MODIFYING FIXATION STIFFNESS TO IMPROVE BONE HEALING

Nicole Bartnikowski

B.Eng. (Hons)

Submitted in fulfilment of the requirements for the degree of Doctor of Philosophy

Institute of Health and Biomedical Innovation

Faculty of Science and Engineering

Queensland University of Technology

2016

Keywords

Bone, external fixator, FE modelling, fracture gap, mechanical environment, mechanobiology, osteotomy, secondary bone healing, stability, stiffness

Abstract

The majority of long bone fractures heal via a secondary bone healing process, with the development of an external callus. Callus size and morphological development are influenced by mechanical stimuli throughout all stages of the healing process. Interfragmentary movement (IFM) has been identified as the most important mechanical factor influencing healing, and is determined by the applied load and the stability of any fixation. Identifying the phases of healing that are most sensitive to mechanical stimulation can provide an opportunity for clinicians to optimise bone healing treatments.

This thesis employs a number of methods to investigate the effect of modifying fixation stiffness on the healing process and outcome. A finite element (FE) model is used as a predictive tool and an *in vivo* small animal osteotomy model is employed to investigate the effect of early flexible fixation, which was later stabilised at different times throughout the healing process.

Finite element models provide an opportunity to assess mechanical stimuli within healing fractures that cannot be measured directly during experimental investigations. These models have the potential to further our understanding of fracture healing, and to ultimately be used to predict and optimise patient-specific treatment strategies in a clinical setting. However, due to limitations in modelling techniques and our current understanding of mechanobiological principles, these goals cannot currently be realised. This limitation was identified after using the FE model to simulate changes in fixation stiffness, whereby the results indicated that constant stable fixation always led to the best healing outcome.

The *in vivo* studies undertaken as part of this project investigated tissue development in response to varied mechanical stimuli. Histological methods were used to characterise changes in callus composition and development throughout the healing process. The outcome of healing was assessed using a combination of mechanical testing, micro-computed tomography, and histological evaluation.

This study clearly identified differences in healing under different constant fixation stabilities. The formation of the periosteal callus via intramembranous ossification was shown to be related to the local mechanical stimulus within the fracture region. As healing progressed under constant fixation, it was observed that higher magnitude IFM led to delayed healing, particularly during the mineralisation of cartilage as part of the endochondral process.

Modification of fixation stiffness at 7 days post-operatively led to a healing pathway dominated by intramembranous ossification, however when implemented 14 days post-operatively, the process was shown to accelerate endochondral ossification. Overall, these results indicates benefits from early fixation flexibility through stimulation of hard callus formation, with further stabilisation required for intracortical bone formation - irrespective of the healing pathway.

Table of Contents

Keywords i

Abstract ii

Table of Contents iv

List of Figures vii

List of Abbreviations xii

Statement of Original Authorship xiii

Acknowledgements xiv

CHAPTER 1: INTRODUCTION 1

1.1 Background 1

1.2 Mechanical Stimulus on Bone Healing 2

1.3 Computation Modelling of Secondary Bone Healing 3

1.4 Purpose for the Research 3

1.5 Thesis Hypothesis and Aims 4

1.6 Overview 5
- 1.6.1 Chapter 2: Literature Review 5
- 1.6.2 Chapter 3: Hypothesis Conceptualisation and Development 5
- 1.6.3 Chapter 4: Computational simulation of fracture healing under modulation of fixation stiffness 5
- 1.6.4 Chapter 5: The Influence of Modifying Fixation Stiffness on the Healing Outcome 6
- 1.6.5 Chapter 6: The Influence of Modifying Fixation Stiffness on Callus Development 6
- 1.6.6 Chapter 7: Summary and Discussion 6

CHAPTER 2: LITERATURE REVIEW 7

2.1 Bone Physiology 7

2.2 Bone Fracture Healing 9
- 2.2.1 Inflammation 11
- 2.2.2 Repair 12
- 2.2.3 Remodelling 14
- 2.2.4 Revascularisation 15

2.3 Factors Influencing Fracture Healing 16
- 2.3.1 Methods of Fixation 17
- 2.3.2 Compression 17
- 2.3.3 Splinting 18
- 2.3.4 Complications 21
- 2.3.5 Fracture Motion 23
- 2.3.6 Assessing the rate of Bone Healing 27
- 2.3.7 Modifying the Mechanical Environment 29

2.4 Mechanobiology During Bone Healing 34
- 2.4.1 Mechanical Stimuli on Cells 34
- 2.4.2 Interfragmentary Strain Theory 36

2.5 Computational Simulation of Bone Healing 38
- 2.5.1 Tissues Modelled as a Single Solid Phase 39
- 2.5.2 Biphasic and Adaptive Finite Element Models 42
- 2.5.3 Models of Callus Growth 43

CHAPTER 3: HYPOTHESIS CONCEPTUALISATION AND DEVELOPMENT 45

3.1 Introduction....45
3.2 Materials and Methods....48
3.3 Results....51
3.4 Discussion....56
3.4.1 Models to Investigate Mechanical Environment....58
3.4.2 Inter-species Comparisons....60
3.4.3 Defining Bone Healing....61
3.5 Conclusion....64
CHAPTER 4: COMPUTATIONAL SIMULATION OF FRACTURE HEALING UNDER MODULATION OF FIXATION STIFFNESS....65
4.1 Introduction....65
4.2 Methods....67
4.2.1 FE Model....69
4.2.2 Fuzzy Logic Controller....71
4.2.3 Iterative Healing Simulation....72
4.3 Results....73
4.3.1 Assessing Fixation Parameters....73
4.3.1 Modifying Fixation Stiffness....76
4.4 Discussion....80
4.5 Conclusion....83
CHAPTER 5: THE INFLUENCE OF MODIFYING FIXATION STIFFNESS ON THE HEALING OUTCOME....84
5.1 Introduction....84
5.2 Materials and Methods....86
5.2.1 Animal Model....86
5.2.2 Fixator Design and Construction....86
5.2.3 Operative Procedure....87
5.2.4 Biomechanical Testing....89
5.2.5 Micro-computed Tomography....91
5.2.6 Histology and Histomorphometry....91
5.2.7 Data Analysis / Statistics....92
5.3 Results....92
5.3.1 Biomechanical Testing....93
5.3.2 Microcomputed Tomography....93
5.3.3 Histology and Histomorphometry....94
5.4 Discussion....100
5.4.1 Stiff versus Flexible Control....100
5.4.2 Modulation from Flexible to Stiff Fixation....101
5.5 Conclusion....106
CHAPTER 6: THE INFLUENCE OF MODIFYING FIXATION STIFFNESS ON CALLUS DEVELOPMENT....107
6.1 Introduction....107
6.2 Materials and Methods....109
6.2.1 Animal Model....109
6.2.2 Fixator Design and Construction....110
6.2.3 Operative Procedure....111
6.2.4 Histology and Histomorphometry....111
6.2.5 Data Analysis / Statistics....111
6.3 Results....112
6.3.1 Stiff versus Flexible Control....112

6.3.2 Modifying Fixation Stiffness and Quantitative Assessment....116
6.3.3 Tissue Formation over the Course of Healing....122

6.4 Discussion....124
6.4.1 Stiff versus Flexible Control....124
6.4.2 Modifying Stiffness....126
6.4.3 Healing Stages....128

6.5 Conclusion....134

CHAPTER 7: SUMMARY AND DISCUSSION....135
7.1.1 Temporal tissue formation....139

7.2 Clinical Implications of Modifying Fixation STiffness....143

7.3 Future Work....145
7.3.1 Further Examination of the Healing Pathway....147
7.3.2 Finite Element Models....148
7.3.3 Further Applications....148

7.4 Conclusion....149

REFERENCE LIST....151

APPENDICES....164
Appendix A Chapter 5 and Chapter 6: Surgical Procedure....165

List of Figures

Figure 2.1: Hierarchical bone organisation over different length scales. A) the cortical outer layer; b) cylindrical osteons (or Haversian systems); c) a range of cell membrane receptors specific to binding sites; and d) the nanoarchitecture of the surrounding extracellular matrix (ECM) (reproduced with permission [21, 22]). 9

Figure 2.2: Intramembranous bone formation occurs forming an initial hard callus while the hematoma is replaced by fibrous tissue (adapted with permission [34]). 13

Figure 2.3: Cartilage formation at the bone ends and bony bridging (adapted with permission [34]). .14

Figure 2.4: Bone remodelling process in which the original structure of the bone is restored (adapted with permission [34]). 15

Figure 2.5: Radiograph of an ankle. A compression plate with cortex screws was used to fix the fibular fracture while the medial melleolar fracture has been fixed with two cancellous screws (reproduced with permission [28]) 18

Figure 2.6: Example of a unilateral external fixator. A number of geometric parameters influence the stiffness of the external fixation. These parameters include the diameter of the screws (d), diameter of the connecting bar (D), free length between the bar and bone (L), shortest distances between inner screw and fracture (L1 and L2), distance between connecting bars (L3) and distance between screws (LS) (reproduced with permission [48]). 19

Figure 2.7: Intramedullary nail fixation used to stabilise a spiral distal tibial fracture a) before and b) after fixation. The insertion of interlocking screws in the proximal and distal ends of the fixator provides axial stability (reproduced with permission [28]). 21

Figure 2.8 Radiological images of a femoral upper diaphysis hypertrophic non-union (left) and a tibial diaphysis atrophic non-union (right) (reproduced with permission [7]). 23

Figure 2.9 Radiographs of experimental tibiae, with greater periosteal callus formation on the far side of the external fixation, where a greater compressive displacement was induced. A greater periosteal response was observed when a greater number of cycles were applied to the fracture (reproduced with permission [82]). 26

Figure 2.10 Histologic appearance of bone healing where the predominant loading was A) axial compression and B) interfragmentary shear (reproduced with permission [92]). 27

Figure 2.11: Throughout the normal bone healing process, interfragmentary movement (red) is at its greatest during the early stages of healing and decreases as the tissues within the fracture mature. It ceases as the fracture callus bridges (dashed vertical red line). Conversely, callus stiffness (green) increases as healing progresses with maximum stiffness (dashed green vertical line) often occurring following bony bridging as the entire callus mineralises (reproduced with permission [12]). 29

Figure 2.12: Illustration of the fixator construct used in the dynamization study [107, 108]. For the more rigid configuration, two bars were used on the fixator, with the offset between the inner bar and the lateral surface of the bone set at 6 mm. For the flexible configuration, one fixator bar was used with a 15mm offset from the surface of the femur (reproduced with permission [107, 108]). 32

Figure 2.13: Deformation of elementary particles of a cube of isotropic elastic material under A) biaxial tensile forces, increasing in volume but retaining the same shape and B) under shearing forces, where the volume remains constant but the spherical shape is deformed to an ellipsoid (adapted with permission [117]). 35

Figure 2.14: A schematic representation of Pauwel's hypothesis regarding the influence of mechanical stimuli on tissue phenotype development (reproduced with permission [117]). 36

Figure 2.15: Interfragmentary strain theory: A tissue cannot exist in an environment where the interfragmentary strain exceed the strain tolerance of the extracellular matrix of the tissue (reproduced with permission [63, 64]). 38

Figure 2.16: The relationship between mechanical loading history and tissue formation in a fracture callus as presented by Carter *et al*. (reproduced with permission [38]). 40

Figure 2.17: Tissue formation driven by different mechanical conditions within a healing fracture as in a fracture callus based on the local mechanical conditions as hypothesised by Claes and Heigele (reproduced with permission [11]).....41

Figure 2.18: Mechano-regulation theory for tissue development at the surface of implants based on strain and fluid flow (reproduced with permission from [137]). 43

Figure 2.19: Fracture healing theory based on strain and fluid flow (reproduced with permission [127]).....43

Figure 2.20. Bone healing simulation produced by the volumetric growth model of Garcia-Aznar *et al*. (2007). Increased load lead initially to larger calls growth however when increased to 750 N healing was delayed. (Figure adapted with permission from [121]). 44

Figure 3.1: The hypothesised benefits of modifying fixation stiffness (increasing) on interfragmentary movement (left) over the course of bone healing. Increasing fixation stiffness will decrease the time taken for IFMs to reduce compared to flexible fixation and potentially stable fixation (reproduced with permission [12]).....48

Figure 3.2 One quarter FE-model of the callus region (reproduced with permission [11]). 49

Figure 3.3 From left to right: One quarter model of initial state and early state with small mineral callus (3 mm width) and early state with large mineral callus (6 mm width). Initial connective tissue (ICT), cortex (C), mineral callus (CA) and facia (F). 50

Figure 3.4 Strain and hydrostatic pressure fields in the initial fracture callus are comparable to those reported by Claes and Heigele [11] (adapted from [11]).....52

Figure 3.5 The reciprocal relationship between the cross-sectional area of the bone at approximately the line of the osteotomy and the resulting IFM.....53

Figure 3.6 Strain and hydrostatic pressure fields in the remaining soft tissue after the formation of mineral periosteal callus, for callus sizes of 3 mm and 6 mm. 54

Figure 3.7 Strain and hydrostatic pressures along the ossification pathway for initial conditions, 3 mm hard callus and 6 mm hard callus models.....55

Figure 3.8 Histology section from an ovine osteotomy model after two weeks of bone healing, stabilised under unilateral external fixation on the medial side. The predominant loading is interfragmentary compression however due to the nature of the fixation, bending occurs, transmitting higher loads to the far cortex than the near, stimulating the production of a larger callus. (reproduced with permission [12]). 57

Figure 3.9: Histological sections of rat (top) and sheep (bottom) osteotomy models at different time points post-operatively. The rat model demonstrates a faster healing process when compared to sheep (reproduced with permission [154]). 61

Figure 4.1: a) Schematic of external ring fixator used in animal experiments (reproduced with permission [40, 59] b) FE model (2D, axisymmetric) of a standardised fracture callus geometry used in FE model by Simon *et al*. (reproduced with permission [98]). 68

Figure 4.2: Fuzzy controller with seven fuzzy input and three fuzzy output variables. (reproduced with permission [129]).7 71

Figure 4.3: Flowchart of the dynamic fracture healing model including the FE method and the fuzzy logic in an iterative loop over time (reproduced with permission [129]). 73

Figure 4.4 Theoretical calculations versus model measured values for interfragmentary movement (for each fixation stiffness). 74

Figure 4.5 Interfragmentary movement measured over time (iterations) in the FE model. Stiffness parameters investigated ranged from 200 $N \cdot mm^{-1}$ to 1600 $N \cdot mm^{-1}$. It may be seen that very low stiffness parameters did not result in healing (200 $N \cdot mm^{-1}$), with higher stiffness fixations producing similar healing outcomes to one another (800-1600 $N \cdot mm^{-1}$). The red line indicates the healed condition, at an IFM of less than 0.1 mm. 75

Figure 4.6 Healing outcome measured in number of iterations required until IFM is less than 0.1 mm. It may be seen that there is a large change in time from 300 to 800 $N \cdot mm^{-1}$, with only small decreases in healing times achieved with stiffness in excess of 800 $N \cdot mm^{-1}$.....75

Figure 4.7 Healing pathways under with different stiffness fixators; 400 $N \cdot mm^{-1}$ (left); 800 $N \cdot mm^{-1}$ (middle) and 1600 $N \cdot mm^{-1}$ (right). No differences were observed in the first 2 weeks of callus development, however differences began to arise by 4 - 6 weeks, with more bone formation under stiffer fixation. 77

Figure 4.8 Interfragmentary movement measured over time (iterations) in the FE model. Fixation stiffness was changed from 400 $N \cdot mm^{-1}$ to 800 $N \cdot mm^{-1}$ (top) and 500 $N \cdot mm^{-1}$ to 800 $N \cdot mm^{-1}$ (bottom). Changes in stiffness were made at iteration 7, 14 and 21. The red line indicates healed condition at IFM of less than 0.1 mm. 79

Figure 4.9 Tissue distribution at time of periosteal bridging for both constant fixation conditions and from stabilising the fixator at iteration 7, 14 and 21.....79

Figure 5.1 The four study groups (3D, 7D, 14D and 21D) with the stiff and flexible control group. In the study groups, the fixation was stiffened at 3, 7, 14 and 21 days, respectively. 87

Figure 5.2: Fixator constructs demonstrating offset difference between stiff and flexible configurations A) schematic of stiff construct with 6 mm offset; B) postoperative *in vivo* radiograph of stiff construct; C) schematic of flexible construct with 12 mm offset; and D) postoperative *in vivo* radiograph of flexible construct.....88

Figure 5.3: Attachment of external fixation to femur and creation of 1 mm osteotomy. 89

Figure 5.4: Three point bending test of callus.....91

Figure 5.5 Effect of the modulation of stiffness from flexible to stiff (3, 7, 14 and 21 days) on bone healing, evaluated by 3-point bending. A) Flexural rigidity of the callus normalised to the contralateral limb, and B) absolute flexural rigidity. $p < 0.05$ was considered significant. Significantly different groups indicated by different symbols (I and II).....93

Figure 5.6 Effects of the modulation of stiffness from flexible to stiff (3, 7, 14 and 21 days) on bone healing evaluated by μCT. A) Total volume of the fracture callus; B) volume of the fracture gap; C) bone mineral density throughout the entire callus, and; D) bone mineral density in the fracture region. $p < 0.05$ was considered significant. Significantly different groups indicated by different symbols (I, II and III).....95

Figure 5.7 Micro-computed tomography images of the osteotomies at 35 days post-operatively, after modulation of stiffness from flexible to stiff at 3, 7, 14 and 21 days post-operatively and compared to stiff and flexible controls.....96

Figure 5.8 Effects of the modulation of stiffness from flexible to stiff (3, 7, 14 and 21 days) on bone healing, evaluated by histomorphometry. A) Cartilage area quantified throughout the entire callus, and; B) cartilage area throughout the fracture gap. $p < 0.05$ was considered significant. Significantly different groups indicated by different symbols.....97

Figure 5.9 Histological images at 35 days post-operatively after stabilisation with stiff and/or flexible fixators, and modulation of stiffness from flexible to stiff at 3, 7, 14 and 21 days. A) Stiff group; B) 3D group; C) 7D group; D) 14D group; E) 21D group and F) flexible group. Histological sections were stained with paragon: fibrous tissue (white and blue), cartilage (purple), and bone (light blue-white). Scale bar indicates 1 mm.....97

Figure 5.10 Expected changes in tissue and analytical parameters over the course of healing in a rat model. Where FT - Fibrous Tissue; CA – Cartilage Area; BMD – Bone Mineral Density and BV/TV – Bone Volume over Total Volume.....105

Figure 6.1: Time points to monitor the progression of healing. Time in the flexible fixation condition is represented in blue, with stiff fixator conditions indicated in grey. Rats were euthanised at 5 days and 14 days postoperatively for the 3D, 7D and controls groups. Rats were euthanised at 28 days for the control groups only. These groups were compared to the results from Chapter 5, where the rats were euthanised at 35 days. 110

Figure 6.2 The callus histology (safranin orange-fast green) after 5 days of healing. A) Stiff fixation; B) periosteal callus response under stiff fixation; C) flexible fixation, and; D) periosteal callus response under flexible conditions, where cartilage formation can be seen at the

periphery of the initial hard callus. Scale bar indicates 1 mm for A) and C) and 100 µm for B) and D).....113

Figure 6.3 The callus histology (safranin orange-fast green) after 14 days of healing. A) Stiff fixation; B) periosteal and intracortical tissue formation under stiff fixation; C) flexible fixation, and; D) periosteal and intracortical tissue under flexible conditions. Scale bar indicates 1 mm for A) and C) and 100 µm for B) and D). 114

Figure 6.4 The callus histology (safranin orange-fast green) after 28 days of healing. A) Stiff fixation; and B) flexible fixation. Scale bar indicates 1 mm. 115

Figure 6.5 The callus histology (safranin orange-fast green) after 5 days of healing. A) Flexible fixation for 3 days (3D) stabilised for the final two days, and; B) periosteal tissue responses after changed fixation stiffness at 3 days. Scale bar indicates 1 mm for A), and 100 µm for B).....117

Figure 6.6 Healing evaluated 5 days post-operatively, comparing stiff and flexible conditions with fixation stiffness modified at 3 days (3D). A) Total callus area; B) callus diameter; C) bone area, and; D) cartilage area within the callus were quantified. $p < 0.05$ was considered significant. Significantly different groups have different symbols. 118

Figure 6.7 The callus histology (safranin orange - fast green) after 14 days of healing. A) 3D group; B) intracortical tissue with changing fixation stiffness at 3 days; C) 7D group, and; D) intracortical tissue with changing fixation stiffness at 7 days. Scale bar indicates 1 mm for A) and C) and 100 µm for B) and D). 119

Figure 6.8 Healing evaluated 14 days post-operatively, comparing stiff and flexible conditions with a changed fixation stiffness at 3 days (3D) and 7 days (7D). A) Total callus area; B) periosteal callus area; C) endosteal callus area, and; D) intracortical area. All graphs display the total area for the callus region, as well as bone and cartilage areas. $p < 0.05$ was considered as significant. Significantly different groups have different symbols. 120

Figure 6.9 Healing evaluated 28 days post-operatively, comparing stiff and flexible conditions. A) Total callus area; B) periosteal callus area, and; C) endosteal callus area. All plots display the total area for the callus region, as well as bone and cartilage areas. $p < 0.05$ was considered significant. Significantly different groups have different symbols. 121

Figure 6.10: Healing evaluated over time for the control groups. A) Total callus; B) periosteal callus; C) endosteal callus, and; D) intracortical region. All figures display the total area for the callus region, as well as bone and cartilage areas. 123

Figure 6.11: Tissue distribution throughout the callus over time for 3D, 7D and control groups. A) Total callus area; B) bone area, and; C) cartilage area. 123

Figure 6.12 Callus histology (safranin orange - fast green) under flexible conditions assessing the callus progression at the time of stabilisation. A) 3 days of healing; B) 7 days of healing, and; C) 14 days of healing. Scale bar indicates 40 µm. 129

Figure 6.13 Healing under constant fixation stiffness in a rat femoral osteotomy model. Stage I with the formation of a haematoma; Stage II with periosteal callus formation and initial cartilage formation; Stage III is indicative of further periosteal callus growth, endosteal bridging and a combination of periosteal, intracortical and endosteal cartilage formation; Stage IV is characterised by mineralisation and bridging of the periosteal callus; Stage V can be represented by intracortical bridging and initial remodelling of the periosteal and endosteal regions; and Stage VI is a continuation of the remodelling process, characterised by the formation of a dual cortex, which is later fully resorbed.....132

Figure 6.14 Healing after modifying fixation stiffness during Stage II of healing in a rat femoral osteotomy model. Stage I with the formation of a haematoma primarily within the fracture region; Stage II with periosteal callus formation and initial cartilage formation; Stage III is indicative of intramembranous ossification at the cortical bone ends; Stage IV is undefined with potential bone formation or cartilage formation (indicated in brown); Stage V can be represented by intracortical bridging and initial remodelling of the periosteal and endosteal regions; and Stage VI is a continuation of the remodelling process, characterised by the formation of a dual cortex, which is later fully resorbed.....133

List of Tables

Table 3-1: Material properties of the different tissue types used in this model.....51

Table 4-1: Material properties of the pure tissue types used in the FE model.....71

Table 4-2 Time to healing after stabilising fixation by increasing stiffness.....78

Table 5-1 Three-point bending and micro-computed tomography results (mean ± standard deviation) determined after 35 days of healing 98

Table 5-2 Histomorphometry results (mean ± standard deviation) determined after 35 days of healing. 99

Table 5-3 Number of animals achieving bony bridging after 5 weeks of healing.....100

Table 6-1 Healing stages observed in sheep 3 mm osteotomy healing (adapted from Vetter *et al*. 2010 [197], with permission). 131

Table 6-2 Healing stages outlined for osteotomy healing in rat femoral osteotomy model (1 mm) ...131

List of Abbreviations

2D	two dimensional
3D	three-dimensional
ANOVA	analysis of variance
BMD	bone mineral density
BMP	bone morphogenetic protein
BV	bone volume
Col I	collagen type I protein
Col II	collagen type II protein
CO_2	carbon dioxide
DNA	deoxyribonucleic acid
ECM	extracellular matrix
EDTA	ethylenediamine tetraacetic acid
FE	finite element
EI	flexural rigidity
IFM	interfragmentary movement
IFS	interfragmentary strain
IL-1	interleukin-1
IL-6	interleukin-6
MSC	mesenchymal stem cell
µCT	microcomputed tomography
NaCl	sodium chloride
NaOH	sodium hydroxide
PDGF	platelet derived growth factor
PBS	phosphate buffered saline
PG-E_2	prostaglandin E_2
TGF-β	transforming growth factor beta group
TV	total volume
QUT	Queensland University of Technology
SD	standard deviation
vWF	von Willebrand Factor

Statement of Original Authorship

The work contained in this thesis has not been previously submitted to meet requirements for an award at this or any other higher education institution. To the best of my knowledge and belief, the thesis contains no material previously published or written by another person except where due reference is made.

QUT Verified Signature

Nicole Bartnikowski

27 July 2016

Acknowledgements

There are many people I would like to thank for their involvement in my work and/or life during my PhD experience. I would first like to thank Dr Devakar Epari for all of his contributions and patience during my PhD journey, even during the most difficult times.

Secondly, I extend my gratitude to Dr Vaida Glatt, who has been a great mentor to me. Vaida and I shared many insightful discussions not only relating to this research project but in all facets of life. To round out my supervisory team, I would like the thank Dr Roland Steck, who spent countless hours assisting throughout the practical work, and without whom, my first year would have been incredibly difficult.

I also thank the Trauma Research group for including me in their community and supporting me through this time. Both past and present members have played an important role in my personal and professional growth and development. I would also like to acknowledge the technical support I received from staff at the Medical Engineering Research Facility, who assisted me in facilitating a vast amount of experimental work.

Lastly I wish to extend my thanks to my friends and family, most notably my husband Michal. Without his help, support and cooking during this period in my life, I would have struggled significantly more.

Chapter 1: Introduction

1.1 BACKGROUND

Bone fractures occur frequently throughout Australia and cost the health care system more than AUD$1.9 billion annually in direct costs [1]. Fractures occur when an accidental load exceeds the physiological 'limit' of the tissue, inducing strains that result in stress greater than the strength of the bone [2]. These can occur from high energy trauma, for example sporting or traffic accidents, or from low energy trauma, such as slips and falls. Whilst many such fractures heal with minimal intervention, particularly in children, a large proportion require surgical intervention to heal appropriately [3].

The intrinsic repair capacity of bone tissue is considerable, with the tissue being able to return to its original strength and anatomy without the formation of scar tissue, given appropriate healing conditions. However, when fracture complexity or the suitability of fixation exceed certain limits, complications may arise, as reported in 5-10 % of all long bone fractures [4-6]. Propensity for complication is highly dependent on a combination of injury and host factors [7].

The regeneration of bone tissue, is a complex, well-orchestrated process of cell recruitment, proliferation and differentiation [8]. The tissues that are formed in the defect, including granulation tissue, fibrous tissue, cartilage, and bone, form different distributions throughout healing that are directly influenced by the mechanical environment of the fracture. It has been hypothesised [9-13] that if this mechanical environment can be optimised, the bone healing response will be enhanced, reducing patient recovery times and complication rates.

1.2 MECHANICAL STIMULUS ON BONE HEALING

The majority of fractures heal via secondary bone healing, with the formation of an external callus, due to mechanical stimulus within the fracture. In this context, movement at the fracture site is referred to as interfragmentary movement (IFM). Such movements induce local mechanical stimuli within the developing callus tissue that can influence cellular differentiation, tissue turnover and hence improve the rate of healing [14]. The magnitude of IFM occurring at an injury site is governed by the load applied to the limb, due to weight bearing and muscle forces, the stiffness of the tissue, and the stability of the fracture site as determined by the stiffness of the fixation.

Past experimental investigations have determined that there is a range of IFM which produces a reliable healing outcome, with stimuli outside of this range resulting in potential complications. On one hand, overly rigid fixation results in delayed healing where callus formation is suppressed, whilst conversely overly flexible fixation leads to hypertrophic non-union, where excessive instability and IFM impairs callus mineralisation. For optimal bone healing, a fixation needs to allow sufficient movement to stimulate callus growth, yet provide enough stability to permit mineralisation and the bony bridging of the fracture.

Whilst it is clear that IFM influences the healing outcome, it is not well understood how IFM-related strain influences specific cellular signalling, leading to the formation of different tissue types. Hence, optimal IFM may vary across different stages of healing. Development in this field may reveal clinically relevant periods where the ability to modify the fracture fixation stiffness may potentiate favourable IFM, enhancing the healing outcome. This would prove advantageous over current methods, where the stiffness of fixation remains unchanged until the end of the healing period unless adverse events are observed.

The concept of modulating fixation stiffness throughout bone fracture healing to optimise the mechanical environment at each healing stage will be investigated in this thesis. A number of methods will be employed to investigate this theory, including *in vivo* studies and computational studies.

1.3 COMPUTATION MODELLING OF SECONDARY BONE HEALING

Determining the mechanical stimuli driving tissue development during secondary fracture healing is critical to optimise clinical treatment of bone fractures. Whilst investigation into this interaction has been explored both clinically and experimentally, limitations in monitoring technology, such as non-invasive measurement of intra-defect strains during healing, have largely impeded advancement. Alternative approaches, namely that of numerical modelling in the form of Finite Element (FE) simulations, have been developed to attempt to combat such issues.

FE techniques may be used to analyse a structure with a known geometry, a proposed load and appropriately detailed material properties. Whilst perfectly suited to purpose conceptually, these models are still often preliminary and require significant assumptions or simplifications to be made in order to be executed. At present, FE models are only used to describe biological and histological outcomes from past *in vivo* experimental investigations. To ultimately develop models capable of predicting healing outcomes from patient specific cases, they require further assessment and development. This thesis will explore the status of current numerical simulations of bone healing in comparison to results obtained through *in vivo* investigations.

1.4 PURPOSE FOR THE RESEARCH

The purpose of this research is to expand knowledge in the field of bone fracture repair. I explored the effect of changing the mechanical environment in the healing of

bone fractures. The majority of this work was conducted in collaboration with colleagues from the Institute of Orthopaedic Research and Biomechanics, University Hospital of Ulm, Germany.

Firstly, I tested the predictive capacity of an established FE bone healing model, to assess if the model had the capacity to predict healing outcomes in a scenario beyond which it was developed. Secondly, I conducted an *in vivo* bone healing study in a rat mid-diaphyseal femoral osteotomy model, whereby the mechanical environment was modulated at different times throughout the healing process, to assess not only a changing mechanical environment on the overall healing outcome, but also on each healing stage. Finally, I conducted a comparison between the FE modelling and the *in vivo* study in order to further describe mechanobiological mechanisms that influence fracture repair.

1.5 THESIS HYPOTHESIS AND AIMS

The overarching aim of this thesis is to determine during the phases of bone healing where mechanical stimulation may enhance the bone healing response. It was hypothesised that the healing outcomes of long bone fractures can be improved through the implementation of appropriate mechanical stimuli that are purposefully modulated as healing progresses. We propose that it will be most beneficial to provide a flexible fixation to the fracture during the earlier stages of healing to promote larger callus formation, and then to increase fixator stiffness to allow for callus maturation and subsequent remodelling to occur.

1.6 OVERVIEW

1.6.1 Chapter 2: Literature Review

This chapter provides a comprehensive review of literature relating to the field of bone healing. Beginning with the anatomy and physiology of diaphyseal bones, followed by a description of the bone fracture healing process. Factors influencing bone healing are then reviewed including methods of fixation, the mechanical environment and fracture motion, and complication arising clinically. Finally the mechanobiological theories driving fracture repair and current computational modelling of the healing process are described.

1.6.2 Chapter 3: Hypothesis Conceptualisation and Development

This chapter provides background justification for the overarching hypothesis investigated throughout this thesis. We hypothesise that bone healing will be enhanced with initial flexible fixation conditions which will be converted to stiff fixation during the later stages of repair. An axisymmetric FE study was conducted as a demonstration of the hypothesis whereby a larger callus lowered the tissue strain within the fracture gap and along the ossification front compared with a smaller callus. Finally, the models which will be implemented in order to investigate this hypothesis are outlined.

1.6.3 Chapter 4: Computational simulation of fracture healing under modulation of fixation stiffness

This chapter implements a current numerical algorithm of bone fracture healing, developed at the Institute of Orthopaedic Research and Biomechanics, University Hospital of Ulm, Germany, to assess the predictive capacity of the simulation. The study was intended to determine if the model can appropriately address the effects of the changing mechanical environment on tissue distribution and the length of time required for healing. Results from this chapter are later compared with the following *in vivo* studies.

1.6.4 Chapter 5: The Influence of Modifying Fixation Stiffness on the Healing Outcome

In this chapter, an *in vivo* study was used to investigate the influence of modifying fixation stiffness on the outcome of healing. The experimental model was a rat femoral osteotomy stabilised with an external fixator. The hypothesis of this thesis was assessed by treating osteotomies with early flexible fixation to promote callus formation, with subsequent stiffening of the fixator to allow for callus mineralisation. Mechanical testing, micro-computed tomography and histological techniques were used to assess the quality of bone healing in each group.

1.6.5 Chapter 6: The Influence of Modifying Fixation Stiffness on Callus Development

The aim of this chapter was to assess the bone healing process under stiff and flexible fixation conditions, and to compare these with modified fixation stiffness at 3 and 7 days post-operatively. Early time points in healing were examined closely, by assessing tissue distributions at 5, 14 and 28 days post-operatively. It was hypothesised that a larger callus will be formed earlier in the post-operative period with flexible fixation conditions, which once stabilised under stiffer fixation conditions, will result in faster intracortical bone formation.

1.6.6 Chapter 7: Summary and Discussion

The final chapter provides a summary and discussion of the results and how they relate to the hypothesis of this project. Future directions are also outlined to progress knowledge in the field of bone fracture healing and mechanobiology.

Chapter 2: Literature Review

2.1 BONE PHYSIOLOGY

Bone is a complex and highly organised connective tissue that performs several important functions in the body including protection of vital organs, structural support, and movement [15]. Across all of these functions, bone is able to withstand considerable load due to its hierarchical structure, which is constantly remodelled in response to varied stimuli [16].

The adult human skeleton is composed of 80 % cortical bone and 20 % trabecular bone by weight [15]. Cortical bone is a dense, strong material that forms the cortex of long bones. Conversely, trabecular bone comprises a network of rod- and plate-like trabeculae with a much larger surface area per unit volume compared with cortical bone [17]. The trabecular network reduces the overall weight of bone without significantly impacting mechanical properties of the bone at an organ level, whilst providing the necessary volume for bone marrow and blood vessel ingrowth.

The external surfaces of long bones are covered by the periosteum, which is a fibrous connective tissue sheath. The periosteum consists of an outer fibrous layer, composed of collagen and reticular fibres, and an inner, proliferative layer (cambium) which lies adjacent to the bone [18]. The outer fibrous layer provides elasticity to the tissue and facilitates the insertion of ligaments, tendons, and muscles [18]. The inner proliferative layer contains osteoblasts and osteoprogenitor cells capable of forming woven bone after a fracture [15].

The majority of bone mass is comprised of extracellular bone matrix. This matrix comprises both mineralised and non-mineralised elements. The non-mineralised

(organic) component includes ground substance (proteoglycans and glycoproteins) and collagen type I fibres, which contribute to the structure of the bone and provide tensile strength and toughness [19]. The mineralised inorganic component is hydroxyapatite, a crystalline calcium phosphate, which forms microscopic, tightly packed crystals in and around the collagen fibres in the extracellular matrix, reinforcing the tissue structure [15]. The function of cells within the bone is to form, maintain and remodel this matrix [18]. The major cell types include: osteoblasts, which produce bone; osteocytes, which maintain bone; and osteoclasts, which resorb bone.

Structurally, cortical bone is made up of osteons (Figure 2.1). Cortical osteons, also known as Haversian systems, are cylindrical in shape and form a branching network within the bone [19]. The walls of Haversian systems are formed of concentric layers of lamellar bone, orientated parallel to the long axis of the bone; giving high compressive strength and resistance to bending. Cells within the bone are responsible for bone production, maintenance and modelling. Osteoblasts are derived from mesenchymal stem cells and are found on the internal and external surfaces of the lamellae. They secrete glycoproteins and mucopolysaccharides to form the organic component of the bone matrix (osteoid) [19]. Osteocytes are mature osteoblast that are located within lacuna (small pit/depression) throughout the bone matrix [15]. They form a large number of cell-cell contacts, making them capable of rapid signal transduction, through an extensive network of cell processes known as canaliculi [20]. Osteocytes are the cell responsible for sensing mechanical forces exerted on bone. In response to this mechanical stimuli, osteocytes will alter the production of a multitude of signally molecules, which may direct the other cells type to initiate bone resorption or formation responses [20]. Osteoclasts are large multinucleated cells found in cavities on bone surface and are responsible for bone resorption [19].

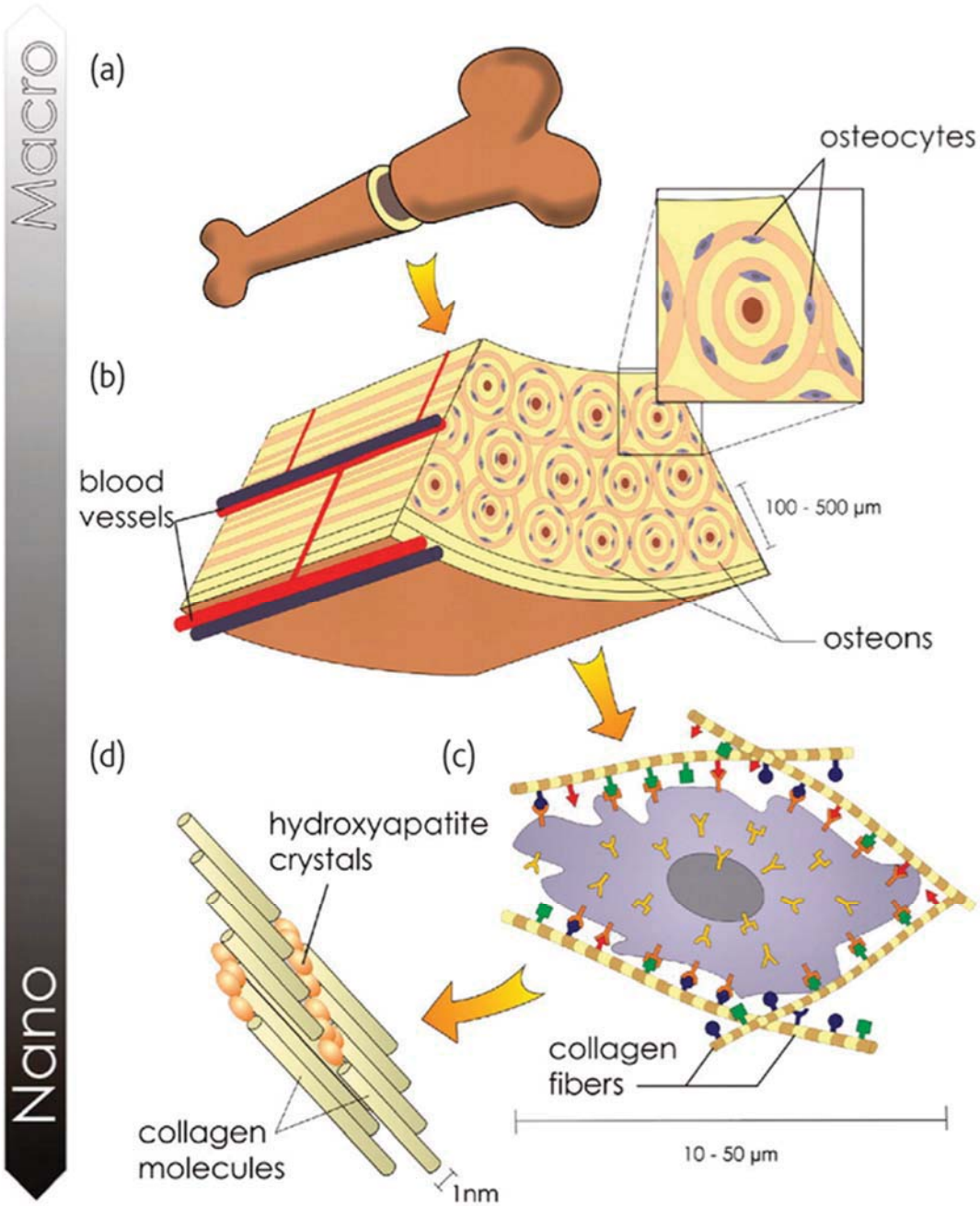

Figure 2.1: Hierarchical bone organisation over different length scales. A) the cortical outer layer; b) cylindrical osteons (or Haversian systems); c) a range of cell membrane receptors specific to binding sites; and d) the nanoarchitecture of the surrounding extracellular matrix (ECM) (reproduced with permission [21, 22]).

2.2 BONE FRACTURE HEALING

A bone fracture occurs when strain exceeding the physiological limits of the tissue is applied [23]. Bone has a substantial capacity for repair following fracture [16], in order to re-establish the continuity and structural integrity of the injured bone, and

subsequently to restore the function of the injured limb [3]. Bone fracture healing is a multistage repair process that involves complex, well-orchestrated steps initiated in response to fracture, and occurs through either primary or secondary healing mechanisms [16, 24, 25].

Primary fracture healing is characterised by direct re-establishment of the cortical bone without the formation of a fracture callus. Primary healing is not a common occurrence, as it requires the anatomical reduction of the fracture ends, with direct cortical bone contact or a small fracture gap, together with an extremely stable fixation compressing the fracture ends. Under these conditions, tissue strain is very low, allowing direct cortical bone remodelling and osteonal bridging without any external callus tissue formation [26, 27].

In this process, osteoclasts act as a cutting head, producing longitudinal cavities known as 'cutting cones', resorbing dead bone at the necrotic ends of the fracture [23, 26]. Behind the cutting head, osteoblasts form new bone within the cutting cones, and subsequently bridge the fracture gap [28]. This process results in the generation of bony union while simultaneously restoring the Haversian systems [29]. It is a slow process which can take anywhere from many months to years until healing is complete [24].

Secondary healing can be outlined in three overlapping stages; inflammation, repair and remodelling. It is a sequential tissue differentiation process that is characterized by periosteal callus formation, with a combination of direct intramembranous ossification and endochondral ossification [3, 16, 24, 25]. This process produces a large volume of woven bone that stiffens the fracture gap, decreasing the movement between the fracture ends and resulting in gradual restoration of the bone tissue [30].

2.2.1 Inflammation

Immediately following a fracture, a haematoma is formed as a result of ruptured blood vessels in the bone, periosteum, surrounding soft tissue, adjacent to the fracture site [4, 31]. Disruption of the blood supply usually leads to the development of hypoxic areas within the tissues due to an initial fall in oxygen tension and nutrient delivery [31]. This deprives the osteocytes of nutrients and gases, which leads to bone necrosis at the fracture site. The extent of this necrosis varies depending on the degree of sustained trauma [30, 32].

The haematoma is rich in platelets and macrophages, which are stimulated to release a series of signalling molecules such as cytokines and growth factors, initiating the inflammatory response by recruiting inflammatory cells [3, 4]. Important cytokines in this stage of fracture healing include platelet derived growth factor (PDGF), the transforming growth factor beta group of proteins (TGF-β), interleukin-1, interleukin-6 (IL-1 & IL-6) and prostaglandin E_2 (PG-E_2) [4]. Many of the cytokines involved in this phase have an angiogenic function, assisting to restore the blood supply through formation of new blood vessels (capillaries) from pre-existing undamaged vessels.

Osteoclasts are activated and begin resorption of bone debris at the fracture site, whilst mesenchymal stem cells (MSCs) are also recruited to the fracture region. The MSCs originate from the periosteum, endosteum, vascular endothelium and bone marrow [4, 19]. They are multi-potent cells and hence capable of differentiating down fibrogenic (fibrous tissue), chondrogenic (cartilage), osteogenic (bone) and lipogenic (fat) cell lineages [31, 32] depending upon the biological and mechanical stimuli they receive. After a few days post-fracture, the haematoma is resorbed leaving fibroblasts which form a loose aggregate of cells that are interspersed with small blood vessels, forming what is known as granulation tissue.

2.2.2 Repair

During the repair phase of secondary fracture healing, both soft and hard calluses are formed through a combination of endochondral and intramembranous ossification [26]. Intramembranous ossification produces a hard callus and occurs predominantly at the periphery of the callus, in a region of low tissue strain, whilst the soft callus is formed centrally in the endochondral ossification zone [3, 16, 24-26].

The intramembranous ossification response occurs predominantly beneath the periosteum, generating a hard callus of woven bone (Figure 2.2). In this region, periosteal osteoblasts synthesize type I collagen (COL I) which leads to the direct generation of calcified tissue [4]. The osteoblasts involved in intramembranous bone formation are said to be derived from periosteal precursor cells and hence removal of the periosteum results in diminished capacity for hard callus formation [30]. Intramembranous bone formation is therefore initiated regions where the periosteum and vascularisation are not disturbed by trauma and where IFM causes minimal tissue strain [33].

A fibrin-rich granulation tissue is formed following the development of the primary haematoma, occurring simultaneously with hard callus formation. This tissue forms between the fracture ends external to the periosteal sites (Figure 2.2). The region is hypoxic and is exposed to high tissue strains [3]. Such conditions encourage the differentiation of MSCs down a chondrogenic lineage, resulting in the formation of a soft callus comprising cartilaginous tissue that stabilises the fracture in this region throughout the calcification and remodelling processes [4, 25, 26].

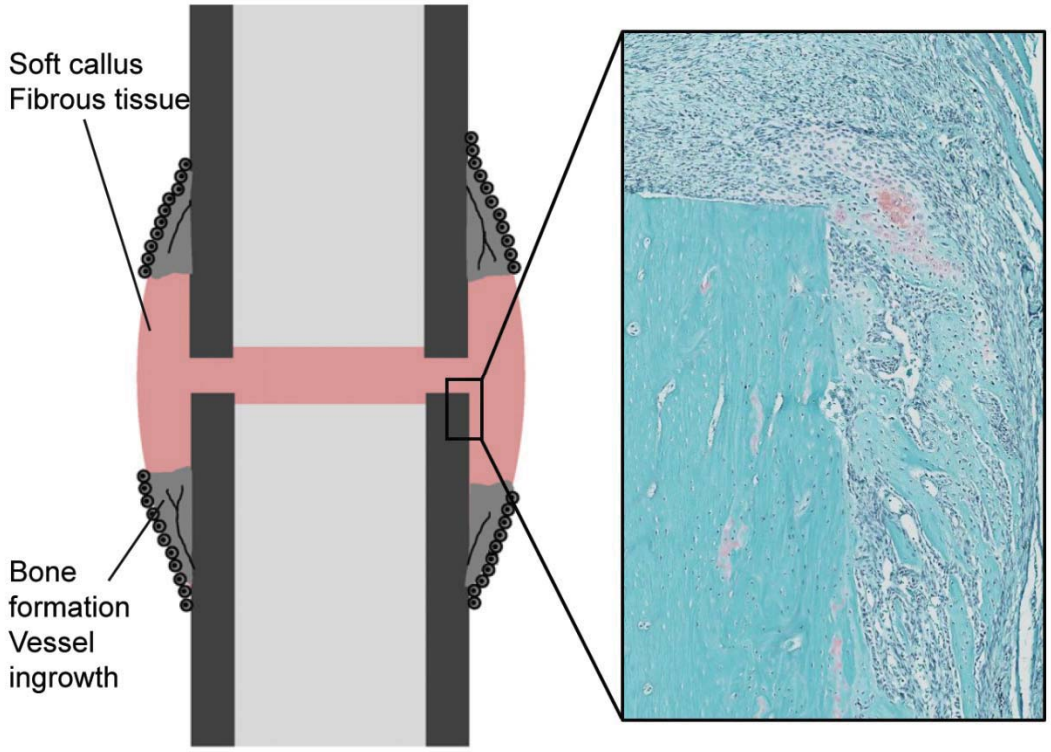

Figure 2.2: Intramembranous bone formation occurs forming an initial hard callus while the hematoma is replaced by fibrous tissue (adapted with permission [34]).

Calcification of the soft cartilaginous callus occurs through the process of endochondral ossification (Figure 2.3), which continues until bone has bridged the fracture site. As chondrocytes in the fracture callus proliferate, they become hypertrophic and start to release calcium and undergo apoptosis [33].This process is similar to the mechanism which occurs in growth plates during embryological bone development. Bridging of the fracture by the cartilaginous matrix provides stability to the region, allowing the ingrowth of blood capillaries into the callus increasing blood supply [26]. The new blood vessels ease chondrocyte and osteoblast infiltration into the tissue, which facilitates the active removal of mineralised cartilage and promotes deposition of woven bone [26].

Throughout this phase of healing, the stiffness and stability of the fracture increases due to an increase in callus volume and the progressive tissue calcification

[4, 24]. By the time the endochondral process has reached the stage of cartilage formation and calcification, a substantial amount of woven bone has already been formed adjacent to the fracture site by intramembranous ossification. Bony bridging will then occur (Figure 2.3) [24], with the resulting fracture callus being composed entirely of woven bone. Ultimately, the final bridging of this hard callus provides the fracture with a semi-rigid structure that allows weight bearing. However, the collagen fibres within this woven bone have random orientations in contrast to those in normal lamellar bone [4], and further remodelling is required to restore the original lamellar structure.

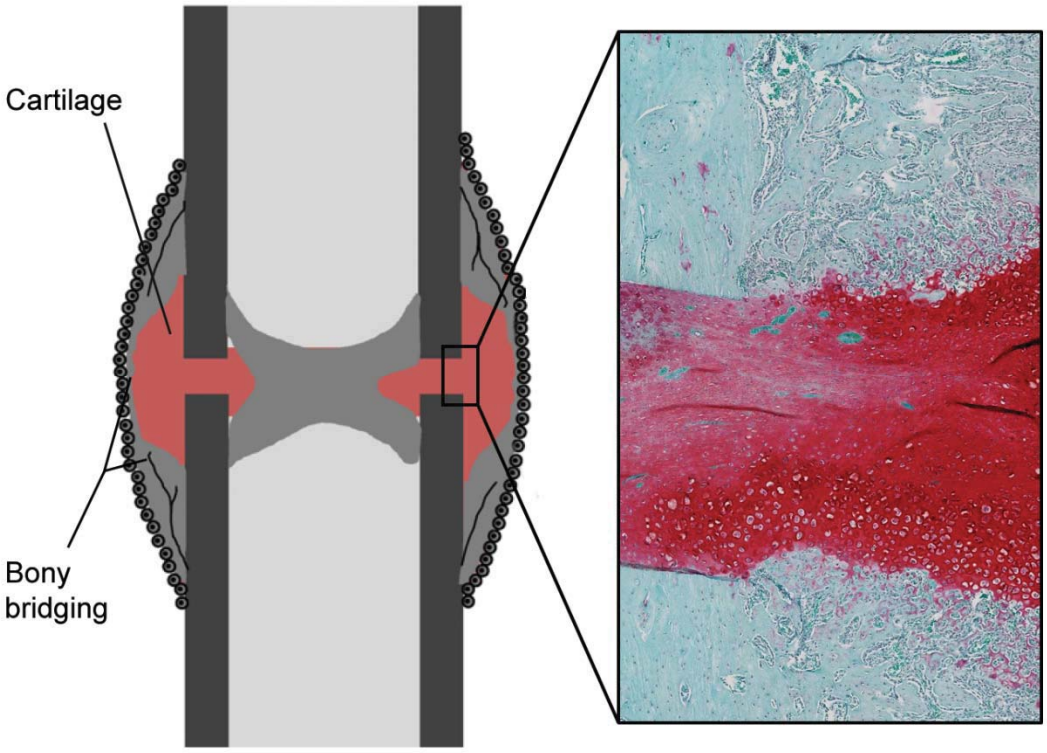

Figure 2.3: Cartilage formation at the bone ends and bony bridging (adapted with permission [34]).

2.2.3 Remodelling

Remodelling of the hard callus restores the lamellar structure, the central medullary cavity, and the normal mechanical characteristics of the bone (Figure 2.4)

[26, 33]. The remodelling process involves a balance of hard callus resorption by osteoclasts and lamellar bone deposition by osteoblasts [24, 30]. It also coincides with the reestablishment of the original blood supply to the bone. The entire process may take multiple years to complete.

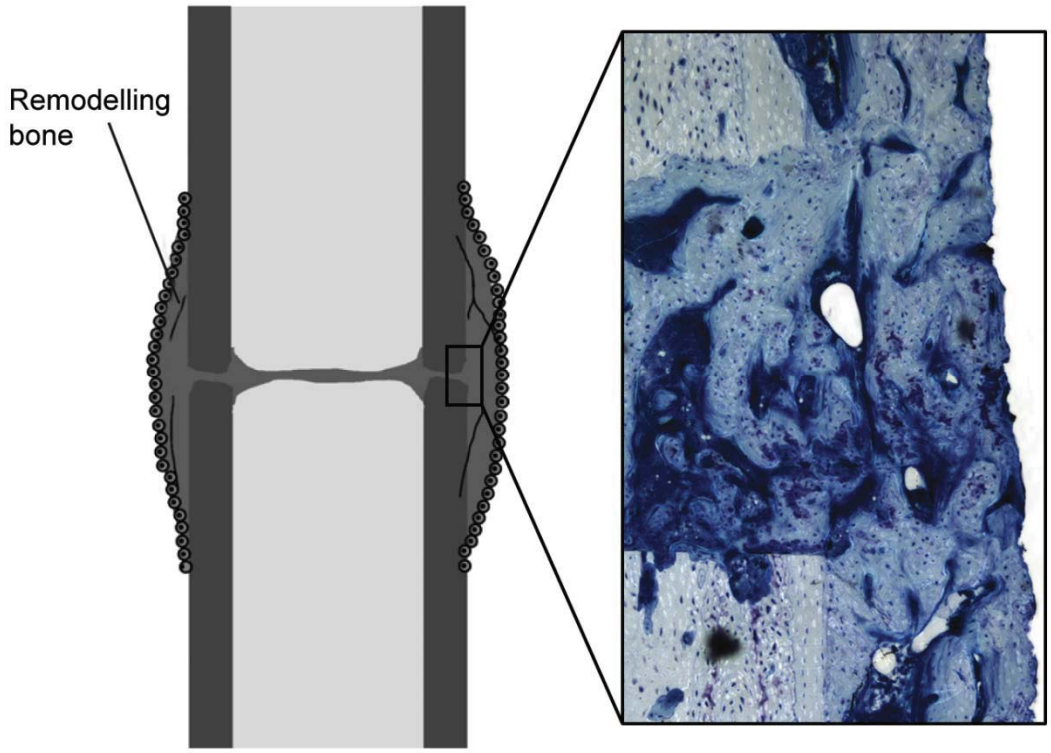

Figure 2.4: Bone remodelling process in which the original structure of the bone is restored (adapted with permission [34]).

2.2.4 Revascularisation

Revascularisation of the callus is critical as it facilitates nutrient and gas exchange to the local cells. In this context, angiogenesis is the outgrowth of new capillaries from existing vessels [35, 36], which is dependent on well-vascularised tissue being present on either side of the fracture gap, as well as sufficient mechanical stability to allow new capillaries to form and survive [29]. Blood supply to the fracture site and throughout the callus is derived primarily from the surrounding tissues, in contrast to the normal centrifugal blood flow from the medullary canal in intact bones [33].

Immediately following fracture, the total blood flow to the affected area of bone is reduced due to the rupture of blood vessels and physiological vasoconstriction in response to the trauma [33]. This hinders the transport of cells, oxygen and other nutrients to the site of repair [36]. The fracture ends are hence generally devascularised and as such cannot contribute to the repair process. The local oxygen tension is believed to influence the differentiation of local MSCs, with low oxygen content tending towards a chondrogenic lineage. Conversely, the periosteal tissue has extensive microvasculature, which drives initial intramembranous ossification.

As healing progresses, if fracture stability is maintained, intramedullary blood vessel bridging can occur. However, in the presence of excessive interfragmentary strain, vessels cannot form between the cortices and will instead form in the soft tissue, circumferential to the fracture gap thus driving the development of periosteal callus. As the callus tissue progressively stabilises the fracture, capillary and bony bridging will occur throughout the fracture gap.

Despite an increase in vascularity throughout the healing process, oxygen tension, measured across a healing callus, remains low until well into the remodelling phase. Brighton and Krebs [37], found that both cartilage and bone are formed in areas of low oxygen tension, despite an increase in vascularity at the fracture site. It has been suggested that this is due to an even greater increase in cellularity due to the healing response, and as such a relative state of hypoxia exists throughout the majority of the callus. Once the fracture has healed and the medullary canal is re-established, vascularity of the region is sufficient to restore normoxia to the bone tissue.

2.3 FACTORS INFLUENCING FRACTURE HEALING

Fracture healing is influenced by the mechanical environment within the healing tissue [10, 14, 38-40]. The mechanical environment varies based on the type of fracture

or fracture geometry, the type of fixation used to stabilise the fracture and the loading throughout the fracture gap.

2.3.1 Methods of Fixation

To enable healing to occur, fractures are stabilised using a variety of fixation techniques. The purpose of fixation is to provide mechanical stability to enable faster healing of the bone, whilst minimising complications and achieving a good functional outcome [23]. Fracture fixation devices can either be internal or external to the body and can provide either absolute stability through compression of the fracture site, or relative stability using splinting techniques. Devices that provide absolute stability include internal devices such as compression plates or lag screw fixators. Splinting techniques provide relative stability to the fracture. Internal devices include intramedullary nails and bridge plates whilst external devices may include casts and external fixators.

2.3.2 Compression

Interfragmentary compression fixation techniques to provide the fracture with absolute stability inducing primary fracture healing. This can be achieved with the use of lag screws and compression plates (Figure 2.5) [3, 23]. In fractures stabilised by compression plating, the fractured cortical ends are compressed in a rigid manner such that there is no motion between the fracture ends [3, 23, 28, 41-43]. This creates a low strain environment throughout the fracture, allowing primary bone healing with little or no external callus [23, 44]. In contrast to secondary bone healing, primary healing is a slow process [42]. Clinically, it is difficult to monitor the progression of healing with compression plates with only the use of radiographs, as such the re-operation rates has been reported at 10 % [45].

Figure 2.5: Radiograph of an ankle. A compression plate with cortex screws was used to fix the fibular fracture while the medial melleolar fracture has been fixed with two cancellous screws (reproduced with permission [28])

2.3.3 Splinting

Splinting fracture fixation techniques provide relative stability to the fracture and hence induce healing through a secondary fracture healing process. Splinting techniques used to stabilise fractures include external fixators, bridging plates and intramedullary nails.

External fixation methods align the fractured bone ends, using percutaneously placed pins secured to external scaffolding in the form of bars or rings, which provide support to the fracture site. These elements can be constructed to form unilateral, bilateral, circular or hybrid external fixation frames. The aim of the fracture fixation technique is to anatomically align the bone fragments and while achieving sufficient stability to enable healing. External fixators allow micromotion of the fracture, which encourages early formation of callus and enables early weight bearing for the patient [23, 46, 47]. The stiffness of the fixation is dependent on a number of factors including the number of bone screws, the diameter of the screws, and the distance between the

connecting rod of the fixator and the bone surface (Figure 2.6) [48]. Clinically, these devices are used in a number of different situations: as a definitive fracture treatment device, particularly when the fracture is accompanied by an open soft tissue wound; for temporary or emergency stabilisation; and for limb reconstruction, including limb lengthening, deformity corrections or treatment of non-unions [48, 49]. However because the fixation is external to the body, this can make it susceptible to pin infections [48].

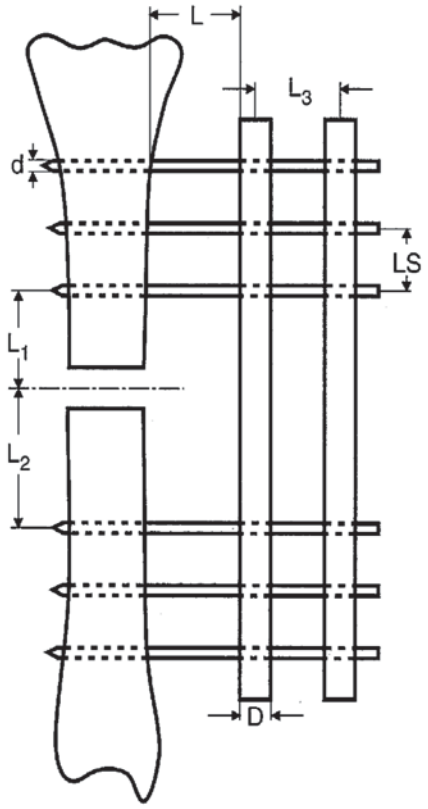

Figure 2.6: Example of a unilateral external fixator. A number of geometric parameters influence the stiffness of the external fixation. These parameters include the diameter of the screws (d), diameter of the connecting bar (D), free length between the bar and bone (L), shortest distances between inner screw and fracture (L1 and L2), distance between connecting bars (L3) and distance between screws (LS) (reproduced with permission [48]).

Internal splinting of fractures can be achieved through the use of bridge plating. This type of plating differs from the compression plating of fractures as there is no contact between the plate and bone, some movement is allowed between the fracture surfaces encouraging callus formation, as well as preservation of the periosteal blood supply [23].

Intramedullary nails are also a splinting technique, whereby a metal rod (or nail) is inserted into the medullary cavity of the bone. They are most commonly used in long bone fractures of the humerus, tibia and femur (Figure 2.7). Fractures fixed with intramedullary nails heal via secondary bone healing as these devices allow for movement between the fracture ends. This technique does cause some disruption to the endosteal blood supply of the bone through the reaming and nailing process [48]. Unreamed intramedullary nails can also be used, reducing the damage to the blood vessels; however bony union and infection rates are similar between reamed and unreamed nails [50]. The torsional stability of these implants can be improved by the inserting of locking screws in the proximal and/or distal ends of the nail, perpendicular to its long axis [23, 51]. The stability of the fixation is determined by its fit within the intramedullary canal, the material and mechanical properties of the nail, and the mechanical properties of the locking screws [23, 51, 52].

Figure 2.7: Intramedullary nail fixation used to stabilise a spiral distal tibial fracture a) before and b) after fixation. The insertion of interlocking screws in the proximal and distal ends of the fixator provides axial stability (reproduced with permission [28]).

2.3.4 Complications

Fracture union is defined clinically as the stage of fracture healing when there is no pain or motion at the fracture site in response to physiological stress, and/or the patient can exercise with full, pain-free weight bearing without additional support (for lower limb fractures) [53]. However despite the substantial capacity of the body to repair bones, not all fractures spontaneously heal. Fracture non-union or delayed union prolongs morbidity and delays the return to function of the fractured limb. The incidence of non-union is highly dependent on a combination of injury and host factors, with the overall occurrence rate being reported as 5-10 % of long bone fractures [4-6].

Non-unions occur when periosteal callus formation ceases prior to bony bridging, leaving union of the fracture fragments dependent upon the endosteal healing [53]. Several adverse mechanical and biological factors influence the occurrence of non-union. Examples of this include excess motion or conversely, inadequate stimulation, loss of blood supply, a large interfragmentary gap, or severe trauma to the periosteum and surrounding soft tissue [54, 55]. Non-unions can be classified into two broad categories, hypertrophic or atrophic non-unions [4]:

- Hypertrophic non-union (Figure 2.8) – occurs when the fracture site is hyper-vascular and retains biological potential. In this case there is good vascularity but unstable fixation, such that healing progresses to form a cartilaginous soft callus that cannot calcify to bridge the fracture [24].
- Atrophic non-union (Figure 2.8) – occurs when that the fracture site is hypo-vascular, inert and seemingly incapable of biological activity. In this situation the fracture gap may be elongated with the bone ends being resorbed and rounded [23, 53]. This scenario requires more than optimisation of the mechanical environment to attain a union. Potential treatments include the use of growth factors to restore the biological potential of the regeneration site.

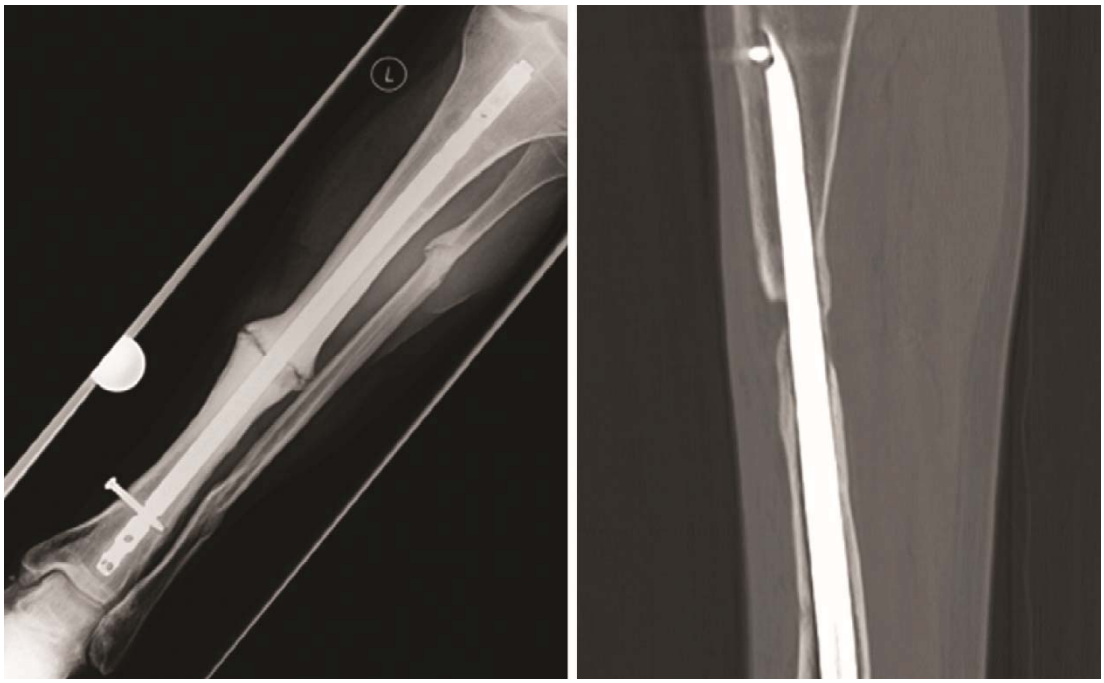

Figure 2.8 Radiological images of a femoral upper diaphysis hypertrophic non-union (left) and a tibial diaphysis atrophic non-union (right) (reproduced with permission [7]).

Without intervention, delayed or non-union fractures may progress to the development of a pseudarthrosis. In this situation, the bone is covered by fibrous tissue or fibrocartilage surrounded by a bursal sac containing synovial fluid, forming a false joint [56].

2.3.5 Fracture Motion

Interfragmentary movement (IFM) is the movement between the fracture fragments and occurs due to mechanical stimulation from physiological or external loading of the fractured limb. It has been demonstrated that IFM has a determining influence on the healing outcome [10, 14, 39, 40, 57-64]. The amplitude and direction of the movements are determined by the stiffness of the fixation device and the load applied to the fracture, by a combination of weight bearing, and muscle forces [65-67].

Many clinical and experimental studies have tried to characterise the influence of these movements. Thus far it has been clearly demonstrated that rigid fixation of a

fracture minimises IFM and results in limited callus formation [13, 32, 44, 49, 62]. Conversely, excessive motion in highly unstable fractures does not allow bone mineralisation or revascularisation within the fracture gap and will lead to a non-union [4, 34, 68-73]. As such, determining the optimal magnitude of IFM has been the target of numerous *in vivo* investigations [9-11, 39, 48, 57-62, 67, 74-91].

Goodship and Kenwright [14] investigated the effect of controlled micromovement with a 3 mm tibial osteotomy in a sheep model. A loading regime of 500 cycles per day was applied using a pneumatically driven cylinder attached to an external fixator. A force of 360 N at a frequency of 0.5 Hz was applied, creating an initial axial IFM of 1 mm and resulting in greater callus formation and superior callus stiffness than a rigid control group. The authors varied the parameters of the applied stimulus in a subsequent study [83], demonstrating that smaller axial IFMs (0.5 mm) and application with a lower force (200 N) led to further improvements in the mineralisation of the fracture callus and thus the increase in fracture stiffness.

The effect of strain rate was investigated by Goodship *et al*. [13] where they showed that short term cyclic IFM applied at a moderate strain rate (40 $mm \cdot s^{-1}$ and 400 $mm \cdot s^{-1}$) induced a greater periosteal callus response than the same stimulus applied at a low (2 $mm \cdot s^{-1}$) strain rate. This study also identified that if the stimulus was delayed until after the initiation of ossification and bony bridging [67], the positive benefits of cyclic loading are eliminated. Stimulating the fracture 1 week post-operatively showed significantly greater healing compared to 6 weeks post-operatively, suggesting that the delayed healing could be attributed to a lack of stimulation during the proliferative phase of the healing process.

The number of loading cycles applied during healing is also an important variable to control however this can be difficult to assess experimentally without the

isolation of functional loading. Hente *et al*. [82] investigated the influence of 0, 10 and 1000 cycles, however the number of cycles resulting from functional loading throughout the experiment was not controlled. It was observed that for a higher number of loading cycles, there was a greater periosteal callus response. This however provided no information as to the quality of the healing outcome, with no analyses on upper and lower loading cycles performed. Notably, it can be clearly observed that unilateral fixation alters the strain gradient within the interfragmentary space, resulting in greater callus formation in the cortex furthest from the fixator, where the compressive strains are of the greatest magnitude (Figure 2.9).

Many *in vivo* experiments have been conducted that isolate the direction of loading (Figure 2.10), such as axial, torsional and shear, to determine their impact on fracture healing [75, 83, 86, 91-95]. Claes *et al.* [60] showed that compressive axial IFM between 0.2 and 1.0 mm in a 3 mm osteotomy was beneficial to fracture healing, whereas IFM greater than 2 mm led to poor healing outcomes. However, clinical and experimental studies confirmed that considerable interfragmentary shear can occur due to asymmetries in both the fractures and fixation device [65, 94-96].

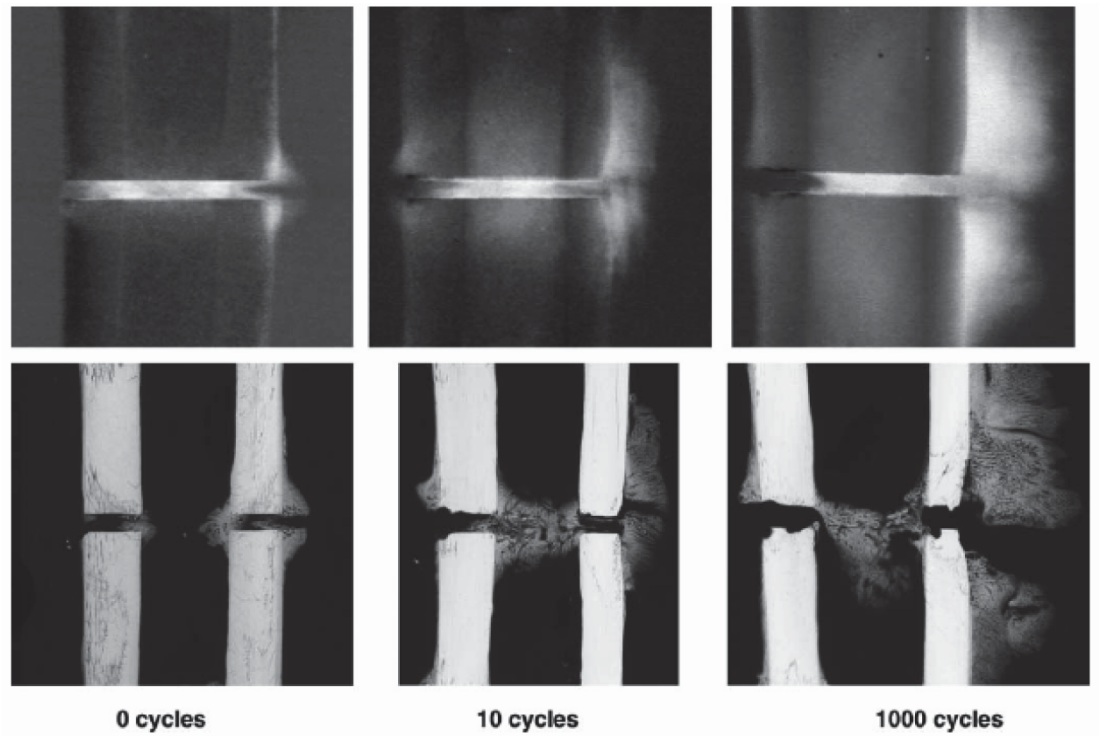

Figure 2.9 Radiographs of experimental tibiae, with greater periosteal callus formation on the far side of the external fixation, where a greater compressive displacement was induced. A greater periosteal response was observed when a greater number of cycles were applied to the fracture (reproduced with permission [82]).

In contrast to axial compressive loading, tensile, torsional and shear movements of similar magnitude were shown to hinder the healing process [38, 91, 97, 98]. In a study conducted by Augat *et al*. [92], shear movement resulted in healing with decreased periosteal callus formation, delayed fracture healing and inferior mechanical stability when compared to the axial movement (Figure 2.10). The combination of high axial strains (47 %) and shearing motion, as demonstrated by Schell *et al.* [99], also appeared to inhibit healing and lead to a non-union.

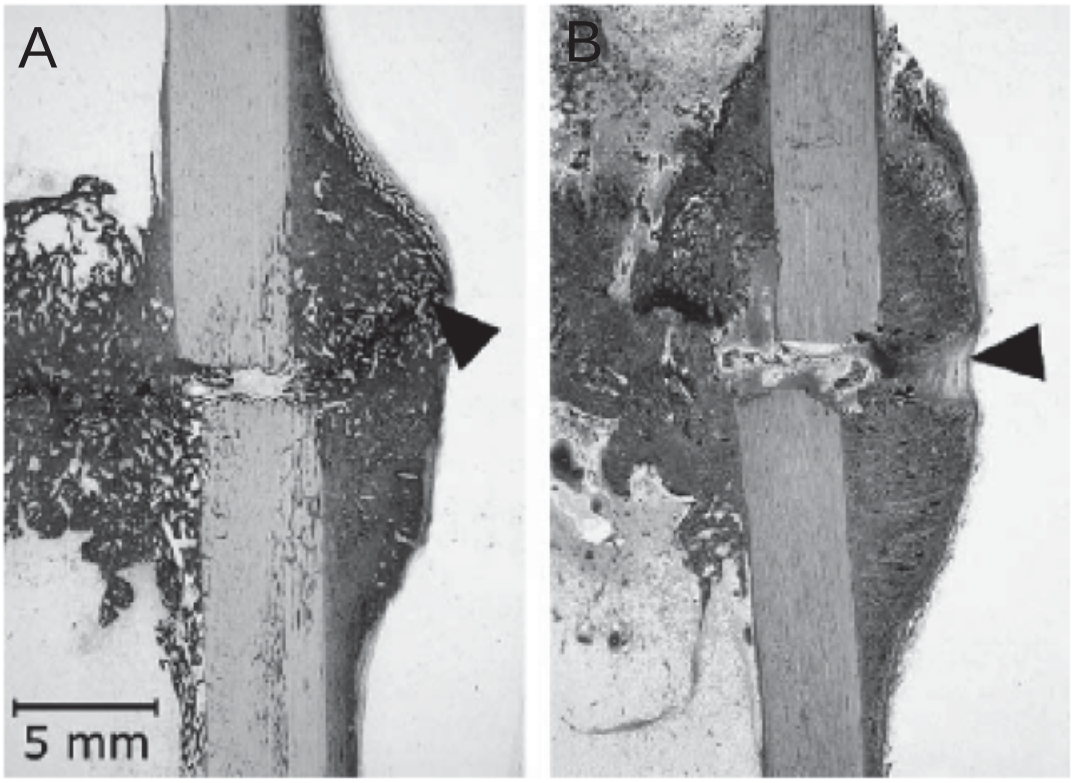

Figure 2.10 Histologic appearance of bone healing where the predominant loading was A) axial compression and B) interfragmentary shear (reproduced with permission [92]).

As interfragmentary gap size changes the mechanical environment within a fracture, it has been shown to influence the healing outcome. Experimental studies conducted by Claes *et al*. [59] and Augat *et al.* [100] investigated fracture gap sizes of 1, 2 and 6 mm, with initial axial strains implemented as 7 or 31 %. It was found that increasing the size of the gap resulted in poorer mechanical and histological outcomes, with significantly reduced strength and bending stiffness for these groups.

2.3.6 Assessing the rate of Bone Healing

Throughout the bone healing process, IFM will decrease due to an increase in stiffness of the healing tissues. During normal bone healing, IFMs are largest during the initial stage of healing, when the callus is filled with haematoma and soft fibrous tissue (Figure 2.11). In this stage, the fracture callus exhibits low strength, low stiffness and large elongation, whereby as healing progresses this is replaced by a harder, stiffer

material phase, consequently eliminating all IFM [101]. The upper and lower portions of the curve (Figure 2.11) represent the remodelling and reparative phases of healing, while the sudden increase in stiffness in the intermediary phase can be attributed to bony bridging of the fracture gap [102-104]. The rate at which the reparative tissue advances towards the fracture gap is likely to determine the rate of healing, an avenue of research that has been thoroughly investigated with few clear conclusions. This sigmoidal relationship has been described in small animal studies when comparing callus stiffness over time [101, 105]. Similarly in ovine fractures, an exponential increase in stiffness was observed between weeks 2-8 prior to the remodelling phase, depending on the model used [61].

It has been shown that IFM in the early stages of healing can positively influence the rate of healing [84]. In a clinical study of tibial fractures, all patients were treated with a rigid fixation, where one group had early axial movements applied in the first 1-3 weeks following fracture and the other group was not loaded [84]. Earlier bending stiffness levels equivalent to clinical union were achieved more rapidly in patients with early axial movement (17.9 weeks), compared to the unloaded patients (23.2 weeks). However, later experimental studies demonstrated that early instability prolongs and/or inhibits bone healing [65, 106], thus this phenomenon will be further investigated.

When strain is applied to the fracture late in the healing process, it can inhibit callus development [13], and mineralisation [67]. Epari *et al*. found that calluses which healed under rigid fixation were found to have higher torsional stiffness after 6 weeks than the less rigid fixation. The study concluded that instability within a fracture prolongs the chondral phase of healing, during which cartilage is mineralising to bone.

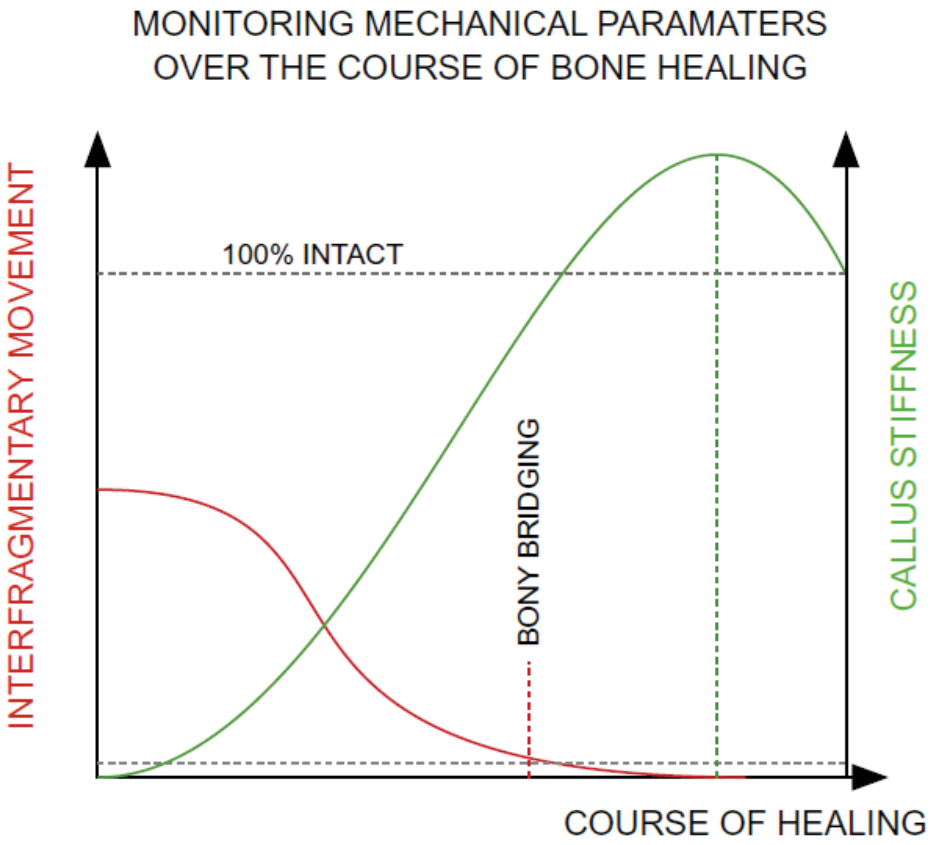

Figure 2.11: Throughout the normal bone healing process, interfragmentary movement (red) is at its greatest during the early stages of healing and decreases as the tissues within the fracture mature. It ceases as the fracture callus bridges (dashed vertical red line). Conversely, callus stiffness (green) increases as healing progresses with maximum stiffness (dashed green vertical line) often occurring following bony bridging as the entire callus mineralises (reproduced with permission [12]).

2.3.7 Modifying the Mechanical Environment

These studies clearly show that IFM has a significant influence on bone healing, however exactly how different types of movement influence the biological process of bone repair is not well understood. Some authors believe that the optimal IFM might be different at various stages of healing [12, 40, 107]. This concept led to experimental and clinical studies where the mechanical stimulus was altered at different stages of the healing process by means of changing fixator stiffness; this process was termed dynamization.

Dynamization is the process where the stiffness of a fixator is reduced during bone healing to increase the IFM through physiological weight bearing and muscle contraction [40, 107-109]. There are two different methods of dynamization: axial and elastic dynamization. Axial dynamization uses a telescoping mechanism within the fixation device that allows free axial movement and closure of the fracture gap, as well as inducing an increase in IFM [107, 110, 111]. This process has been studied both experimentally and clinically. Elastic dynamization involves the destabilisation of the fixator frame from a stable to a more flexible fixation, which causes an increase in IFM while holding the fracture gap constant [107, 108]. Although both axial and elastic dynamization have been used experimentally and clinically in the treatment of fractures, it remains unclear at which time point during the healing process dynamization should be applied.

An experimental study in dogs examined the effect of axial dynamization using a telescoping mechanism versus elastic dynamization through the destabilisation of the fixator [112]. These processes were applied two weeks postoperatively. After two months of healing it was found that there was no significant difference in biomechanical properties between the two groups. However, this study was limited through a lack of comparable control groups by not including a constant fixation stiffness group. It also provided no insights into the timing of application of the dynamization process.

A study in rats conducted by Claes *et al*. [107, 108] investigated the effect of early and late elastic dynamization on bone healing. This model used an external fixation system that controlled the biomechanical environment and maintained the fracture gap (Figure 2.12). Elastic dynamization was achieved through destabilisation, where the inner fixator bar was removed, thereby decreasing the stiffness of the

fixation. Assuming the load bearing capacity of the operated leg did not change, this led to an increase in the IFM.

The results of this study showed that early dynamization, 1 week postoperatively, led to significantly lower flexural rigidity compared with constant rigid fixation. It also showed that there was no significant difference in flexural rigidity of the callus, callus volume, or bone mineral density between early dynamization and constant flexible fixation groups. These results indicate that rigid fixation for 1 week followed by flexible fixation for 4 weeks does not induce improved healing compared to flexible fixation for 5 weeks. This study cannot therefore confirm a positive effect of increasing IFM early during the fracture healing process, indicating that the improved fracture healing found through early dynamization in the aforementioned studies was through the effects of closing the fracture gap.

These results are similar to a study conducted by Utvag *et al*. [89], where it was demonstrated that dynamization of intramedullary nails after 20-30 days of healing in a rat femoral fracture model resulted in increased callus formation [89], but decreased bone mineral content compared to rigid nails. The results from the late dynamization groups at 3 and 4 week postoperatively showed that they had similar flexural rigidity and bone mineral density to the rigid group, and that was significantly higher than the early dynamization and flexible groups. The results showed that the 4 week dynamization group had a significantly greater elastic modulus and significantly smaller callus bone volume compared with the rigid group. These parameters suggest that there were increased bone properties at the level of the osteotomy and advanced remodelling occurred in the 4 week group, indicating more advanced healing. These data suggest that once bony bridging has started, dynamization may accelerate the bone remodelling processes.

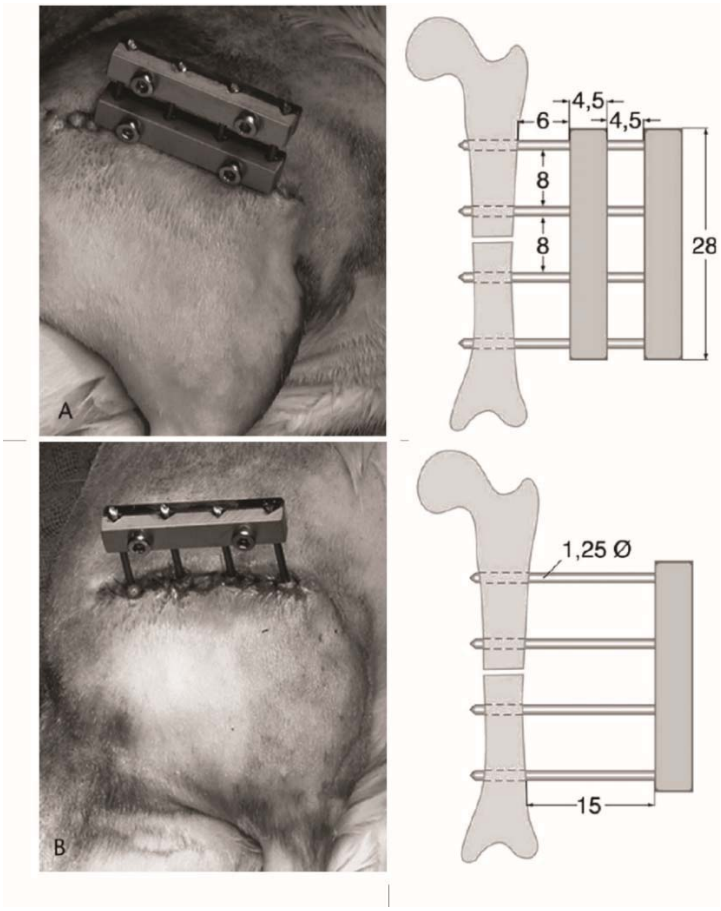

Figure 2.12: Illustration of the fixator construct used in the dynamization study [107, 108]. For the more rigid configuration, two bars were used on the fixator, with the offset between the inner bar and the lateral surface of the bone set at 6 mm. For the flexible configuration, one fixator bar was used with a 15mm offset from the surface of the femur (reproduced with permission [107, 108]).

A clinical study assessing the healing rates of patients using the Dynamic Axial Fixator (Orthofix) was conducted to assess the timing of dynamization [113]. The healing process was compared between 22 pairs of patients, one with dynamization occurring in the first 4 weeks postoperatively, and one patient with dynamization occurring after 4 weeks. The timing of the dynamization process was determined at the surgeons' discretion, defined by when the fracture site was deemed to have evidence of radiological bridging, and when the patient was able to walk independently without pain. Patients were paired based on four factors: age, site of tibial fracture, stability of the fibula and Gustilo wound grading. These factors were selected as they

were thought to be the most likely to affect the rate of healing. This study showed that healing rates can be significantly improved through early dynamization - within four weeks postoperatively. Furthermore, this study also found that early dynamization was more advantageous over late dynamization [113]. However, it should be noted that this study did not include a group with a constant stiffness fixation throughout the healing period, and therefore it cannot be conclusively confirmed that dynamization in fact caused improved healing.

In a similar clinical investigation of axial dynamization using the Orthofix external fixator, patients were divided into three treatment groups [114]. Group 1 consisted of patients with a standard Orthofix external fixator. Axial dynamization was carried out four weeks postoperatively. Group 2 had a modified fixator which contained a silicone cushion. This allowed the fixator to shorten by 2 mm under a deforming force of 200 N and return to its original length when the force was released. Axial dynamization was performed at four weeks postoperatively for this group. Group 3 patients had a cushioned fixator like that in group 2, but it was left in the unstable configuration for the entire healing period. The results of this study showed that in scenarios where axial dynamization was performed leading to a closure of the fracture gap, an improved healing outcome compared to limiting the IFM to 2 mm [114]. This indicates that rather than an increase in IFM, the positive outcomes of performing axial dynamization are caused by the closure of the fracture gap.

Both of these clinical studies suggest that early dynamization stimulates the fracture healing process, however isolation or non-inclusion of the telescoping mechanism is required to provide clarity on the effects of decreasing fixation stability. While these studies both used the same fixator, the results are difficult to compare as the test conditions vary greatly between each study.

In summary, results from experimental and clinical dynamization studies are somewhat contradictory. From a clinical point of view, early dynamization studies were beneficial only when closure of the fracture gap was permitted, rather than from an increase in IFM alone. This might indicate that elastic dynamization should not be performed prior to callus bridging, although potential benefits may be achieved late in the healing process through enhancement of the remodelling phase. The concept of dynamization itself is in contrast to the outcomes of studies describing the rate of healing where initial mechanical stimulation is found to accelerate the healing response [13, 83, 84].

2.4 MECHANOBIOLOGY DURING BONE HEALING

Mechanobiology describes the mechanisms by which mechanical loads and physical conditions regulate biological processes [38, 48, 66, 115, 116]. The local mechanical environment at the fracture site can be determined through these factors, and it provides the mechanobiological signal for the regulation of the fracture repair process and the stimulation of cellular reactions [66].

2.4.1 Mechanical Stimuli on Cells

The concept of mechanobiology whereby biological processes (cellular level) are regulated by mechanical loads, was originally described by Roux in the late 1800s (as discussed by Pauwels, 1980; Claes and Ito, 2005). His theory of functional adaptation proposed that mechanical irritations in the fracture environment stimulated the formation of three different types of supporting or connective tissues [117]. Based on this theory, compression was the specific stimulus for the formation of bony tissue, tension stimulated connective tissue and relative displacement (tissues moving relative to each other) together with compression or tension was the stimulus for cartilage tissue [117].

Pauwels, drawing on these ideas from Roux, developed a theory for tissue differentiation in response to the local mechanical stresses [117]. He suggested that further examination of stress and strain invariants (scalar quantities that are independent of a coordinate system) could supply important information. These scalars can be calculated from the full stress and strain tensors. Two stress invariants are octahedral shear (or distortional) stress, S, and hydrostatic (or dilatational) stress, D. These are defined as:

$$S = \frac{1}{3}\sqrt{(\sigma_1 - \sigma_2)^2 + (\sigma_2 - \sigma_3)^2 + (\sigma_3 - \sigma_1)^2} \quad (2\text{-}1)$$

$$D = \frac{1}{3}(\sigma_1 + \sigma_2 + \sigma_3) \quad (2\text{-}2)$$

where σ_1, σ_2 and σ_3 are the principal stresses. The corresponding strains are octahedral shear (or distortional) strain, and volumetric strain. In a compressible, elastic, isotropic material, hydrostatic stresses cause a change in material volume, or volumetric strain, but no distortion. Conversely, octahedral shear stress causes material deformation, or distortional strain, but no change in volume (Figure 2.13).

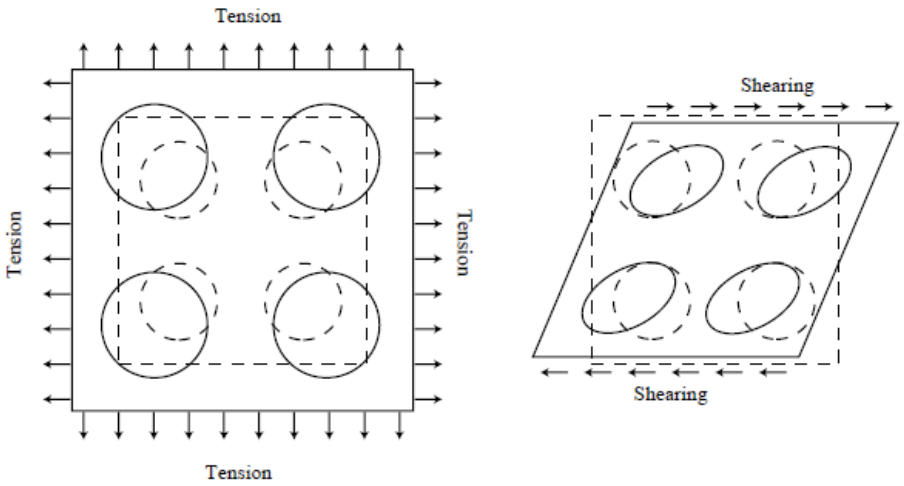

Figure 2.13: Deformation of elementary particles of a cube of isotropic elastic material under A) biaxial tensile forces, increasing in volume but retaining the same shape and B) under shearing forces, where the volume remains constant but the spherical shape is deformed to an ellipsoid (adapted with permission [117]).

Pauwels [117] proposed that hydrostatic compression, causing a volumetric change, would result in cartilage formation, and that distortional stress or elongation would result in fibroblastic differentiation (fibrous tissue). His theory is presented in Figure 2.14 where deformation of shape (shear) is indicated on the horizontal axis and hydrostatic compression on the vertical axis. It can be seen that a combination of these stimuli will influence tissues formed within the fracture, leading to hyaline cartilage, fibrocartilage or fibrous tissue. Depending on the stimuli, intramembranous or endochondral bone formation will ensue, and finally through remodelling, a lamellar bone structure may be formed.

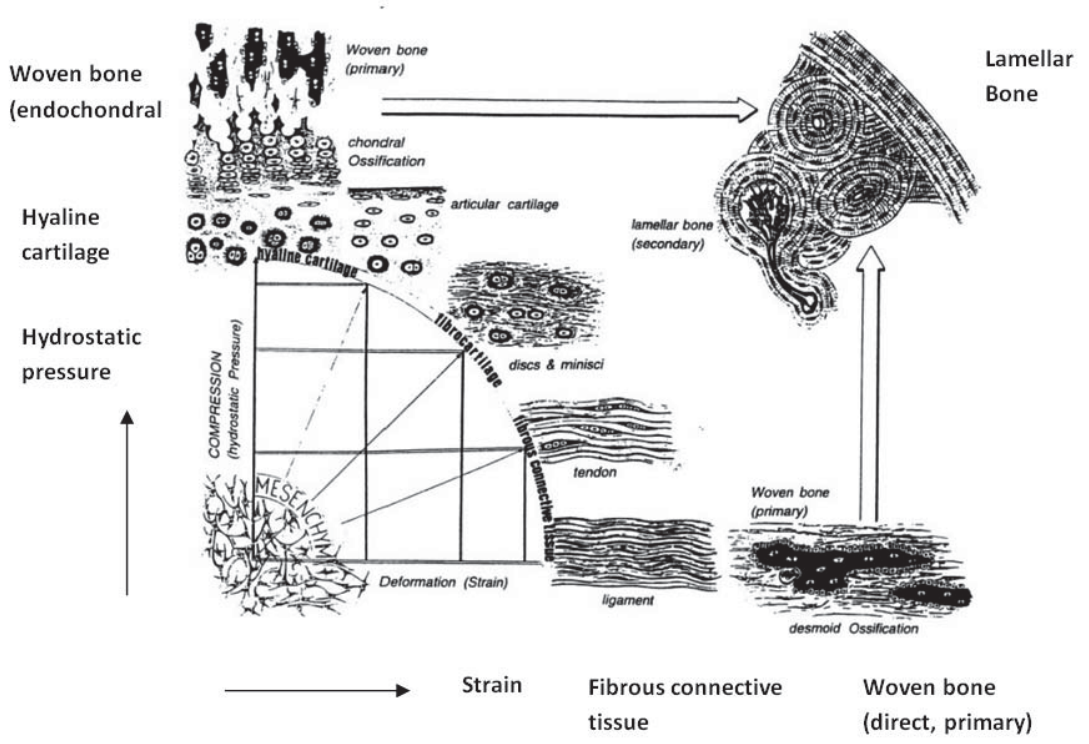

Figure 2.14: A schematic representation of Pauwel's hypothesis regarding the influence of mechanical stimuli on tissue phenotype development (reproduced with permission [117]).

2.4.2 Interfragmentary Strain Theory

Based on qualitative observations from clinical fracture healing, Perren and Cordey [63] proposed a much simpler theory, the "Interfragmentary Strain Theory"

[63, 64], whereby tissue differentiation was controlled by the tolerance of various tissues to strain. The basis of this theory is that a tissue cannot be produced under strain conditions which exceed the elongation at rupture of the given tissue element. Only the tissues that can withstand this interfragmentary strain without rupturing can exist in the fracture gap. The interfragmentary strain (IFS) is defined as the magnitude of interfragmentary motion (axial) divided by the fracture gap size.

$$Interfragmentary\ strain = \frac{Interfragmentary\ movement}{Fracture\ gap\ size} \qquad (2\text{-}3)$$

Lamellar bone would theoretically rupture under a strain of 2 %, cartilage at 10 %, and granulation tissue up to 100 % (Figure 2.15). Based on this theory, bone healing occurs by a progressive tissue differentiation from initial granulation tissue to fibrous tissue, cartilaginous tissue, and finally bony tissue. The formation of each tissue will stiffen the fracture gap, reducing the IFM and allowing progression to the next tissue type.

This theory however only considers axial strains in the interfragmentary regions without consideration of radial or circumferential strains, and therefore cannot predict tissue changes in other regions of the fracture callus. Moreover, the theory was conceptualised from cases of primary bone healing and therefore does not account for a different or changing mechanical environment due to external callus formation. This theory would suggest that for a given IFM, an increasing gap size would produce a better healing result which is in direct contrast to later experimental results [59, 100].

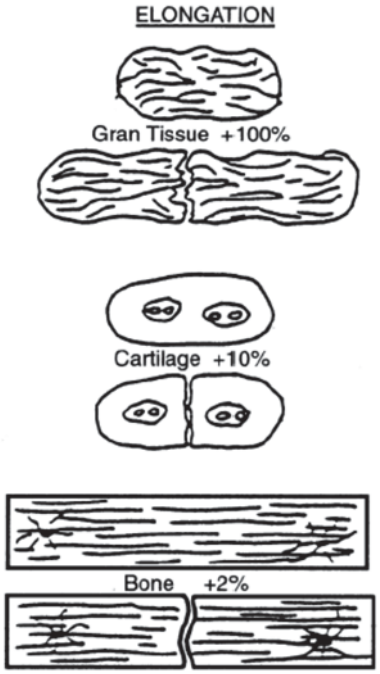

Figure 2.15: Interfragmentary strain theory: A tissue cannot exist in an environment where the interfragmentary strain exceed the strain tolerance of the extracellular matrix of the tissue (reproduced with permission [63, 64]).

Further investigations into the development of mechanobiological theories have since been conducted, with refinements made in terms of mechanical stimuli [118] and biological factors [119]; however these are based primarily on the initial theories. For this field of study to continue to advance, it requires both experimental and computational studies [34, 120, 121].

2.5 COMPUTATIONAL SIMULATION OF BONE HEALING

In mechanobiology, computational models have been developed and used together with *in vivo* and *in vitro* experiments to quantitatively determine the rules that govern the effects of mechanical loading on bone cell differentiation and tissue growth, adaptation and maintenance [34, 120, 121]. Numerical models of the fracture callus have been developed to predict the pattern of mechanical stimuli in the healing tissue [2], since it has not been possible to measure them. Constant finite FE models [11, 122] have been used to predict stress, strain and pressure distributions at particular

healing stages based on experimental evidence whereas dynamic models [73, 118, 120, 123-132] simulate healing processes using time-dependent iterative loops. In most of these simulations, tissue development depends on local mechanical signals such as strain invariants, hydrostatic pressure or the strain energy density. Some models include biological factors like local concentrations of growth factors [119, 133], or concentrations of different cell types. The merits of each of these methods are discussed below.

2.5.1 Tissues Modelled as a Single Solid Phase

Building on the work conducted by Pauwels, Carter *et al.* [38] developed a new tissue differentiation theory which correlated new tissue formation with the local stress histories [38]. In the early callus material they proposed that compressive hydrostatic stress history dictates the formation of cartilage, whereas tensile strain history guides synthesis of fibrous connective tissue. Bone can only be formed in regions without significant levels of either of these stimuli (Figure 2.16). Unlike Pauwels, they also recognised the influence of vascular perfusion and proposed that low oxygen tension diverts cells down a chondrogenic lineage. Using FE models, Carter showed that normal differentiation patterns in fracture healing at various stages were consistent with patterns of pressure and strain in the fracture callus. This tissue differentiation theory is again limited however, as it only qualitatively describes the relationship between the ossification pattern and the loading history.

The relationships employed by Carter *et al*. [38] have been further developed to investigate healing in oblique fractures [76], pseudoarthrosis formation [56], asymmetric fractures [134] and distraction osteogenesis [135].However, all of these studies are limited by not predicting tissue differentiation adaptively over time.

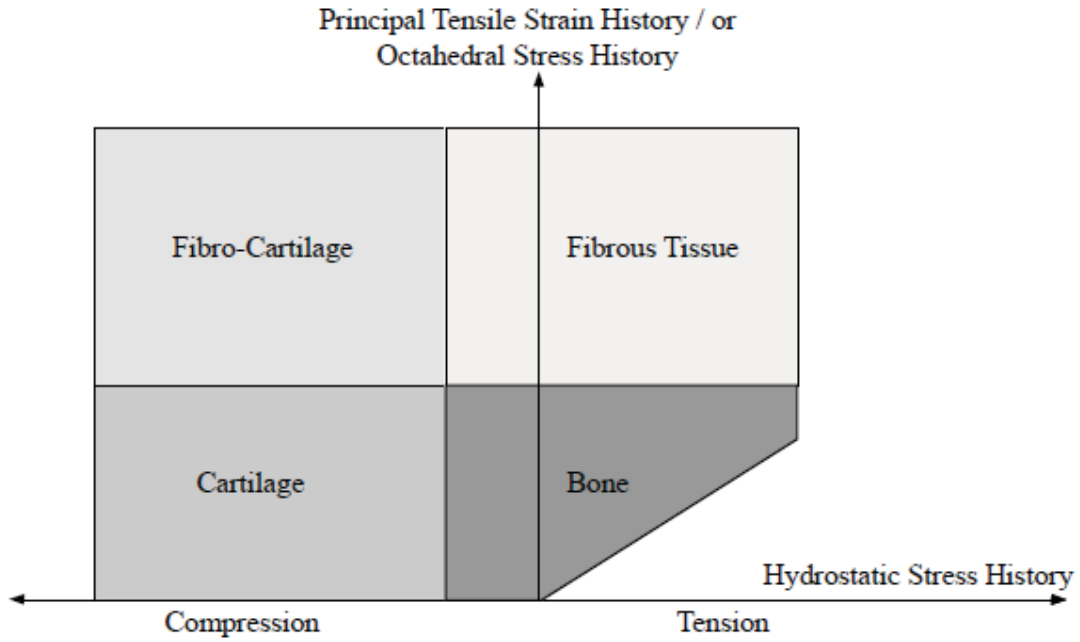

Figure 2.16: The relationship between mechanical loading history and tissue formation in a fracture callus as presented by Carter *et al*. (reproduced with permission [38]).

Claes and Heigele [11] proposed the hypothesis that new bone formation in fracture healing occurs primarily along fronts of existing calcified tissue and that the type of bone healing (intramembranous or endochondral) is dependent on the local stain and stress magnitudes (Figure 2.17). The formulation of this theory involved a study that compared the local strains and stresses in the callus as calculated from FE models developed from histological findings from an animal fracture model. From this study, Claes and Heigele established intramembranous bone formation over the range of strain less than ±5 % and hydrostatic pressure less than ± 0.15 MPa (Figure 2.17). Conversely, endochondral ossification was stimulated with hydrostatic pressures less than - 0.15 MPa (compression) at strain levels of less than 15 %. All other loading conditions corresponded to the formation of fibrous cartilage or connective. These results were similar to that of Carter, however they defined the requirements in quantitative terms.

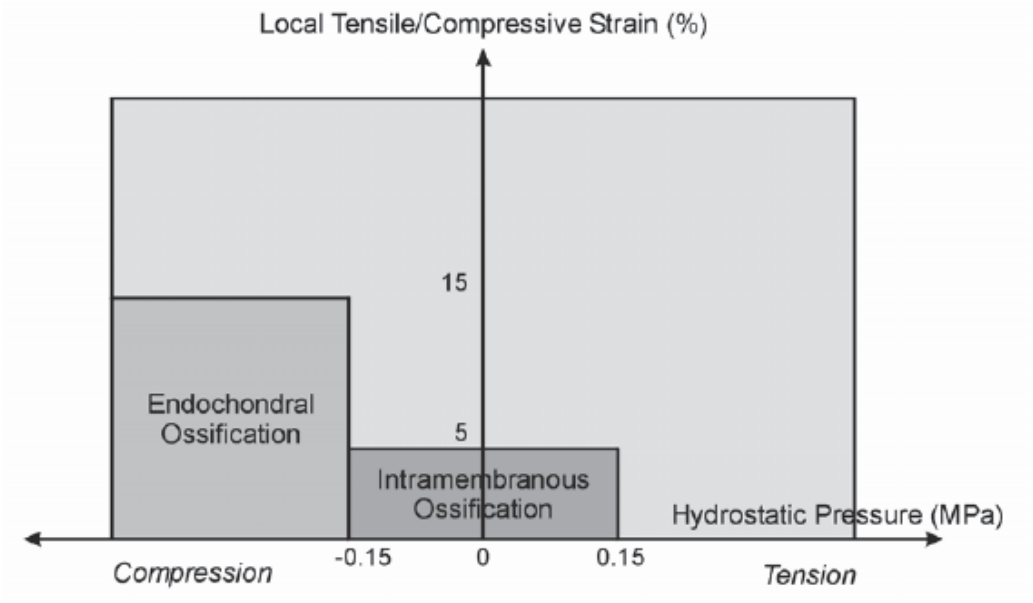

Figure 2.17: Tissue formation driven by different mechanical conditions within a healing fracture as in a fracture callus based on the local mechanical conditions as hypothesised by Claes and Heigele (reproduced with permission [11]).

Ament and Hofer [120] presented a healing simulation which implemented a fuzzy logic controller. This simulation used Strain Energy Density (SED) and the concentration of bone in neighbouring elements to control tissue differentiation within a fixed rectangular domain. Results from this study showed strong similarities to the work of Claes *et al*. [11], where the reduction of IFM induced formation of a typical *in vivo* callus i.e. periosteal expansion and endosteal bridging. This model is more advanced than previous studies as it simulates a dynamic change in the tissue properties which correspond to a change in mechanical stimuli. However the model was only verified against one interfragmentary strain case (IFS = 36 %), and as such it is not possible to determine the behaviour of the model under different initial interfragmentary stains, or different fracture geometries. It is also limited by representing tissues as linear elastic materials with numerous rules required to predict tissue differentiation, which may have the potential to over govern the fracture healing process.

2.5.2 Biphasic and Adaptive Finite Element Models

Soft tissues primarily comprise collagen and water and as such can be considered as a two-phase or biphasic material. The interaction between the solid and fluid phases, where fluid flows through a solid matrix, gives rise to inherent viscoelasticity, a property which describes a delay or lag between initial stress or strain input and material response [136]. Viscoelasticity provides the tissue with a strain-rate dependent response that allows for dramatic changes in elastic modulus with varied loading regimens, and manifests properties such as creep or stress relaxation.

Prendergast *et al*. [137] developed a model of tissue development at the surface of implants, using a biphasic poroelastic FE model (Figure 2.18). They proposed two biophysical stimuli: shear strain (deviatoric) in the solid phase, and fluid velocity in the interstitial fluid phase. Under high magnitudes of either of these stimuli, fibrous tissue would form and when both stimuli were low enough, bone formation could occur.

Lacroix *et al*. [118, 127] then applied this algorithm in a 2D axisymmetric FE model, to investigate tissue maturation during fracture healing (Figure 2.19). This dynamic model could simulate a number of parameters in bone healing including intramembranous bone formation away from the fracture site, endochondral ossification occurring centrally, within the callus, the gradual stabilisation of the bone fragments as healing progressed, and callus resorption [127]. Lacroix *et al*. modelled cell concentrations, using a diffusive mechanism to simulate migration, proliferation and differentiation of cells. However, this was a limited representation as the maturation of the tissue was highly dependent on the cell density. This model was since further develop for osteochondral healing by Kelly *et al.* [138].

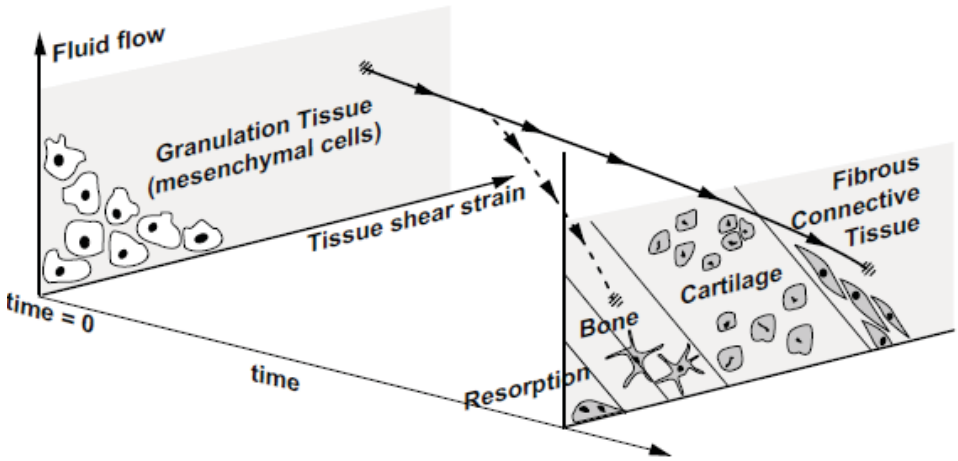

Figure 2.18: Mechano-regulation theory for tissue development at the surface of implants based on strain and fluid flow (reproduced with permission from [137]).

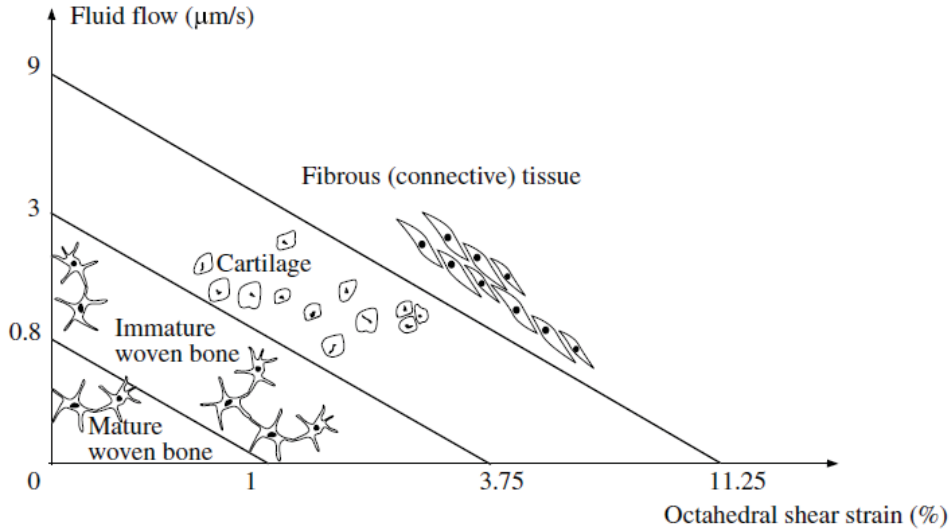

Figure 2.19: Fracture healing theory based on strain and fluid flow (reproduced with permission [127]).

2.5.3 Models of Callus Growth

Throughout the development of the fracture callus, cell density, tissue distribution, and callus stiffness change over time, as does the shape and size of the callus. However, the studies described previously, neglected tissue volumetric growth. Garcia-Aznar *et al*. [121], following the theoretical basis proposed by Prendergast *et al*. [137], modelled the fracture callus as an expanding formation from an initial

cylindrical geometry. The investigation used the second invariant of the deviatoric strain tensor as the stimulus for tissue differentiation, with volumetric growth modelled based on thermal expansion; aiming to characterise changing callus size, shape and tissue distributions for different load conditions.

This technique was able to capture increased periosteal callus growth with increased IFM (Figure 2.20), however, the predicted callus geometries were not physiologically accurate at the boundaries. The model failed to account for initial immature callus tissue that surrounds the fracture fragments, which act as a medium within which differentiation occurs [139]. This study also predicted a negative correlation between initially applied interfragmentary strain and the rate of healing.

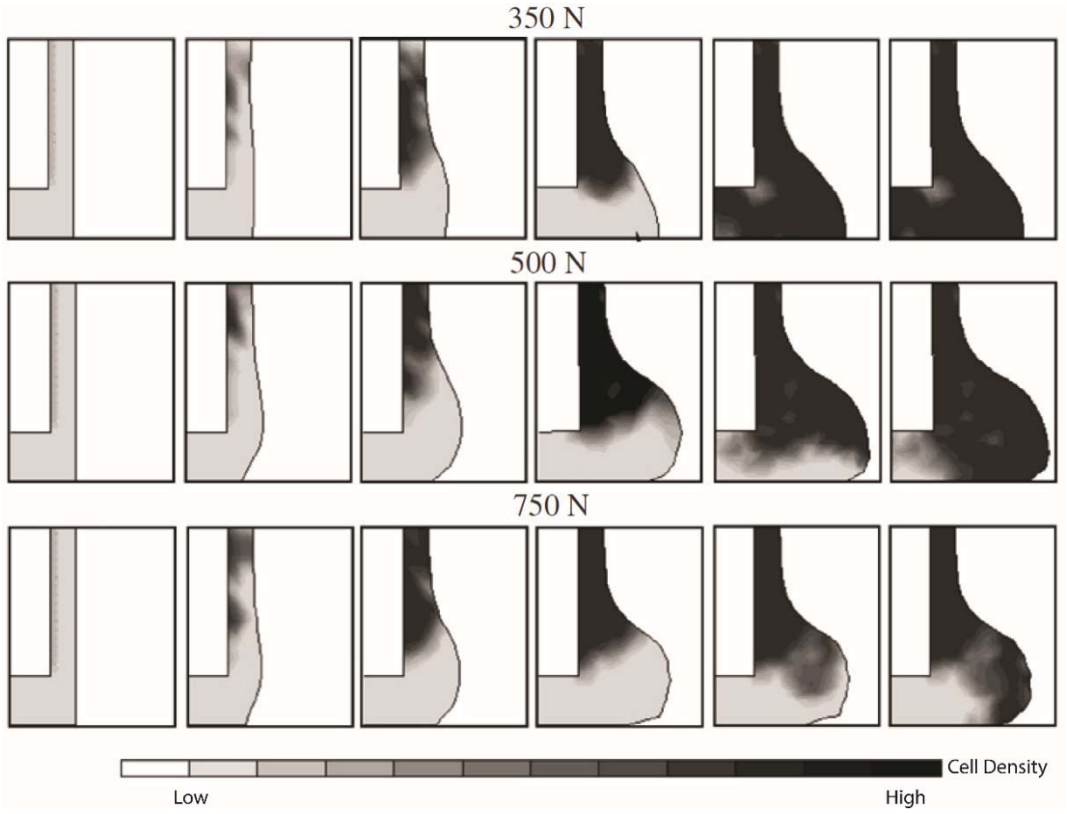

Figure 2.20. Bone healing simulation produced by the volumetric growth model of Garcia-Aznar *et al*. (2007). Increased load lead initially to larger calls growth however when increased to 750 N healing was delayed. (Figure adapted with permission from [121]).

Chapter 3: Hypothesis Conceptualisation and Development

3.1 INTRODUCTION

The rate and success of the healing of a bone fracture is determined largely by the mechanical environment. Identifying the mechanical stimuli that regulate the development of specific skeletal tissue phenotypes during healing can be applied to improve treatment of skeletal injuries. Many studies have identified interfragmentary movement (IFM) as the most important mechanically-determined parameter of fracture healing [14, 60]. These IFMs, or relative movements of the fracture fragments, are governed by a complex relationship between fixation stiffness, fracture gap size and configuration, and limb loading (weight bearing and muscle forces) [40, 90, 140]. IFMs are typically largest post-operatively, when the callus predominantly comprises haematoma and soft fibrous tissue, and decline over the course of healing as the tissues mature and mineralize into new bone. The size of the callus formed during healing is related to the magnitude of IFM [30, 59, 60], with the amplitude and direction of IFMs influenced by the stiffness of the fixation device [65, 66]. Extremely rigid fixation suppresses callus formation [14], conversely instability created by overly flexible fixation leads to formation of large callus that can fail to bridge, also known as a hypertrophic non-union [141]. Moderate IFMs are known to reliably produce a good healing outcome [14, 30, 60, 79, 140].

The influence of mechanics on the healing outcome is well established, however it is not clear which stages of repair are most sensitive to mechanical stimulus. The multiple stages of the healing process may all respond differently to biophysical stimuli, with strain, pressure and fluid flow [9, 11, 118] all likely to induce cellular responses that may also vary over time.

Although fractures may heal under a broad spectrum of mechanical conditions, the modification of fixator stiffness has the potential to enhance tissue regeneration by combining desired mechanical stimulation during periods of healing, and shielding tissues from potentially disruptive IFMs when stimulation is not required [12].

The first stage of healing is inflammation, which involves the formation of a haematoma. A haematoma callus is largely rubber-like; it exhibits low strength, low stiffness, and may be subject to large elongation without inducing material failure [11, 142, 143]. However, despite such material properties, it has been shown that when the haematoma is undisturbed during initial healing, it may lead to a positive healing outcome compared with unstable conditions [144].

The repair phase of healing can be further broken into a proliferative phase and a callus consolidation phase, both of which may be sensitive to different mechanical conditions. It is in the proliferative phase that the fracture callus develops calcified regions along the cortex of the bone whilst cartilage formation begins in the fracture gap, with the IFM magnitude determining the size of the callus. Flexible conditions with larger IFMs will produce a larger callus than fixation under stable conditions with small IFMSs [10, 38]. The formation of a larger mineralized callus through intramembranous ossification, acts to increase the load-sharing area and thereby reduce tissue strains in the fracture gap.

At this stage of healing, the proliferative soft callus within the intracortical region has a high strain tolerance. However, as healing progresses and the fracture gap narrows during the consolidation phase, the same relative movement of the fracture fragments can produce larger tissue strains, exceeding the strain tolerance of the callus inhibiting ossification of this region. Studies have demonstrated that that healing periods may be lengthened unnecessarily by the influence of tissue stresses that cause callus failure demonstrated by experimental models when excess displacements are imposed on healing fractures at this stage [67]. Thus, it may be

inferred that mineralization and bridging of the callus may be impaired by excessive tissue strains manifesting through large IFM, and for bony bridging to occur the fracture requires stability. Likewise, Kenwright and Gardner [145] demonstrated faster bone healing when loading through the fracture is reduced as healing progresses. Hence, it may be beneficial to stiffen fixation during the callus consolidation phase to reduce the IFM and resulting tissue strains, enabling mineralization and bony bridging through eliminating potentially disruptive loading events. In addition, the increase in fixation stiffness would also provide the stability needed for revascularisation.

In the final phase of healing when bone remodelling is occurring, a flexible fixation would be most advantageous to accelerate this process, as demonstrated in the dynamization study [107, 108]. However as this phase occurs after callus bridging, at a time when the bone is capable of bearing loads, optimising or accelerating this phase is not as critical as it is for the healing stages prior to bridging.

We therefore hypothesise that healing times of fractures in long bones can be reduced by the implementation of an appropriate mechanical environment that is purposefully modulated as healing progresses. We propose that it may be most beneficial to flexibly stabilise the fracture during the earlier stages of healing to enhance the healing response by promoting larger callus formation which decreases tissue stress, and then increase fixator stiffness, allowing callus maturation and remodelling to occur (Figure 3.1).

There is no experimental or otherwise obtained evidence in support of this mechanism and to what degree the magnitude of biophysical stimuli may be modulated. Direct measurement of the biophysical stimuli in the healing tissue is not feasible. Whilst some attempts have been made to measure mechanical stimulus *in vivo* (e.g. pressure) [36], these techniques do not provide information as to the distribution of these stimuli throughout the callus. Computational methods such as FE models offer a possibility to investigate the

mechanical environment and have been used previously to estimate the magnitude and distribution of potential biophysical stimuli in a fracture callus [11, 80, 118, 126, 146].

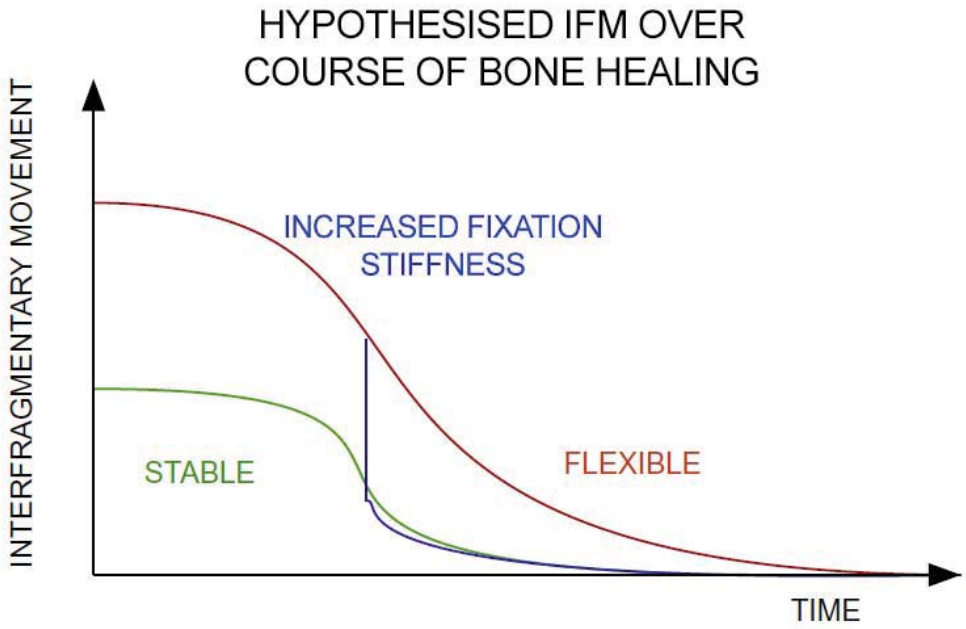

Figure 3.1: The hypothesised benefits of modifying fixation stiffness (increasing) on interfragmentary movement (left) over the course of bone healing. Increasing fixation stiffness will decrease the time taken for IFMs to reduce compared to flexible fixation and potentially stable fixation (reproduced with permission [12]).

The aim of this theoretical investigation is to analyse the influence of the size of the early hard callus on the biophysical stimuli in the remaining soft callus. We hypothesise that a larger early hard callus will lead to lower magnitudes of strain and pressure in the callus. In this study a previously validated computational model is used to investigate the mechanical environment of a fracture callus with different configurations of early hard callus [11].

3.2 MATERIALS AND METHODS

Two-dimensional axisymmetric FE models of a diaphyseal bone fracture callus were generated in ANSYS Workbench version 15 (ANSYS, Inc., Canonsburg, USA). The model of the fracture callus was based on that previously described by Claes and Heigele [11]. Mirror

image symmetry through the osteotomy (*x*) and rotational symmetry along the long bone axis (y) were assumed and therefore a quarter of the total geometry was modelled (Figure 3.2).

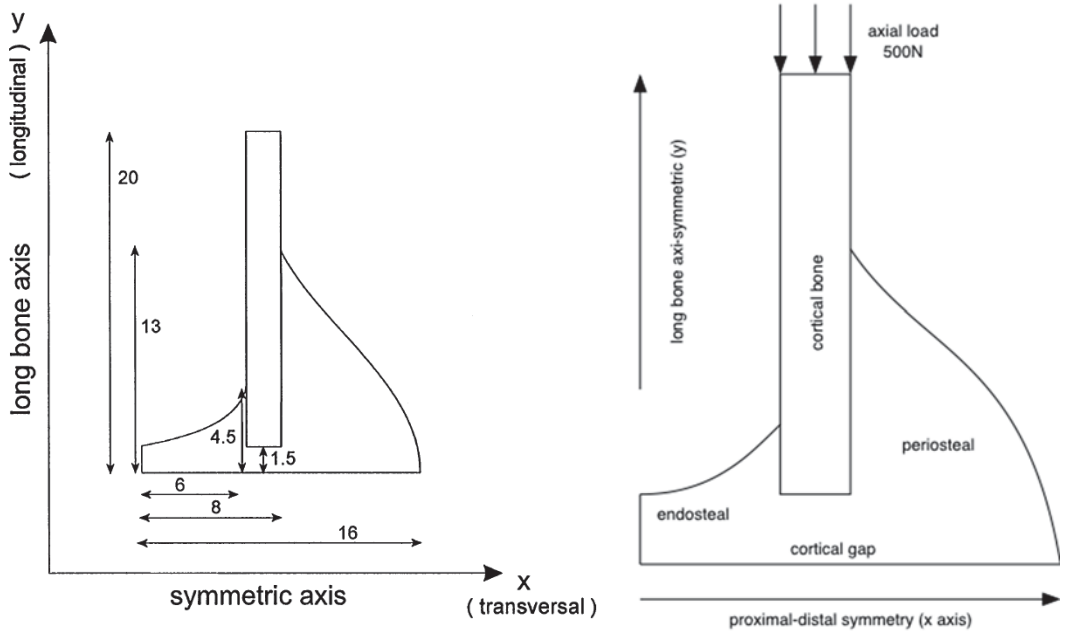

Figure 3.2 One quarter FE-model of the callus region (reproduced with permission [11]).

A model of the initial callus prior to bone formation identical to that presented by Claes and Heigele [11] was created and analysed for comparison. Subsequent models were created to be representative of an approximate 3 week time point based on the morphological patterns of healing in a previously described animal study [67]. In the first model a small mineralised hard callus was modelled, and in the second a larger mineralised hard callus. The sizes of the mineralised calluses were based on those observed by Epari *et al.* [67], while the inner and outer diameters of the cortical bone was modelled at 12 mm and 16 mm, respectively [11]. The external diameter of the periosteal tissue area was constant in all models at 32 mm.

Similar to Claes and Heigele, meshing was performed using 8-node quad axisymmetric elements. The mesh was found to converge sufficiently with approximately 5,000 elements. For testing the mesh convergence, an additional analysis was performed by increasing the number of elements (approx. 10,000 elements), to evaluate strain and hydrostatic pressure

under the cortical fragments and to confirm these elements showed the highest strain and hydrostatic pressure values.

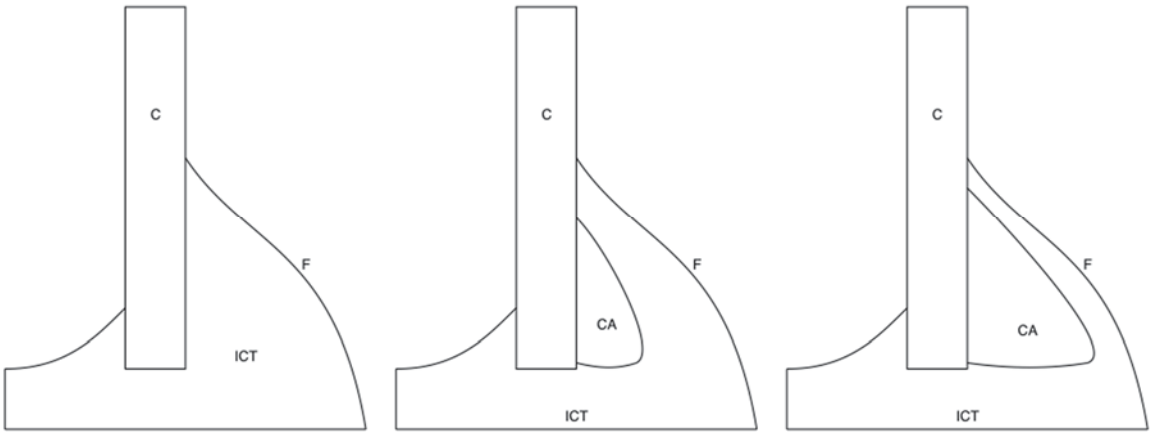

Figure 3.3 From left to right: One quarter model of initial state and early state with small mineral callus (3 mm width) and early state with large mineral callus (6 mm width). Initial connective tissue (ICT), cortex (C), mineral callus (CA) and facia (F).

In the initial healing stage, the callus consisted of connective tissue only. In the later (3 weeks) model, the callus contained a mineralised hard callus adjacent to the periosteum, while the remainder of the callus consisted of connective tissue. Due to order of magnitude difference in the material properties of the mineralised callus (> 1000 MPa), and the connective tissue (approximately 3 MPa), the model was simplified and did not differentiate between intermediate and soft callus as in the study of Claes and Heigele [11]. This was justified on the basis that the mineralised callus undergoes negligible deformation and behaves as a rigid indenter in the connective tissue. Therefore, only the shape of the initial hard callus was deemed important.

The initial connective tissue within the fracture callus is said to exhibit rubberlike behaviour, therefore we used the nonlinear hyperelastic Mooney-Rivlin Potential (ANSYS 15 User's Manual). The displacement pressure (u/p) finite element formulation was employed for calculating stress and strain in the initial connective tissue. Isotropic elastic linearity was

assumed for all other tissue types. The tissue material properties were taken from Claes and Heigele [11], and are reproduced in Table 3-1.

The cortex was loaded with an axial force of 500 N. The boundary conditions were implemented following the model of Claes and Heigele where the displacement degree of freedom (DOF) of the nodes on the *x*-axis in the *y*-direction were set to zero; the displacement DOF in the *x*-direction of the nodes on the *y*-axis were restricted. For each healing stage, the global strain field and the global hydrostatic pressure distribution was determined. For the verification of our results, we compared the IFM, strain, and pressure from the initial healing stage with the results from Claes and Heigele [11].

Table 3-1: Material properties of the different tissue types used in this model.

Tissue Type	Elastic Modulus (MPa)	Poisson's ratio	Mooney-Rivlin constants
Initial connective tissue (ICT)	3	0.4	0.293 0.177
Mineral callus (CA)	6000	0.3	
Cortex (C)	20 000	0.3	
Facia (F)	250	0.4	

3.3 RESULTS

The strain and pressure fields for the model of the initial condition, were found to be in good agreement with the pattern of strain and hydrostatic pressure distribution found by Claes and Heigele [11](Figure 3.4).

Under a 500 N axial load, the largest IFM (1.00 mm) occurred in the initial fracture callus, prior to the formation of the mineralised callus. A small periosteal hard callus (width = 3 mm) produced an axial IFM of 0.48 mm, and a larger periosteal hard callus (width = 6 mm) reduced the IFM to 0.20 mm. An exponential relationship was found between the increase in

bone cross-sectional area and relative decrease in IFM throughout the fracture gap (Figure 3.5). Increasing bone cross-sectional area was directly proportional to increasing callus width.

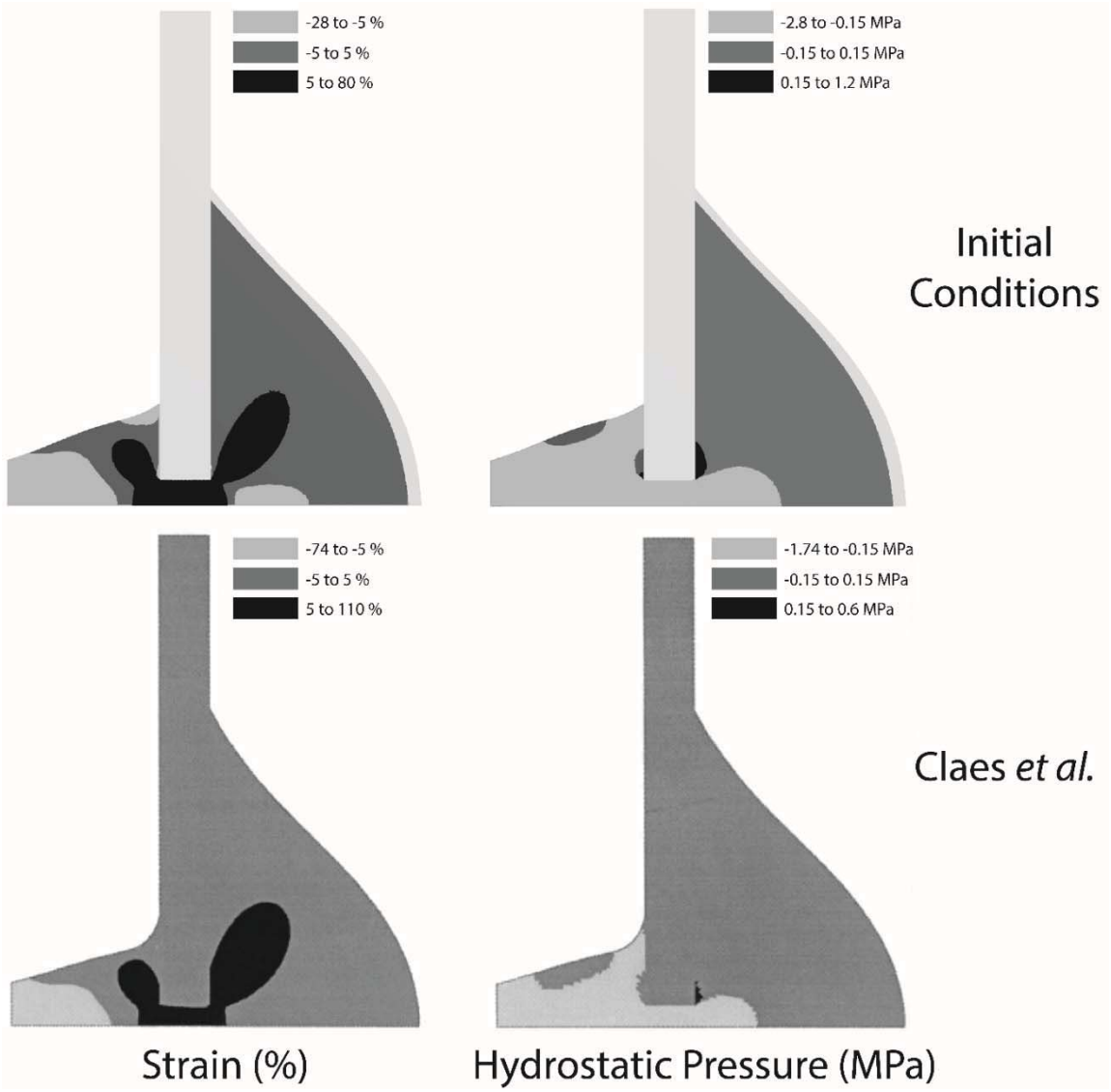

Figure 3.4 Strain and hydrostatic pressure fields in the initial fracture callus are comparable to those reported by Claes and Heigele [11] (adapted from [11]).

Claes and Heigele [11] identified the importance of investigating areas of low ($< \pm 5$ %) and areas of high strain ($> \pm 5$ %) within the callus, based on comparisons between histological tissue distribution and calculated stain and hydrostatic pressure fields. Prior to the formation of the mineralised callus, the maximum strain in the gap was approximately 50 % and the hydrostatic pressure was 2.8 MPa (Figure 3.4). The maximum strain in the fracture gap

was reduced with a small periosteal callus to 30 %, which was further reduced with the larger callus model, to approximately 12 % (Figure 3.6). In the case of the small callus, it can be seen that high strains exist in the entire intracortical region, however as the callus size increases, a drop in strain can be seen in this region, with strain in some intracortical areas observed at less than ± 5 %. Similarly, a larger periosteal hard callus reduced the maximum hydrostatic pressure in the osteotomy gap from approximately 1.6 to 1.0 MPa.

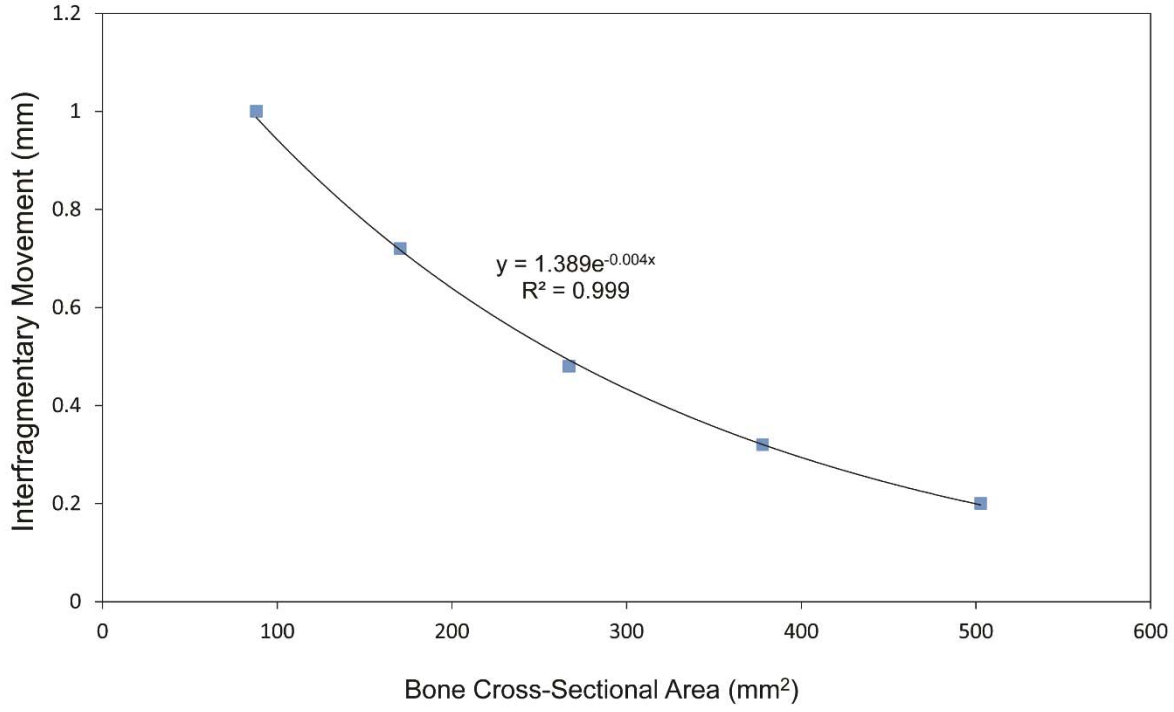

Figure 3.5 The reciprocal relationship between the cross-sectional area of the bone at approximately the line of the osteotomy and the resulting IFM.

Examination of the peak strains and hydrostatic pressures along the ossification path for each model (Figure 3.7) show that in the initial condition the peak magnitudes occur at the fracture gap and decrease as the distance from the gap increases. However, with the presence of a hard callus, strain values are lowest at the cortex and increase in magnitude the greater the distance from the fracture gap. With hydrostatic pressure, it can be seen that it peaks at either extremity of the hard callus for both 3 mm and 6 mm models

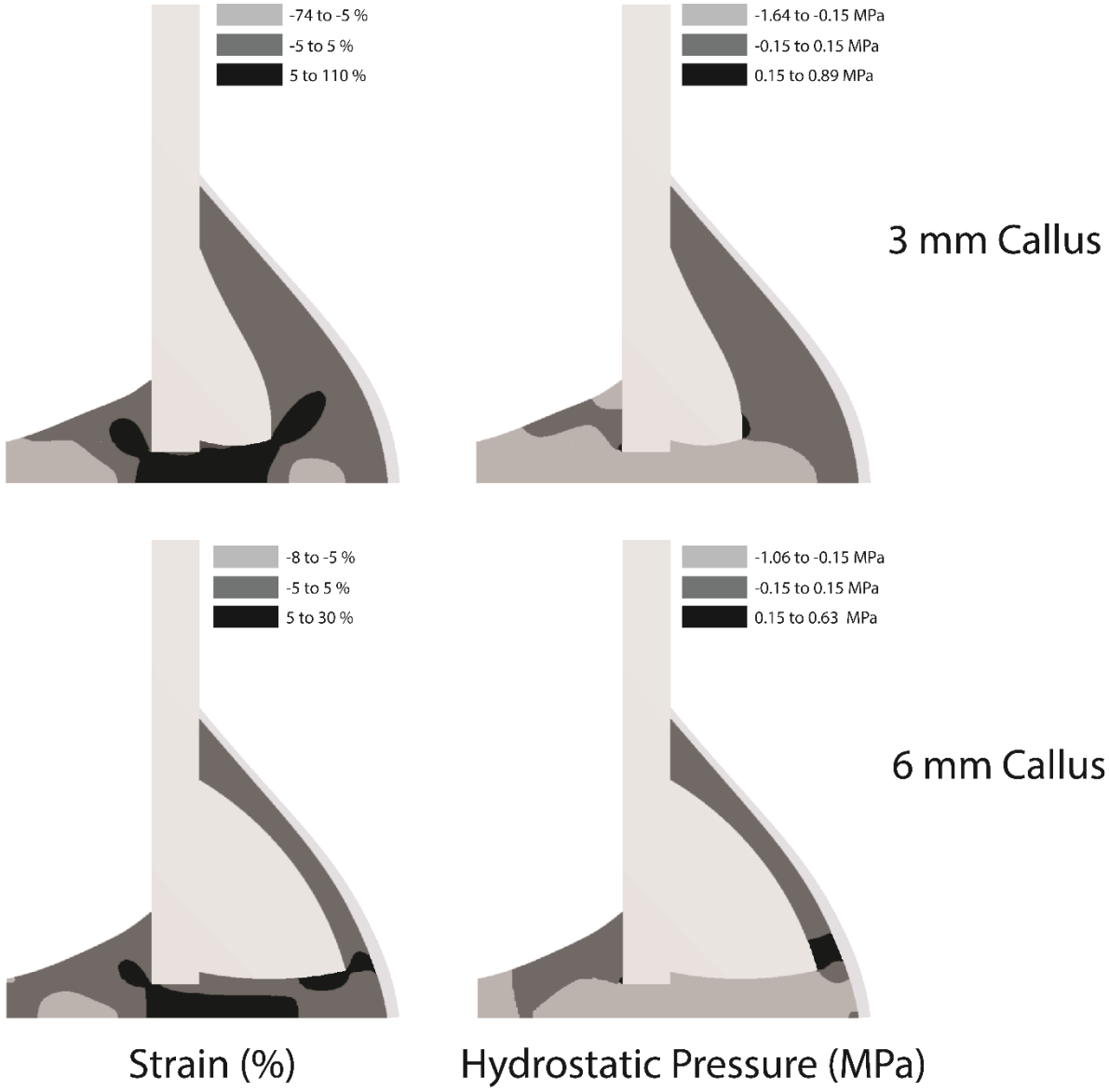

Figure 3.6 Strain and hydrostatic pressure fields in the remaining soft tissue after the formation of mineral periosteal callus, for callus sizes of 3 mm and 6 mm.

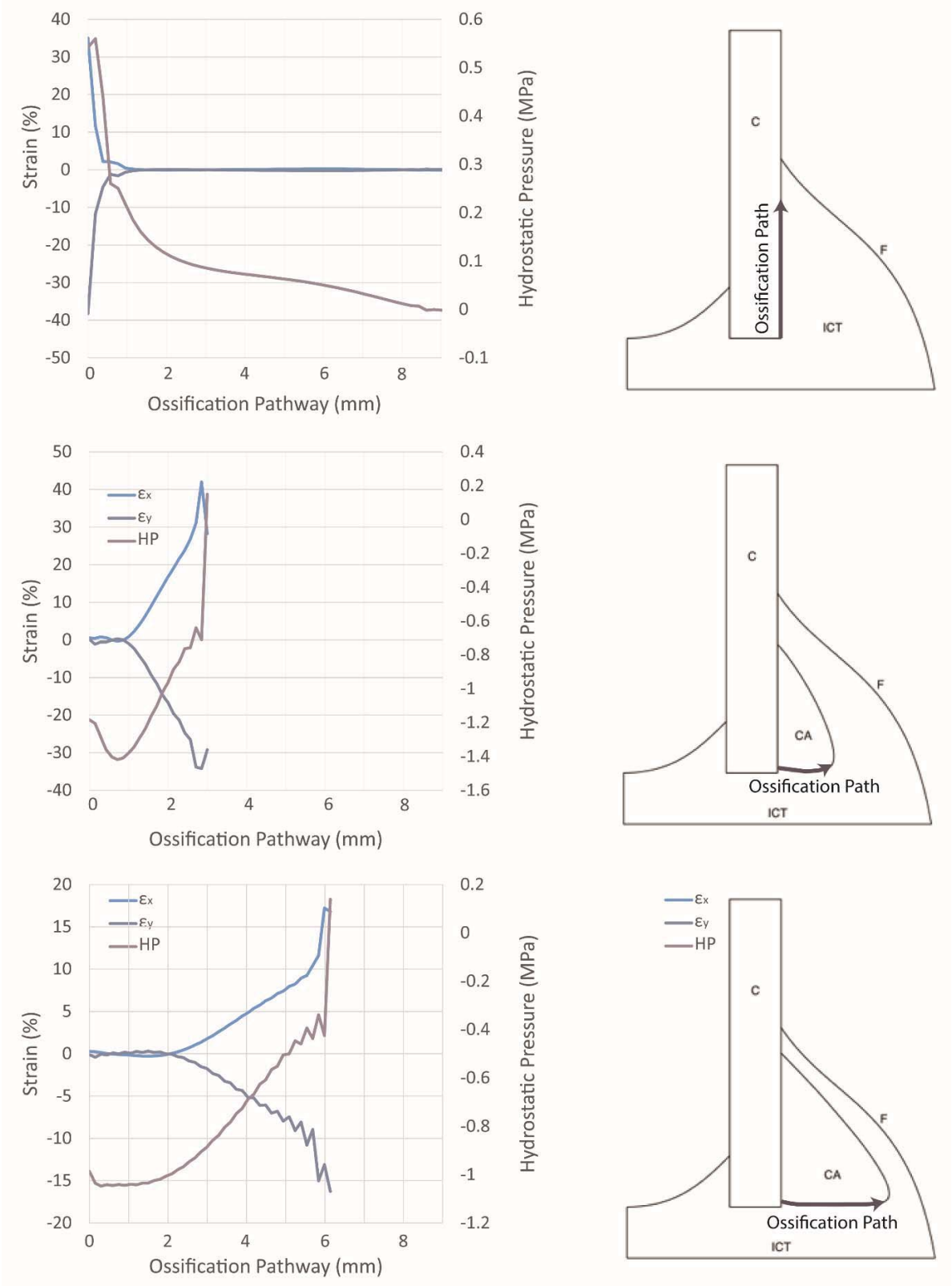

Figure 3.7 Strain and hydrostatic pressures along the ossification pathway for initial conditions, 3 mm hard callus and 6 mm hard callus models.

3.4 DISCUSSION

In this theoretical study, FE models were applied to investigate the influence the size of the early mineral callus on the mechanical environment with in a fracture callus. It was demonstrated that the width of the mineral callus alone has a significant influence on the IFM and thus the biophysical stimuli in the remaining soft callus. The FE model was based on that reported by Claes and Heigele [11] and included justifiable simplifications of geometry, material properties and loading.

From the demonstrated models, it may be seen that the early mineralised callus formed by intramembranous ossification served to reduce the magnitude of strain and hydrostatic pressure in the fracture gap. Increasing the width of the hard callus increased the area of soft callus that is engaged in weight bearing and load transfer thereby reducing the IFM and corresponding biophysical stimuli. A reciprocal relationship was found between the area of the mineral callus and cortex surface in contact with the soft callus in the gap and the magnitude of the IFM. Consequently, relatively small increases in callus width result in substantial decreases in fracture movement. Once callus width reaches a certain size, there is only a marginal benefit of further increases.

The results of this study illustrate the importance of the early hard callus formed by intramembranous ossification on the mechanical environment in the fracture region. A larger hard callus can be produced under more flexible fixation conditions, as demonstrated with histological analysis of an ovine bone healing model (Figure 3.8). This osteotomy was stabilised with a unilateral external fixator, whereby the predominant loading mode within the fracture gap is axial compression. However due to eccentric loading of the fixator, greater magnitude of IFM occur in the far cortex compared to the near cortex. The results of which demonstrate firstly, that the size of the hard callus produced is closely related to the local

mechanical conditions and secondly, that within the same time frame a larger callus can form when higher IFMs are present [12].

Applying this concept clinically, the ideal fixation would then be flexible fixation during the early stages of callus proliferation followed by stiffening to permit uninterrupted callus consolidation and bony bridging. The reduction in tissue strain in the fracture gap provides a more ideal environment for soft callus mineralisation and bony bridging, which has the potential to accelerate these processes compared to bone healing with a constant stable fixation stiffness.

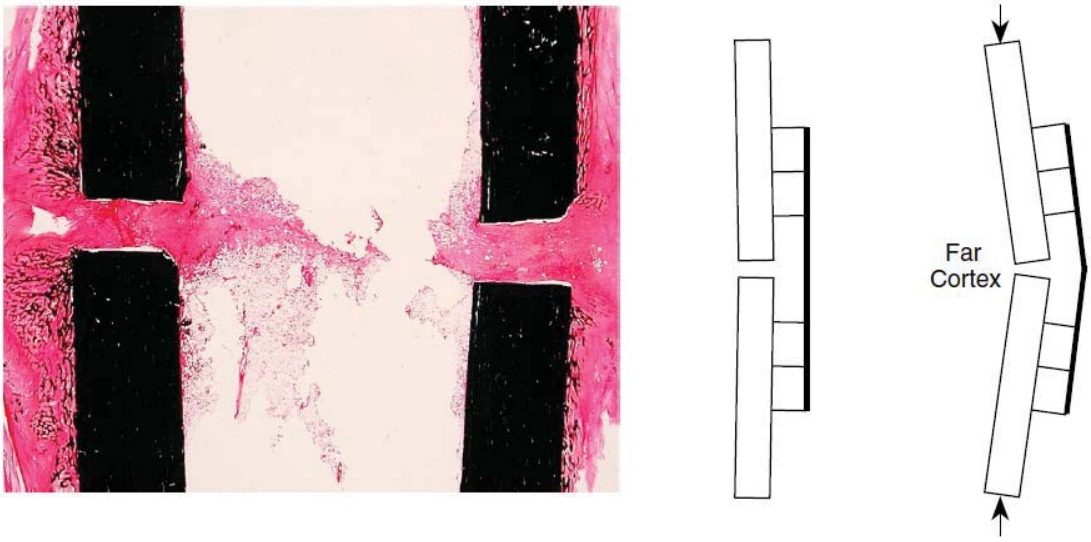

Figure 3.8 Histology section from an ovine osteotomy model after two weeks of bone healing, stabilised under unilateral external fixation on the medial side. The predominant loading is interfragmentary compression however due to the nature of the fixation, bending occurs, transmitting higher loads to the far cortex than the near, stimulating the production of a larger callus. (reproduced with permission [12]).

The models presented in this study are not intended to give precise determination of strain and pressure values in the callus. Although this study is limited through the simplified geometry and ossification pathway, it provides a simple demonstration of the concept of reducing tissue strains by producing a larger hard callus through intramembranous ossification. This concept will be further investigated throughout this thesis by modulating fixation stiffness at different time points throughout the healing process. The predicted benefits of initial flexible fixation which is later stabilised have previously been stated as (1) shortened healing in comparison to

very flexible fixation and healing time comparable or faster than optimum fixation and (2) greater callus stiffness [12]. Where optimum fixation can be defined as a stable fixation stiffness that results in the shortest time to healing with respect to reduced IFM and time to bony bridging.

3.4.1 Models to Investigate Mechanical Environment

The proposed hypothesis of modulating fixation stiffness, will be investigated with the use of *in vivo* models combined with Finite Element (FE) modelling. Common *in vivo* models used in investigating the influence of mechanics on bone healing include large and small animals. Large animal models used include the dog, rabbit and sheep. The reasons for this are that the bone healing processes in these animals have been shown to closely follow that of humans and implants for fracture stabilisation, as well as surgical techniques are able to be transferred from clinical practice. Sheep in particular are frequently used as orthopaedic models. Advantages of using sheep models are that they begin to use their treated limbs for weight-bearing as soon as they can [147], whereas other animals such as dogs will not load the fractured limb because they can move well with the use of only three limbs.

Small animal fracture models, namely rats and mice, have increased in prevalence in fracture healing studies over recent times [147]. The benefit of using a small animal model over a large animal model are that animal housing is easier and less expensive, space and housing requirements are significantly lower and breeding cycles are shorter with relatively fast availability of animals for large study groups [147]. Molecular assays and genetic manipulation of rodent models, particularly mice, also allow in-depth examination and signalling pathways and molecular mechanisms involved in fracture healing, that are not possible in larger animal models [148]. For these reasons, a wide number of fracture fixation techniques have been developed for use in rats and mice.

For this investigation, an external fixation system to stabilise femoral fractures in a rat model will be used. This external fixator has been recently developed at the Institute of Orthopaedic Research and Biomechanics, University Hospital of Ulm, and has been used in a number of studies investigating bone healing in rats [105, 149, 150], with a similar fixation system implemented by Claes *et al.* [107, 108] to investigate the effect of dynamization on bone healing. This fixator enables the modification of the degree of stability from flexible to rigid or vice-versa without the need for surgical intervention. For this study, it will be used to create initial flexible conditions which can then be modified to stiff fixation conditions as the healing period continues.

As well as conducting an *in vivo* investigation, this hypothesis will be applied to and investigated with Finite Element modelling of fracture healing. Numerous mechanobiological algorithms have been developed to simulate the mechanical influences on fracture healing [11, 73, 80, 118-126, 128-131, 151-153]. The results from the majority of these models have been compared against pre-existing experimental data. Our approach is to use a current model as a predictive tool to investigate the effect of reverse dynamization and to establish whether the model has the capacity to predict the effects of reverse dynamization.

The FE model that will be used for this investigation is an extension of the one presented by Simon *et al.* [129] The mechanisms within this model will be assessed to determine how they predict tissue proliferation and differentiation for the applied stimuli. This predictive study will then be compared with the results from the *in vivo* experimental study to provide further corroboration of the model or to potentially reveal weaknesses in the model which may require addressing to improve its predictive capabilities. As the *in vivo* model for this investigation is a rat model and the FE model is based on sheep studies, it is important to consider inter-species variations when comparing the results.

3.4.2 Inter-species Comparisons

It has been well established that the mechanical conditions of a fracture will influence the course of bone healing. Many studies have characterised the healing pathway in different species exclusively, however few have translated this across species. It is unknown whether different mechanobiological rules apply to different species and how this may affect the pattern of the healing tissue [154].

Two of the most common animal models used are that of the rat and sheep. Several rat osteotomy models stabilized with external fixators have been studied and it is clear that fracture healing progresses significantly faster in rats when compared with sheep (Figure 3.9) [154]. In the rat, the initial healing response is characterized by periosteal and endosteal bone formation [85] with bony bridging occurring 4-5 weeks postoperatively. However, in an externally stabilized sheep study there was no sign of endosteal intramembranous ossification in the early stages of healing and time to callus bridging was much longer [98]. These differences may indicate that bone formation in these models may be respondent to different mechanical stimuli.

Rats also have a more primitive bone structure than sheep and humans as they don't have a Haversian system [147]. Rats remodel bone at the fracture site using resorption cavities that form near the fracture surface [155]. Osteoblasts fill in the resorption cavities as bone heals. This process has been shown to be similar to the Haversian remodelling in larger animals however there is little understanding of the importance of this anatomic difference between large animals, humans and rats.

Checa *et al.* [154] performed an *in silico* investigation into the mechanobiological regulation of tissue regeneration across species to investigate whether the same mechanobiological model can explain the bone healing patterns observed in two different *in vivo* bone healing situations. The results indicated that there was a significant difference in the mechanical stimuli within the callus region in the initial state of the model, which may have

contributed to the differences in the healing patterns at later time points. The higher levels of strain in the sheep may be a contributing factor as to why bone formation in the early stages of healing is not observed whilst significant amounts of bone formation are shown in the rat (Figure 3.9). Due to limitations in the model, it cannot be conclusively stated that fracture healing in these animals operates under different mechanobiological rules, however the findings suggest that careful consideration is required when transferring results from one animal to another.

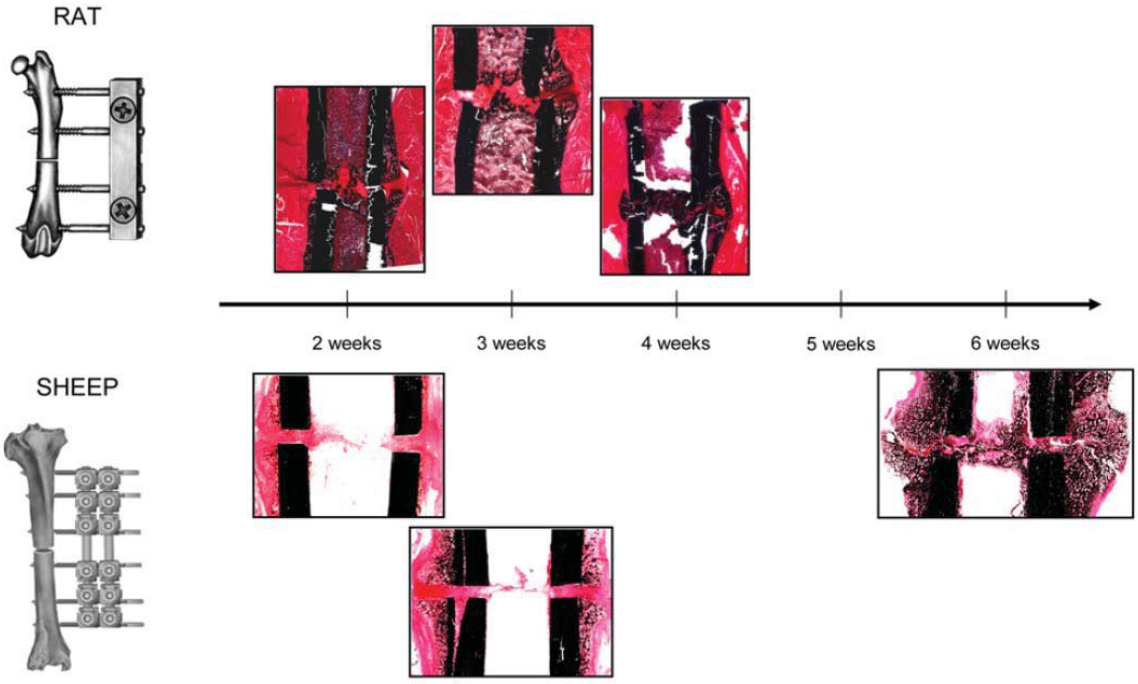

Figure 3.9: Histological sections of rat (top) and sheep (bottom) osteotomy models at different time points post-operatively. The rat model demonstrates a faster healing process when compared to sheep (reproduced with permission [154]).

3.4.3 Defining Bone Healing

The assessment of bone fracture healing is a clinically relevant and frequently used outcome measure following trauma. The outcome of fracture healing can be defined as the restoration of the mechanical properties of the fractured bone, such that the healed fracture achieves and maintains mechanical characteristics similar to those of the bone prior to fracture [156]. However this can be difficult to assess through non-invasive methods. Clinically, the

determination of bone fracture union is almost always based upon serial clinical and radiographic assessments [157]. More specifically these include a patient's pain response to weight bearing, pain during deflection of the fracture site, and radiographic assessment [29, 53, 158]. Radiographic evaluation of fracture union includes several parameters such the assessment of the diameter and shape of the callus, monitoring the disappearance of fracture lines and cortical bridging or continuity [53, 102, 159, 160]. This overall process can be quite complex relying largely on judgment and experience of clinicians as no methods for quantitatively monitoring healing have been validated and implemented in treatment [53, 159, 161]. Thus clinicians often exhibit caution by extending fracture treatment far longer than may be necessary. The imprecise nature of this definition makes it difficult to compare healing outcomes between different clinical and experimental scenarios. Therefore emphasis should be placed on defining this criterion when conducting an experimental fracture healing study.

Experimentally, bone healing has often been defined by the strength or stiffness of the bone. The strength is measured by the maximum stress it can withstand before re-fracture. This is measured experimentally with bending or torsional loads applied to the bone until destruction. However due to the destructive nature of strength measurements, which prevent histological analysis of the specimens, a related parameter such as stiffness may be assessed for a non-destructive quantification.

Stiffness describes the resistance of a material to deformation under an applied load. It has been shown that stiffness increases within fractured, healing bone tissue as healing progresses. Because measurements of stiffness are predominantly determined non-destructively, they are used both clinically and experimentally to monitor bone healing.

When performing stiffness measurements to determine progression of healing it is important to consider how this relates to the strength of the fracture callus. In a study conducted by Chehade *et al.* [162] investigated the relationship between stiffness and strength of tibial

fractures in sheep, it was found that the relationship between these two properties differed throughout the healing period. It was found that there was a strong correlation between stiffness and strength in the early phases of healing as they result from the same healing process: the formation of woven bone. After this phase, the organisation and remodelling of callus with an increasing amount of lamellar bone increases fracture strength with little or no effect on fracture stiffness. Hence increases in stiffness may be used to monitor changes in fracture strength until stiffness reaches approximately two thirds of the normal range. After this is achieved, stiffness can only determine a baseline of fracture strength.

However as outlined above, stiffness measurements can produce large variability with experimental errors up to 60 %. Therefore callus stiffness should be de-emphasised as bone healing definition and instead used to correlate the mechanical changes in the callus to the progression of healing.

Mechanical testing of bone can produce considerable errors [163] and is particularly challenging with small animal models due to the size of the bone. As such this parameter to assess healing should be coupled with radiographic, microcomputed tomographic (μCT) and histological assessment of the healing outcome. These evaluation techniques can give an overview of the cortical continuity of the bone fracture, the volume of bone produced, the quality of the bone produced and the tissue distribution throughout the callus. Coupled with mechanical integrity, these parameters can provide a much clearer outcome of the experimental fracture healing outcome. Panjabi *et al.* [164] studied correlations of radiographic analysis of healing fractures with strength using experimental osteotomies in rabbits. This study reported that the best single predictor of strength of a healing bone was cortical continuity.

Therefore throughout this project, bone healing was assessed primarily by the formation of bone in the intracortical region restabilising the cortical continuity of the fractured limb. Further advances in the healing were evaluated by the quality and quantity of bone within the

fracture region, the resorption of bone within the medullary canal as well as remodelling of the periosteal callus.

3.5 CONCLUSION

Modifying the fixator stiffness during the healing period has the potential to enhance tissue regeneration. We hypothesize that bone healing will be enhanced with initial flexible fixation conditions which will be converted to stiff fixation during the later stages of repair. A simple axisymmetric FE study was conducted as a demonstration of the hypothesis whereby a larger callus lowered the tissue strain within the fracture gap and along the ossification front compared with a smaller callus. This investigation will be conducting using a combination of an *in vivo* small animal study and a computational Finite Element (FE) study.

Chapter 4: Computational simulation of fracture healing under modulation of fixation stiffness

4.1 INTRODUCTION

Fixation stability has been shown to influence the rate and quality of the healing of bone fractures as it governs the mechanical environment within the fracture. The stability will determine the magnitude of movements between the fractured bone ends (IFM), through which mechanical stimuli to the local cells is provided. Loading causes deformation within the immature callus tissue, with this strain encouraging the adjacent pluripotent cells to differentiate down a specific cell lineage; osteogenic, chondrogenic or fibrogenic, depending on the strain magnitude and rate [165-167]. Under more flexible fixations, where greater strain magnitudes occur, cells are induced down a chondrogenic pathway, whilst conversely under very low strain, differentiation down the osteogenic pathway will be encouraged. Subsequently, the fracture fragments will reunite with a combination of bone formed by intramembranous (direct bone formation) and endochondral (via a cartilage intermediate) ossifications.

There is conflict between experimental studies regarding the significance of mechanical stimuli on the rate of bone healing due to dissimilarities in the models used to investigate this parameter. For example, there is no standard methodology for loading during fracture healing [168]. This has been implemented actively [14], passively to allow a limited amount of movement [59], or using fixations of varied stiffness [65, 80, 98], all of which load the fracture differently in terms of magnitude and direction. Hence it is not only difficult to measure and monitor the mechanical environment *in vivo,* but also challenging to assess and interpret previous data [104].

In order to overcome these limitations, finite element (FE) modelling has been explored extensively [11, 73, 118, 120, 123-132]. Numerical models of the fracture callus have been developed to predict physiological responses under various mechanical loads, and simulate their subsequent influence on tissue healing [2]. Current mechanobiological models are highly complex in terms of implementation of mechanical and biological factors, however model complexity does not ensure accuracy in determining biological outcomes. Further, interpretation of results from highly complex models becomes increasingly difficult due to an increased number of assumptions and estimations required in the initial definition of the system [34].

Despite differences in FE model development - the majority of studies have attempted to quantitatively verify their simulations based on experimental data. However, if the experimental data are not obtained by the same investigators, sufficient information is not always available to adequately corroborate the FE model. Data presented in publication form may also fail to provide adequate information regarding tissue mechanical properties or boundary conditions. As such, qualitative comparisons are often used to establish model parameters.

Whilst there are limitations within current mechanobiological models, they have potential to advance research in bone fracture healing and management through their implementation within the development of new clinical therapies, such as implant design, or bone tissue engineering [168]. However, the predictive power of the current methodologies needs to be rigorously analysed prior to their use in clinical medicine, to determine how accurately they simulate natural responses. This requires both quantitative and qualitative comparisons with physical evidence, which largely lie outside the domain under which the model was developed.

The aim of this study was to use an established numerical algorithm that models the fracture healing process to predict the effect of changing fixation stiffness on the rate of fracture healing. The numerical algorithm used is a FE model developed by Simon *et al*. [129] from the Institute of Orthopaedic Research and Biomechanics, University Hospital of Ulm, based on the fracture healing process observed in previous sheep studies [60, 100, 140]. This axisymmetric fracture healing model was used herein and adapted by varying the stiffness of the fixator at different time points throughout the healing process. This study was intended to determine if the model can appropriately address the effects of the changing mechanical environment on tissue distribution, and on the length of time required for healing. The interfragmentary movement between the fracture ends was assessed, as well as the healing pattern of the fracture callus, with respect to cartilage and bone concentration. It was hypothesised that conditions where stable fixation provides 'optimal' mechanical stimulus would result in the fastest healing because this is a fixed domain model, and therefore changes in callus size based on the magnitude of mechanical stimulus would not be observed.

4.2 METHODS

Simon *et al*. [129] developed a dynamic axisymmetric finite element model to simulate the interactions of mechanical stability, revascularisation and tissue differentiation during fracture healing [129]. The model will be described briefly, however as this model was not developed throughout this study and only adapted to test its predictive capacity, more specific details regarding model function and development may be examined in the relevant publication [129].

Load and boundary conditions for the FE model were based on previous animal experiments [40, 59]. The external fixator used in the previously performed animal experiment (Figure 4.1) was incorporated into the FE model to allow axial movement of the bone fragments up to a predefined magnitude, whilst limiting movement in all other directions (Figure 4.1).

This enabled the simulation of both stable and unstable conditions across the fracture gap, through the manipulation of the stiffness values of the fixator [100, 140].

The numerical model described the healing process using three main state variables: blood perfusion, cartilage concentration and bone concentration. The model then predicted the stress and strain distribution throughout the fracture callus using time-dependent iterative loops. Solving of the model was conducted by applying fuzzy logic rules to the initial state (100 % soft tissue, 0 % cartilage, 0 % bone). These rules dictate biological processes within the simulation including angiogenesis, intramembranous ossification, chondrogenesis, cartilage calcification and endochondral ossification, all of which are dependent on the local strain state and local blood perfusion within each element [98].

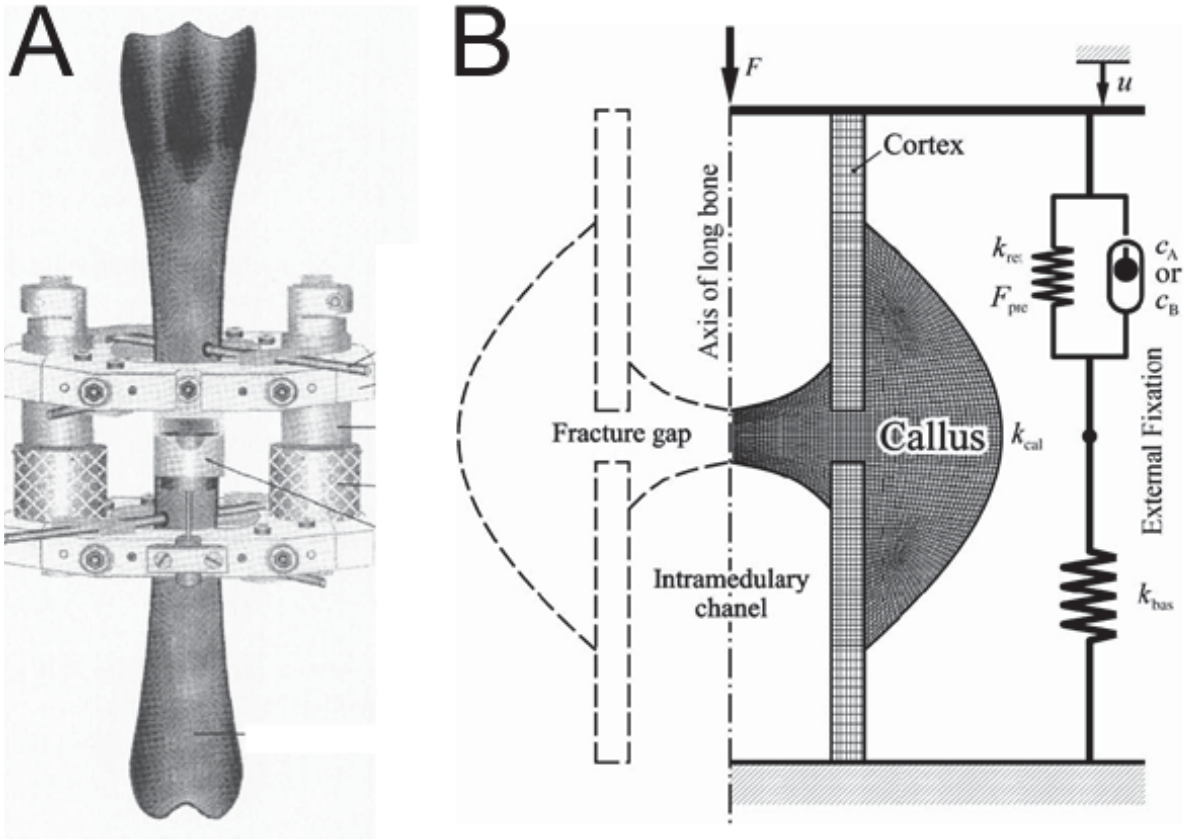

Figure 4.1: a) Schematic of external ring fixator used in animal experiments (reproduced with permission [40, 59] b) FE model (2D, axisymmetric) of a standardised fracture callus geometry used in FE model by Simon *et al*. (reproduced with permission [98]).

4.2.1 FE Model

The numerical model describes the healing process in time and space using three main variables:

$$\underline{C}(\underline{x},t) := \begin{bmatrix} Blood\ perfusion \\ Cartilage\ concentration \\ Bone\ concentration \end{bmatrix},$$

$$\underline{C}(\underline{x},t) := \begin{bmatrix} c_{perf}(\underline{x},t) \\ c_{cart}(\underline{x},t) \\ c_{bone}(\underline{x},t) \end{bmatrix}. \tag{4-1}$$

The tissue differentiation process is described by a changing tissue mixture consisting of soft tissue, fibrocartilage and woven bone. The volume fraction of fibrocartilage $c_{cart}(\underline{x},t)$ and woven bone $c_{bone}(\underline{x},t)$ are calculated with soft tissue comprising the remainder of the callus composition ($c_{cart} + c_{bone} + soft\ tissue = 100\ \%$).

The progression of the variables was modelled as an initial value problem where change in perfusion and tissue concentrations was calculated from a complex function $\underline{f}$, depending on a combination of the current state $\underline{C}$ of the tissue and the local mechanical stimuli within the element.

$$\frac{\partial \underline{C}}{\partial t} = \underline{f}\left[\underline{C}, \underbrace{\underline{S}(\underline{C},F)}_{\text{Callus mechanics}}\right] \quad \underbrace{\phantom{\underline{f}\left[\underline{C}, \underline{S}(\underline{C},F)\right]}}_{\text{Biological processes}} \tag{4-2}$$

Fuzzy logic was chosen to describe the function $\underline{f}$ as analytical expressions have not been developed for all mechanobiological processes.

The model was loaded axially with a force of 500 N, representing the amplitude of the major metatarsal loading during normal gait in a sheep, as measured previously [40, 59]. All FEs had linear

elastic material properties, with cortex elements comprising compact bone, and callus elements consisting of the changing tissue mixtures. Each callus element was assigned a material property, which was then updated at each time step based on the tissue concentrations and properties of the pure tissues (Table 4-1Table 4-1) [129].

Table 4-1Elastic modulus for each element was taken as the tissue concentration to the power of three multiplied by the tissue modulus. This was based on a previously determined experimental relation where the apparent compressive modulus of trabecular bone specimens was proportional to the cube of their apparent density [129].

$$E_{el} = \sum_{tiss} E_{tiss}\, c_{el,tiss}^{3} \tag{4-3}$$

A linear mixture model was implemented to determine Poisson's ratio, ν_{el} for each element:

$$\nu_{el} = \sum_{tiss} \nu_{tiss} c_{el,tiss} \tag{4-4}$$

Based on the tissue differentiation hypothesis of Pauwels [117], two independent strain invariants were used as mechanical stimuli:

$$\underline{S} = \begin{bmatrix} \varepsilon_0 \\ \gamma_0 \end{bmatrix}. \tag{4-5}$$

From the principle strains $\varepsilon_1, \varepsilon_2, \varepsilon_3$ of each element: the dilatational strain (hydrostatic strain) representing a volumetric change was defined as:

$$\varepsilon_0 = \frac{1}{3}(\varepsilon_1 + \varepsilon_2 + \varepsilon_3), \tag{4-6}$$

and the distortional strain representing a change in shape:

$$\gamma_0 = \frac{1}{3}\sqrt{(\varepsilon_1 - \varepsilon_2)^2 + (\varepsilon_1 - \varepsilon_3)^2 + (\varepsilon_2 - \varepsilon_3)^2}. \tag{4-7}$$

Table 4-1: Material properties of the pure tissue types used in the FE model.

Tissue, tiss	Elastic modulus (MPa)	Poisson's ratio
Cortical bone	10 000	0.36
Woven bone	4000	0.36
Fibrocartilage	200	0.45
Connective tissue	3	0.3

4.2.2 Fuzzy Logic Controller

The fuzzy logic tool in MATLAB 2014a (The MathWorks, Inc., Natick, MA) was used to implement the biological processes within the simulation and to predict changes in seven variables, as previously described [128, 129, 153, 169]. The main variables were perfusion, cartilage and bone concentration, the mechanical stimuli (dilatational and distortional strain) and two variables describing bone and perfusion concentrations in adjacent elements (Figure 4.2). These comprised the input variables of the fuzzy controller which consisted of eight linguistic if-then rules. The rules described the processes of angiogenesis, intramembranous ossification, chondrogenesis, cartilage calcification, endochondral ossification and tissue destruction. The output variables dictated change in perfusion, cartilage or bone for each iteration.

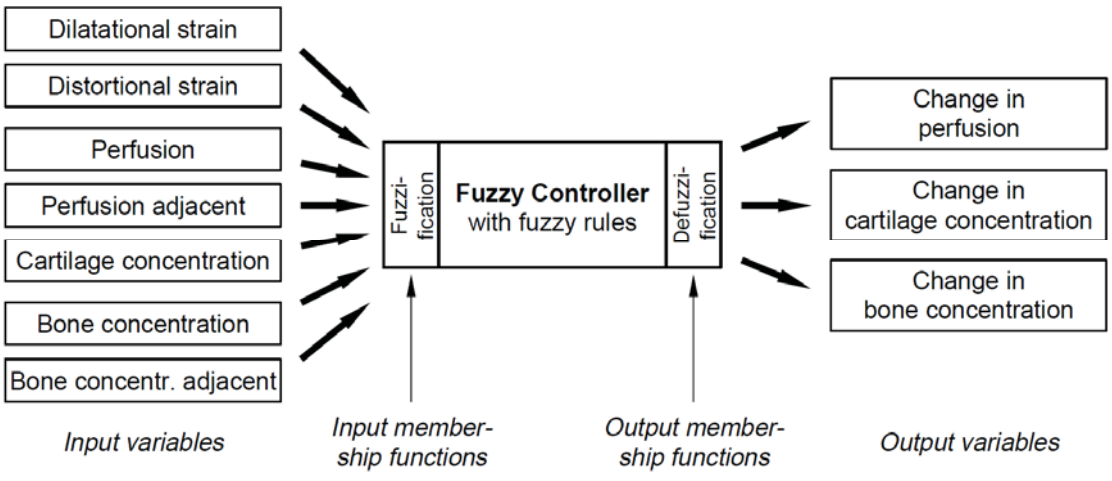

Figure 4.2: Fuzzy controller with seven fuzzy input and three fuzzy output variables. (reproduced with permission [129]).7

4.2.3 Iterative Healing Simulation

The callus healing process was described numerically as an initial value problem and simulated using time-dependent iterative loops over equidistant time steps (Figure 4.3). The simulation was started with a pre-processor that generates geometry, element mesh, external fixation, load and boundary conditions. Following this, initial values for the tissue composition, the material properties and the blood supply were assigned to each of the elements, creating a representation of the fractured bone immediately following fixation. The iterative pattern of the simulation was then followed, beginning with the FE analysis, calculating local mechanical stimuli in each element of the model. These stimuli together with the tissue composition and local blood supply were used as inputs to the fuzzy logic controller, producing a resulting tissue composition and blood perfusion within each element. A subsequent FE pre-processor updated the material properties of the elements according to the new tissue compositions, completing one iteration before beginning the next.

For this study, it was necessary to be able to manipulate the stiffness of the fixator modelled throughout the healing period. This required altering the original numerical script to allow a changing fixator stiffness at any chosen iteration. A number of fixation configurations were assessed throughout this analysis. Initially, a range of constant fixation stiffness parameters were modelled to ascertain the responsiveness of the model to different conditions. Thereafter flexible and more stable fixation values were selected for analysis. The model was then analysed with the flexible fixation stiffness, which was increased at iterations 7, 14 and 21.

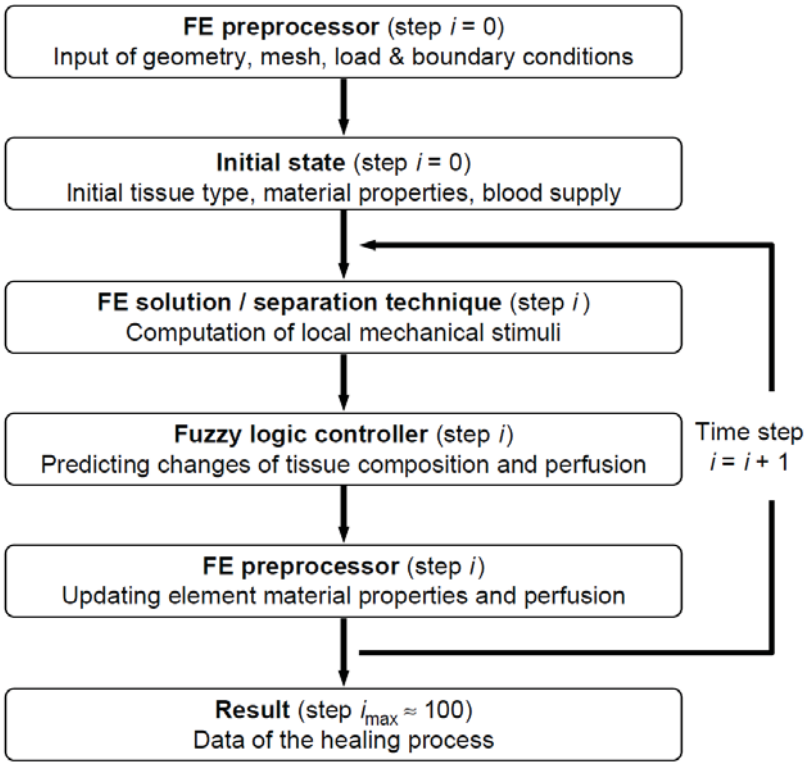

Figure 4.3: Flowchart of the dynamic fracture healing model including the FE method and the fuzzy logic in an iterative loop over time (reproduced with permission [129]).

The measured parameter used to monitor and define healing was IFM. The bone was considered healed when the IFM (axial) was less than 0.1 mm [129]. The resulting outputs were the number of iterations required to reach an IFM of less than 0.1 mm, as well as the tissue formation and mechanical conditions for each iteration.

4.3 RESULTS

4.3.1 Assessing Fixation Parameters

For each fixation stiffness the theoretical IFM (load/fixation stiffness) was calculated for the initial condition and compared to the measured value within the model. It was found that there was good agreement between the theoretical and measured values, however they did deviate slightly for the lowest fixation stiffness values (Figure 4.4). There was a considerable decrease in IFM and IFS observed between 200 $N \cdot mm^{-1}$ and 1000 $N \cdot mm^{-1}$, however for stiffness values greater than 1000 $N \cdot mm^{-1}$, the changes in these parameters were less noticeable, especially in the case of a 3 mm fracture gap. The range of fixation stiffness

examined in the model were therefore from 200 N·mm^{-1} to 1000 N·mm-1. A simulation of 1600 N·mm^{-1} was used to verify small changes in the results for stiffness greater than 1000 N·mm^{-1}.

The changes in IFM for each iteration produced results where the stiffer the fixation the faster the decline in IFM, and the faster the achievement of the healing outcome (Figure 4.5). It can be seen (Figure 4.5) that there is little reduction in IFM for the first 10 – 20 iterations, irrespective of fixation stability. Following this, from iterations 20 – 30 there is a sharp decline in IFM, as the callus tissues stiffen. For the lowest stability conditions (< 400 N·mm^{-1}) this change does not occur until after iteration 35.

For the lowest fixation stiffness that could produce a healing outcome (300 N·mm^{-1}), healing occurred within 83 iterations, whereas a threshold appeared to be reached by 800 N·mm^{-1}, with healing occurring after 35 iterations, similarly to the limit of 32 days observed with the 1600 N·mm^{-1} condition. This result again indicated that negligible benefit may be drawn from stiffness values in excess of 800 N·mm^{-1} (Figure 4.6).

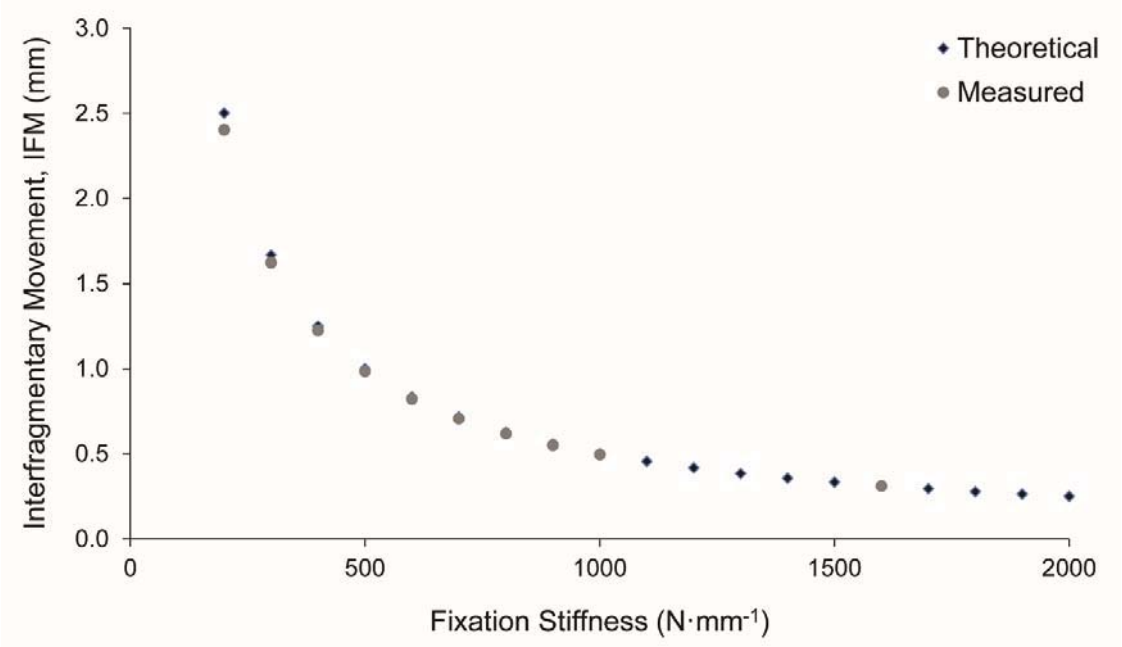

Figure 4.4 Theoretical calculations versus model measured values for interfragmentary movement (for each fixation stiffness).

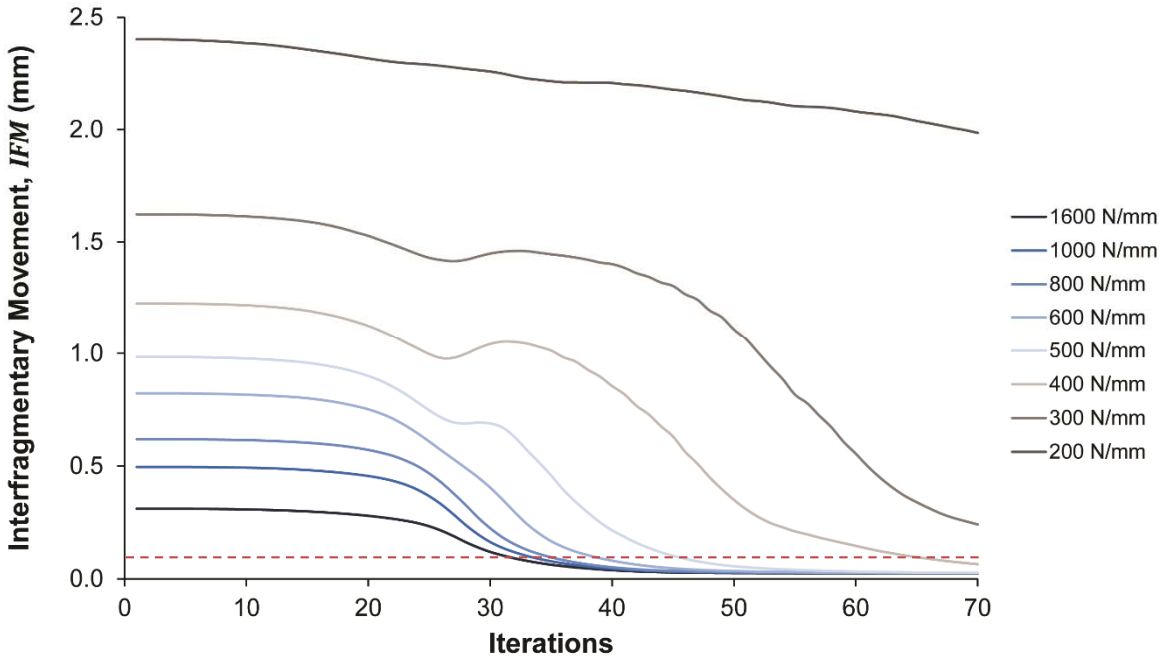

Figure 4.5 Interfragmentary movement measured over time (iterations) in the FE model. Stiffness parameters investigated ranged from 200 N·mm^{-1} to 1600 N·mm^{-1}. It may be seen that very low stiffness parameters did not result in healing (200 N·mm^{-1}), with higher stiffness fixations producing similar healing outcomes to one another (800-1600 N·mm^{-1}). The red line indicates the healed condition, at an IFM of less than 0.1 mm.

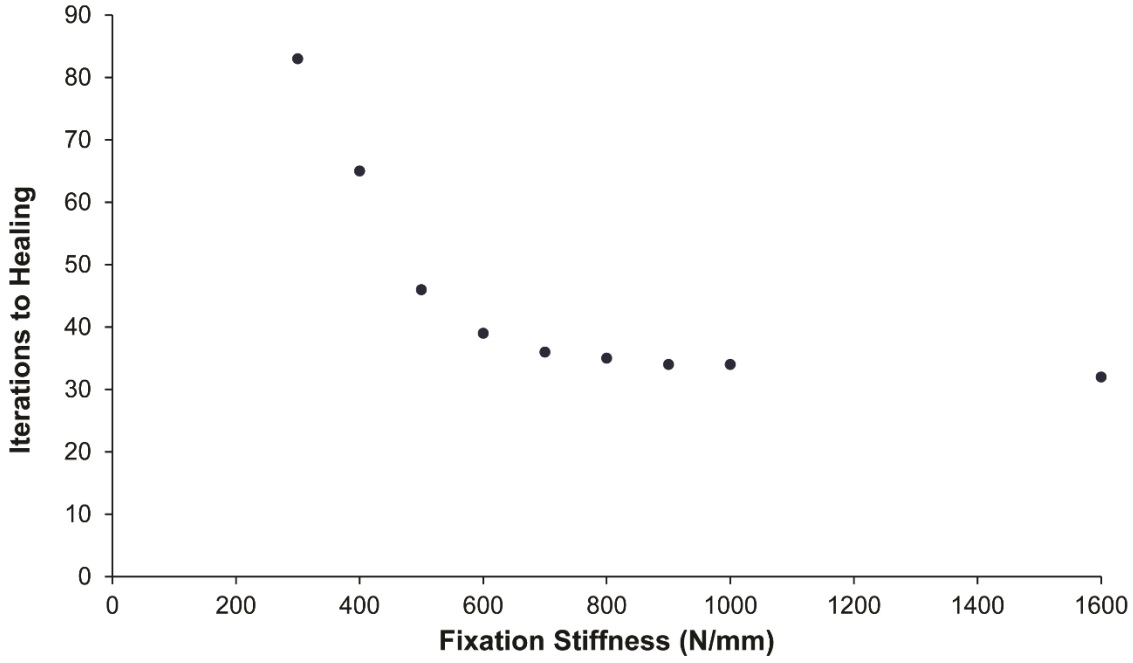

Figure 4.6 Healing outcome measured in number of iterations required until IFM is less than 0.1 mm. It may be seen that there is a large change in time from 300 to 800 N·mm^{-1}, with only small decreases in healing times achieved with stiffness in excess of 800 N·mm^{-1}.

Concentrations of cartilage and bone throughout the fracture healing process were analysed and compared to the predicted distributions of distortional and dilatational strain (Figure 4.7). The highest absolute strain values were predicted to occur within the fracture gap during the initial stages of healing. It may be seen that these values were in fact higher with lower fixation stiffness, as more load and hence IFM was transferred through the fracture itself. As the healing progressed, particularly in the case of the development of periosteal bone callus, the strain throughout the fracture gap decreased.

There were few observable differences within the first two weeks of healing despite different fixation conditions. By week 4 however, it became evident that there was increased cartilage development in the intracortical and endosteal callus regions under stiffer fixation, whilst the low stiffness fixation resulted in the greatest concentration of cartilage developing in the periosteal callus adjacent to the fracture gap. Bone formation at this stage was however quite consistent amongst all groups, with a trend of slightly more bone formation under stiffer fixation. By 6 weeks, periosteal callus bridging was observed under all stiffer fixation conditions aside from 400 $N \cdot mm^{-1}$, where a band of soft tissue was noted.

4.3.1 Modifying Fixation Stiffness

Initial fixation stiffness values were modelled as 400 $N \cdot mm^{-1}$, resulting in IFS of 42 %. An IFS of 42 % has been shown to delay healing *in vivo* compared to more stable conditions, with the optimal range for healing being between 7 - 30 % [59]. The fixation stability was increased to 800 $N \cdot mm^{-1}$ (IFS 21 %) at iteration 7, 14 and 21.

Initially, under all conditions there was limited bone development and only slight reduction in IFM over the first 20 iterations, irrespective of fixation condition. When the fixator was changed to a more stable configuration, there was a steep decline in IFM, purely due to the more stable fixation. This was clearly demonstrated when fixator conditions were changed within the first 20 – 25 iterations (Figure 4.8).

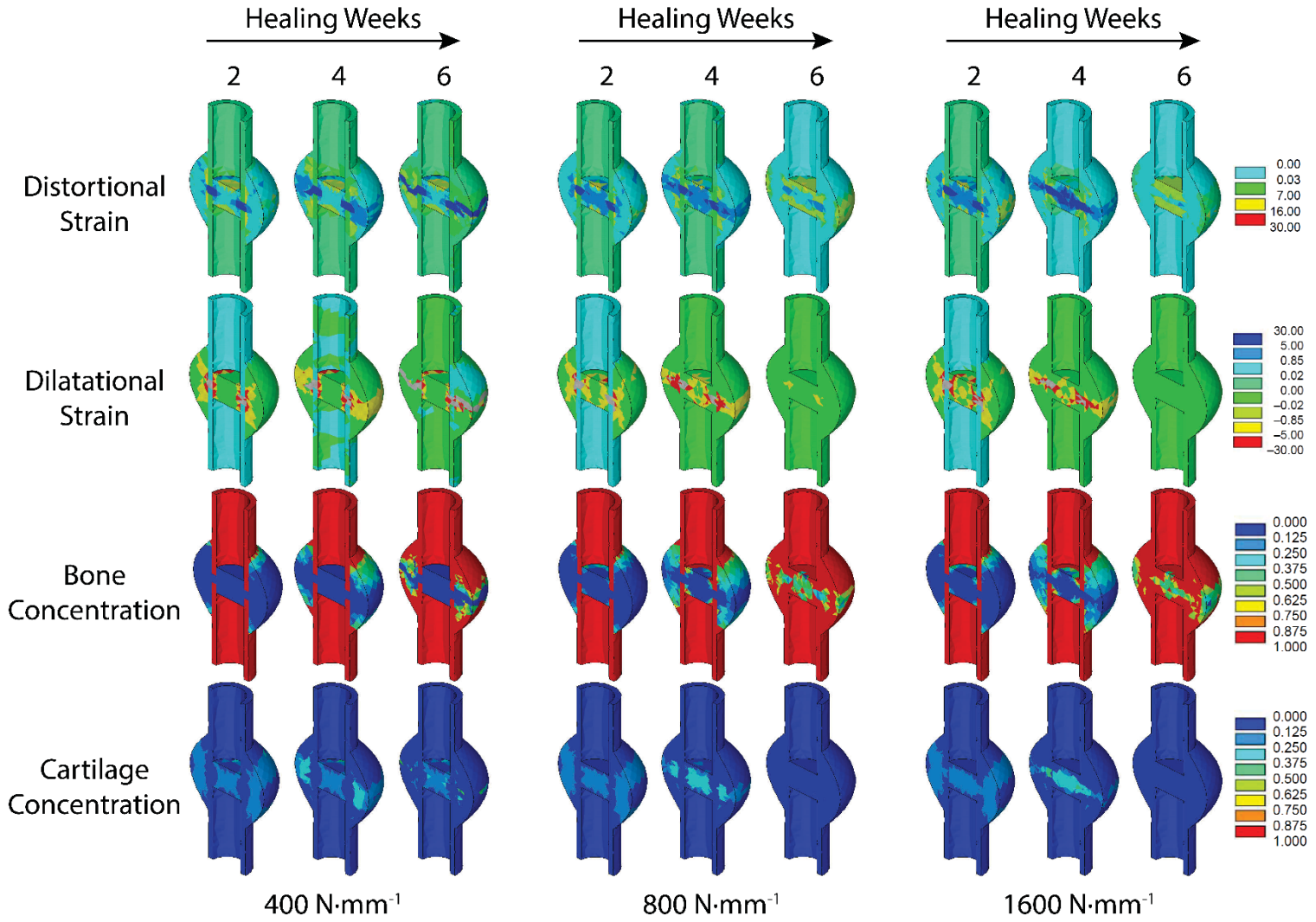

Figure 4.7 Healing pathways under with different stiffness fixators; 400 N·mm^{-1} (left); 800 N·mm^{-1} (middle) and 1600 N·mm^{-1} (right). No differences were observed in the first 2 weeks of callus development, however differences began to arise by 4 - 6 weeks, with more bone formation under stiffer fixation.

The results demonstrated that changing the stiffness allowed less stiff conditions to 'catch up' to the most stable condition, however there did not appear to be potential to ever exceed this outcome (Table 4-2). The initial pattern of healing observed with the changing fixation did not differ from that of a constant 800 $N \cdot mm^{-1}$, as the initial flexibility and IFM did not influence the pattern of tissue development within the callus of this model. However, as the bone approached the periosteal bridging stage, a few differences were noted between the simulation groups. For the 400 $N \cdot mm^{-1}$ fixation condition, a band of soft tissue throughout the intracortical region was present until periosteal bridging was seen at the periphery of the callus. For the other fixation conditions however, some bone formation was observed throughout the intracortical region by this stage. The 800 $N \cdot mm^{-1}$ fixation and 7 day conditions were quite similar in tissue appearance at bridging, with a large bone portion formed endosteally, whilst this region in the 14 day and 21 day conditions primarily comprised soft tissue. The 14 day condition varied in terms of periosteal bridging, as it occurred at the periphery of the callus, whereas the 800 $N \cdot mm^{-1}$, 7 day and 21 day conditions bridged mid-periosteal callus.

Table 4-2 Time to healing after stabilising fixation by increasing stiffness

	Iterations to healing	**Iterations to bridging**
Constant 800 $N \cdot mm^{-1}$	35	43
7 Day	36	45
14 Day	38	47
21 Day	39	47
Constant 400 $N \cdot mm^{-1}$	65	70

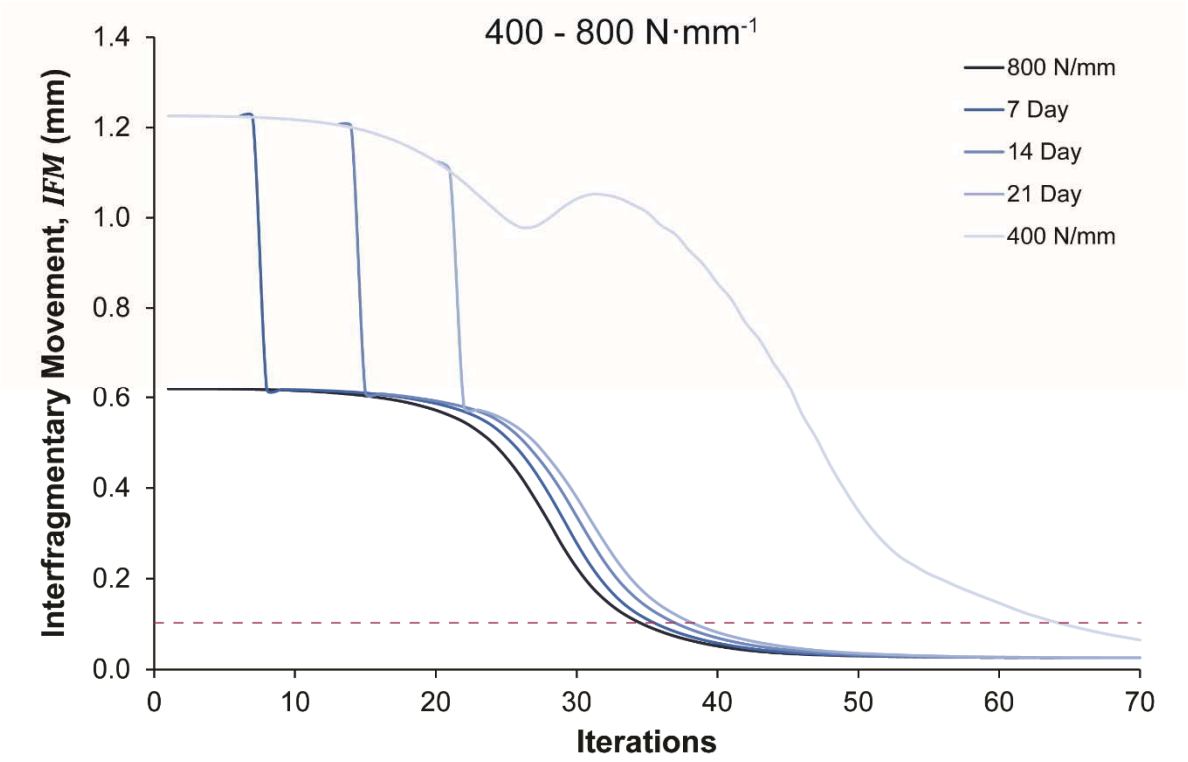

Figure 4.8 Interfragmentary movement measured over time (iterations) in the FE model. Fixation stiffness was changed from 400 N·mm^{-1} to 800 N·mm^{-1} (top) and 500 N·mm^{-1} to 800 N·mm^{-1} (bottom). Changes in stiffness were made at iteration 7, 14 and 21. The red line indicates healed condition at IFM of less than 0.1 mm.

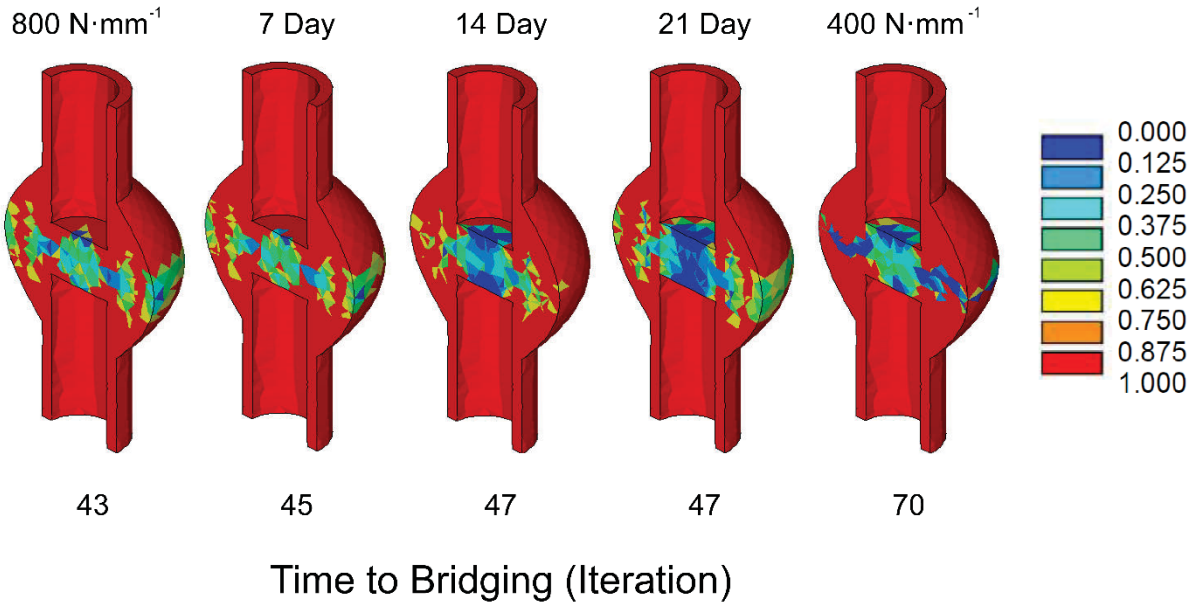

Figure 4.9 Tissue distribution at time of periosteal bridging for both constant fixation conditions and from stabilising the fixator at iteration 7, 14 and 21.

4.4 DISCUSSION

The major objective of this predictive modelling was to assess the mechanisms within the model itself, the fuzzy logic rules, and their ability to predict bone healing through simulating cellular proliferation and differentiation patterns under the chosen stimuli. Hence examination was not limited to the final result or outcome of the model, but extended to the mechanisms and pathways of the model used in establishing the solution. By performing this analysis prior to obtaining the results of the *in vivo* study (Chapter 5:), the conclusions reached from the interpretation of these results will not be biased by prior knowledge of the effect of stiffening fixation on bone healing.

The progression of healing, as well as the end point of the healing process, were both investigated in this study. Under constant fixation, the dilatational strain distribution was similar amongst all fixation conditions, however the distortional strain differed across the groups. After two weeks, the distortional strains were concentrated in the intracortical region under low fixation stiffness, however extended throughout the endosteal region under higher fixation stiffness. By 4 weeks, the strain had distributed to span the entire fracture region for the high stiffness fixations, however for low stiffness, it extended into the periosteal region (Figure 4.7). It may be seen that this influenced the development of cartilage tissue, with cartilage concentration increasing endosteally by 4 weeks under a higher fixation stiffness, whereas the increased cartilage resulting from low fixation was found in the periosteum. By 8 weeks, no cartilage remained in the higher fixation conditions, and for the low stiffness condition it was resorbed into the periosteal callus, with low concentrations remaining in the endosteal region. This was particularly interesting for the low stiffness fixation condition, as the periosteal cartilage did not transform to bone by 6 weeks and it instead appeared there was only soft tissue within the fracture gap. This result appeared to be consistent with findings in the literature, where high IFMs during the callus consolidation phase can prolong the healing

duration [67]. For the low fixation condition, this time translated to a slight increase in IFM over time (Figure 4.5) before healing was eventually continued.

Under constant fixation, IFM was initially at its peak when the callus completely comprised of soft tissue. It remained at this high level for the first 20 iterations, which was consistent with i*n vivo* monitoring of mechanical stability over the course of healing [65, 80]. Experimental models have shown that IFM peaks approximately one week postoperatively, and remains high over the first three to four weeks [65]. Over this time frame, only a small volume of periosteal callus was formed, both proximal and distal to the fracture region. As such, this hard callus development appeared to have very little influence on the mechanical conditions and resultant strain within the fracture gap. Changing the fixation stiffness at 7, 14 and 21 days all occurred during this plateau period, which essentially allowed healing to occur with limited delay compared to the more stable fixation (800 $N \cdot mm^{-1}$; Figure 4.8). Importantly, this demonstrated that the model does not describe the rate of healing based on the initial IFS, but rather the magnitude of strain later in the healing period affects the outcome more significantly [67].

Evidently there were limitations with both this investigation and the finite element model itself. Firstly, many experimental studies have determined that a higher loading causes larger external callus formation, however the influences on callus size cannot be assessed with this model [38, 59, 60]. The premise of a larger callus reducing strain within the fracture region therefore cannot be investigated thus there is no potential for early flexible conditions to enhance the healing through this mechanism. Wilson *et al*. [139] recently demonstrated that predefining a field of soft tissue in which callus can form strongly influences the strain field and thereby the predicted pattern of bone formation. They found that starting with only a thin layer of periosteal soft tissue and allowing bone and cartilage to grow within the callus domain produced tissue deposition patterns that were consistent with histological results, where the

callus growth appeared to radiate from the cortical surface of the fracture site. The authors suggested that this may be confirmed by testing alternative regulatory algorithms for the early stages of fracture healing.

Another limitation of the model shown in this study was that under-stimulation of the fracture, which occurs with overly rigid fixation, was not considered. It has been shown clinically that under-stimulation of a fracture may lead to a poor healing outcome, with in fact no callus formation [1], [116]. The present model was tested with an extremely rigid fixation of 5000 $N \cdot mm^{-1}$. The initial IFM in this conditions was already less than 0.1 mm, however direct intracortical bridging with a small volume of callus formation was observed during the simulation, demonstrating the clinically relevant limit of the model. Further to this, the geometry and loading applied to this model was simplified, with loads assumed to be acting axially with no additional inclusion of muscle loading.

The model may be enhanced by defining healing by a parameter other than the reduction of IFM to less than 0.1 mm. Whilst this forms a useful simple comparison of healing times for this predictive study, more information could be obtained about the healing process and the mechanisms in the model if the healing result could be alternately quantified. For example, if the changes in callus stiffness could be monitored along with the IFM, more data for the comparison of healing situations would be obtained. Despite the above limitations, conclusions about the current capabilities of the model cannot yet be made without the comparison with *in vivo* results, which forms part of the future work for this investigation.

Currently the model has been created based on experimental work and results from sheep studies [140], however it essentially represents universal rules and understanding of mechanobiology. The comparison between the FE model and the experimental study will not be performed in terms of finite healing times, but rather a qualitative comparison between the relevant phases of healing.

4.5 CONCLUSION

Further work with this numerical model will be carried out to qualitatively assess and compare the tissue distributions generated computationally at different stages of healing by comparing the model data to the histological analysis of rat femurs from *in vivo* studies. It can thus be determined if the biological processes implemented in the model are sufficient to predict accurate healing patterns. Initially, these comparisons will be made for the control groups where the fixation stiffness is constant throughout the entire healing period. All of the above suggest that present model needs to be further developed to enable predictions of clinical value in the future.

Chapter 5: The Influence of Modifying Fixation Stiffness on the Healing Outcome

5.1 INTRODUCTION

The majority of diaphyseal long bone fractures heal via the secondary bone healing process with the formation of an external callus. Secondary healing occurs in the presence of fracture interfragmentary movement (IFM) [170], with the magnitude of IFM being critical to healing outcome. The healing process is composed of several overlapping stages beginning with inflammation and the formation of a hematoma. Callus proliferation is the next stage of healing with the conversion of the hematoma to a soft callus composed primarily of fibrous tissue and cartilage. Simultaneously a hard callus is formed at the periphery of the fracture via intramembranous ossification. Callus consolidation follows whereby the soft cartilaginous callus undergoes mineralization via endochondral ossification, leading to bridging of the fracture. Finally, the callus is gradually remodelled and resorbed [32].

The size of the fracture callus formed is primarily related to the stability of the fracture site influenced by the fixation [78]. Extremely rigid fixation has been shown to suppress callus formation [171], whilst instability in the fracture resulting from overly flexible fixation may lead to the formation of a large callus that cannot bridge, resulting in a hypertrophic non-union [141]. Previous studies have determined that moderate axial IFMs consistently produce a reliable healing outcome [60, 79, 171, 172], characterised by the return of strength and function to the limb, as well as bony bridging across the cortices. The magnitude of IFM is determined by the stiffness of fixation, the degree of limb loading (a combination of weight bearing and muscle forces), as well as the mechanical competence of the healing tissues. Throughout the normal bone healing process, IFMs are largest during the initial stage of healing and reduce as the fracture callus increases in size and mineralises [172, 173].

Despite previous studies demonstrating that the mechanical environment plays a critical role in the development of fracture callus tissue [63, 145, 171, 172], it is not clear whether various stages or processes of repair are differentially mechano-sensitive. Therefore, remains unknown if mechanical stimulation is required during all stages of bone healing and how the optimal magnitude IFM may differ at various phases.

A number of experimental investigations have been conducted, analysing the modification of fixation stiffness over the course of healing [71, 73, 106, 108, 159, 174]. The focus of these studies has been on the concept of elastic dynamization, whereby the fixation stiffness is reduced at a certain time point during the healing process [71, 73, 106, 108, 159]. This increases the IFM of the fracture gap [108, 159], and has been tested both clinically and experimentally. Claes *et al*. [108] showed that elastic dynamization at 3 or 4 weeks in a similar rat model enhanced healing indicated by a greater elastic modulus of the callus, particularly when the callus was largely calcified and close to bridging, or at the remodelling stage of healing. However performing dynamization earlier in the healing period led to a poor healing outcome. As such, the benefits of dynamization and the optimal modulation time during healing remain unclear.

Through comparisons of healing under different degrees of stability, it has been established that very flexible fixation delays healing with respect to bony bridging and leads to the formation of a larger callus. Furthermore, it was previously concluded that the later chondral (cartilaginous) phase of healing was prolonged under more flexible conditions [67]. Based on this observation, it might be inferred that mineralisation of the callus and bridging are both impaired by excessive tissue strain, and that callus bony bridging requires stability. Hence, it may be beneficial to stiffen fixation during the callus consolidation phase, enabling ossification and bony bridging to occur.

The ability to modulate the stiffness of fixation provides the potential to enable mechanical stimulation during periods of healing when they are needed, and to shield the tissues from potentially disruptive loading when stimulation is not required [12]. Based on the influences theorised above, we hypothesise that it may be most beneficial to flexibly stabilise the fracture during the earlier stages of healing to promote larger callus formation, and to then increase fixation stiffness, allowing for callus maturation and remodelling to occur. More specifically, the predicted benefits of an initial flexible fixation which is later stabilised are (1) shortened healing time in comparison to very flexible fixation and healing time comparable or faster than optimum fixation, and (2) greater callus stiffness [12].

5.2 MATERIALS AND METHODS

5.2.1 Animal Model

Forty-eight male Wistar rats (weight 400–450 g) were randomly divided into six groups ($n = 8$) consisting of two control groups, a stiff fixation group (S group) and a flexible fixation group (F group), and four modulated experimental groups designated 3D, 7D, 14D and 21D. The experimental groups were fixed flexibly for 3, 7, 14 and 21 days respectively, followed by stiff fixation for the remainder of the 5-week healing period. Time points for transition from flexible to stiff fixation were been selected to correspond with different bone healing phases (Figure 5.1). The 3D group was selected to target the inflammation stage of the fracture healing process. The 7D group, with flexible fixation for 1 week followed by stiff fixation for 4 weeks, was aimed at assessing the effects after inflammation in the early phases of callus proliferation, with the 14D group assessing the late proliferation stage. The 21D group was selected to target the consolidation stage of healing.

5.2.2 Fixator Design and Construction

The fixator was designed by our collaborators at the Institute of Orthopaedic Research and Biomechanics, University Hospital of Ulm, and has been used in previous studies [105,

149, 150]. The unilateral external fixator (Figure 5.2) comprised bars (28 × 4.5 × 5 mm): a front-side component made of stainless steel and a back-side component made of aluminium, which clamp onto four threaded stainless steel pins (Jagel Medizintechnik, Bad Blankenburg, Germany) spaced 8 mm apart. For a stiff fixation, the inner bar of the fixator was set at an offset of 6 mm and for the flexible configuration the offset was set to 12 mm (Figure 5.2). The offset distance was defined as the free length of the pins, between the lateral surface of the femur of the rat and the inner side of the fixator bar. This resulted in an axial stiffness of 119 $N \cdot mm^{-1}$ for the stiff configuration, and 31 $N \cdot mm^{-1}$ for the flexible configuration [149, 150].

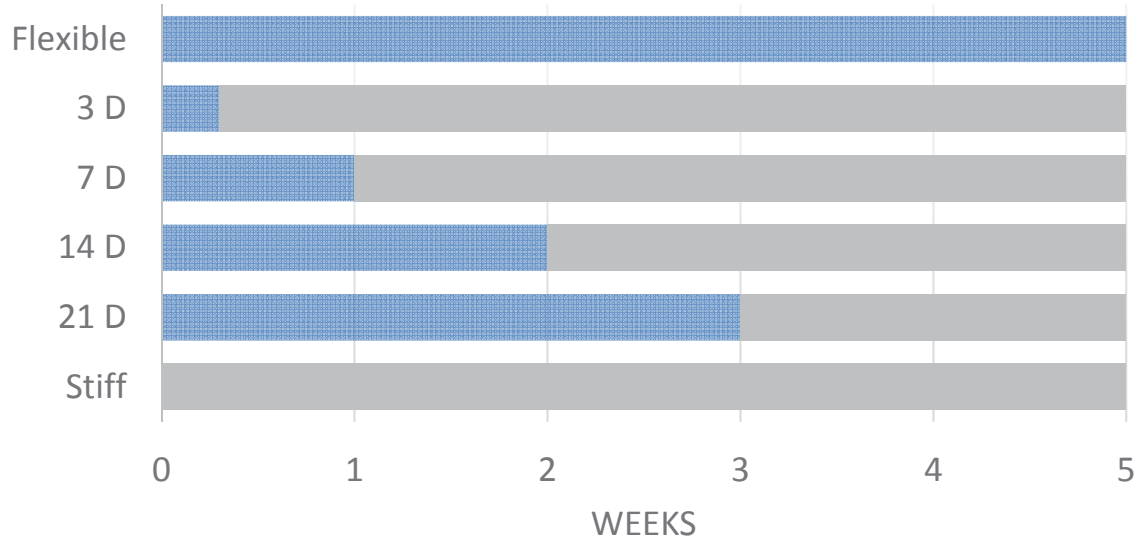

Figure 5.1 The four study groups (3D, 7D, 14D and 21D) with the stiff and flexible control group. In the study groups, the fixation was stiffened at 3, 7, 14 and 21 days, respectively.

5.2.3 Operative Procedure

The rats were anaesthetised with isoflurane (2 % with 2 $L \cdot min^{-1}$ O_2 by air mask). Preoperatively, a 5 mL subcutaneous injection of normal saline was administered along with an antibiotic and analgesic. The antibiotic clindamycin-2 -dihydrogenphosphate (Sobelin; Pfizer, Karlsruhe, Germany), was administered subcutaneously at 45 $mg \cdot kg^{-1}$ prior to surgery, and at three days postoperatively. The analgesic tramadol (Tramal; Gruenenthal, Aachen,

Germany) was administered subcutaneously at 20 $mg \cdot kg^{-1}$, and was diluted in the drinking water of each animal at 25 $mg \cdot L^{-1}$ for three days postoperatively.

An incision of 3-4 cm was made through the skin, and the shaft of the femur was exposed. An external fixator bar with drill guides was used to permit reproducible positioning of four drill holes, to accommodate the screws used to secure the fixator. After the fixator was in place, a saw was used to make a 1 mm osteotomy (Figure 5.3). The wound was then closed in layers. A detailed surgical procedure can be found in Appendix A.

Animal care and experimental protocols were followed in accordance with the National Health and Medical Research Council (NHMRC) guidelines and approved by the Animal Ethics committee of Queensland University of Technology.

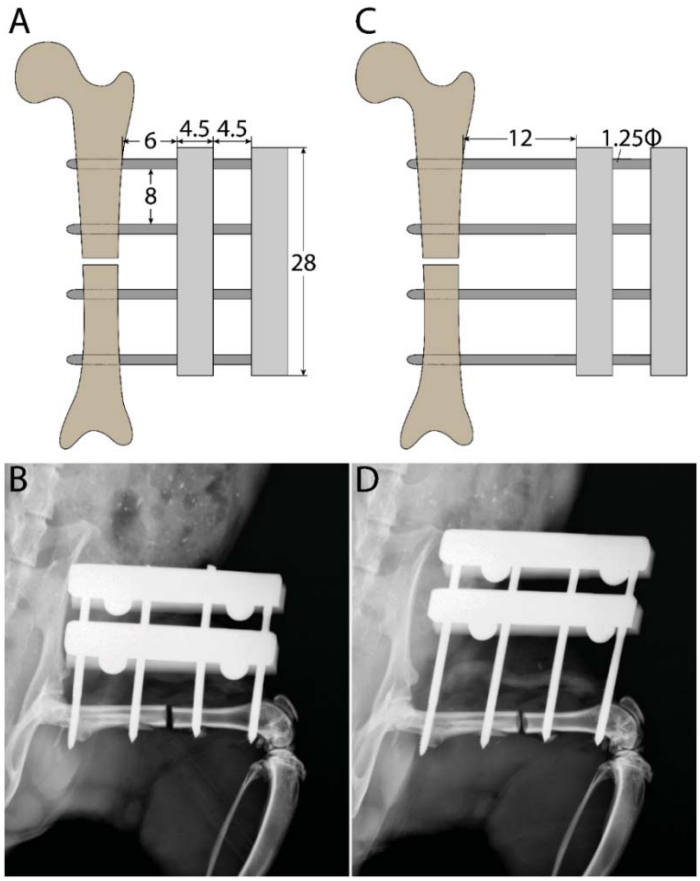

Figure 5.2: Fixator constructs demonstrating offset difference between stiff and flexible configurations A) schematic of stiff construct with 6 mm offset; B) postoperative *in vivo* radiograph of stiff construct; C) schematic of flexible construct with 12 mm offset; and D) postoperative *in vivo* radiograph of flexible construct.

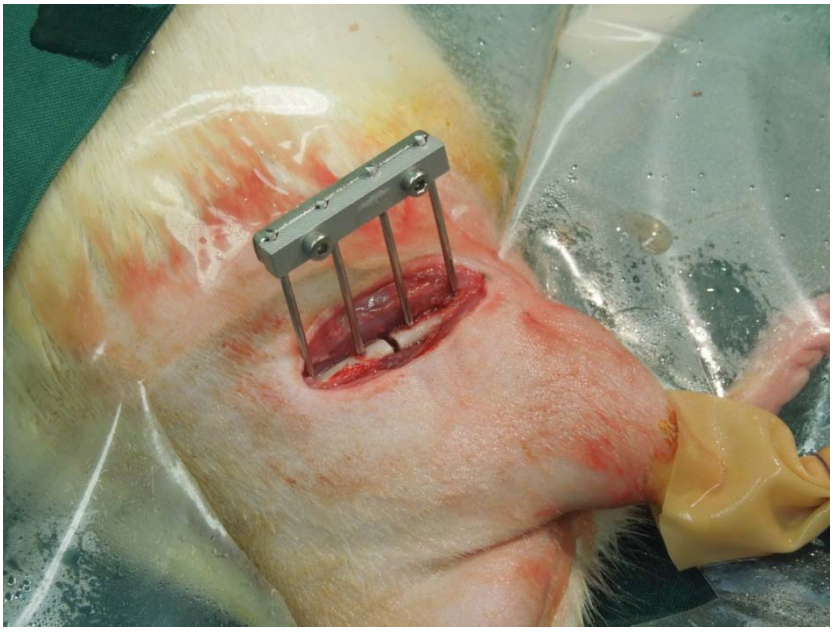

Figure 5.3: Attachment of external fixation to femur and creation of 1 mm osteotomy.

Each animal was housed in its own cage, with mobility and signs of infection monitored daily. Immediately after surgery, the rats were given unrestricted access to food and water and resumed normal activity. The rats were given the analgesic tramadol (25 $mg \cdot L^{-1}$) via their drinking water for three days post-operatively, and an antibiotic by subcutaneous injection, as described above.

In the four experimental groups, the fixator offset was decreased from 12 mm to 6mm (Figure 5.2) under anaesthesia after 3, 7, 14 and 21 days respectively. After 35 days, the rats were euthanised. This time point was expected to represent bony bridging in this model.

5.2.4 Biomechanical Testing

After 35 days of healing, all rats were euthanised by carbon dioxide (CO_2) asphyxiation. Femurs were then dissected, with all soft tissue removed. The contra-lateral limbs were used as paired internal controls. The flexural rigidity of the experimental femur was evaluated using a non-destructive three-point bending test (Figure 5.4). The fixator and pins were removed before mechanical testing. The femurs were potted in cylinders with polymethylmethacrylate

(PMMA) (Paladur, Heraeus Kulzer GmbH, Hanau, Germany) with a 30 mm free length (l) between the bending supports for the bone. Bending was applied at the level of the osteotomy, in the anterior–posterior direction.

The load was applied with a materials testing machine (Instron 5848 MicroTester; Instron, Norwood, MA) at a deflection rate of 1 mm·min^{-1} to a maximum force of 10 N [107]. During the protocol, the bone was hydrated with a 0.5 % NaCl solution. The bending load (F) was applied on top of the callus and was recorded continuously versus sample deflection (d). Flexural rigidity, a product of Elastic Modulus (E) and second moment of inertia (I): EI, was calculated from the slope, k, of the linear region of the load–deflection curve. As the callus was not always located at the middle of the supports (l/2), the distances between the load and the proximal support (a) and the distal support (b), were used to calculate the flexural rigidity according to (Equation 5.1):

$$EI = k\left(\frac{a^2 b^2}{3l}\right) \tag{5-1}$$

Where:

$E =$ Elastic $Modulus$

$I = Second\ moment\ of\ Area$

$k = slope\ of\ load - deflection\ curve$

$l = free\ length\ between\ bending\ supports$

$a = distance\ from\ centre\ osteotomy\ to\ proximal\ support$

$b = distance\ centre\ osteotomy\ to\ distal\ support$

The bending load was applied three times, with the first two tests necessary to condition each sample, and the third application used for the measurement, thus minimising potential artefacts resulting from contact settlements. The flexural rigidity was then reported as a percentage of the intact contralateral limb.

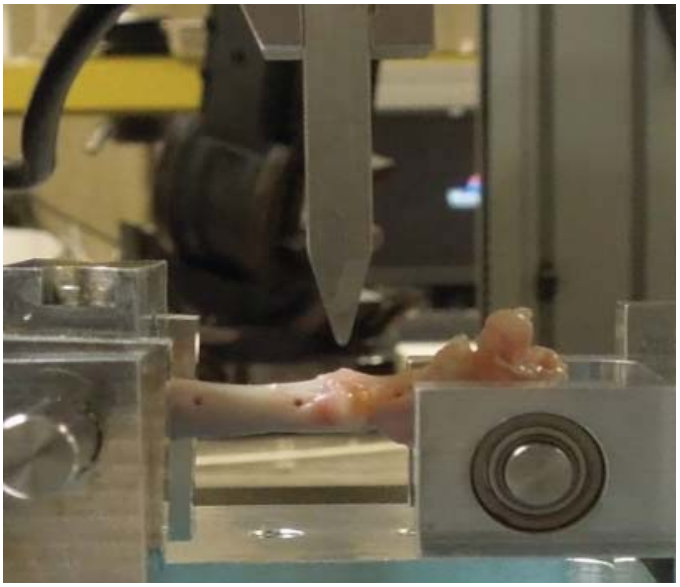

Figure 5.4: Three point bending test of callus.

5.2.5 Micro-computed Tomography

Femora were scanned using a micro computed tomography (μCT) scanner (μCT40; Scanco Medical, Bassersdorf, Switzerland), with a 20 μm isotropic voxel size and a 250 ms integration time, at 70 keV of energy. Two volumes of interest (VOI) were selected for analysis using the μCT evaluation software (V6.5-3, Scanco Medical, Bassersdorf, Switzerland)[107]. The first, VOI_{callus} included the callus between the two inner pins of the fixator, subtracting the cortical bone. The second, $VOI_{fracture}$ encompassed only the callus formed at the level of the osteotomy. To evaluate these regions of interest, the following variables were assessed: total callus volume (TV), mineralised bone tissue volume (BV), and bone volume over total volume (BV/TV). Additionally, average callus diameter was calculated at the level of the osteotomy. Bone mineral density (BMD) was calculated after conversion of the gray-level values using a correction algorithm [107].

5.2.6 Histology and Histomorphometry

Femora were fixed for histological analysis in 4 % paraformaldehyde and then dehydrated in ascending grades of ethanol, infiltrated, and embedded in methyl methacrylate (MMA) (Technovit 9100, Heraeus Kulzer, Germany). Samples were sectioned in the

longitudinal direction and stained with paragon [109], which enables differentiation between fibrous tissue (white and light blue), cartilage (purple), and bone (white-yellow). Quantitative histomorphometry was performed using light microscopy to analyse tissue differentiation in two regions of interest (ROI). The ROI_{callus} included the complete outer diameter of the periosteal callus in the radial direction and extended 2 mm proximally and distally from the centre of the gap. The $ROI_{fracture}$ included the complete outer diameter of the periosteal callus in the radial direction but was limited in height to the fracture gap. The cortical bone was excluded from both ROIs. The total callus area was measured using OsteoMeasure (OsteoMetrics, Atlanta, USA) and the proportions of bone, cartilage and fibrous tissue were quantified. The number of animals achieving bony bridging in the periosteal, intracortical and endosteal regions was counted and a bridging score from 0 to 4 was calculated based on the number of bridged cortices [109].

5.2.7 Data Analysis / Statistics

Statistical analysis was performed using SPSS 21.0, to determine differences in the mechanical, μCT and histological parameters. Analysis of variance (ANOVA) tests were used to assess differences, with a post-hoc test (Tukey) used to determine inter-group relationships, with p-values < 0.05 taken as significant. Data are presented as the mean with error bars indicating the standard deviation

5.3 RESULTS

The animals tolerated the experimental procedure. Pin breakage occurred in three animals reducing the sample size of the stiff group ($n = 7$); the 3D group ($n = 7$) and the 14D group ($n = 7$). At the time of operation, the rats weighed an average of 438 ± 26 g. The average increase in body weight from the time of operation to 5 weeks postoperatively was 19 ± 2 %.

5.3.1 Biomechanical Testing

No significant difference was determined between the flexural rigidity of the contralateral limbs of the stiff, flexible and experimental groups (data reported in Table 5-1). The flexural rigidity (% of intact contralateral) of the S group was found to be 150 % greater than the F group ($p = 0.001$). The flexural rigidity of all four experimental groups was significantly different ($p < 0.015$) to the flexible control group Figure 5.5) with the 3D group showing 159% greater; 7D 186% greater; 14D 145% greater and 21D 116% greater rigidity. No significant difference was determined in the flexural rigidity between any of the experimental groups and the stiff control group (Table 5-1).

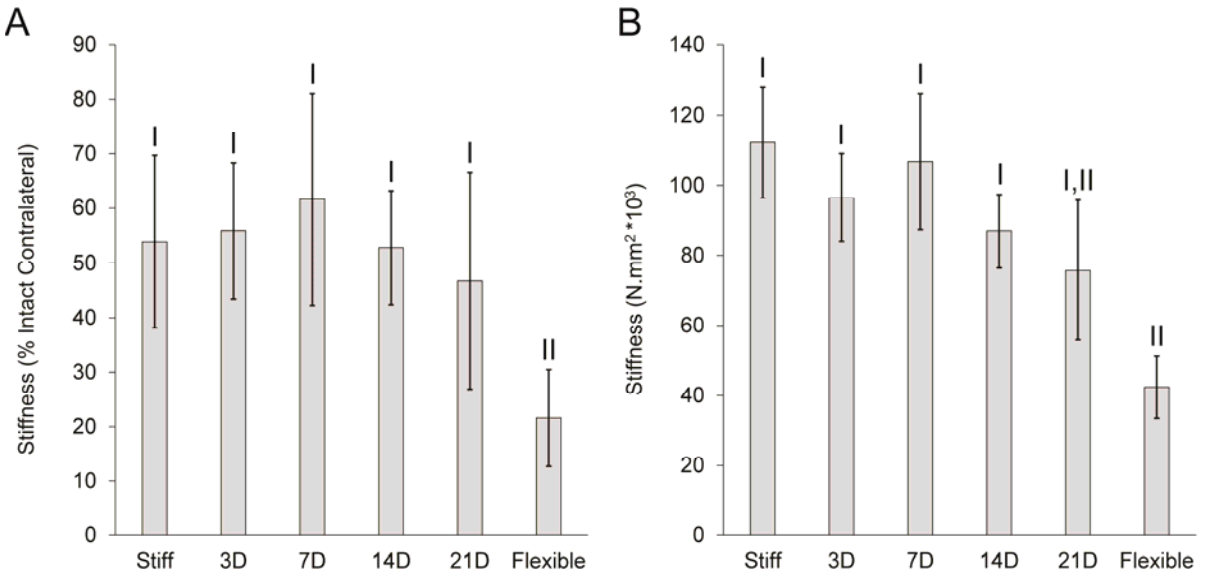

Figure 5.5 Effect of the modulation of stiffness from flexible to stiff (3, 7, 14 and 21 days) on bone healing, evaluated by 3-point bending. A) Flexural rigidity of the callus normalised to the contralateral limb, and B) absolute flexural rigidity. $p < 0.05$ was considered significant. Significantly different groups indicated by different symbols (I and II).

5.3.2 Microcomputed Tomography

The flexible group showed characteristics of the least advanced healing of all groups; a large periosteal callus, incomplete periosteal and intracortical bony bridging, and substantial endosteal bony callus (Figure 5.7). The stiff control and experimental groups in contrast showed

signs of complete bony bridging and remodelling with formation of a neo-cortex in the periosteal callus and resorption of endosteal callus and re-establishment of marrow canal.

The flexible group possessed the largest callus (106 mm^3) at 5 weeks in the ROI_{callus}. Total callus volume (TV) was 31% less in the 3D ($p = 0.026$), 31% less in the 14D ($p = 0.033$) and 36% less in S group ($p = 0.008$) than in the F group, but not significantly less in the 7D and 21D groups (Figure 5.6). Bone volume tended to be largest in the 21D and F groups, but there were no significant differences in the bone volume. The BMD in the flexible group was found to be significantly lower compared to all other groups across the entire callus ($p < 0.042$). No other statistically significant parameters were found when assessing the entire callus.

In the fracture gap, the volume was 27 % less in the 3D ($p = 0.024$); 24 % less in the 7D ($p = 0.043$); 31 % less in the 14 D ($p=0.007$) and 30 % in the S group ($p = 0.01$) than the F group. The 21D group showed no differences in this parameter compared to any other group. The BV/TV was found to be significantly higher in the 3D, 7D and stiff group ($p < 0.01$) compared with the flexible group, with no observable differences with the 14D and 21D groups (Table 5-1). The BMD in the F group (706 mgHA/cm^3) measured at the level of the osteotomy ($ROI_{fracture}$) was significantly lower compared to all experimental groups ($p < 0.03$) but not compared to the S group. The BMD in the 14D group (927 mgHA/cm^3) was significantly greater than the 21D group (818 mgHA/cm^3, $p = 0.047$) and the stiff control group (806 mgHA/cm^3, $p = 0.027$).

5.3.3 Histology and Histomorphometry

Defects stabilized for 5 weeks under flexible conditions contained a prominent band of cartilage throughout the osteotomy in all animals (Figure 5.9). Correspondingly, the largest cartilage area (1.8 mm^2) was determined in the F group (Figure 5.8). Cartilage area was 85% less in S group, 80% less in the 3D, 90% less in the 7D, 92% less in the 14D and 65% less in the 21D group ($p < 0.002$) than in the F group, when assessed throughout the entire callus.

The S group was characterized by a high degree of periosteal and intracortical bridging (79%) compared to the F group (25%). The highest bridging score was determined in the 7D (94%) and 14D (96%) groups. Resorption of endosteal callus is a sign of advanced healing, 1/7 animals in the 14D group and 3/8 animals in the 7D group were still bridged endosteally compared to 7/8 in the F and 3/7 in S control groups (Table 5-2).

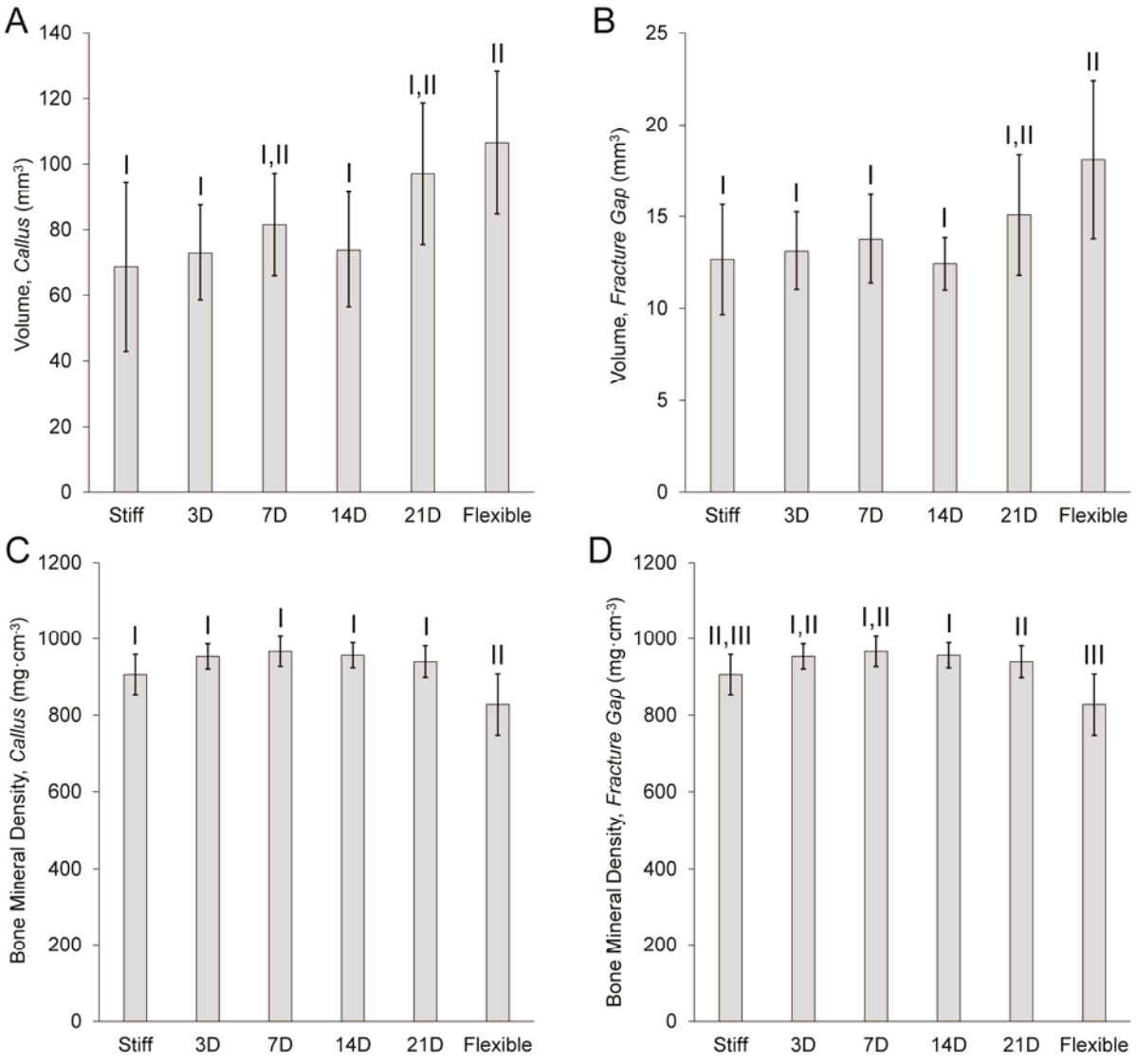

Figure 5.6 Effects of the modulation of stiffness from flexible to stiff (3, 7, 14 and 21 days) on bone healing evaluated by μCT. A) Total volume of the fracture callus; B) volume of the fracture gap; C) bone mineral density throughout the entire callus, and; D) bone mineral density in the fracture region. $p < 0.05$ was considered significant. Significantly different groups indicated by different symbols (I, II and III).

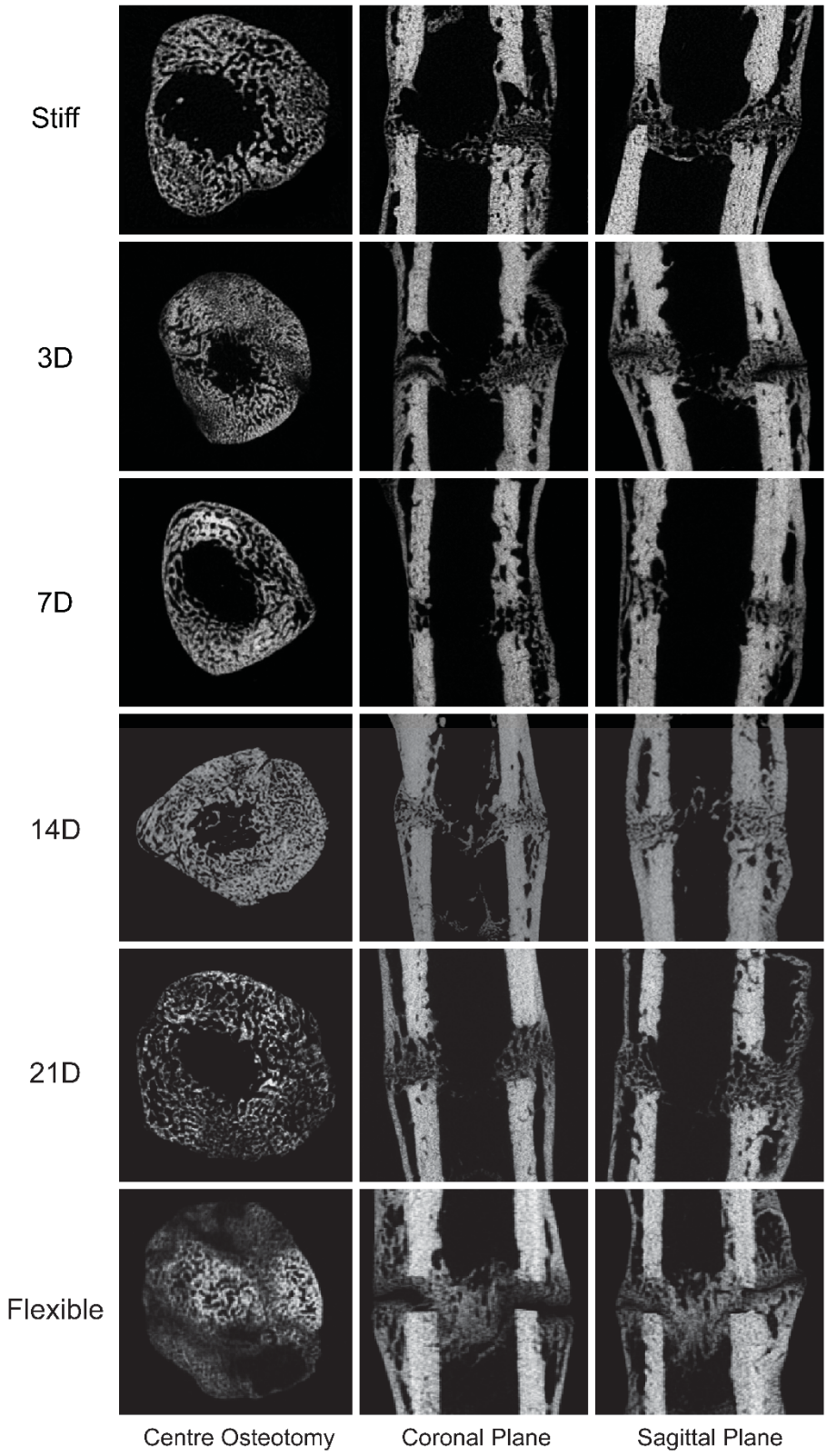

Figure 5.7 Micro-computed tomography images of the osteotomies at 35 days post-operatively, after modulation of stiffness from flexible to stiff at 3, 7, 14 and 21 days post-operatively and compared to stiff and flexible controls.

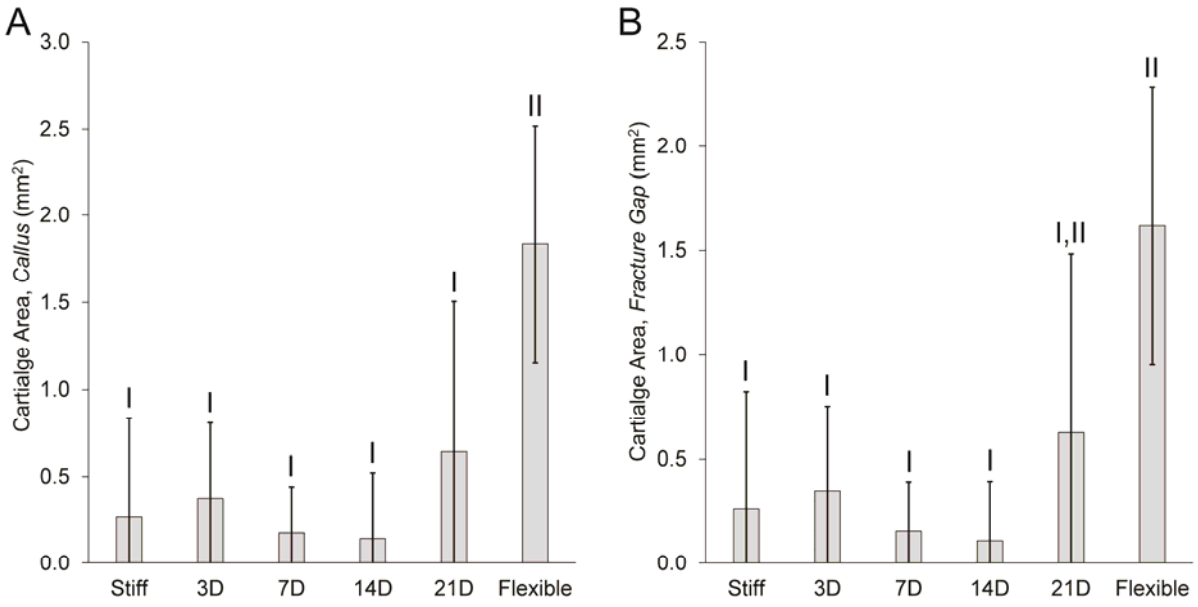

Figure 5.8 Effects of the modulation of stiffness from flexible to stiff (3, 7, 14 and 21 days) on bone healing, evaluated by histomorphometry. A) Cartilage area quantified throughout the entire callus, and; B) cartilage area throughout the fracture gap. $p < 0.05$ was considered significant. Significantly different groups indicated by different symbols.

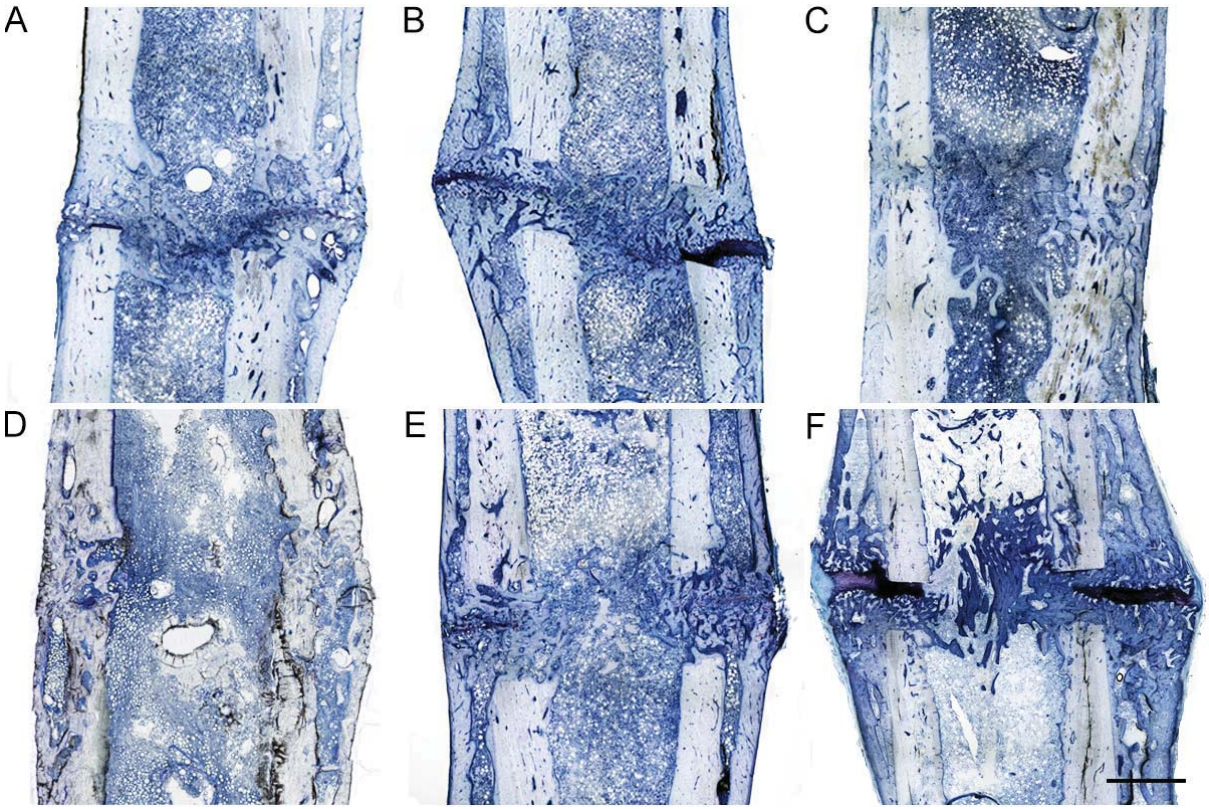

Figure 5.9 Histological images at 35 days post-operatively after stabilisation with stiff and/or flexible fixators, and modulation of stiffness from flexible to stiff at 3, 7, 14 and 21 days. A) Stiff group; B) 3D group; C) 7D group; D) 14D group; E) 21D group and F) flexible group. Histological sections were stained with paragon: fibrous tissue (white and blue), cartilage (purple), and bone (light blue-white). Scale bar indicates 1 mm.

Table 5-1 Three-point bending and micro-computed tomography results (mean ± standard deviation) determined after 35 days of healing

Measure	S	3D	7D	14D	21D	F
Flexural Rigidity ($kNmm^2$)						
Operated Femur	112 ± 39	96 ± 21	107 ± 33	87 ± 12	76 ± 29	42 ± 16
Intact Femur	204 ± 30	174 ± 7	174 ± 13	164 ± 26	165 ± 20	203 ± 26
Percent Intact Contralateral	54 ± 16	56 ± 12	62 ± 19	53 ± 10	47 ± 20	22 ± 9
Total Volume (mm^3)						
Callus	68.6 ± 25.8	73.0 ± 14.5	81.5 ± 15.6	73.9 ± 17.5	97.1 ± 21.5	106.5 ± 21.7
Fracture Gap	12.7 ± 3.0	13.1 ± 2.1	13.8 ± 2.1	12.4 ± 1.4	15.1 ± 3.3	18.1 ± 4.3
Bone Volume (mm^3)						
Callus	49.4 ± 15.3	52.8 ± 9.8	57.5 ± 12.5	48.8 ± 10.7	64.3 ± 22.0	68.7 ± 24.4
Fracture Gap	9.2 ± 2.8	9.0 ± 1.8	9.6 ± 2.2	7.7 ± 0.8	9.3 ± 2.8	9.0 ± 4.1
BV/TV						
Callus	0.73 ± 0.09	0.73 ± 0.04	0.70 ± 0.04	0.66 ± 0.05	0.65 ± 0.10	0.63 ± 0.13
Fracture Gap	0.72 ± 0.10	0.68 ± 0.05	0.69 ± 0.05	0.62 ± 0.09	0.61 ± 0.10	0.47 ± 0.15
Bone Mineral Density ($mgHA \cdot cm^{-3}$)						
Callus	907 ± 52	954 ± 33	967 ± 39	957 ± 32	940 ± 41	828 ± 80
Fracture Gap	806 ± 73	831 ± 63	841 ± 67	927 ± 14	818 ± 70	706 ± 99

Table 5-2 Histomorphometry results (mean ± standard deviation) determined after 35 days of healing.

Measure	S	3D	7D	14D	21D	F
Callus Diameter (mm)						
Total Area (mm^2)						
Callus	9.5 ± 3.4	13.0 ± 1.9	12.9 ± 3.2	11.2 ± 3.1	15.1 ± 4.2	17.9 ± 2.0
Fracture Gap	4.6 ± 2.1	6.6 ± 1.7	4.8 ± 1.3	4.5 ± 0.9	6.5 ± 1.3	7.4 ± 1.3
Bone Area (mm^2)						
Callus	6.1 ± 2.1	8.8 ± 1.4	8.4 ± 2.4	7.7 ± 2.4	8.9 ± 3.2	10.8 ± 2.0
Fracture Gap	2.4 ± 1.2	3.8 ± 1.1	2.8 ± 1.0	2.5 ± 0.4	3.4 ± 1.4	3.4 ± 1.1
Fibrous Tissue Area (mm^2)						
Callus	3.2 ± 1.3	3.9 ± 0.7	4.3 ± 1.1	3.4 ± 1.2	5.6 ± 1.8	5.3 ± 0.9
Fracture Gap	2.0 ± 0.7	2.5 ± 0.6	1.8 ± 0.7	1.8 ± 0.8	2.4+1.1	2.4 ± 0.7
Cartilage Area (mm^2)						
Callus	0.3 ± 0.6	0.4 ± 0.4	0.2 ± 0.3	0.1 ± 0.4	0.6 ± 0.9	1.78 ± 0.7
Fracture Gap	0.3 ± 0.6	0.3 ± 0.4	0.2 ± 0.2	0.1 ± 0.3	0.6 ± 0.9	1.6 ± 0.7

Table 5-3 Number of animals achieving bony bridging after 5 weeks of healing.

Measure	S	3D	7D	14D	21D	F
Total % bridging (periosteal + intracortical)	82	71	94	96	66	25
Endosteal callus bridging (%)	43	57	38	14	38	88

5.4 DISCUSSION

In the treatment of fractures, the stiffness of fixation is typically unchanged over the course of healing. Experimental studies have demonstrated that timely fracture healing requires the optimisation of fixation stability [79]. In cases of overly rigid fixation, dynamization may be performed to stimulate callus formation and healing [108, 175, 176]. If healing is delayed through excess strain, the formation of a hypertrophic non-union may result, which may be rectified by stiffening the fixation [71, 159]. In these cases, the modulation of fixation is in response to an adverse healing progression. It has been proposed that fracture healing maybe further optimised through the purposeful conversion of fixation from a flexible to stiff configuration [12]. This study investigated the influence of modulation of fixation from a flexible to a stiff configuration on the healing of a rat osteotomy model. Time points of modulation were selected corresponding to the early, mid and late phases of callus healing.

5.4.1 Stiff versus Flexible Control

Before discussing the results from stiffening fixation, it is first necessary to characterize the degree of stability provided by the stiff and flexible fixators and describe healing in the respective control groups. The terminology frequently used (rigid, semi-rigid, stiff, flexible) to label fixation groups of differing stiffness [105, 106] is not ideal in this case, and rigid and stiff fixation may be misinterpreted as creating absolute stability, typically associated with primary bone healing. Interfragmentary strain (IFS) is a useful description of the mechanical environment that relates interfragmentary movement to gap size [63]. IFM may then be

estimated from knowledge of the external and internal loads and fixation stiffness. The peak axial load in the rat femora during gait (6-8 times body weight) has been calculated with musculoskeletal modelling [174]. This yields initial interfragmentary movements of 0.25 and 1 mm (25 % and 100 % IFS for a 1 mm osteotomy) for the stiff and flexible fixation groups respectively, assuming an average weight of 430 g. Interfragmentary strains that lie within the range of 7 – 30% have been previously shown to support good healing [172]. Hence, the stiff fixator was expected to create mechanical conditions conducive to timely healing, whilst the flexible fixator was overly flexible and should delay healing. In the present study, both control groups were characterised by the formation of external callus and secondary bone healing, and supported the above mentioned assumption. At 5 weeks, fractures treated with the stiff fixator were biomechanically superior and morphologically more advanced than the flexible group, exhibiting bony bridging, a resorbing periosteal callus and the re-establishment of a marrow canal. In a concurrent study, fracture callus stiffness was monitored *in vivo* and determined that maximum callus stiffness was achieved at 4 weeks with the stiff fixator compared to 9 weeks with the flexible fixator [105]. Therefore, the fixation of the stiff group can be considered to provide constant fixation within a good range whilst the flexible fixator may be considered overly flexible.

5.4.2 Modulation from Flexible to Stiff Fixation

The predicted benefits of modulating the fixation stiffness (flexible to stiff) are (1) greater callus stiffness and (2) shortened healing in comparison to very flexible fixation and healing time comparable or faster than optimum fixation [12].

(1) Greater Callus Stiffness

Callus size increases with more flexible fixation [177]. It was hypothesized that flexible fixation during the proliferative phase of healing and subsequent stiffening of fixation would lead to increased callus size and translate into greater callus stiffness. As expected the callus

formed in the flexible group was the largest but was biomechanically inferior as it was not completely bony bridged and contained less dense bone and a greater proportion of cartilage. Stiffening fixation at all time-points significantly increased callus stiffness compared to the flexible group. However the callus stiffness in the modulated groups was comparable to that achieved with constant stable fixation in the stiff group. Greater callus stiffness through modulation from flexible to stiff fixation could not be confirmed by this study.

(2) Shortened Healing Time

During the course of secondary bone healing the callus passes through a number of distinctive stages [178]. The stage of healing can be distinguished through examination of morphological data from μCT and histology. As stated above, healing the flexible group lagged significantly behind healing in the stiff group and experimental groups. The differences between the experimental groups and the stiff control group were less pronounced and are discussed below with respect to early, mid and late time-points of modulation.

Early Modulation

The treatment in the 3D group differed from the stiff control group in that flexible fixation was applied for only the first three days out of the 5 week healing period. Biomechanical and morphological results demonstrated that early modulation did not affect healing outcome compared to the stiff control. Previous studies have suggested that the initial phase of bone healing is particularly sensitive to mechanical stimulus, and the mechanical environment during this phase may direct the healing process [179]. Early instability for as little as 24 h was sufficient to influence chondrocyte differentiation, resulting in more cartilage formation at 10 days post-operatively [180]. Any effects created by very flexible fixation initially in this study had no significant impact on the state of healing at 5 weeks.

Mid Modulation

Stiffening fixation during the middle of the repair phase, groups 7D and 14D, produced morphological characteristics that were suggestive of the most advanced healing state of all groups. Notably, these groups had a high degree of callus bridging (periosteal and intracortical), with a low degree of endosteal bridging which is associated with callus remodelling and reestablishment of the marrow canal. The bone mineral density (BMD) in the fracture gap of the 14D group was also significantly greater than the stiff control group. In an apparent contradiction to this result, the mean of bone volume to total volume (BV/TV) was higher in the Stiff group compared with the 14D. This may be explained however by the unusual callus remodelling observed in rodents, and the formation of a double cortex [181]. As healing progresses, woven bone is remodelled into lamellar bone and hence BMD increases, approaching the value of mature cortical bone. In contrast to BMD, BV/TV can be expected to increase as the callus mineralisation reaches a peak prior to the onset of callus resorption during remodelling. The un-mineralised space between the two cortices decreases the apparent BV/TV of the callus as remodelling progresses. This may explain why the 14D group has a larger BMD than the stiff control group, yet a lower BV/TV and indicates a more advanced state of repair in the 14D group.

Late Modulation

Stabilisation after 21 days significantly improved healing with respect to the very flexible fixation, demonstrating that delayed healing can be prevented by providing stability to an unstable situation. The 21D group did not differ significantly from the stiff group but the biomechanical values tended to be lower and the cartilage area was larger in this group. This supports the theory that decreased callus strain due to increased stability of fixation permits cartilage mineralisation and accelerates bony bridging.

This study is the first to investigate the controlled modification of fixation stability, with initial flexible conditions followed by stiffening the fixation as different time points throughout healing of an experimental fracture. Prior studies have investigated the influence of time of stabilisation on fracture healing [182]. However, this involved going from a scenario of no fixation and instability to fixation and therefore was more akin to the situation of delayed presentation or treatment. Miclau *et al*. [180] demonstrated that there was a trend towards more cartilage formation with delayed fracture stabilization, suggesting that early instability for as little as 24 h may be sufficient to influence chondrocyte differentiation. This trend appeared to be shared by our results, with more cartilage present in the 3D and flexible groups at 5 days than the stiff group. However beyond this, the models differ too much for further comparison or extrapolation of results.

Studies have addressed the conversion from external fixator to intramedullary nail or internal fixation [183]. Whilst this typically stiffens fixation, the second surgery impacts the biology of repair, which has been shown to further delay healing. The most similar biomechanical situation to that presented herein was conducted by Gardner *et al*. [61] who demonstrated that a reduction in the IFM applied to a fracture site over the course of healing could result in a more rapid maturation of callus tissue. It demonstrated in that sufficient mechanical stimulus is essential early in the healing period for tissue proliferation and reduced throughout the process to avoid tissue damage which can arise from large displacements that exceed the maximum strain tolerance of the tissue. The method applied in this study differs from our approach of altering the fixation stiffness, however the rationale is very similar and closely aligns with the results obtained in this thesis. Unfortunately a suitable healing control with constant fixation stiffness was lacking, limiting the usefulness of the obtained results.

A number of limitations were identified regarding the *in vivo* study design. Firstly, the evaluation of healing through mechanical testing to obtain flexural rigidity. Mechanical testing

in rodent bones is difficult to execute accurately due to difficulties in alignment and embedding resulting from the small size of the bones. A recent analysis of biomechanical testing methods concluded that three point bending tests are highly sensitive to callus shape and may induce experimental errors of up to 60 % [163]. Torsional testing may provide a more robust alternative method, however gaining access to the equipment necessary to facilitate this testing may also prove to be difficult.

Early fracture healing studies were primarily based on large animal models [147], particularly in sheep [40, 58, 61]. As a consequence, parameters used to assess healing are generally based on these studies, which may not be related directly to fracture healing in small animal models. In particular parameters such as bone volume/total volume (BV/TV) can be skewed in small animals by the remodelling process. Remodelling of small animal fractures tends to originate at the cortical bone surface [184]. This forms a dual cortex rather than remodelling from the periphery of the callus as seen in larger animals [79]. Therefore as healing proceeds, there should be an observable increase in this parameter, which declines after the initiation of remodelling (Figure 5.10). BMD on the other hand, is a parameter that would be expected to increase until restoration of the density of the original cortical bone.

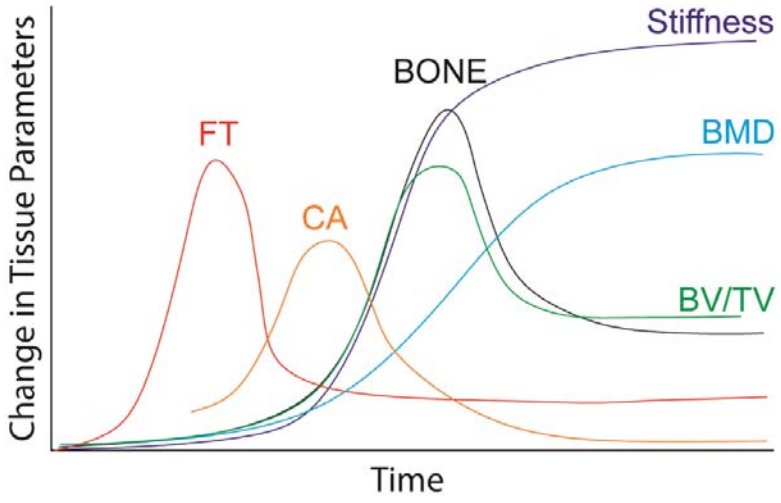

Figure 5.10 Expected changes in tissue and analytical parameters over the course of healing in a rat model. Where FT - Fibrous Tissue; CA – Cartilage Area; BMD – Bone Mineral Density and BV/TV – Bone Volume over Total Volume.

The fixation system used in the present study created defined stability and permitted modulation of the stiffness of fixation without the need for surgical intervention and the subsequent impact on the biology of the tissue. However, limb loading remained an uncontrolled variable. The rat model, due its relatively low-cost and short healing time, is useful in studies such as this where multiple time points are investigated. Ultimately, the findings of this study must be confirmed in a large animal model that can overcome the limitations and challenges with respect to controlled mechanical conditions, monitoring of healing and biomechanical testing.

Evidently this study, which is limited in addressing a single end point of 35 days, was not comprehensive enough to detect an accelerated rate of healing. Thus, multiple time points evaluating the course of healing will be necessary to provide an understanding of the different healing patterns between these fixation conditions, which could lead to an improved understanding of bone regeneration.

5.5 CONCLUSION

Overall, it was demonstrated that stiffening a flexible construct realizes an improved healing outcome, resulting in comparable tissue formation to that achieved through stable fixation. Although some effects of modulation of fixation stiffness during healing were demonstrated, it was not possible to isolate the effects of callus size itself on when assessing only the healing outcome. Further investigations of this phenomenon in large animal models may yield clinically relevant data. Whilst some studies have suggested that the mechanical conditions during the initial stage of healing may define the healing path and outcome, this study has shown at all time-points the benefits of stabilizing a flexible construct to achieve timely healing. Concurrently, we have shown that modulation of fixation stability is a potential avenue for improvement of healing by manipulating the local environment and promoting favourable strain conditions.

Chapter 6: The Influence of Modifying Fixation Stiffness on Callus Development

6.1 INTRODUCTION

Both clinical and research investigations have confirmed that bone healing depends on the mechanical conditions at the fracture site [9, 11, 14, 67, 82, 166, 185, 186]. Defining an optimal set of mechanical conditions to promote osseous healing has the potential to contribute to clinical device design optimisation and the selection of optimal patient fracture treatments relative to specific injuries.

Presently, our understanding of bone repair suggests that this is a multifaceted process that involves complex interactions between mesenchymal stem cell types that are located in the marrow, cortex, periosteum, and in the surrounding bone and fracture environment. Loading conditions of the fracture influence the differentiation of these cells, resulting in the formation of the various connective tissues that compose skeletal organs [26, 30, 181, 187]. Histological examination of fracture repair may reflect the interaction of the mechanical environment and the healing tissues, which is essential to complete our understanding of the processes that re-establish the biomechanical competency and the original tissue structure of the injured bone [165].

Callus size and development, and subsequently tissue morphology and biomechanics, may hence be influenced by mechanical stimulus throughout all stages of tissue development and maturation. Several theories outlining the mechanical stimulus responsible for guiding the formation of different tissue types have been presented. These stimuli include shear strain and interstitial fluid flow [118, 137], strain and hydrostatic pressure [11], tensile strain and hydrostatic pressure [38], and shear strain only [64, 123]. These theories have been

predominantly tested using computational simulations, which estimate the mechanical environment, thereby predicting the healing outcome. However, somewhat contradictory results have been produced [125, 188] that question the reliability of these models as predictive tools.

Further *in vivo* investigations are thus required to more completely assess the effects of the mechanical environment throughout the healing process, and obtain further information that in turn can be implemented into numerical simulations, enhancing their capabilities. The outcome of *in vivo* experiments are often reported by way of histological images, either at the end-point of healing, or at different time points post-operatively, providing accurate qualitative histological descriptions and outcomes [85, 166]. Histological sections can show an intricate pattern of different tissue types. Depending on the harvesting time the tissues observed can include the haematoma, fibrous tissue, cartilage, mineralised callus and newly formed bone. The majority of studies have focused on differences in the early phases of healing [180], late phases of healing [184], in the development of non-union models [189, 190] or in different biological treatments [191-195]. Few studies have investigated different healing patterns under different fixator conditions throughout the entire healing period [67, 196].

Investigations in temporal tissue formation and distribution could provide key information when assessing the optimal mechanical environment for fracture healing. It has been hypothesised that the ability to modify the fixation stiffness could promote large callus formation under initial flexible conditions, which is then later stabilised to allow callus consolidation and mineralisation to occur. A model where fixation stiffness was modified from a flexible to a stiff configuration throughout healing in a rat femoral osteotomy to assess the effect on the healing outcome was previously presented (Chapter 5).

Flexible fixation was changed to stiff at 3, 7, 14 and 21 days postoperatively, to stabilise the fracture and thus decrease strain in the intracortical space, allowing callus mineralisation

to occur. The total healing response was evaluated after 5 weeks. The study found that whilst fixator modification was able to produce comparable outcomes to the stiff control, additional healing was not achieved. Overall, whilst being unable to demonstrate advantage over an ideal stiff fixation, the previous results showed that the latent stabilisation of an undesirably flexible fixation may produce comparable healing. This result was contradictory to current literature, which suggests the healing pathway and outcome are defined by the initial fixation conditions [65, 98]. I conversely was able to demonstrate that stable fixation although occurring later in the healing process, could still produce equivalent results to optimal fixation. This study alone was not able to assess the rate of healing as it only examined a single end time-point in the healing response, and consequently further investigation was required to test this hypothesis.

The aim of this study was therefore to assess tissue formation during the course of healing of the stiff and flexible fixation conditions, and to compare these with modified fixation stiffness at 3 and 7 days post-operatively. In this case, particular focus was given to the early stages of fracture repair, with time points at 5, 14 and 28 days post-operatively. Tissue distribution and topological patterns will be described qualitatively and quantitatively to assess the healing pathway that results in the outcomes previously examined (Chapter 5:). It is hypothesised that a larger callus will be formed earlier in the post-operative period under flexible fixation conditions, which once stabilised, will result in faster intracortical bone formation.

6.2 MATERIALS AND METHODS

6.2.1 Animal Model

Ninety six male Wistar rats (weight 400–450 g) were randomly divided into nine groups (n = 8 each; Figure 6.1). The six groups served as control groups, with three receiving a stiff fixation configuration, and three receiving flexible fixation. These groups were euthanised at three time points, either 5 days, 14 or 28 days postoperatively. Two experimental groups had

their fixation changed from the flexible configuration to the stiff configuration at 3 days post-operatively (3D). These groups were also euthanised at either 5 days or 14 days post-operatively. One experimental group had the fixation changed from flexible to stiff at 7 days post-operatively, with euthanasia occurring at 14 days. These time points were selected to focus on differences immediately post-modulation in the early phases of healing. Finally, an additional two study groups for the flexible control were examined (n = 5). These were euthanised at 3 days and 7 days post-operatively to assess the healing progression and callus development at these times.

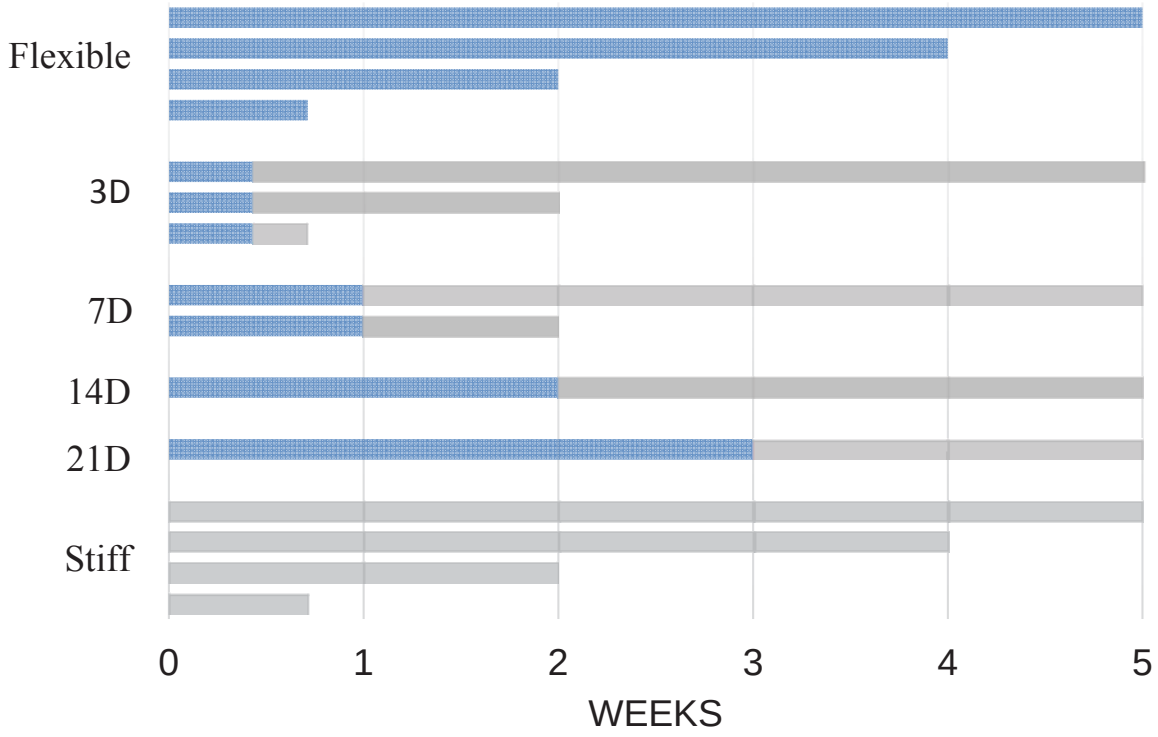

Figure 6.1: Time points to monitor the progression of healing. Time in the flexible fixation condition is represented in blue, with stiff fixator conditions indicated in grey. Rats were euthanised at 5 days and 14 days postoperatively for the 3D, 7D and controls groups. Rats were euthanised at 28 days for the control groups only. These groups were compared to the results from Chapter 5, where the rats were euthanised at 35 days.

6.2.2 Fixator Design and Construction

An external fixator, as described previously (Chapter 5.2.2), was used to stabilise the rat femoral osteotomy. The stiff configuration was offset 6 mm from the surface of the femur and

the flexible configuration was set at 12 mm creating axial stiffness of 119 and 31 $N \cdot mm^{-1}$, respectively.

6.2.3 Operative Procedure

The operative procedure for this study was the same as described previously (Chapter 5.2.3 and Appendix A). Animal care and experimental protocols were followed in accordance with the National Health and Medical Research Council (NHMRC) guidelines and approved by the Animal Ethics committee of Queensland University of Technology.

6.2.4 Histology and Histomorphometry

Femora were fixed using 4 % paraformaldehyde for 3 days and then were decalcified for four weeks in 10 % EDTA solution at 4 °C with agitation. After decalcification, the samples were processed by graded ethanol solutions to dehydration, cleared in xylene and embedded in paraffin wax. Embedded samples were sectioned at a thickness of 5 μm, collected onto poly-l-lysine microscope slides and dried overnight. Serial sections from each sample were stained with safranin orange–fast green to detect cartilage. The morphological features of the periosteal, intracortical, and endosteal zones were qualitatively described using light microscopy. Additionally, quantitative histomorphometry was performed using light microscopy (KS400; Zeiss, Eching, Germany) to analyse tissue morphology. The total callus area was measured using OsteoMeasure, a bone histomorphometry system (OsteoMetrics, Atlanta, USA) and the proportions of bone, cartilage and fibrous tissue were quantified. The cortical bone was excluded from the analysis.

6.2.5 Data Analysis / Statistics

Statistical analysis was performed to determine differences in the mechanical, histological and μCT parameters. Analysis of variance (ANOVA) tests were used to assess differences, with a post-hoc test (Tukey) used to determine inter-type relationships. Tests were

conducted using SPSS 21.0 with *p*-values < 0.05 taken as significant. Data are presented as the mean with error bars indicating standard deviation.

6.3 RESULTS

The animals tolerated the experimental procedure. Pin breakage occurred in 5 animals reducing the sample size of the stiff group at 5 days (*n* = 7); the stiff group at 14 days (n = 7), the stiff group at 28 days, the 3D group at 5 days (*n* = 7), and the 3D group at 14 days (n = 7). At the time of operation, the rats weighed an average of 426 ± 39 g. The average increase in body weight from the time of operation to 5 weeks postoperatively was 6 ± 2 %

6.3.1 Stiff versus Flexible Control

The healing progression was examined closely for the control groups with time points assessed at 5 days, 14 days and 28 days postoperatively.

5 Days Postoperatively

After five days (Figure 6.2), woven bone had formed on the periosteal surface of the cortical bone fragments in both control fixation groups. This bone formation was found to be larger and more structurally organised in the flexible group. The thickness of the newly formed periosteal bone appeared to be relatively constant over the length of the bone from the fracture gap to the inner fixator pin. At this time, no bone formation was observed endosteally or intracortically. However, some hypertrophic chondrocytes were visible at the periphery of the periosteal callus in the flexible group. The remaining soft callus at this healing time was composed of fibrous tissue, with signs of hematoma present in the intracortical and endosteal regions in the stiff group (6/8) and flexible group (5/8).

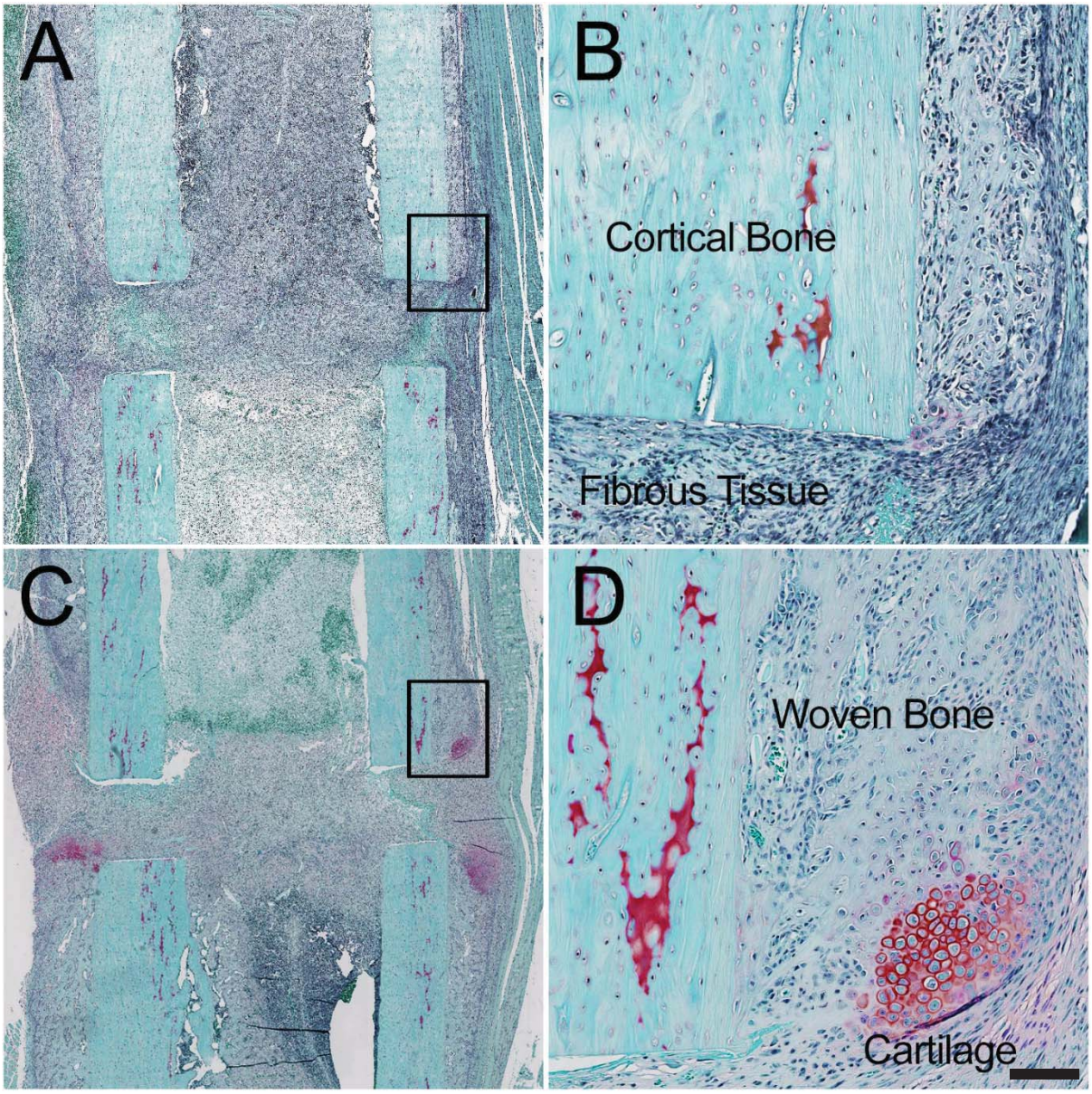

Figure 6.2 The callus histology (safranin orange-fast green) after 5 days of healing. A) Stiff fixation; B) periosteal callus response under stiff fixation; C) flexible fixation, and; D) periosteal callus response under flexible conditions, where cartilage formation can be seen at the periphery of the initial hard callus. Scale bar indicates 1 mm for A) and C) and 100 μm for B) and D).

14 Days Postoperatively

By 14 days (Figure 6.3), the callus size had visibly increased with continued woven bone formation in the periosteal region in both groups. However, across all samples, this bone formation appeared to be larger under more flexible fixation. At this time point, there was a large amount of cartilage formed in both groups. In the stiff group, this formed predominantly in the intracortical region, whereas the flexible group had the greatest cartilage formation in

the periosteal callus. Endosteal bone formation was present in the flexible control group with all samples exhibiting endosteal bony bridging. This occurred in only a few (3/8) samples in the stiff group. In the intracortical region of the stiff group, there was some woven bone formation on the surfaces of the pre-existing cortical bone whereas in this region in the flexible group, the predominant tissue appeared to be fibrocartilage or a dense fibrous tissue. At this time, there was no bony bridging in any samples either intracortically or periosteally.

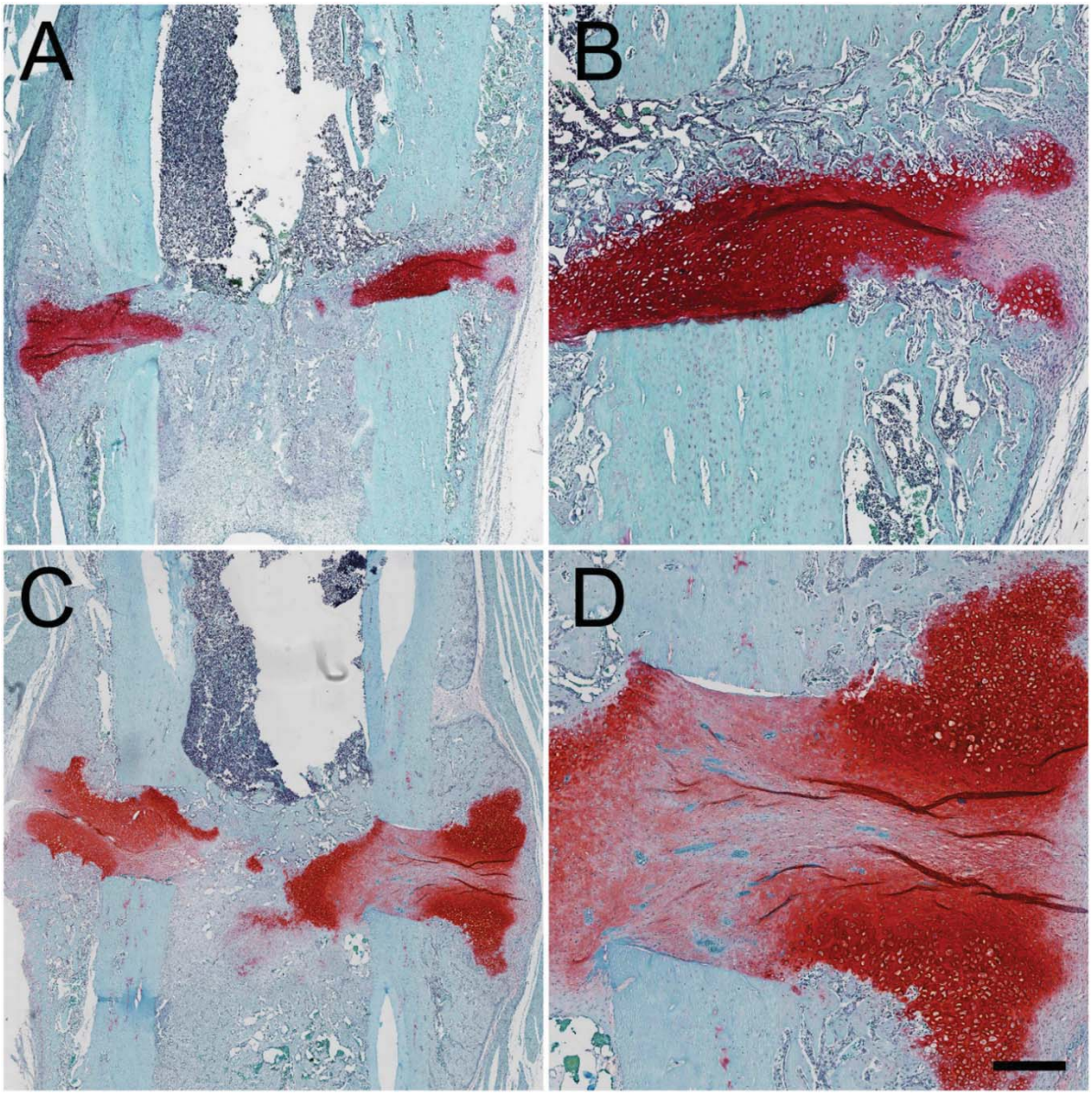

Figure 6.3 The callus histology (safranin orange-fast green) after 14 days of healing. A) Stiff fixation; B) periosteal and intracortical tissue formation under stiff fixation; C) flexible fixation, and; D) periosteal and intracortical tissue under flexible conditions. Scale bar indicates 1 mm for A) and C) and 100 μm for B) and D).

28 Days Postoperatively

At 28 days postoperatively, bridging of the periosteal callus had occurred in all animals of the stiff group for at least one side of the callus, and half of the animals of the flexible group (4/8). In the flexible groups all animals were bridged endosteally, which appeared to be more organised and larger in magnitude than at 14 days, while the stiff group was bridged endosteally in half of the animals, with the appearance of remodelling in this region. Intracortically, there was increased bone deposition in both groups compared to 14 days, with the majority of the stiff group exhibiting bridging in this region (6/7). However, only two animals of the flexible group had bridged intracortically. The presence of cartilage seemed to decrease by 28 days in both control groups. (Figure 6.4). The stiff group had cartilage present mainly in the intracortical region, whereas the flexible group had cartilage present throughout all callus regions. The stiff group was also characterised by more extensive remodelling in the periosteal callus, with the formation of dual cortices, a common characteristic pattern during bone remodelling in small animals.

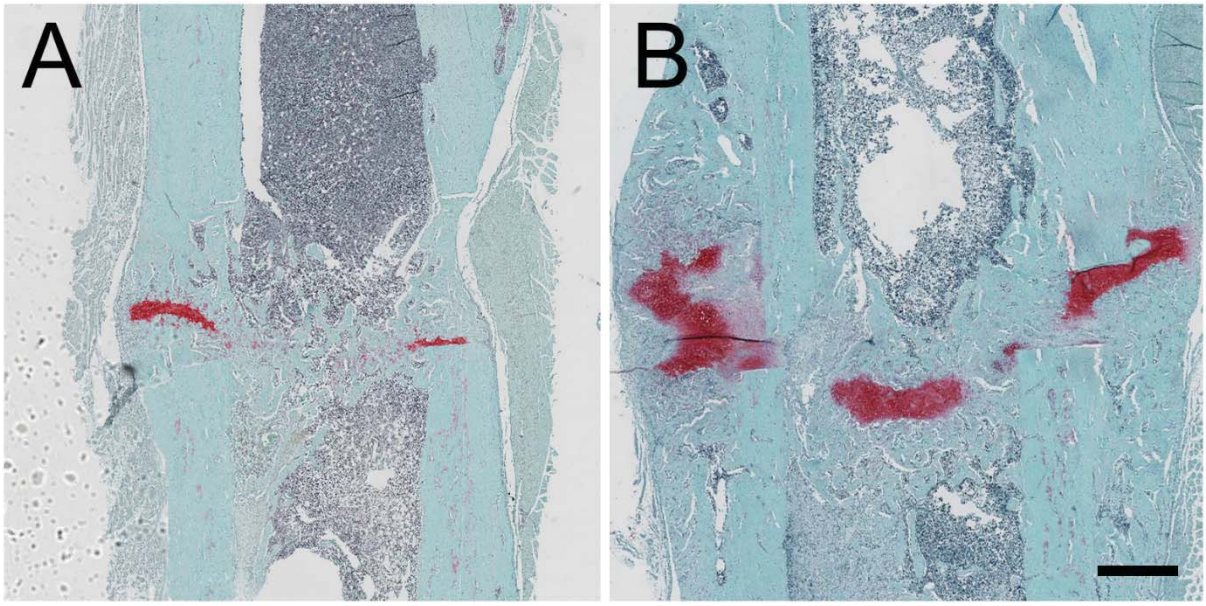

Figure 6.4 The callus histology (safranin orange-fast green) after 28 days of healing. A) Stiff fixation; and B) flexible fixation. Scale bar indicates 1 mm.

6.3.2 Modifying Fixation Stiffness and Quantitative Assessment

Fixation stiffness was modified at 3 days (3D) post-operatively, the results of which were assessed at 5 days and 14 days. Fixation stiffness was also modified at 7 days (7D) post-operatively and assessed at 14 days.

5 Days Postoperatively

After five days of healing, the 3D group was compared to the stiff and flexible control groups (Figure 6.5) both qualitatively and quantitatively. Similarly to the control groups, woven bone had formed on the periosteal surface of the cortical bone fragments, appearing to be greater in the 3D and flexible groups than the stiff group. While there was very little cartilage present in the stiff group, the 3D group had more cartilage formation visible at the periphery of the periosteal callus. However, this initial cartilage formation did not appear to be as consistent among all samples as the flexible group. The remaining soft callus comprised fibrous tissue in the 3D group, with remnants of haematoma visible in 5 animals. These observations were confirmed quantitatively by assessing the callus area, as well as bone and cartilage formation within the callus. The overall callus area was significantly greater in the flexible and 3D groups compared to the stiff group ($p < 0.01$). This trend was also reflected in the bone formation with significantly larger areas of bone measured in the 3D group compared to the stiff group ($p = 0.04$; Figure 6.6). The flexible group was found to be significantly larger than both ($p < 0.01$ and $p = 0.046$) for the stiff and 3D groups, respectively. Cartilage area measurements were also greater in the 3D and flexible groups, however no statistical significance was found in this parameter.

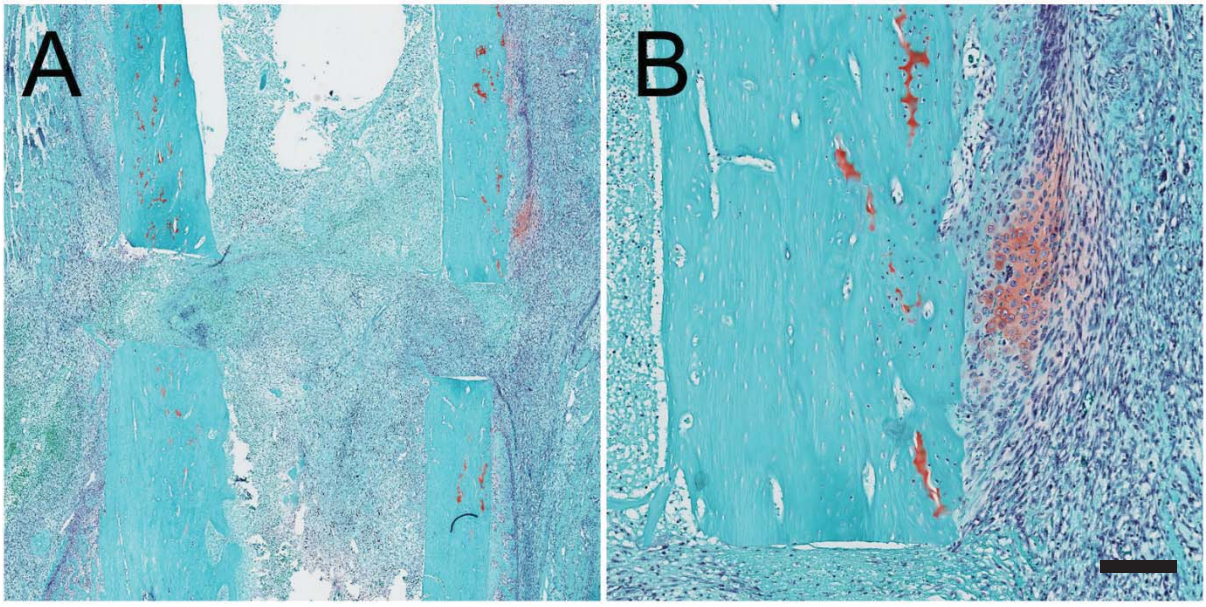

Figure 6.5 The callus histology (safranin orange-fast green) after 5 days of healing. A) Flexible fixation for 3 days (3D) stabilised for the final two days, and; B) periosteal tissue responses after changed fixation stiffness at 3 days. Scale bar indicates 1 mm for A), and 100 µm for B).

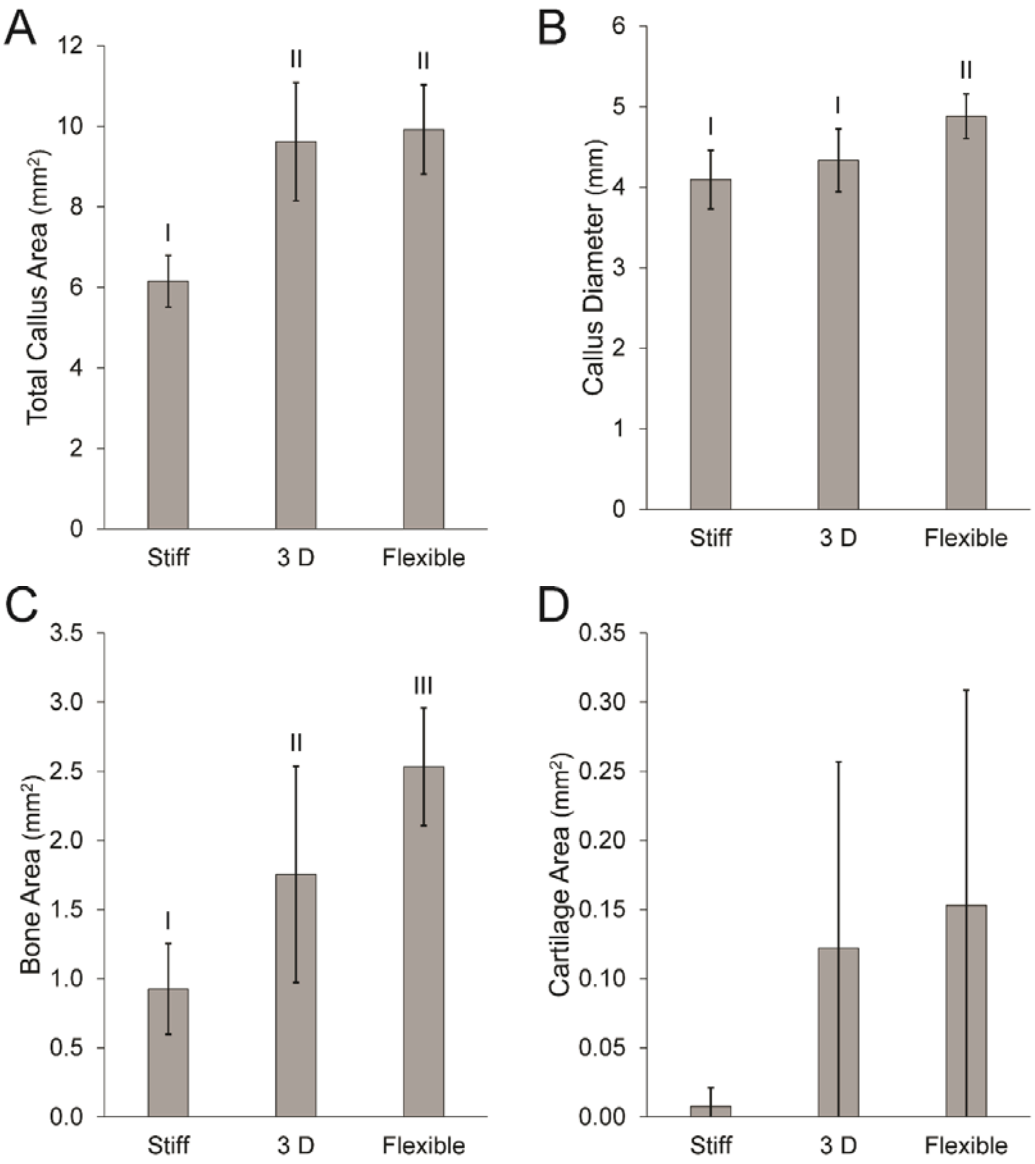

Figure 6.6 Healing evaluated 5 days post-operatively, comparing stiff and flexible conditions with fixation stiffness modified at 3 days (3D). A) Total callus area; B) callus diameter; C) bone area, and; D) cartilage area within the callus were quantified. $p < 0.05$ was considered significant. Significantly different groups have different symbols.

14 Days Postoperatively

The 3D and 7D groups (Figure 6.7) showed very different healing outcomes after 14 days compared to both of the control groups (Figure 6.3). In these experimental groups, it may be seen that the periosteal callus was far smaller than under the constant fixation situation of the control groups. There was also limited cartilage formation throughout the entire callus in the experimental groups, particularly in comparison to the control groups, where there was extensive callus formation. In the intracortical region, the tissue formation appeared to be

predominantly bone and fibrous tissue, compared to the stiff group, which appeared to be predominantly cartilage in this region. At this time point, there was no intracortical or periosteal bridging observed in the control groups however the 7D (4/8) and 3D (3/8) samples exhibited bridging in these regions, in at least one cortex. Similarly to the flexible group however, the majority of samples in these group were bridged endosteally.

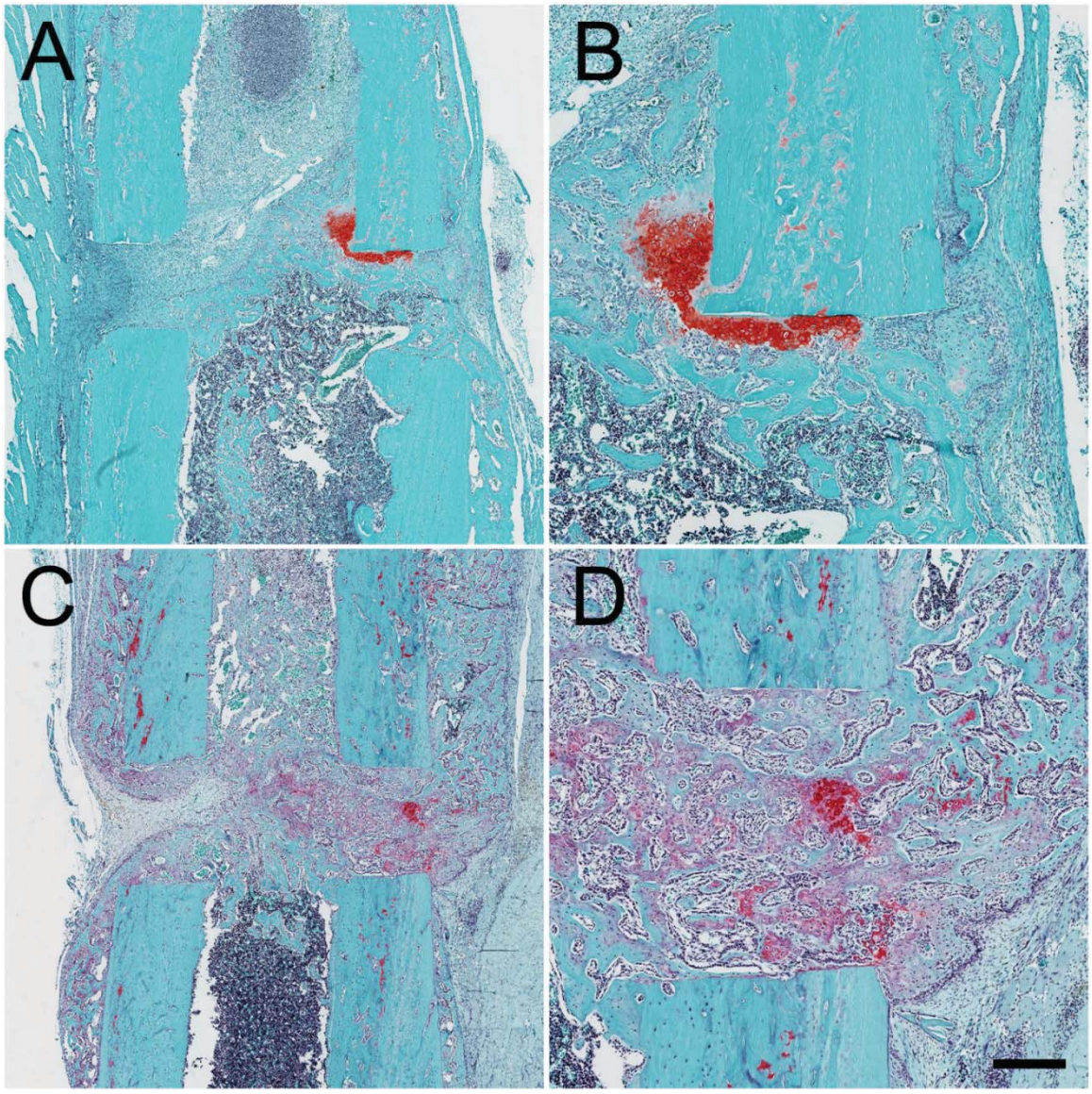

Figure 6.7 The callus histology (safranin orange - fast green) after 14 days of healing. A) 3D group; B) intracortical tissue with changing fixation stiffness at 3 days; C) 7D group, and; D) intracortical tissue with changing fixation stiffness at 7 days. Scale bar indicates 1 mm for A) and C) and 100 μm for B) and D).

The quantitative analysis revealed a number of differences between the experimental and control groups in all callus regions (Figure 6.8). Throughout the entire callus, the flexible group had a significantly greater callus area (16.0 mm^2) than all other groups. The stiff group (12.2 mm^2) had a significantly greater callus area than the 3D group (8.0 mm^2), however the 7D (10.1 mm^2) did not differ from either. This trend was observed with both the bone and cartilage area throughout the entire callus, however both the 3D and 7D groups had developed significantly less cartilage than the control groups.

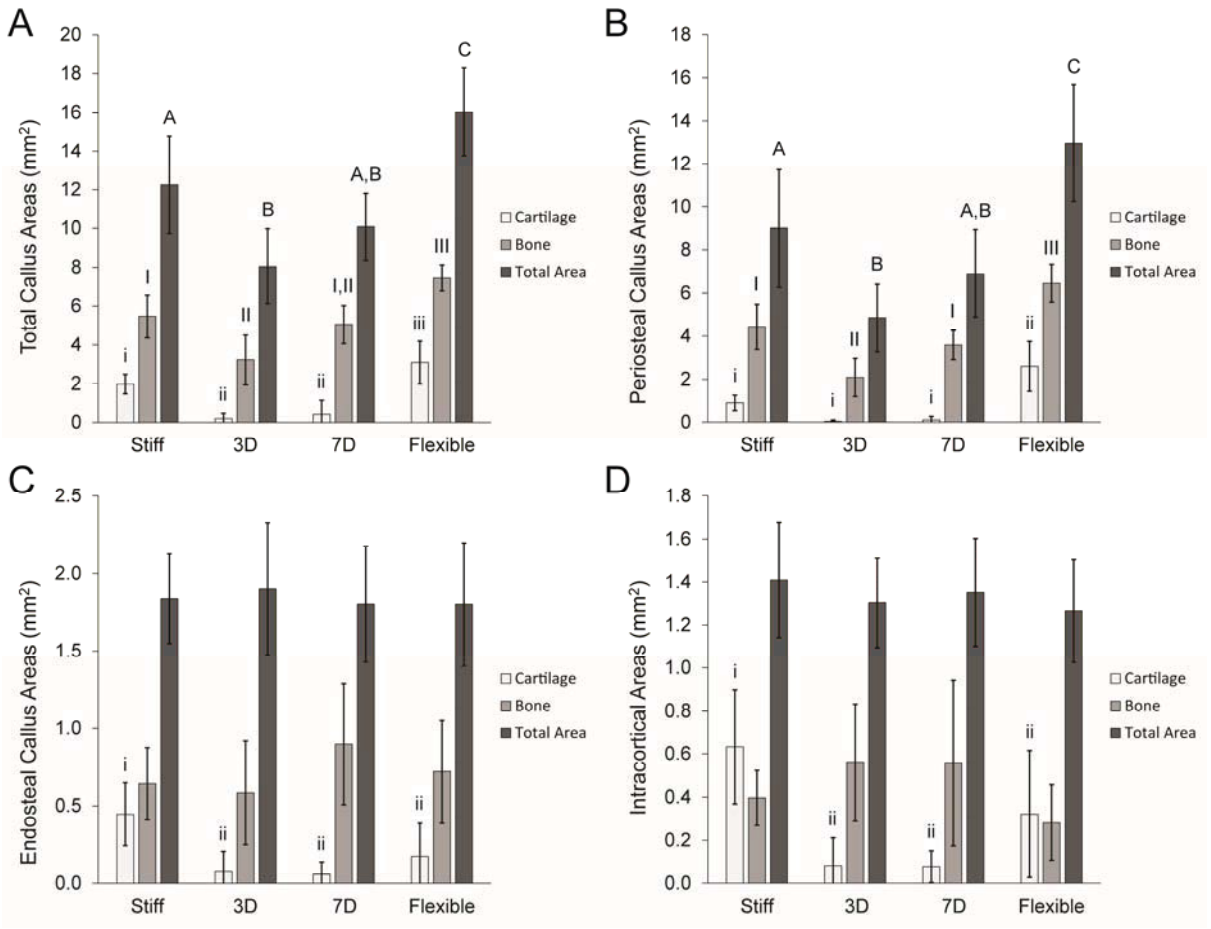

Figure 6.8 Healing evaluated 14 days post-operatively, comparing stiff and flexible conditions with a changed fixation stiffness at 3 days (3D) and 7 days (7D). A) Total callus area; B) periosteal callus area; C) endosteal callus area, and; D) intracortical area. All graphs display the total area for the callus region, as well as bone and cartilage areas. $p < 0.05$ was considered as significant. Significantly different groups have different symbols.

The periosteal callus region exhibited similar differences between groups, however the 3D group was found to have significantly less bone formation than the other groups. Cartilage

area did not differ between the 3D, 7D, and stiff group in the periosteal callus. Interestingly, in the endosteal callus and intracortical regions, cartilage formation in the stiff group was found to be significantly greater than all other groups. No other parameters in these regions demonstrated significant differences.

28 Days Postoperatively

The qualitative results comparing the stiff and flexible groups were confirmed by quantitative histomorphometry (Figure 6.9), with significant differences observed between the flexible and stiff groups in total callus (16.2 vs. 9.5 mm^2; $p < 0.01$) and periosteal callus areas (12.5 vs. 6.2 mm^2; $p < 0.01$). The bone and cartilage areas were significantly higher in the flexible group compared to the stiff throughout the total callus and the periosteal callus ($p < 0.01$ all parameters). The endosteal region showed significantly greater areas of both cartilage and bone formation under flexible conditions ($p = 0.01$ and $p = 0.039$, respectively), reflective of the remodelling occurring in this region in the stiff fixation group. In the intracortical region however, there were no statistically significant differences in bone and cartilage area, despite a much larger number of the stiff group exhibiting bony bridging at this time point.

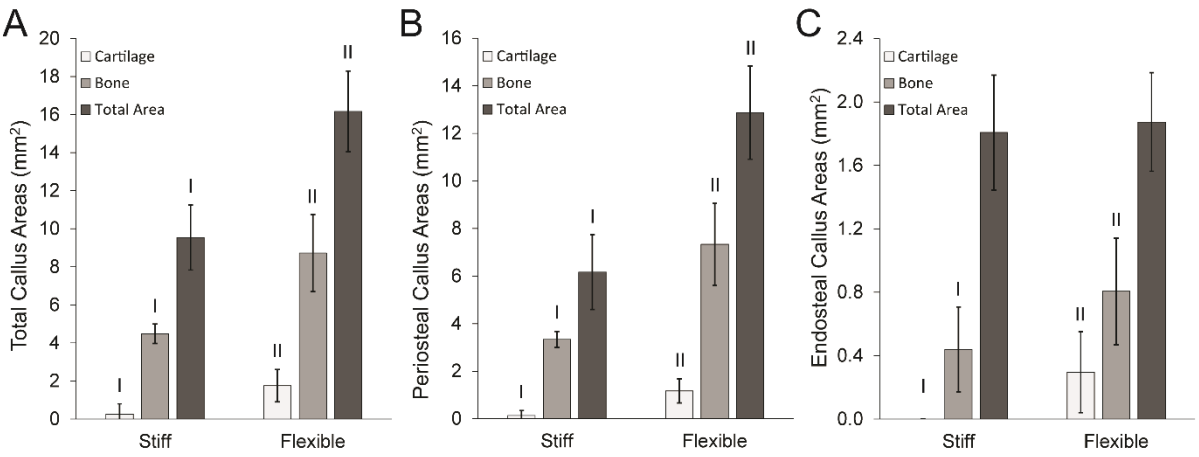

Figure 6.9 Healing evaluated 28 days post-operatively, comparing stiff and flexible conditions. A) Total callus area; B) periosteal callus area, and; C) endosteal callus area. All plots display the total area for the callus region, as well as bone and cartilage areas. $p < 0.05$ was considered significant. Significantly different groups have different symbols.

6.3.3 Tissue Formation over the Course of Healing

Tissue distribution throughout the callus was analysed over time, based on the presented results (Figure 6.10). Throughout the total callus, it may be seen that the size of the callus increased up to 35 days for the flexible group, whereas the callus size peaked at 14 days for the stiff group and then decreased until 35 days [181]. The bone area increased consistently for the flexible group, however at a slower rate from 14 days to 28 days. Conversely the stiff group decreased slightly from 14 to 28 days, before increasing to 35 days. When comparing the control groups, the cartilage parameter demonstrated similar trends, despite differences in magnitudes, with cartilage formation peaking at 14 days before decreasing by 35 days.

In all other callus regions, bone and cartilage formation peaked at 14 days and then decreased by 28 days, with the exception of intracortical bone formation, which was at its greatest at 28 days. On the other hand, flexible conditions caused an increase in bone measurements throughout the healing periods. Cartilage however, peaked at 14 days in the periosteal callus and intracortical region before declining by 28 days as this tissue in this region ossified. In the endosteal region, cartilage increased throughout the healing period, however the magnitude of cartilage in this region was notably lower than the stiff fixation at 14 days.

Comparison of the tissue distributions in the control groups to the experimental groups across the entire callus (Figure 6.11) demonstrated clear differences noted previously at 14 days. It may be seen whilst the callus area peaked for the stiff group at 14 days, the 3D and 7D demonstrated a decline at this time in callus area compared to their size at 5 and 7 days respectively. The callus area then continued to increase until 35 days. For the experimental groups there was a steady increase in bone formation through the entire healing period. Cartilage in the 3D group increased slowly throughout the entire healing period, however in the 7D group, cartilage peaked at 14 days before declining by 35 days.

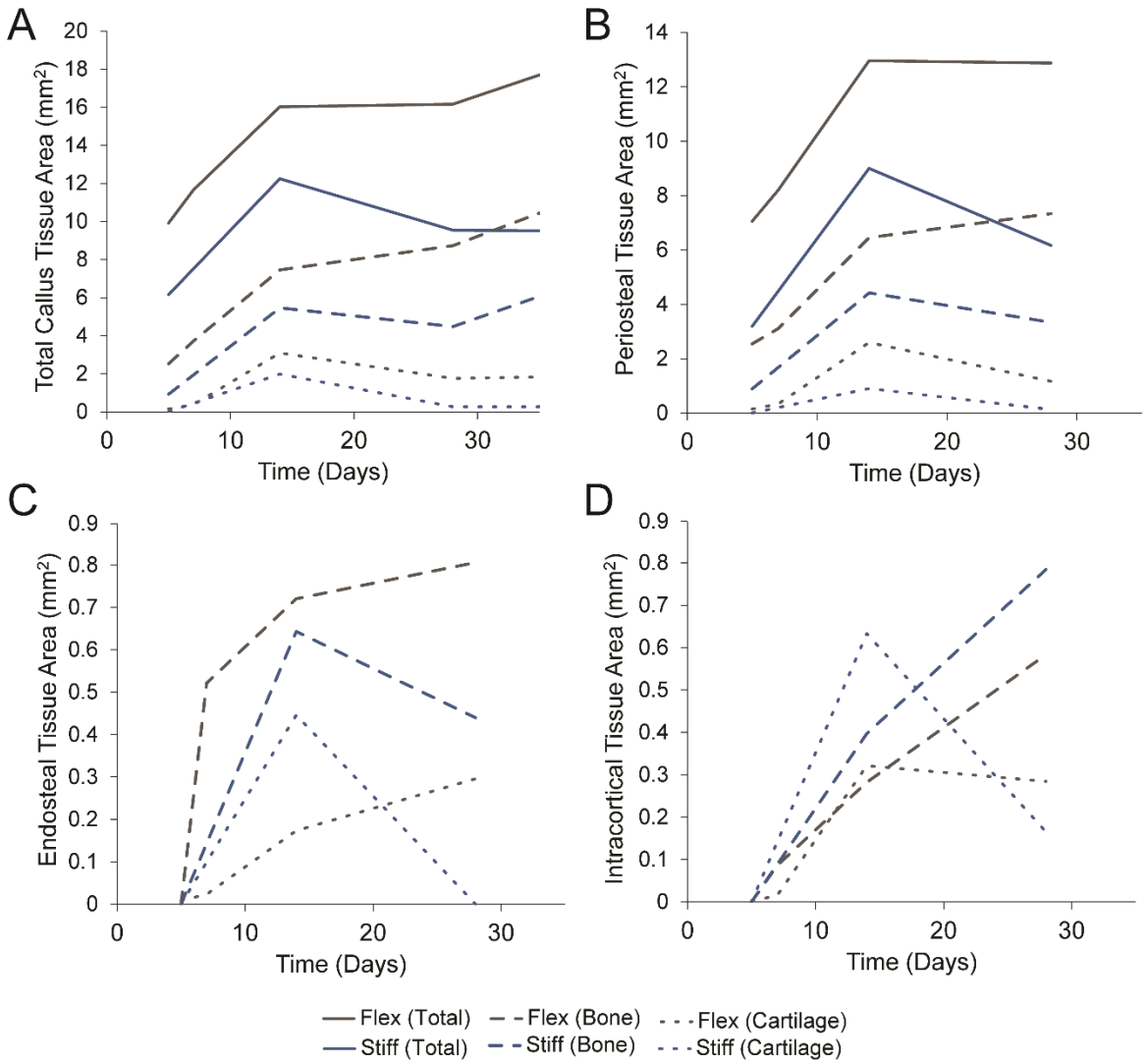

Figure 6.10: Healing evaluated over time for the control groups. A) Total callus; B) periosteal callus; C) endosteal callus, and; D) intracortical region. All figures display the total area for the callus region, as well as bone and cartilage areas.

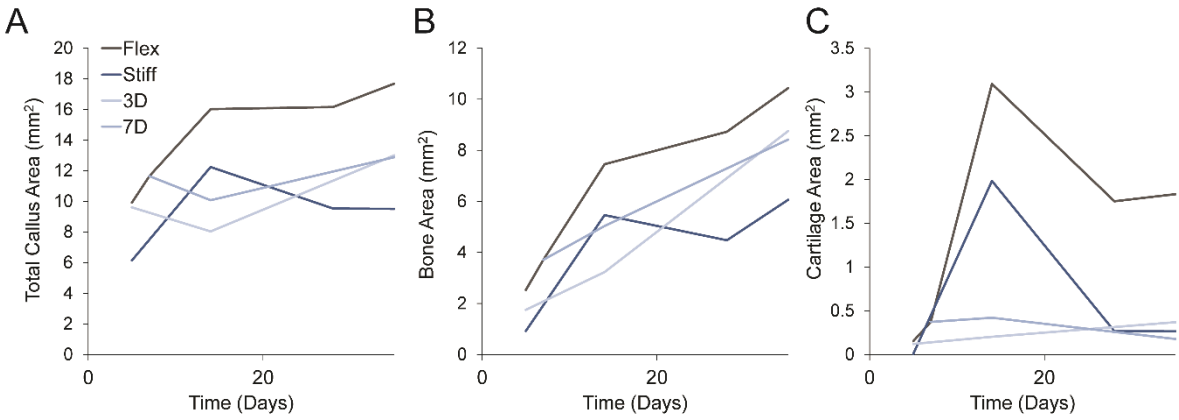

Figure 6.11: Tissue distribution throughout the callus over time for 3D, 7D and control groups. A) Total callus area; B) bone area, and; C) cartilage area.

6.4 DISCUSSION

This study examined the effect of fixation stiffness on tissue formation through fracture healing, with particular focus on the early phases of healing. The data shows that both the course of healing (tissue formation) and healing outcome are not negatively affected by early instability (flexible conditions), if the fracture is later stabilised. The difference between the stiff and flexible conditions in our model were first evaluated, followed by changing fixation stiffness to stabilise the fracture site.

6.4.1 Stiff versus Flexible Control

In the initial phase of healing, significant differences existed between the two fixation conditions, where a greater callus area, diameter and bone area were measured under flexible fixation. This confirms our hypothesis that more mechanical strain early in the healing period stimulates the formation of a larger callus. Despite the larger strain, resolution of the haematoma did not appear to differ between the stiff and flexible fixation conditions. This is contrary to previous temporal tissue distribution studies in sheep [67] and rats [85], which found that tissue development in the early phases of healing was not dependant on fixation stiffness.

By 14 days, the periosteal callus continued to expand in both control groups through intramembranous bone formation, however under flexible conditions this was significantly greater. It has previously been reported that peak callus area is reached in the rat by 14 days postoperatively [85, 154, 181]. This study found that under stiff fixation (25 % IFS), this outcome was confirmed, potentially as the IFS falls within optimal values [140], whereas under the more flexible conditions, callus size continues to increase until 35 days. Wehner *et al.* [105] implemented the same fixation stabilities to investigate changes in callus stiffness over time. Their study demonstrated that the repair phase was significantly extended under flexible conditions, however by 12 weeks there were few differences remaining between the groups.

Based on the callus development throughout this study, there are few identifiable differences between the groups in terms of overall healing progression by 14 days of healing. However, closer examination of the tissue distributions indicated that cartilage was formed in different regions of the callus under different fixation stabilities.

Under flexible conditions, cartilage predominantly formed in the periosteal callus, which peaked in this region at 14 days. Whilst the stiff group also exhibited periosteal cartilage formation, it had significantly higher areas of cartilage compared to the flexible group in the intracortical and endosteal regions of the callus. All cartilage areas peaked at 14 days in the stiff group, however in the flexible group, the intracortical and endosteal cartilage increased by 28 days.

Similarly, endosteal bone formation differed in these groups. While there was no significance found in magnitude, all of the samples in the flexible group and only a few in the stiff group (3/8) had bridged across this region at 14 days. The development of bone in this region seemed to increase significantly in the flexible group with an increase in area as well as thicker trabecular structures observed at 28 days. Notably, in this rat osteotomy model, endosteal bone formation and bridging preceded periosteal bone formation for both fixation stabilities. This phenomenon was not observed in the sheep, with periosteal bony bridging occurring before other regions of the callus [67, 197].

These results fundamentally suggest that while tissue distribution patterns may differ under different fixation conditions, healing does not appear to be delayed significantly by the early flexible condition, when examined at 14 days. The main indication of a slight delay in healing is the greater cartilage formation in the stiff group in the intracortical region. However, by 28 days, differences in the healing progression between the groups is far greater, suggesting that the delay is primarily caused by flexible conditions in the later reparative stage of healing. This finding aligns with finding from sheep studies [67] despite differences in the healing

process between the species. Looking at the results from the previous experimental chapter (Chapter 5), this outcome was further demonstrated when fixation stiffness was stabilised at 14 days (14D) producing an equivalent healing outcome to the stiff control group. Furthermore, the 21 day group, which would have had delayed healing conditions for a further 7 days, essentially reached comparable tissue maturity to the other experimental and stiff control groups despite stabilisation only occurring late in the reparative phase of healing.

6.4.2 Modifying Stiffness

It was hypothesised that a larger callus will be formed earlier in the post-operative period under flexible fixation conditions, which once stabilised, will result in faster intracortical bone formation compared to constant fixation conditions. This study clearly demonstrated that under flexible fixation, a larger callus was produced at both 5 days and 14 days of healing, confirming findings from previous large animal experiments [67, 96, 145]. Further examination of the experimental groups within this study is required to assess the second part of the hypothesis, of accelerated intracortical bone formation.

Firstly, examining the healing process in the 7D group, it may be seen that as expected, the callus size in this group was significantly lower at 14 days than the flexible group and did not differ statistically from the stiff group. The bone formation across all areas of the callus did not differ statistically from the stiff control group, however there was a trend of more bone formation throughout the intracortical and endosteal regions. This is indicated by the greater number of animals within this group achieving bony bridging either intracortically or periosteally. The most notable differences was that of cartilage distribution, with minimal cartilage produced in all regions of the callus. These results suggest that intracortical and periosteal bone formation were both primarily deposited through an intramembranous ossification pathway rather than a combination of intramembranous and endochondral ossification, as clearly demonstrated by the control groups and in other experimental bone

healing studies [67]. By 35 days, virtually all animals in this experimental group had fully bridged fractures, with minimal cartilage remaining. Healing 7 days post-operatively under flexible fixation (Figure 6.12) indicates large periosteal bone formation with cartilage at the periphery of the callus. The geometry of this initial callus would have increased the load sharing area of the bone, which when combined with a more stable fixation, could have reduced tissue strains within the intracortical region sufficiently to allow intramembranous ossification without the need for a cartilage intermediate phase [12]. This could be further examined with computational studies assessing the mechanical environment at the time of stabilisation, as measuring the mechanical stimulus is not possible, particularly at the small scale of a rat model. Further examination of this group could also be conducted to assess the tissue formation between 14 days and 35 days. It would be interesting to observe if the remaining cortices bridge purely by intramembranous formation, or if cartilage formation occurs, which is then mineralised by the 35 day time point.

The 3D group exhibited similarly limited cartilage formation, however less bone formation than the 7D group, with fewer samples achieving bridging. Examining the tissue formation after 3 days under flexible fixation, it may be seen that there is limited periosteal bone formation, and haematoma is present within the osteotomy (Figure 6.12). However, by 5 days the callus size and bone area in this group was significantly greater than the stiff group (Figure 6.5). This would suggest that tissue strains in the intracortical region at 5 days would be lower in the 3D group than the stiff group, both under the same fixation stiffness. Similarly to the 7D group, this seemingly has allowed an intramembranous response throughout the intracortical region. However the bone formation and bridging is less extensive than the 7D group and all areas of the callus have not been engaged in this process. This would be due to the shorter time under flexible conditions in this group limiting the periosteal response comparative to the 7D group. Further examination and analysis is required to confirm that the

bone formation throughout the intracortical region for these groups was produced predominantly through via intramembranous ossification.

The 3D and 7D groups appeared to form intracortical bone through intramembranous ossification unlike the control groups which indicated endochondral ossification in this region. However, based on the results from Chapter 5, it can be observed that the 14D group produced a similar healing outcome to the 7D and stiff control groups. It may be therefore inferred after examining the flexible condition at 14 days that both intramembranous ossification and endochondral ossification can occur more rapidly under stable fixation conditions, if sufficient mechanical stimulus is provided to the fracture region early in the healing process. Further investigation into the cellular processes instigated by this stimulation is necessary to ascertain the mechanism of improved healing under these conditions.

Limitations exist with assessing fracture healing with small animal models as this process is greatly accelerated compared with large animals and humans. As such, it is not necessarily possible to examine every step of the healing process, as some processes may occur too rapidly to be examined at discreet time points. It may thus be necessary to characterise the general healing phases, especially in order to extrapolate the results in relation to alternate animal models or for clinical applications.

6.4.3 Healing Stages

The outcome of this animal experiment was reported by means of histological images at different time points post-operatively, assessed predominantly by qualitative histology and supported with simple histomorphometric analyses. Description of the average healing progression seen in this study provided a platform for interspecies comparisons, assessment of mechanobiological theories and a means to clearly identify enhanced healing.

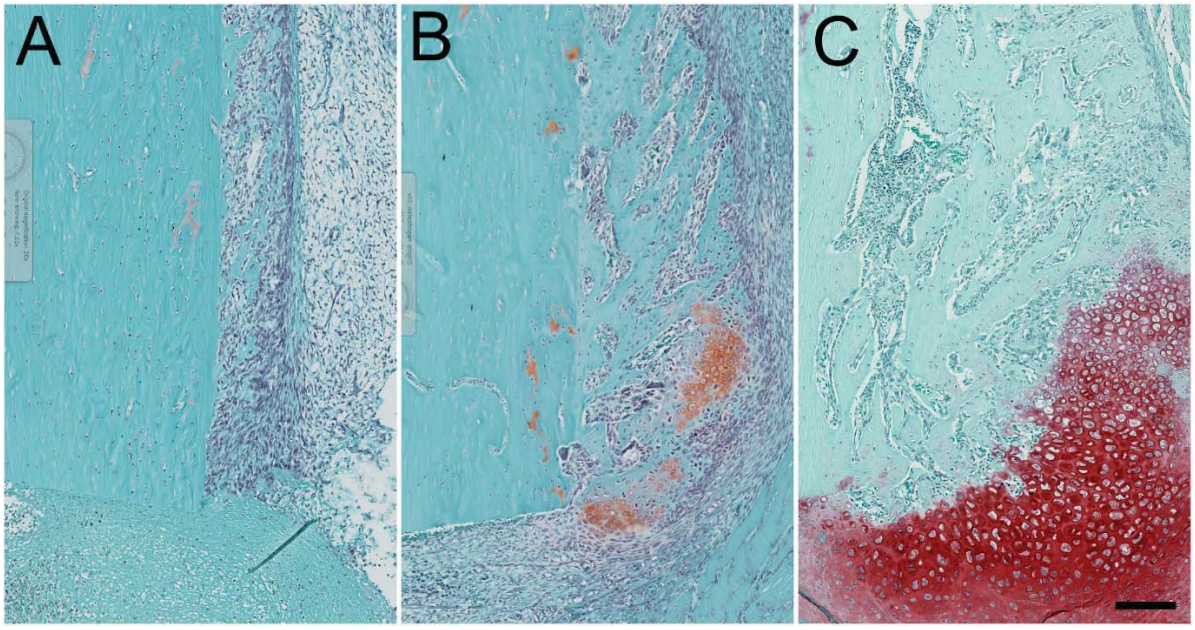

Figure 6.12 Callus histology (safranin orange - fast green) under flexible conditions assessing the callus progression at the time of stabilisation. A) 3 days of healing; B) 7 days of healing, and; C) 14 days of healing. Scale bar indicates 40 μm.

Vetter *et al*. [197] introduced a new method to describe the progression of healing reflecting the topology of the different tissue types formed (Table 6-1). They found that healing under different fixation conditions showed no qualitative difference in topology using this method despite measurable differences quantitatively. These healing stages were used as a basis for comparison with the current rat osteotomy healing model. Comparison of relationships between species is essential to further research in this field and is critical to advance research project findings to a clinical scenario.

Differences were identified between healing stages in a rat (Table 6-2) and sheep osteotomy. The inflammatory phase had similar haematoma formation, the resolution of which was much faster in a rat - with no signs of hematoma present by 7 days post-operatively irrespective of fixation stability. Conversely in the sheep model, signs of the haematoma were present for far longer under less stable fixation conditions [67].

The second stage of healing identified in both species were very similar, with the dissolution of the haematoma as well as initial periosteal callus formation via intramembranous ossification. By the third healing stage, the processes diverged. In the rat, endosteal bone formation was present with bridging in this region that was not observed in the sheep until far later in the healing process (Stage V). This difference could potentially be related to restoration of the intramedullary blood supply in the rat occurring faster than in larger models, a parameter that should be investigated in future work). Both species however bridged in the periosteal callus via endochondral ossification.

As healing proceeded, bony bridging in the periosteal callus then occurred in both groups, with significant cartilage formation in the intracortical region that did not occur to the same extent in the sheep. Finally, intracortical bony bridging in conjunction with the initiation of callus remodelling was observed. In the sheep, the remodelling process involved a slow decrease in periosteal and endosteal callus. In the rat, remodelling initiated along the cortical bone surface rather than the outer periosteal callus surface and as a consequence a dual cortex was formed [184]. When analysing healing outcomes, this is an important consideration in the rat, as it can skew quantitative parameters that do not reflect regional differences in callus tissue distributions. The healing stages for the rat model were defined from observed callus development under constant fixation conditions.

Table 6-1 Healing stages observed in sheep 3 mm osteotomy healing (adapted from Vetter *et al*. 2010 [197], with permission).

Healing Stage	Topological Criteria	Classification According to Healing Phase
Stage I	Remnant of hematoma still present in the callus	Late inflammatory phase
Stage II	No remnants of hematoma left, cartilage not yet formed	Early reparative phase
Stage III	Bridging via cartilage in the outer osteotomy zone, but no bony bridging of the osteotomy gap	Reparative phase
Stage IV	Formation of a periosteal bony bridge between the proximal and distal parts of the osteotomy callus	Late reparative phase
Stage V	Formation of an endosteal bony bridge between medial and lateral parts of the osteotomy callus	Early remodelling phase
Stage VI	Reduced size of the hard callus, resorption of the endosteal bony bridge	Remodelling phase

Table 6-2 Healing stages outlined for osteotomy healing in rat femoral osteotomy model (1 mm)

Healing Stage	Topological Criteria	Classification According to Healing Phase
Stage I	Remnant of hematoma present in the callus	Late inflammatory phase
Stage II	Periosteal bone formation, uniform along cortex with initial periosteal cartilage formation.	Early reparative phase
Stage III	Bridging via cartilage formation within the periosteal callus and intracortical region. Endosteal bridging via woven bone.	Reparative phase
Stage IV	Periosteal bony bridging. Cartilage with initial bone formation intracortically.	Late reparative phase
Stage V	Intracortical bridging with resorption of periosteal callus adjacent to cortical bone forming a dual cortex. Endosteal callus beginning to remodelling however still bridged in this region.	Early remodelling phase
Stage VI	Final resorption of endosteal callus and resorption of dual cortex	Remodelling phase

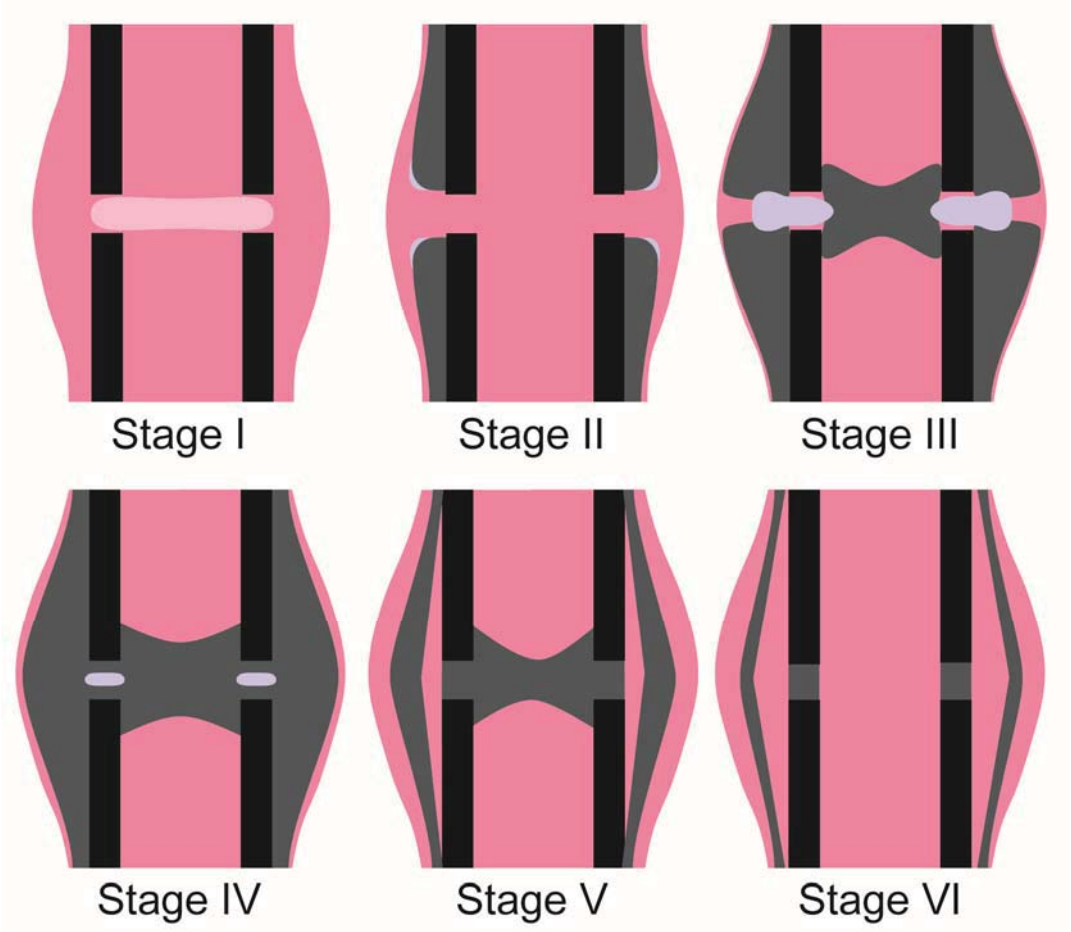

Figure 6.13 Healing under constant fixation stiffness in a rat femoral osteotomy model. Stage I with the formation of a haematoma primarily within the fracture region; Stage II with periosteal callus formation and initial cartilage formation at the periphery of the callus; Stage III is indicative of further periosteal callus growth, endosteal bridging and a combination of periosteal, intracortical and endosteal cartilage formation; Stage IV is characterised by mineralisation and bridging of the periosteal callus; Stage V can be represented by intracortical bridging and initial remodelling of the periosteal and endosteal regions; and Stage VI is a continuation of the remodelling process, characterised by the formation of a dual cortex, which is later fully resorbed.

When the fixation stability was changed (3D and 7D groups) during stage II of the healing process (Figure 6.13) the healing pathway was altered from that of constant fixation conditions. Bone formed via intramembranous ossification on the cortical bone ends with very little cartilage formation observed (Figure 6.14). Stage IV of the healing process, following the change in fixation stability, is yet to be defined. Based on the results it is postulated that bony bridging of these groups is driven via intramembranous ossification with little or no contribution from the endochondral process. However the healing phases converge at Stage V

and VI for constant and modified stiffness groups, suggesting there is no impact on bone remodelling following fixation stiffness modification. When the fixation stiffness was modified in Stage III of healing (14D group), the phases of healing were not changed, however there seemed to be an acceleration in the progression from Stage III to V.

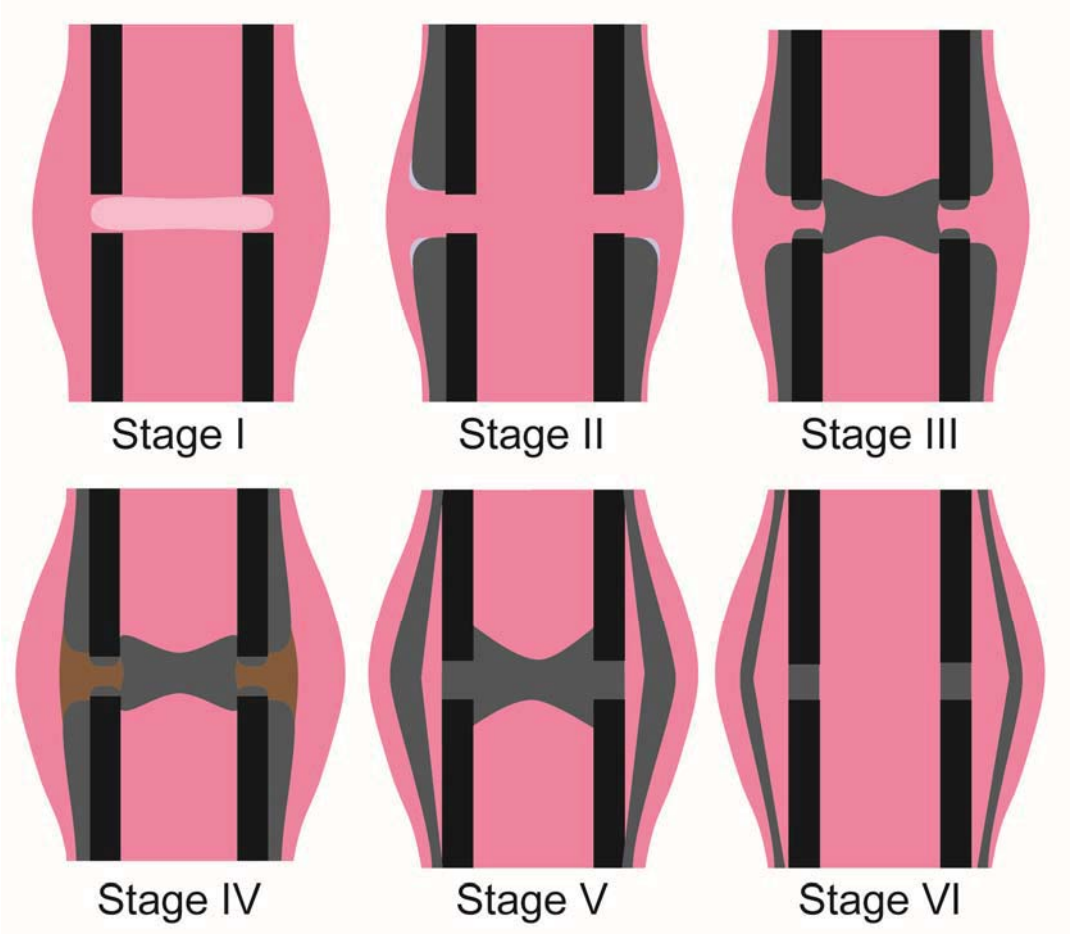

Figure 6.14 Healing after modifying fixation stiffness during Stage II of healing in a rat femoral osteotomy model. Stage I with the formation of a haematoma primarily within the fracture region; Stage II with periosteal callus formation and initial cartilage formation at the periphery of the callus; Stage III is indicative of intramembranous ossification at the cortical bone ends; Stage IV is undefined with potential bone formation or cartilage formation (indicated in brown); Stage V can be represented by intracortical bridging and initial remodelling of the periosteal and endosteal regions; and Stage VI is a continuation of the remodelling process, characterised by the formation of a dual cortex, which is later fully resorbed.

6.5 CONCLUSION

From this study, it has been demonstrated that modifying the fixation stiffness can alter the healing pathway, differences of which are not detectable as a healing outcome. Further investigation is required into the mechanisms triggered by stabilising the fixation, to assess the clinical applicability of this process. The healing stages described for both animal models relate to healing situations of constant fixation stiffness (Figure 6.13). The use of small animal models is increasing due to their low cost, short breeding cycles and well defined genome, as such characterising healing and callus development is crucial to enable the extrapolation and comparison of results for a pre-clinical (large animal) and clinical setting.

Chapter 7: Summary and Discussion

The majority of long bone fractures heal via a secondary bone healing process, involving the development of an external callus. Overall, it has been widely reported that the course of fracture healing is influenced by the interfragmentary movement of the fractured bone, as determined by the applied load and the stability of any fixation [11, 14, 40, 84]. Accurately describing the mechanisms through which bone healing is influenced by mechanical factors may likely have a profound clinical impact by permitting the optimisation in treatment of bone injuries.

Callus size and morphological development are influenced by mechanical stimuli throughout all stages of the healing process. Whilst this fact is commonly known, a sizeable challenge remains in identifying the mechanisms by which differing mechanical environments regulate the formation of various tissue types. A number of mechanobiological theories have been proposed, attributing cell differentiation and hence tissue formation to a number of specific mechanical cues [11, 38, 64, 117, 118]. These theories are continually improved upon as *in vivo* studies increase our understanding of the fracture healing process as a whole.

Proposed in this project is the concept that healing times of fractures may be reduced by modulating the mechanical environment as healing progresses. We proposed that it may be most beneficial to flexibly stabilise fractures during the early stages of healing to stimulate the formation of a larger periosteal callus, and then to increase fixation stiffness, enabling a more rapid mineralisation of the tissue [12]. This concept was explored using a combination of computational and *in vivo* experimental techniques.

The first step in exploring this hypothesis was to perform a theoretical investigation analysing the influence of the size of a hard periosteal callus on the mechanical environment within a model fracture (Chapter 3). A previously validated axisymmetric finite element model of a fracture callus was used, which was modified to accommodate different sizes of the periosteal callus, as demonstrated in a previous *in vivo* study [67]. This study clearly supported the load-sharing effect of the periosteal callus, where under the same magnitude of loading, tissue strain and hydrostatic pressure were reduced within the intracortical region. This was the phenomenon we aimed to illustrate in our *in vivo* studies, where a larger callus was produced in the same time frame under flexible conditions. After then stabilising the fracture, the loading conditions would be equivalent to those under initial stiff fixation. Furthermore, the larger callus size may then lead to reduced strain within the callus tissue, potentially of such magnitude as to induce an increased rate of mineralisation within the cortices.

The above work was expanded in Chapter 4, where the predictive capacity of a FE model developed by Simon *et al*. [129] from the Institute of Orthopaedic Research and Biomechanics, University Hospital of Ulm was assessed. This model was developed based on previous sheep studies [60, 100, 140], and was adapted to allow for the modification of fixation stiffness at any iteration throughout the healing process. The aim of the study was to determine if the model may appropriately address the effects of the changing mechanical environment on tissue distribution, and more significantly on the length of time required for healing to occur. The results of this assessment demonstrated that conditions where the fixation was most stable produced the fastest healing outcome, as defined by the achievement of an IFM threshold value. This indicated that within this model, the modulation of fixation stiffness would never

be able to improve the healing times of a constant stiff fixation. The primary limitation identified with this model was the fixed radius of the periosteal callus. Without the development of a larger callus through higher strains, it was impossible to assess the hypothesis discussed in Chapter 3. The tissue distribution over time required further assessment with the planned *in vivo* studies conducted in following chapters (Chapters 5 and 6).

Chapter 5 implemented the proposed fixation regimen in an *in vivo* study using a rat femoral osteotomy model stabilised with an external fixation system [105, 149, 150]. This fixator enabled the modification of the degree of stability from flexible to stiff and vice-versa without the need for surgical intervention. Under initial conditions assuming an average body weight of 430 g, the stiff fixation would allow IFMs of 0.25 mm (IFS 25 %) while the flexible fixator would allow 1 mm of movement (IFS 100%). With these fixator conditions, it was expected that the stiff fixator would enable optimal bone healing, falling within an optimal interfragmentary strain condition as determined by previous studies (7 - 30%) [172]. The flexible conditions however would result in delayed healing. The modification of fixation stiffness and hence the mechanical environment (as described above), was investigated at various time points throughout healing; inflammation (day 3), proliferation (day 7, 14), and consolidation (day 21) with an end time point of 35 days. We found that stabilising the fixation significantly improved the healing outcome when compared to flexible fixation. Likewise, stiff fixation also led to faster bone healing than flexible fixation, which confirmed the findings of previous studies [107, 108]. Our study found no significant differences between the stiff and the experimental groups in majority of measured parameters (mechanical testing, μCT and histology), although some trends were noted.

Differences between the stiff group and 3 day (3D) group were minimal in terms of the overall healing outcome, despite previous studies suggesting that the mechanical environment in the early phase of healing can direct the entire healing process [179]. Notably, the bone mineral density in the fracture gap of the 14D group was significantly greater than the stiff group, suggesting more mature bone in this region. Finally, stabilisation after 21 days (21D) was found to significantly improve the healing outcome with respect to flexible group. This was an important finding as it confirmed clinical experience [71, 159] of stabilising hypertrophic non-unions to allow mineralisation of the callus tissue. It was, however, difficult to form clear conclusions with a single termination time point of 35 days. As a result of this, the study was expanded to include an earlier intermediate time point to assess the healing pathway and allow for a clearer description of the phenomena occurring in this process.

This expansion formed the study described in Chapter 6, where the time course of healing was evaluated at 5, 14 and 28 days post-operatively. This study showed interesting tissue distributions associated with the modification of fixation stiffness, driving intracortical bridging via different pathways. In both control groups (initial IFS 25% and 100%), periosteal callus formation via intramembranous ossification was observed 5 days post-operatively. By 14 days, periosteal callus development had continued, with large amounts of cartilage formation in the periosteal and intracortical regions, in this case driven via endochondral ossification. At this stage of healing, endosteal bone formation had also initiated, with bridging across this region under flexible conditions. By 28 days, the cartilage found in the stiff group had predominantly mineralised, with some mineralisation occurring under flexible conditions and a large amount of cartilage present even at 35 days. By 35 days, healing and bony bridging had occurred in the majority of samples in the stiff condition. From

these findings a healing pathway for rat diaphyseal bones was developed (Figure 6.13) and compared to a pre-existing model developed based on sheep histology.

This healing pathway was then compared to experimental groups, where fixation was stabilised at 3 days (3D) and 7 days (7D) postoperatively with healing evaluated at 14 days. Interestingly, these groups appeared to follow an alternate healing pathway to the control groups, with minimal cartilage formation and increased intracortical bone formation, with slightly larger bone areas found in the 7D group than the 3D group. The results indicated that bone formation in the intracortical region may have formed via intramembranous ossification, rather than endochondral as previously observed in the control groups. However, further assessment is necessary to confirm these findings, potentially through the use of more detailed biological analyses such as immunohistochemical staining and imaging.

7.1.1 Temporal tissue formation

The predictive capacity of a pre-established FE model of bone healing was assessed in Chapter 4 as previously described. The tissue distributions however were not previously assessed in comparison to *in vivo* histological sections. The sections obtained in Chapter 6, assisted in defining a healing pathway for rat bone healing.

In the FE model, bone formation initiated along the cortical surface of the bone, however this occurred at some distance from the osteotomy. The growth then expanded toward the fracture region whilst the size of the callus was confined to the initial soft tissue domain. This differs from healing observed in experimental studies, where in the rat, healing initiated along the full length of the cortical bone, with this response appearing to be relatively uniform along the length. Similarly, previous experimental sheep studies also demonstrated such a uniform development of the periosteal hard callus [67, 80, 197]. The callus in these experimental studies radiated

away from the fracture region, rather than growing toward the fracture. This is not an uncommon trend within FE models, with this pattern of bone development observed previously in 2D [118, 129], 3D [124] and callus growth models [121].

Despite differences in fixation stability, few differences were observable throughout the healing process in the FE model, contrary to experimental outcomes. The exception to this was the simulation of the lowest fixation stiffness (400 $N \cdot mm^{-1}$), where a band of soft tissue remained throughout the periosteal and intracortical regions; a phenomenon which occurred due to the strain magnitude being too high for bone to develop. Interestingly, however, there was also no cartilage formation in this region, which would be expected based on data from the experimental studies presented here or from other sheep studies [67].

More recently, the FE model used throughout this project was adapted to simulate healing in a rat model [73], which may provide more accurate comparisons for the healing pathway observed herein. This model was adapted by matching the increase in callus stiffness in the FE simulation to experimental data. As a result, strain thresholds were implemented at higher magnitudes than for the previous model of sheep healing [73]. This suggests that a rat fracture callus may develop and mineralise under higher loads than in humans and sheep; a finding that has not been previously elucidated, discussed or assessed.

Qualitative comparison of the numerical model of healing in the rat and experimental data revealed a greater correlation, with both indicating initial periosteal callus formation along the cortex. The size of the callus was marginally smaller under more stable fixation conditions, which was not included in the previous version of this numerical model. However the model also implemented a fixed domain approach, where the more flexible condition remained limited to a callus size within that domain.

Further, endosteal bone formation occurring prior to periosteal bridging was not observed in the simulation, and the amount of cartilage produced did not differ greatly for different fixation stability conditions. Whilst this modification demonstrated improvements in terms of matching experimental data, the adaptation was not tested for its predictive capacity or based on all findings, and thus it seems unlikely that it could adequately model the effects of stabilising fixation.

With the data presented here, it is clear that with the current processes involved in the presented FE model, further development is required to improve correlation with previous histological data and to enable use of the model in future predictive scenarios, both clinically and experimentally. There are a number of limitations across all current FE models restricting their predictive capacity. These include but are not limited to simplifications in loading, material properties, representing callus growth, modelling biological processes and validation of FE models with experimental data.

Loading is applied as a constant parameter in the majority of bone healing simulations. However in reality, limb loading is intermittent (during gait and patient weight bearing) and loading often increases as healing occurs. Loading in FE models is often only applied axially to the proximal bone end, while the distal end of the bone is constrained. There have been efforts to incorporate shear loading / movement, however these are greatly simplified without the addition of muscle, tendon and joint forces, which provide much more complex loading conditions *in vivo* than in the simulation. However the difficulty in increasing the complexity of the loading conditions, is that there is limited information attainable as to patient loading or loading throughout *in vivo* experiments. As this area develops experimentally, with the focus on attaining loading conditions *in vivo*, this knowledge can then be implemented computationally.

Material properties also prove to be difficult to accurately represent with different values reported throughout literature. For example the initial connective tissue or granulation tissue has been reported implemented differently, which can greatly affect the estimations of stress, strain and interstitial fluid velocities as they are sensitive to assumed of material properties [184]. Gardner *et al*. [198] implemented granulation tissue as a linear elastic model with an elastic modulus of 0.2 MPa, whereas Lacroix *et al*. [118, 127] implemented the same elastic modulus however modelling the tissue as a biphasic, poroelastic material. However, Comiskey *et al*. [151] implemented this material as pseudoelastic with an elastic modulus of 1 MPa based on experimental findings of Leong and Morgan [199]. Finally, Claes and Heigele [11] assumed that the granulation tissue behaved as a Mooney-Rivlin hyperelastic material. These vast differences in material properties implemented, makes it difficult to compare models and simulated bone healing outcomes. This also has a vast impact on the magnitude of the initial mechanical stimuli driving the healing process.

The majority of FE models have failed to model callus growth, generally beginning with a field of soft tissue surrounding the bone fracture, in which fibrous tissue, cartilage and bone can develop, modelled as changes in material properties [73, 118, 119, 124, 125, 127-129, 131, 153, 188]. Numerous studies have now identified the importance of a growing callus geometry with changes in mechanical conditions [121, 123, 125, 139] as demonstrated experimentally with larger callus sizes achieved with greater mechanical stimulus [78, 140]. While limitations remain with these FE models of callus growth, future development should enable more realistic determination of mechanical stimuli within the healing callus tissue with this approach.

There also remains a significant challenge in the implementation within an FE model of biological processes during fracture healing, such as cell migration, differentiation, proliferation and apoptosis as well as angiogenesis [35, 129]. A number of models have attempted to characterise these cellular behaviours, however many assumptions are required to model these parameters. For example Lacroix and Prendergast [118] used a diffusion mechanism to simulate migration, proliferation and differentiation of cells. However all of the cellular parameters occur at varying rates leading Isaksson *et al* [200] to describe temporal and spatial distributions of skeletal tissue as being regulated by four cell types, mesenchymal stem cells, chondrocytes, fibroblast and osteoblasts. These cells at each time point could migrate, proliferate, differentiate and/or undergo apoptosis depending on the mechanical stimulation and activity of surrounding cells. Other approaches have reduced the complexity of the models by restricting the formation of fibrous tissue, cartilage and bone to existing surfaces [139], consistent with histological observations.

Finally, validation of the FE model outcome can be difficult as this process generally involves comparisons between the mechanical environment with histological patterns of tissue formation. This approach can only demonstrate correlations and not cause-effect relationships. It can be useful however in assessing the predictive power of current methodologies – an essential step for improving the modelling processes for translation to clinical use.

7.2 CLINICAL IMPLICATIONS OF MODIFYING FIXATION STIFFNESS

Currently in clinical practice, when a fixation device is applied, there is no modulation of the fixation stiffness over the course of healing i.e. the fixation stiffness remains constant. Although this approach is mostly successful in the clinical setting, complications do occur as a result of fixation stiffness that is overly rigid or overly

flexible [175]. Moreover, clinical and experimental studies have shown that there is a greater risk of extremely flexible fixation leading to a delay in bone healing (hypertrophic non-union) [79, 85, 89] compared to a rigid fixation, as extreme rigidity with no mechanical stimulus is difficult to achieve.

Currently there are few scenarios where fixation stability is increased clinically. The first case is when there is delayed healing or hypertrophic non-union resulting from insufficient fixation stability [71, 159]. When this occurs, clinicians usually treat it by increasing the fixation stability, which requires a secondary surgery and the addition of screws or modification of the device entirely [159].

The second case where fixation stability is increased clinically is when severe trauma patients with multiple injuries are initially treated with an external fixator, which is later changed to internal fixations, most commonly an intramedullary nail [183, 201, 202]. External fixators are less invasive than intramedullary nails, so to avoid an excessive inflammatory response, these devices are used in preference to initially stabilised the fracture, particularly when the patient is at high risk of multiple organ dysfunction syndrome. Once the patient is stable, the external fixators are often replaced by intramedullary nails [202] however this process is largely performed for patient comfort and convenience rather than through necessity.

Sigurdsen *et al*. [201] demonstrated that converting from an external fixator to intramedullary nail at 1 week post-operatively in a rat model, produced similar healing outcomes as maintaining external fixation throughout the entire healing period. However there were definitive delays in healing when converting to a nail at 14 or 30 days post-operatively. Further to this Recknagel *et al*. [183] assessed this process in a multiple injury model finding that conversion to a nail at 4 days post-operatively lead to prolonged healing times, potentially due to the disruption and damage of the healing

callus tissues. Clinically studies have demonstrated similar trends, where it has been reported that acute conversion to internal fixation is associated with a higher rate of successful healing, with poorer outcomes associated with longer external fixation time [203]. In one clinical study [204], 40 % of patients who underwent secondary orthopaedic surgery within 3 days post trauma developed multiple organ failure, a finding confirmed with the outcome of the study by Recknagel *et al*. [183]. Therefore there is potential to continue treatment via external fixation, however the fixator may require stabilisation to increase patient mobility.

The advantages of using an external fixation in fracture treatment, particularly for the application of the hypothesis discussed throughout this thesis, is the ability to modify the fixation stability with minimal invasive approaches compared to those discussed with internal fixation devices. However an understandable drawback is patient discomfort and potential pin site infections. However, implementation of the hypothesis clinically, does not need to be directly related to changes in fixation stability. Instead this could be applied as a loading regimen during patient rehabilitation. For example, the patient could weight bear as early as allowable post-operatively. Once there is evidence of callus formation via x-ray, the patient could de-load their fracture limb – potentially producing the same effect as physically stabilising the fracture. Future work is required to examine the mechanistic bone healing pathway and outcomes, in combination with patient rehabilitation studies in order to implement a modification of the mechanical environment within a fracture for potential clinical application.

7.3 FUTURE WORK

There is a great deal of further research that may be derived from the work of this thesis. Firstly the assessment of whether fracture healing time was reduced by

modifying the fixation stiffness compared to the constant stable condition. To assess this further animals would need to be included to the study, to determine the mechanical integrity of the bones throughout in the healing period. Mechanical testing could be conducted on samples as early as 14 days to ascertain the strength differences between the largely cartilaginous callus structure observed in both control groups and the bone formation observed in the 3D and 7D groups. This could be repeated at 28 days post-operatively, where larger differences between the groups would be expected compared to the results after 35 days of healing (Chapter 5:).

The healing pathway (Chapter 6:) of the 7D and 14D groups could be further investigated. It is critical to further assess and confirm if the 7D group formed bone throughout the intracortical region via intramembranous ossification while the 14D group showed an accelerated endochondral ossification response. Early time point samples from these groups could be analysed further via immunohistochemical staining techniques with particular focus on markers indicating cartilage versus bone deposition. Differences in the revascularisation of the callus for these ossification processes could also be examined.

Second to this, assessment of the *in vivo* mechanical environment could be assessed through representative FE models, which could elucidate the mechanical environment conducive to the differing healing pathways. The mechanical stimuli could then be related more closely to the changes in tissue deposition observed experimentally.

Finally, this fixation protocol could be applied to models of disease, where healing is compromised such that without optimised conditions fracture healing can be very difficult. Implementing this process could assist in reducing the margin of error for clinicians.

7.3.1 Further Examination of the Healing Pathway

Further examination of the samples obtained in Chapter 6, could assist in providing more information regarding the healing pathway particularly the differences between intramembranous and endochondral ossification regions across all groups. Firstly, investigating angiogenesis within the fracture callus could assist in determining differences between the control and experimental groups with respect to cartilage formation. Revascularisation of the fracture callus is essential to facilitate nutrient and gas exchange to the cells within the fracture region. It has been postulated that healing situations with low oxygen content are thought to drive MSCs toward a chondrogenic lineage (endochondral ossification), whereas regions with extensive microvasculature are thought to direct MSCs toward an osteogenic lineage (intramembranous) [36, 205]. This may assist in interpreting differences in the bone formation throughout the intracortical region. Potential antibodies that could be used to examine these differences are CD31 [206, 207]; anti-vascular endothelial growth factor (VEGF) [3, 35, 70, 208]; anti-alpha smooth muscle actin [209]; and von Willebrand factor (vWF) [205].

Further to this, investigation into bone tissue macrophages (osteomacs) could provide further insights into the healing pathway as they have been shown to enhance osteoblast mineralization *in vitro* and have been are associated with sites of intramembranous bone deposition *in vivo* [210]. Osteomacs reside within bone lining tissues have thus far been identified in both mice [211] and humans [211, 212]. Specific antibodies that could be used to investigate the role of osteomacs and further to that intramembranous bone formation within the healing fracture include F4/80; CD68 (general marker); CD163 (Mac 2) [210], osteocalcin and Collagen type I. To

examine regions of endochondral ossification more closely, staining for Collagen type X, prior to cartilage formation could be examined [213].

7.3.2 Finite Element Models

Further evaluation is required to identify the features of the mechanical microenvironment most strongly associated with different skeletal tissue formation during bone healing. Building on the previous works of Claes and Heigele [11], a series of FE models could be developed from the histological sections obtained in Chapter 6. The purpose of this investigation would be to determine the mechanical environment under different fixation conditions and to relate this to changes in tissue distribution observed *in vivo*. This could lead to a better understanding of the optimal mechanical conditions for healing by determining the strains and hydrostatic stresses in the callus and how these change with hard callus maturation. It would be interesting then to assess how the mechanical stimuli vary with the increase in fixation stiffness, specifically the changes that influence faster mineralisation within the fracture (as observed experimentally in the 14D group). The results from this FE study could be coupled with the immunohistochemical investigation to enhance understanding of the mechanisms involved in the mechanical regulation of bone healing.

7.3.3 Further Applications

The concept of modifying fixation stiffness from initial flexible conditions to stiff throughout the healing period is a relatively novel concept, as this is the first study to investigate this concept in normal fracture healing. Thus the effect of this process is not fully characterised under normal bone healing conditions. Despite this, there is potential that this process could be applied to disease models where fracture healing is a significantly impaired process and difficult to achieve clinically under constant fixation. Osteoporosis is a skeletal disease characterised by micro-architectural

deterioration and low bone mass, resulting in increased bone fragility and hence susceptibility to fracture [214]. While common osteoporotic fractures are of the hip, distal radius and vertebral body, it is a systemic condition with a heightened risk of many fracture types [215]. Worldwide 100 – 200 million people are at risk of an osteoporotic fracture each year, with this number rising due to the ageing population in many of the developed countries [216]. Clinical experience and outcomes are inconsistent with respect to delayed bone healing for osteoporotic patients due to a lack of comparative studies with normal bone. However recently a retrospective clinical investigation determined that healing was significantly delayed in osteoporotic bone [217]. Several experimental studies have outlined poorer healing outcomes in osteoporotic models, namely reduced fracture callus cross-sectional area [218] and reduced mechanical properties of the fracture callus [219]. Implementing a modification of fixation stiffness has the potential as demonstrated to produce a large callus volume, which upon stabilisation could mineralise to produce a more robust callus.

7.4 CONCLUSION

This project proposed the hypothesis that fracture healing may be enhanced with flexible fixation conditions during the early stages of healing that are later stabilised to allow callus mineralisation. It is the first study in fracture healing to assess the effect of modification of fixation stability, by examining histological outcomes at various healing time-points in a rat femoral osteotomy model.

This study clearly demonstrates differences in healing under constant fixation and after fixation stabilisation. The formation of the periosteal callus via intramembranous ossification was shown to be related to the local mechanical stimulus within the fracture region. It was identified that intramembranous and endochondral

ossification were overlapping processes, with the initiation of the later occurring at the periphery of the periosteal callus. As healing progressed under constant fixation, it was observed that higher magnitude IFM led to a delayed healing, particularly the endochondral response with the presence of cartilage throughout the entire healing process under less stable fixation.

The modification of fixation stiffness at 7 days post-operatively, led to a healing pathway dominated by intramembranous ossification, however when implemented at 14 days post-operatively the process was shown to accelerate endochondral ossification compared to both control groups under constant fixation. Overall these results indicate benefits from early fixation flexibility to stimulate hard callus formation, with stabilisation required for intracortical bone formation, irrespective of the healing pathway.

Reference List

[1] Bradley C, Harrison J. Descriptive epidemiology of traumatic fractures in Australia. In: Ageing DoHa, editor. Adelaide: Flinders University; 2004.
[2] Doblaré M, García JM, Gómez MJ. 2004. Modelling bone tissue fracture and healing: a review. *Engineering Fracture Mechanics* 71: 1809-40.
[3] Yuasa M, Mignemi NA, Barnett JV, Cates JMM, Nyman JS, Okawa A, et al. 2014. The temporal and spatial development of vascularity in a healing displaced fracture. *Bone* 67: 208-21.
[4] Harwood PJ, Newman JB, Michael ALR. 2010. (ii) An update on fracture healing and non-union. *Orthopaedics and Trauma* 24: 9-23.
[5] Tosounidis T, Kontakis G, Nikolaou V, Papathanassopoulos A, Giannoudis PV. 2009. Fracture healing and bone repair: An update. *Trauma* 11: 145-56.
[6] Hayda RA, Brighton CT, Esterhai JL. 1998. Pathophysiology of delayed healing. *Clinical Orthopaedics and Related Research* 355S: S31-40.
[7] Gómez-Barrena E, Rosset P, Lozano D, Stanovici J, Ermthaller C, Gerbhard F. 2015. Bone fracture healing: Cell therapy in delayed unions and nonunions. *Bone* 70: 93-101.
[8] Carlier A, Geris L, Lammens J, Van Oosterwyck H. 2015. Bringing computational models of bone regeneration to the clinic. *Wiley Interdisciplinary Reviews: Systems Biology and Medicine* 7: 183-94.
[9] Carter DR, Blenman PR, Beaupré GS. 1988. Correlations between mechanical stress history and tissue differentiation in initial fracture healing. *Journal of Orthopaedic Research* 6: 736-48.
[10] Carter DR, Van der Muelen MC, Beaupré GS. 1996. Mechanical Factors in bone growth and development. *Bone* 18: S5-10.
[11] Claes LE, Heigele CA. 1999. Magnitudes of local stress and strain along bony surfaces predict the course and type of fracture healing. *J Biomech* 32: 255-66.
[12] Epari DR, Wehner T, Ignatius A, Schuetz MA, Claes LE. 2013. A case for optimising fracture healing through inverse dynamization. *Medical Hypotheses* 81: 225-7.
[13] Goodship AE, Cunningham JL, Kenwright J. 1998. Strain Rate and Timing of Stimulation in Mechanical Modulation of Fracture Healing. *Clinical Orthopaedics and Related Research* 355: S105-S15.
[14] Goodship AE, Kenwright J. 1985. The influence of induced micromovement upon the healing of experimental tibial fractures. *Journal of Bone & Joint Surgery* 67: 650-5.
[15] Clarke B. 2008. Normal Bone Anatomy and Physiology. *Clinical Journal of the American Society of Nephrology : CJASN* 3: S131-S9.
[16] Fazzalari NL. 2011. Bone fracture and bone fracture repair. *Osteoporos Int* 22: 2003-6.
[17] Childs SG. 2003. Stimulators of bone healing: Biologic and biomechanica. *Orthopaedic Nursing* 22: 421-8.
[18] Reichert JC, Hutmacher DW. Bone Tissue Engineering. In: Pallua N, Suscheck CV, editors. Tissue Engineering. Heidelberg: Springer Berlin
2011. p. 431-56.

[19] Fratzl P, Weinkamer R. Hierarchical Structure and Repair of Bone: Deformation, Remodelling, Healing. In: van der Zwaag S, editor. Self Healing Materials: Springer Netherlands; 2007. p. 323-35.
[20] Klein-Nulend J, Bacabac RG, Bakker AD. 2012. Mechanical loading and how it affects bone cells: The role of the osteocyte cytoskeleton in maintaining our skeleton. *European Cells and Materials* 24: 278-91.
[21] Stevens MM, George JH. 2005. Exploring and Engineering the Cell Surface Interface. *Science* 310: 1135-8.
[22] Stevens MM. 2008. Biomaterials for bone tissue engineering. *Materials Today* 11: 18-25.
[23] Wraighte PJ, Scammell BE. 2007. Principles of fracture healing. *The Foundation Years* 3: 243-51.
[24] Marsell R, Einhorn TA. 2011. The biology of fracture healing. *Injury* 42: 551-5.
[25] Merloz P. 2011. Macroscopic and microscopic process of long bone fracture healing. *Osteoporos Int* 22: 1999-2001.
[26] Einhorn TA. 1998. The Cell and Molecular Biology of Frature Healing. *Clinical Orthopaedics and Related Research* 355S: S7-21.
[27] Claes LE, Cunningham JL. 2009. Monitoring the Mechanical Properties of Healing Bone. *Clinical Orthopaedics and Related Research* 467: 1964-71.
[28] Rafiee B. Imaging and Understanding Fracture Fixation. In: Bonakdarpour A, Reinus WR, Khurana JS, editors. Diagnostic Imaging of Musculoskeletal Diseases: A Systematic Approach. Totowa: Springer Science; 2010. p. 203-38.
[29] Marsh DR, Li G. 1999. The biology of fracture healing: optimising outcome. *British Medical Bulletin* 55: 856-69.
[30] McKibbin B. 1978. The biology of fracture healing in long bones. *Journal of Bone & Joint Surgery, British Volume* 60-B: 150-62.
[31] Kolar P, Gaber T, Perka C, Duda GN, Buttgereit F. 2011. Human Early Fracture Hematoma Is Characterized by Inflammation and Hypoxia. *Clinical Orthopaedics and Related Research* 469: 3118-26.
[32] Claes L, Ignatius A, Stefan R. 2012. Fracture healing under healthy and inflammatory conditions. *Nat Rev Rheumatol* 8: 1-11.
[33] Claes L, Recknagel S, Ignatius A. 2012. Fracture healing under healthy and inflammatory conditions. *Nature Reviews Rheumatology* 8: 133-43.
[34] Isaksson H. 2012. Recent advances in mechanobiological modeling of bone regeneration. *Mechanics Research Communications* 42: 22-31.
[35] Geris L, Gerisch A, Sloten JV, Weiner R, Oosterwyck HV. 2008. Angiogenesis in bone fracture healing: A bioregulatory model. *Journal of Theoretical Biology* 251: 137-58.
[36] Chim SM, Tickner J, Chow ST, Kuek V, Guo B, Zhang G, et al. 2013. Angiogenic factors in bone local environment. *Cytokine & Growth Factor Reviews* 24: 297-310.
[37] Brighton CT, Krebs AG. 1972. Oxygen Tension of Healing Fractures in the Rabbit. *Journal of Bone and Joint Surgery* 54: 323-32.
[38] Carter DR, Beaupré GS, Giori NJ, Helms JA. 1998. Mechanobiology of skeletal regeneration. *Clinical Orthopaedics and Related Research* 355: S41-55.
[39] Cheal EJ, Mansmann KA, Digioia AM, Hayes WC, Perren SM. 1991. Role of interfragmentary strain in fracture healing: Ovine model of a healing osteotomy. *Journal of Orthopaedic Research* 9: 131-42.
[40] Claes LE, Wilke HJ, Augat P, Rübenacker S, Margevicius KJ. 1995. Effect of dynamization on gap healing of diaphyseal fractures under external fixation. *Clinical Biomechanics* 10: 227-34.

[41] Miller DL, Goswami T. 2007. A review of locking compression plate biomechanics and their advantages as internal fixators in fracture healing. *Clinical Biomechanics* 22: 1049-62.
[42] Perren SM. 2002. Evolution of the Internal Fixation of Long Bone Fractures. *Journal of Bone & Joint Surgery* 84: 1093.
[43] Riemer B. 2004. Controversies and Perills Plating Diaphyseal Fractures. *Techniques in Orthopaedics* 18: 360-7.
[44] Stiffler KS. 2004. Internal fracture fixation. *Clinical Techniques in Small Animal Practice* 19: 105-13.
[45] Schmidt-Rohlfing B, Heussen N, Knobe M, Pfeifer R, Kaneshige JR, Pape H-C. 2012. Reoperation Rate After Internal Fixation of Intertrochanteric Femur Fractures With the Percutaneous Compression Plate: What Are the Risk Factors? *Journal of Orthopaedic Trauma* 27: 312-7.
[46] Al-Rashid M, Khan W, Vemulapalli K. 2010. Principles of fracture fixation in orthopaedic trauma surgery. *Journal of Perioperative Practice* 20: 113+.
[47] Moss DP, Tejwani NC. 2007. Biomechanics of External Fixation: a review of the literature. *Bulletin of the NYU Hospital for Joint Diseases* 65: 294.
[48] Claes L, Ito K. Biomechanics of Fracture Fixation and Fracture Healing. In: Mow VC, Huiskes R, editors. Basic Orthopaedic Biomechanics and Mechano-Biology. Philadelphia: Lippincott Williams and Wilkins; 2005.
[49] Burgers PTPW, Van Riel MPJM, Vogels LMM, Stam R, Patka P, Van Lieshout EMM. 2011. Rigidity of unilateral external fixators—A biomechanical study. *Injury* 42: 1449-54.
[50] Larsen LB, Madsen JE, Hoiness PR, Ovre S. 2004. Should Insertion of Intramedullary Nails for Tibial Fractures Be With or Without Reaming?: A Prospective, Randomized Study With 3.8 Years' Follow-up. *Journal of Orthopaedic Trauma* 18: 144-9.
[51] Wehner T, Penzkofer R, Augat P, Claes L, Simon U. 2011. Improvement of the shear fixation stability of intramedullary nailing. *Clinical Biomechanics* 26: 147-51.
[52] Miles AW, Goodwin MI. 1994. An investigation into the load transfer in interlocking intramedullary nails during simulated healing of a femoral fracture. *Proceedings of the Institution of Mechanical Engineers, Part H: Journal of Engineering in Medicine* 208: 19-26.
[53] Marsh D. 1998. Concepts of fracture union, delayed union and nonunion. *Clinical Orthopaedics and Related Research* 355S: S22-30.
[54] Geris L, Sloten JV, Oosterwyck HV. 2010. Connecting biology and mechanics in fracture healing: an integrated mathematical modeling framework for the study of nonunions. *Biomechanics and Modeling in Mechanobiology* 9: 713-24.
[55] Jenkins PJ, Keating JF, Simpson AH. 2010. Fractures of the tibial shaft. *Surgery* 28: 489-93.
[56] Loboa EG, Beaupré GS, Carter DR. 2001. Mechanobiology of initial pseudarthrosis formation with oblique fractures. *Journal of Orthopaedic Research* 19: 1067-72.
[57] Augat P, Merk J, Genant HK, Claes L. 1997. Quantitative Assessment of Experimental Fracture Repair by Peripheral Computed Tomography. *Calcif Tissue Int* 60: 194-9.
[58] Augat P, Merk J, Ignatius A, Margevicius KJ, Bauer G, Rosenbaum D, et al. 1996. Early, full weightbearing with flexible fixation delays fracture healing. *Clinical Orthopaedics and Related Research* 328: 194-202.

[59] Claes L, Augat P, Gebhard S, Wilke HJ. 1997. Influence of size and stability of the osteotomy gap on the success of fracture healing. *Journal of Orthopaedic Research* 15: 577-84.
[60] Claes L, Heigele CA, Neidlinger-Wilke C, Kaspar D, Seidl W, Margevicius K, et al. 1998. Effects of mechanical factors on the fracture healing process. *Clin Orthop Relat Res* 355S: S132-47.
[61] Gardner TN, Evans M, Simpson H. 1998. Temporal variation of applied inter fragmentary displacement at a bone fracture in harmony with maturation of the fracture callus. *Med Eng Phys* 20: 480-4.
[62] Goodship AE, Watkins PE, Rigby HS, Kenwright J. 1993. The role of fixator frame stiffness in the control of fracture healing. An experimental study. *Journal of Biomechanics* 26: 1027-35.
[63] Perren S, Cordey J. The concept of interfragmentary strain. In: Uhthoff H, editor. Current Concepts of Internal Fixation of Fractures. Heidelberg: Springer-Verlag; 1980. p. 63-77.
[64] Perren SM. 1979. Physical and biological aspects of fracture healing with special reference to internal fixation. *Clinical Orthopaedics and Related Research* 138: 175-96.
[65] Klein P, Schell H, Streitparth F, Heller M, Kassi J-P, Kandziora F, et al. 2003. The initial phase of fracture healing is specifically sensitive to mechanical conditions. *Journal of Orthopaedic Research* 21: 662-9.
[66] Augat P, Simon U, Liedert A, Lutz C. 2005. Mechanics and mechano-biology of fracture healing in normal and osteoporotic bone. *Osteoporos Int* 16: S36-43.
[67] Epari DR, Schell H, Bail HJ, Duda GN. 2006. Instability prolongs the chondral phase during bone healing in sheep. *Bone* 38: 864-70.
[68] Calisir C, Fayad LM, Carrino JA, Fishman EK. 2012. Recognition, assessment, and treatment of non-union after surgical fixation of fractures: Emphasis on 3D CT. *Japanese Journal of Radiology* 30: 1-9.
[69] Geris L, Reed AAC, Vander Sloten J, Simpson AHRW, Van Oosterwyck H. 2010. Occurrence and Treatment of Bone Atrophic Non-Unions Investigated by an Integrative Approach. *PLoS Computational Biology* 6: e1000915.
[70] Keramaris NC, Calori GM, Nikolaou VS, Schemitsch EH, Giannoudis PV. 2008. Fracture vascularity and bone healing: A systematic review of the role of VEGF. *Injury* 39, Supplement 2: S45-S57.
[71] Moulder E, Sharma HK. 2008. Tibial non-union: a review of current practice. *Current Orthopaedics* 22: 434-41.
[72] Watson L, Elliman SJ, Coleman CM. 2014. From isolation to implantation: a concise review of mesenchymal stem cell therapy in bone fracture repair. *Stem Cell Research & Therapy* 5: 51-.
[73] Wehner T, Steiner M, Ignatius A, Claes L. 2014. Prediction of the Time Course of Callus Stiffness as a Function of Mechanical Parameters in Experimental Rat Fracture Healing Studies - A Numerical Study. *PLoS One* 9.
[74] Andreykiv A, van Keulen F, Prendergast PJ. 2008. Simulation of fracture healing incorporating mechanoregulation of tissue differentiation and dispersal/proliferation of cells. *Biomechanics and Modeling in Mechanobiology* 7: 443-61.
[75] Bishop NE, Schneider E, Ito K. 2003. An experimental two degrees-of-freedom actuated external fixator for in vivo investigation of fracture healing. *Medical Engineering & Physics* 25: 335-40.

[76] Blenman PR, Carter DR, Beaupré GS. 1989. Role of mechanical loading in the progressive ossification of a fracture callus. *Journal of Orthopaedic Research* 7: 398-407.
[77] Bruder SP, Fink DJ, Caplan AI. 1994. Mesenchymal stem cells in bone development, bone repair, and skeletal regenaration therapy. *Journal of Cellular Biochemistry* 56: 283-94.
[78] Claes L, Laule J, Wenger K, Suger G, Liener U, Kinzl L. 2000. The influence of stiffness of the fixator on maturation of callus after segmental transport. *J Bone Joint Surg* 82-B: 142-8.
[79] Epari DR, Kassi J-P, Schell H, Duda GN. 2007. Timely fracture-healing requires optimization of axial fixation stability. *J Bone Joint Surg* 89: 1575-85.
[80] Epari DR, Taylor WR, Heller MO, Duda GN. 2006. Mechanical conditions in the initial phase of bone healing. *Clinical Biomechanics* 21: 646-55.
[81] Hente R, Cordey J, Rahn BA, Maghsudi M, von Gumppenberg S, Perren SM. 1999. Fracture healing of the sheep tibia treated using a unilateral external fixator. Comparison of static and dynamic fixation. *Injury* 30, Supplement 1: SA44-SA51.
[82] Hente R, Fuchtmeier B, Schlegel U, Ernstberger A, Perren SM. 2004. The influence of cyclic compression and distraction on the healing of experimental tibial fractures. *Journal of Orthopaedic Research* 22: 709-15.
[83] Kenwright J, Goodship AE. 1989. Controlled mechanical stimulation in the treatment of tibial fractures. *Clinical Orthopaedics and Related Research* 241: 36-47.
[84] Kenwright J, Goodship AE, Kelly DJ, Newman JH, Harris JD, Richardson JB, et al. 1986. Effect of Controlled Axial Micromovement on Healing of Tibial Fractures. *The Lancet* 328: 1185-7.
[85] Mark H, Nilsson A, Nannmark U. 2004. Effects of Fracture Fixation Stability on Ossification in Healing Fractures. *Clinical Orthopaedics and Related Research* 419: 245-50.
[86] Park S, O'Connor K, McKellop H, Sarmiento A. 1998. The influence of active shear or compressive motion on fracture-healing. *Journal of Bone and Joint Surgery* 80: 868-78.
[87] Sigurdsen U, Reikeras O, Utvag SE. 2011. The influence of compression on the healing of experimental tibial fractures. *Injury* 42: 1152-6.
[88] Smith-Adaline EA, Volkman SK, Ignelzi MA, Jr., Slade J, et al. 2004. Mechanical environment alters tissue formation patterns during fracture repair. *Journal of Orthopaedic Research* 22: 1079-85.
[89] Utvåg SE, Korsnes L, Rindal DB, Reikerås O. 2001. Influence of flexible nailing in the later phase of fracture healing: Strength and mineralization in rat femora. *Journal of Orthopaedic Science* 6: 576-84.
[90] Wolf S, Janousek A, Pfeil J, Veith W, Haas F, Duda G, et al. 1998. The effects of external mechanical stimulation on the healing of diaphyseal osteotomies fixed by flexible external fixation. *Clinical Biomechanics* 13: 359-64.
[91] Yamagishi M, Yoshimura Y. 1955. The biomechanics of fracture healing. *The Journal of Bone & Joint Surgery* 37-A: 1035-68.
[92] Augat P, Burger J, Schorlemmer S, Henke T, Peraus M, Claes L. 2003. Shear movement at the fracture site delays healing in a diaphyseal fracture model. *Journal of Orthopaedic Research* 21: 1011-7.
[93] Bishop NE, van Rhijn M, Tami A, Corveleijn R, Schneider E, Ito K. 2006. Shear does not necessarily inhibit bone healing. *Clinical Orthopaedics and Related Research* 443: 307-14.

[94] Duda GN, Sollmann M, Sporrer S, Hoffmann JE, Kassi JP, C. K, et al. 2002. Interfragmentary motion in tibial osteotomies stabilized with ring fixators. *Clinical Orthopaedics and Related Research* 396: 163-72.
[95] Klein P, Opitz M, Schell H, Taylor WR, Heller MO, Kassi JP, et al. 2004. Comparison of unreamed nailing and external fixation of tibial diastases-mechanical conditions during healing and biological outcome. *Journal of Orthopaedic Research* 22: 1072-8.
[96] Gardner TN, Evans M, Hardy J, Kenwright J. 1998. Is the stability of a tibial fracture influenced by the type of unilateral external fixator? *Clin Biomech* 13: 603-7.
[97] Röntgen V, Blakytny R, Matthys R, Landauer M, Wehner T, Göckelmann M, et al. 2010. Fracture healing in mice under controlled rigid and flexible conditions using an adjustable external fixator. *Journal of Orthopaedic Research* 28: 1456-62.
[98] Schell H, Epari DR, Kassi JP, Bragulla H, Bail HJ, Duda GN. 2005. The course of bone healing is influenced by the initial shear fixation stability. *Journal of Orthopaedic Research* 23: 1022-8.
[99] Schell H, Thompson MS, Bail HJ, Hoffmann J-E, Schill A, Duda GN, et al. 2008. Mechanical induction of critically delayed bone healing in sheep: Radiological and biomechanical results. *Journal of Biomechanics* 41: 3066-72.
[100] Augat P, Margevicius KJ, Simon J, Wolf S, Gebhard S, Claes L. 1998. Local tissue properties in bone healing: Influence of size and stability of the osteotomy gap. *Journal of Orthopaedic Research* 16: 475-81.
[101] Christel P, Cerf G, Pilla A. 1981. Time evolution of the mechanical properties of the callus of fresh fractures. *Ann Biomed Eng* 9: 383-91.
[102] Richardson JB, Kenwright J, Cunningham JL. 1992. Fracture stiffness measurement in the assessment and management of tibial fractures. *Clinical Biomechanics* 7: 75-9.
[103] Liu Y, Manjubala I, Schell H, Epari DR, Roschger P, Duda GN, et al. 2010. Size and habit of mineral particles in bone and mineralized callus during bone healing in sheep. *Journal of Bone and Mineral Research* 25: 2029-38.
[104] Richardson J, Cunningham J, Goodship A, O'Connor B, Kenwright J. 1994. Measuring stiffness can define healing of tibial fractures. *Journal of Bone & Joint Surgery, British Volume* 76-B: 389-94.
[105] Wehner T, Gruchenberg K, Bindl R, Recknagel S, Steiner M, Ignatius A, et al. 2014. Temporal delimitation of the healing phases via monitoring of fracture callus stiffness in rats. *J Orthop Res* 32: 1589-95.
[106] Schell H, Epari DR, Kassi JP, Bragulla H, et al. 2005. The course of bone healing is influenced by the initial shear fixation stability. *J Orthop Res* 23: 1022-8.
[107] Claes L, Blakytny R, Göckelmann M, Schoen M, Ignatius A, Willie B. 2009. Early dynamization by reduced fixation stiffness does not improve fracture healing in a rat femoral osteotomy model. *J Orthop Res* 27: 22-7.
[108] Claes L, Blakytny R, Besse J, Bausewein C, Ignatius A, Willie B. 2011. Late Dynamization by reduced fixation stiffness enhances fracture healing in a rat femoral osteotomy model. *J Orthop Trauma* 25: 169-74.
[109] Willie BM, Blakytny R, Glöckelmann M, Ignatius A, Claes L. 2011. Temporal Variation in Fixation Stiffness Affects Healing by Differential Cartilage Formation in a Rat Osteotomy Model. *Clinical Orthopaedics and Related Research* 469: 3094-101.
[110] Durall I, Falcón C, Díaz-Bertrana MC, Franch J. 2004. Effects of Static Fixation and Dynamization after Interlocking Femoral Nailing Locked with an External Fixator: An Experimental Study in Dogs. *Veterinary Surgery* 33: 323-32.

[111] Larsson S, Kim W, Caja VL, Egger EL, Inoue N, Chao EYS. 2001. Effect of Early Axial Dynamization on Tibial Bone Healing: A Study in Dogs. *Clinical Orthopaedics and Related Research* 388.
[112] Arazi M, Yalcin H, Tarkcioglu N, Dasci Z, Kutlu A. 2002. The effects of dynamization and destabilization of the external fixator on fracture healing: A comparative biomechanical study in dogs. *Orthopaedics* 25: 521-4.
[113] Foxworthy M, Pringle RM. 1995. Dynamization timing and its effect on bone healing when using the Orthofix Dynamic Axial Fixator. *Injury* 26: 117-9.
[114] Noordeen M, Lavy C. 1995. Cyclical micromovement and fracture healing. *Journal of Bone & Joint Surgery* 77: 645-8.
[115] Epari DR, Duda GN, Thompson MS. 2010. Mechanobiology of bone healing and regeneration: in vivo models. *Proceedings of the Institution of Mechanical Engineers, Part H: Journal of Engineering in Medicine* 224: 1543-53.
[116] Wang JC, Thampatty BP. 2006. An Introductory Review of Cell Mechanobiology. *Biomechanics and Modeling in Mechanobiology* 5: 1-16.
[117] Pauwels F. Gesammelte Abhandlungen zur Funktionellen Anatomie des Bewegungsapparates (Translated by P. Maquet and R. Furlong as Biomechanics of the locomotor apparatus) Berlin: Springer-Verlag; 1980.
[118] Lacroix D, Prendergast PJ. 2002. A mechano-regulation model for tissue differentiation during fracture healing: analysis of gap size and loading. *Journal of Biomechanics* 35: 1163-71.
[119] BailÓN-Plaza A, Van Der Meulen MCH. 2001. A Mathematical Framework to Study the Effects of Growth Factor Influences on Fracture Healing. *Journal of Theoretical Biology* 212: 191-209.
[120] Ament C, Hofer EP. 2000. A fuzzy logic model of fracture healing. *Journal of Biomechanics* 33: 961-8.
[121] García-Aznar JM, Kuiper JH, Gómez-Benito MJ, Doblaré M, Richardson JB. 2007. Computational simulation of fracture healing: Influence of interfragmentary movement on the callus growth. *Journal of Biomechanics* 40: 1467-76.
[122] Gardner TN, Weemaes M. 1999. A mathematical stiffness matrix for characterising mechanical performance of the Orthofix DAF. *Medical Engineering & Physics* 21: 65-71.
[123] Gómez-Benito MJ, García-Aznar JM, Kuiper JH, Doblaré M. 2005. Influence of fracture gap size on the pattern of long bone healing: a computational study. *Journal of Theoretical Biology* 235: 105-19.
[124] Isaksson H, van Donkelaar CC, Huiskes R, Ito K. 2006. Corroboration of mechanoregulatory algorithms for tissue differentiation during fracture healing: comparison with in vivo results. *Journal of Orthopaedic Research* 24: 898-907.
[125] Isaksson H, Wilson W, van Donkelaar CC, Huiskes R, Ito K. 2006. Comparison of biophysical stimuli for mechano-regulation of tissue differentiation during fracture healing. *Journal of Biomechanics* 39: 1507-16.
[126] Lacroix D, Prendergast PJ. 2002. Three-dimensional Simulation of Fracture Repair in the Human Tibia. *Computer Methods in Biomechanics and Biomedical Engineering* 5: 369-76.
[127] Lacroix D, Prendergast PJ, Li G, Marsh D. 2002. Biomechanical model to simulate tissue differentiation and bone regeneration: Application to fracture healing. *Med Bio Eng Comput* 40: 14-21.
[128] Shefelbine SJ, Augat P, Claes L, Simon U. 2005. Trabecular bone fracture healing simulation with finite element analysis and fuzzy logic. *Journal of Biomechanics* 38: 2440-50.

[129] Simon U, Augat P, Utz M, Claes L. 2011. A numerical model of the fracture healing process that describes tissue development and revascularisation. *Computer Methods in Biomechanics and Biomedical Engineering* 14: 79-93.
[130] Steiner M, Claes L, Ignatius A, Simon U, Wehner T. 2014. Disadvantages of interfragmentary shear on fracture healing—mechanical insights through numerical simulation. *Journal of Orthopaedic Research* 32: 865-72.
[131] Steiner M, Claes L, Ignatius A, Simon U, Wehner T. 2014. Numerical Simulation of Callus Healing for Optimization of Fracture Fixation Stiffness. *PLoS One* 9.
[132] Wilson C, Schuetz M, Epari D. 2015. Effects of strain artefacts arising from a pre-defined callus domain in models of bone healing mechanobiology. *Biomechanics and Modeling in Mechanobiology* 14: 1129-41.
[133] Geris L, Gerisch A, Maes C, Carmeliet G, Weiner R, Vander Sloten J, et al. 2006. Mathematical modeling of fracture healing in mice: comparison between experimental data and numerical simulation results. *Med Bio Eng Comput* 44: 280-9.
[134] Gardner TN, Mishra S, Marks L. 2004. The role of osteogenic index, octahedral shear stress and dilatational stress in the ossification of a fracture callus. *Medical Engineering and Physics* 26: 493-501.
[135] Morgan EF, Longaker MT, Carter DR. 2006. Relationships between tissue dilatation and differentiation in distraction osteogenesis. *Matrix Biology* 25: 94-103.
[136] Mow VC, Kuei SC, Lai WM, Armstrong CG. 1980. Biphasic Creep and Stress Relaxation of Articular Cartilage in Compression: Theory and Experiments. *Journal of Biomechanical Engineering* 102: 73-84.
[137] Prendergast PJ, Huiskes R, Søballe K. 1997. Biophysical stimuli on cells during tissue differentiation at implant interfaces. *Journal of Biomechanics* 30: 539-48.
[138] Kelly DJ, Prendergast PJ. 2005. Mechano-regulation of stem cell differentiation and tissue regeneration in osteochondral defects. *Journal of Biomechanics* 38: 1413-22.
[139] Wilson CJ, Schuetz MA, Epari DR. 2015. Effects of strain artefacts arising from a pre-defined callus domain in models of bone healing mechanobiology. *Biomechanics and Modeling in Mechanobiology* 14: 1129-41.
[140] Claes L, Augat P, Suger G, Wilke H. 1997. Influence of Size and Stability of the Osteotomy Gap on the Success of Fracture Healing. *Journal of Orthopaedic Research* 15: 577-84.
[141] Muller J, Schenk R, Willenegger H. 1968. Experimental studies on the development of reactive pseudarthroses on the canine radius *Helv Chir Acta* 35: 301-8.
[142] Kolar P, Schmidt-Bleek K, Schell H, Gaber T, Toben D, Schmidmaier G, et al. 2010. The Early Fracture Hematoma and Its Potential Role in Fracture Healing. *Tissue Engineering Part B* 16: 427-34.
[143] Horst K, Eschbach D, Pfeifer R, Hübenthal S, Sassen M, Steinfeldt T, et al. 2015. Local Inflammation in Fracture Hematoma: Results from a Combined Trauma Model in Pigs. *Mediators of Inflammation* 2015: 126060.
[144] Carreira AC, Alves GG, Zambuzzi WF, Sogayar MC, Granjeiro JM. 2014. Bone Morphogenetic Proteins: Structure, biological function and therapeutic applications. *Archives of Biochemistry and Biophysics* 561: 64-73.
[145] Kenwright J, Gardner TN. 1998. Mechanical Influences on tibial fracture healing. *Clinical Orthopaedics and Related Research* 355: S179-90.
[146] DiGioia IAM, Cheal EJ, Hayes WC. 1986. Three-Dimensional Strain Fields in a Uniform Osteotomy Gap. *Journal of Biomechanical Engineering* 108: 273-80.

[147] Histing T, Garcia P, Holstein JH, Klein M, Matthys R, Nuetzi R, et al. 2011. Small animal bone healing models: Standards, tips, and pitfalls results of a consensus meeting. *Bone* 49: 591-9.
[148] Borgiani E, Duda GN, Willie B, Checa S. 2015. Bone healing in mice: does it follow generic mechano-regulation rules? *Facta Universitatis Series: Mechanical Engineering* 13: 217-27.
[149] Recknagel S, Bindl R, Kurz J, Wehner T, Ehrnthaller C, Knöferl MW, et al. 2011. Experimental blunt chest trauma impairs fracture healing in rats. *Journal of Orthopaedic Research* 29: 734-9.
[150] Willie B, Adkins K, Zheng X, Simon U, Claes L. 2009. Mechanical characterization of external fixator stiffness for a rat femoral fracture model. *Journal of Orthopaedic Research* 27: 687-93.
[151] Comiskey DP, MacDonald BJ, McCartney WT, Synnott K, O'Byrne J. 2010. The role of interfragmentary strain on the rate of bone healing--A new interpretation and mathematical model. *Journal of Biomechanics* 43: 2830-4.
[152] Steiner M, Volkheimer D, Meyers N, Wehner T, Wilke H, Claes L, et al. 2015. Comparison between different methods for biomechanical assessment of ex vivo fracture callus stiffness in small animal bone healing studies. *PLoS One* 10.
[153] Wehner T, Claes L, Ignatius A, Simon U. 2012. Optimization of intramedullary nailing by numerical simulation of fracture healing. *Journal of Orthopaedic Research* 30: 569-73.
[154] Checa S, Prendergast PJ, Duda GN. 2011. Inter-species investigation of the mechano-regulation of bone healing: Comparison of secondary bone healing in sheep and rat. *Journal of Biomechanics* 44: 1237-45.
[155] Nunamaker DM. 1998. Experimental models of fracture repair. *Clinical Orthopaedics and Related Research* 355: S56-65.
[156] Watanabe Y, Nishizawa Y, Takenaka N, Kobayashi M, Matsushita T. 2009. Ability and Limitation of Radiographic Assessment of Fracture Healing in Rats. *Clinical Orthopaedics and Related Research* 467: 1981-5.
[157] Bhandari M, Guyatt GH, Swiontkowski MF, Tornetta PI, Sprague S, Schemitsch EH. 2002. A lack of consensus in the assessment of fracture healing among orthopaedic surgeons. *Journal of Orthopaedic Trauma* 16: 562-6.
[158] Wade R, Richardson J. 2001. Outcome in fracture healing: a review. *Injury* 32: 109-14.
[159] Balogh ZJ, Reumann MK, Gruen RL, Mayer-Kuckuk P, Schuetz MA, Harris IA, et al. 2012. Advances and future directions for management of trauma patients with musculoskeletal injuries. *The Lancet* 380: 1109-19.
[160] Goldhahn J, Scheele WH, Mitlak BH, Abadie E, Aspenberg P, Augat P, et al. 2008. Clinical evaluation of medicinal products for acceleration of fracture healing in patients with osteoporosis. *Bone* 43: 343-7.
[161] Giannoudis PV, Einhorn TA, Marsh D. 2007. Fracture healing: The diamond concept. *Injury* 38, Supplement 4: S3-S6.
[162] Chehade MJ, Pohl AP, Pearcy MJ, Nawana N. 1997. Clinical implications of stiffness and strength changes in fracture healing. *The Journal of Bone & Joint Surgery* 79: 9-12.
[163] Steiner M, Volkheimer D, Meyers N, Wehner T, Wilke H-J, Claes L, et al. 2015. Comparison between Different Methods for Biomechanical Assessment of Ex Vivo Fracture Callus Stiffness in Small Animal Bone Healing Studies. *PLoS One* 10.

[164] Panjabi MM, Walter SD, Karuda M, White AA, Lawson JP. 1985. Correlations of radiographic analysis of healing fractures with strength: A statistical analysis of experimental osteotomies. *Journal of Orthopaedic Research* 3: 212-8.
[165] Miller GJ, Gerstenfeld LC, Morgan EF. 2015. Mechanical microenvironments and protein expression associated with formation of different skeletal tissues during bone healing. *Biomechanics and Modeling in Mechanobiology* 14: 1239-53.
[166] Thompson Z, Miclau T, Hu D, Helms JA. 2002. A model for intramembranous ossification during fracture healing. *Journal of Orthopaedic Research* 20: 1091-8.
[167] Morgan EF, Salisbury Palomares KT, Gleason RE, Bellin DL, Chien KB, Unnikrishnan GU, et al. 2010. Correlations between local strains and tissue phenotypes in an experimental model of skeletal healing. *Journal of Biomechanics* 43: 2418-242

[168] Betts DC, Müller R. 2014. Mechanical Regulation of Bone Regeneration: Theories, Models and Experiments. *Frontiers in Endocrinology* 5.
[169] Wehner T, Claes L, Niemeyer F, Nolte D, Simon U. 2010. Influence of the fixation stability on the healing time — A numerical study of a patient-specific fracture healing process. *Clin Biomech* 25: 606-12.
[170] Willenegger H, Perren S, Schenk R. 1971. Primary and secondary healing of bone fractures. *Chirurg* 42: 241–52.
[171] Goodship A, Kenwright J. 1985. The influence of induced micromovement upon the healing of experimental tibial fractures. *J Bone Joint Surg* 67-B: 650-5.
[172] Claes L, Augat P, Suger G, Wilke H-J. 1997. Influence of size and stability of the osteotomy gap on the success of fracture healing. *J Orthop Res* 15: 577-84.
[173] Klein P, Opitz M, Schell H, Taylor WR, et al. 2004. Comparison of unreamed nailing and external fixation of tibial diastases-mechanical conditions during healing and biological outcome. *J Orthop Res* 22: 1072-8.
[174] Wehner T, Wolfram U, Henzler T, Niemeyer F, Claes L, Simon U. 2010. Internal forces and moments in the femur of the rat during gait. *J Biomech* 43: 2473-9.
[175] Bottlang M, Doornink J, Lujan TJ, Fitzpatrick DC, Marsh JL, Augat P, et al. 2010. Effects of Construct Stiffness on Healing of Fractures Stabilized with Locking Plates. *Journal of Bone & Joint Surgery, British Volume* 92: S12-22.
[176] Tsai S, Fitzpatrick DC, Madey SM, Bottlang M. 2015. Dynamic locking plates provide symmetric axial dynamization to stimulate fracture healing. *Journal of Orthopaedic Research* 33: 1218-25.
[177] Claes L, Laule J, Wenger K, Suger G, Liener U, Kinzl L. 2000. The influence of stiffness of the fixator on maturation of callus after segmental transport. *J Bone Joint Surg Br* 82: 142-8.
[178] Vetter A, Epari D, Seidel R, Schell H, Fratzl P, Duda G, et al. 2010. Temporal tissue patterns in bone healing of sheep. *J Orthop Res* 28: 1440-7.
[179] Klein P, Schell H, Streitparth F, Heller M, Kassi J-P, Kandziora F, et al. 2003. The initial phase of fracture healing is specifically sensitive to mechanical conditions. *J Orthop Res* 21: 662-9.
[180] Miclau T, Lu C, Thompson Z, Choi P, Puttlitz C, Marcucio R, et al. 2007. Effects of delayed stabilization on fracture healing. *J Orthop Res* 25: 1552-8.
[181] Gerstenfeld L, Alkhiary Y, Krall E, Nicholls F, Stapleton S, Fitch J, et al. 2006. Three-dimensional Reconstruction of Fracture Callus Morphogenesis. *J Histochem Cytochem* 54: 1215-28.
[182] Coutts R, Woo S, Boyer J, Doty D, Gonsalves M, Amiel D, et al. 1982. The effect of delayed internal fixation on healing of the osteotomized dog radius. *Clin Orthop Relat Res* 163: 254-60.

[183] Recknagel S, Bindl R, Wehner T, Göckelmann M, Wehrle E, Gebhard F, et al. 2013. Conversion from external fixator to intramedullary nail causes a second hit and impairs fracture healing in a severe trauma model. *J Orthop Res* 31: 465-71.
[184] Isaksson H, Gröngröft I, Wilson W, van Donkelaar CC, van Rietbergen B, Tami A, et al. 2009. Remodeling of fracture callus in mice is consistent with mechanical loading and bone remodeling theory. *Journal of Orthopaedic Research* 27: 664-72.
[185] Giannoudis PV, Jones E, Einhorn TA. 2011. Fracture healing and bone repair. *Injury* 42: 549-50.
[186] Thompson MS, Epari DR, Bieler F, Duda GN. 2010. In vitro models for bone mechanobiology: Applications in bone regeneration and tissue engineering. *Proceedings of the Institution of Mechanical Engineers, Part H: Journal of Engineering in Medicine* 224: 1533-41.
[187] McKinley T. 2003. Principles of Fracture Healing. *Surgery (Oxford)* 21: 209-12.
[188] Steiner M, Claes L, Ignatius A, Niemeyer F, Simon U, Wehner T. 2013. Prediction of fracture healing under axial loading, shear loading and bending is possible using distortional and dilatational strains as determining mechanical stimuli. *Journal of the Royal Society Interface* 10: 20130389.
[189] Garcia P, Holstein JH, Maier S, Schaumlöffel H, Al-Marrawi F, Hannig M, et al. 2008. Development of a Reliable Non-Union Model in Mice. *Journal of Surgical Research* 147: 84-91.
[190] Kaspar K, Matziolis G, Strube P, Sentürk U, Dormann S, Bail HJ, et al. 2008. A new animal model for bone atrophic nonunion: Fixation by external fixator. *Journal of Orthopaedic Research* 26: 1649-55.
[191] Burgers TA, Hoffmann MF, Collins CJ, Zahatnansky J, Alvarado MA, Morris MR, et al. 2013. Mice Lacking Pten in Osteoblasts Have Improved Intramembranous and Late Endochondral Fracture Healing. *PLoS One* 8.
[192] Guzel Y, Karalezli N, Bilge O, Kacira B, Esen H, Karadag H, et al. 2015. The biomechanical and histological effects of platelet-rich plasma on fracture healing. *Knee Surg Sports Traumatol Arthrosc* 23: 1378-83.
[193] Ho C-Y, Sanghani A, Hua J, Coathup M, Kalia P, Blunn G. 2015. Mesenchymal Stem Cells with Increased Stromal Cell-Derived Factor 1 Expression Enhanced Fracture Healing. *Tissue Engineering Part A* 21: 594-602.
[194] Issa JPM, Ingraci de Lucia C, dos Santos Kotake BG, Gonçalves Gonzaga M, Tocchini de Figueiredo FA, Mizusaki Iyomasa D, et al. 2015. The effect of simvastatin treatment on bone repair of femoral fracture in animal model. *Growth Factors* 33: 139-48.
[195] Rapp AE, Bindl R, Heilmann A, Erbacher A, Muller I, Brenner RE, et al. 2015. Systemic mesenchymal stem cell administration enhances bone formation in fracture repair but not load-induced bone formation. *European Cells and Materials* 29: 22-34.
[196] Peters A, Schell H, Bail HJ, Hannemann M, Schumann T, Duda GN, et al. 2010. Standard bone healing stages occur during delayed bone healing, albeit with a different temporal onset and spatial distribution of callus tissues. *Histology and Histopathology* 25: 1149-62.
[197] Vetter A, Epari DR, Seidel R, Schell H, Fratzl P, Duda GN, et al. 2010. Temporal tissue patterns in bone healing of sheep. *Journal of Orthopaedic Research* 28: 1440-7.
[198] Gardner TN, Stoll T, Marks L, Mishra S, Knothe Tate M. 2000. The influence of mechanical stimulus on the pattern of tissue differentiation in a long bone fracture — an FEM study. *Journal of Biomechanics* 33: 415-25.

[199] Leong PL, Morgan EF. 2008. Measurement of fracture callus material properties via nanoindentation. *Acta Biomaterialia* 4: 1569-75.
[200] Isaksson H, van Donkelaar CC, Huiskes R, Yao J, Ito K. 2008. Determining the most important cellular characteristics for fracture healing using design of experiments methods. *Journal of Theoretical Biology* 255: 26-39.
[201] Sigurdsen U, Reikeras O, Utvag SE. 2010. Conversion of External Fixation to Definitive Intramedullary Nailing in Experimental Tibial Fractures. *Journal of Investigative Surgery* 23: 142-8.
[202] Sigurdsen U, Reikeras O, Utvag SE. 2011. The Effect of timing of conversion from external fixation to secondary intramedullary nailing in experimental tibial fractures. *Journal of Orthopaedic Research* 29: 126-30.
[203] Monni T, Birkholtz FF, de Lange P, Snyckers CH. 2013. Conversion of external fixation to internal fixation in a non-acute, reconstructive setting: a case series. *Strategies in Trauma and Limb Reconstruction* 8: 25-30.
[204] Waydhas C, Nast-Kolb D, Trupka A, Zettl R, Kick N, Wiesholler J, et al. 1996. Posttraumatic Inflammatory Response, Secondary Operations, and Late Multiple Organ Failure. *The Journal of Trauma: Injury, Infection, and Critical Care* 40: 624-31.
[205] Huang Y-C, Kaigler D, Rice KG, Krebsbach PH, Mooney DJ. 2005. Combined Angiogenic and Osteogenic Factor Delivery Enhances Bone Marrow Stromal Cell-Driven Bone Regeneration. *Journal of Bone and Mineral Research* 20: 848-57.
[206] Garcia P, Pieruschka A, Klein M, Tami A, Histing T, Holstein JH, et al. 2012. Temporal and Spatial Vascularization Patterns of Unions and Nonunions: Role of Vascular Endothelial Growth Factor and Bone Morphogenetic Proteins. *Journal of Bone & Joint Surgery* 94: 49-58.
[207] Lu C, Marcucio R, Miclau T. 2006. Assessing Angiogenesis during Fracture Healing. *The Iowa Orthopaedic Journal* 26: 17-26.
[208] Street J, Bao M, deGuzman L, Bunting S, Peale FV, Ferrara N, et al. 2002. Vascular endothelial growth factor stimulates bone repair by promoting angiogenesis and bone turnover. *Proceedings of the National Academy of Sciences* 99: 9656-61.
[209] Lienau J, Schell H, Duda G, Seebeck P, Muchow S, Bail HJ. 2005. Initial vascularization and tissue differentiation are influenced by fixation stability. *Journal of Orthopaedic Research* 23: 639-45.
[210] Alexander KA, Chang MK, Maylin ER, Kohler T, Müller R, Wu AC, et al. 2011. Osteal macrophages promote in vivo intramembranous bone healing in a mouse tibial injury model. *Journal of Bone and Mineral Research* 26: 1517-32.
[211] Hume DA, Loutit J, Gordon S. 1984. The mononuclear phagocyte system of the mouse defined by immunohistochemical localization of antigen F4/80: macrophages of bone and associated connective tissue. *Journal of Cell Science* 66: 189-94.
[212] Chang MK, Raggatt LJ, Alexander KA, Kuliwaba JS, Fazzalari NL, Schroder K, et al. 2008. Osteal Tissue Macrophages Are Intercalated throughout Human and Mouse Bone Lining Tissues and Regulate Osteoblast Function In Vitro and In Vivo *The Journal of Immunology* 181: 1232-44.
[213] Radomisli TE, Moore DC, Barrach HJ, Keeping HS, Ehrlich MG. 2001. Weight-bearing alters the expression of collagen types I and II, BMP 2/4 and osteocalcin in the early stages of distraction osteogenesis. *Journal of Orthopaedic Research* 19: 1049-56.
[214] Sambrook P, Cooper C. 2006. Osteoporosis. *The Lancet* 367: 2010-8.
[215] Nanes MS, Kallen CB. 2014. Osteoporosis. *Seminars in Nuclear Medicine* 44: 439-50.

[216] Giannoudis P, Tzioupis C, Almalki T, Buckley R. Fracture healing in osteoporotic fractures: Is it really different? *Injury* 38: S90-S9.
[217] Nikolaou V, Lindner T, Kanakaris N, Giannoudis P. 2010. IS FRACTURE HEALING DELAYED IN OSTEOPOROTIC PATIENTS? *Journal of Bone & Joint Surgery, British Volume* 92-B: 332.
[218] Namkung-Matthai H, Appleyard R, Jansen J, Hao Lin J, Maastricht S, Swain M, et al. 2001. Osteoporosis influences the early period of fracture healing in a rat osteoporotic model. *Bone* 28: 80-6.
[219] Walsh WR, Sherman P, Howlett CR, Sonnabend DH, Ehrlich MG. 1997. Fracture healing in a rat osteopenia model. *Clinical Orthopaedics and Related Research* 342: 218-27.

Appendices

A. Chapter 5 and Chapter 6: Surgical Procedure

Appendix A
Chapter 5 and Chapter 6: Surgical Procedure

The surgeries for this study have been conducted at QUT Medical Engineering Facility (MERF) and ethics approval was obtained by from the university ethics committee (ethics approval number: 1100000717). Animal care and experimental protocols were followed in accordance with the National Health and Medical Research Council (NHMRC) guidelines and approved by the Animal Ethics committee of Queensland University of Technology.

Table A-1: Instruments and consumables necessary for surgical procedure.

Instruments	Consumables
Fixator bars and screws	Gauze squares
1 mm stainless steel pins	Gauze balls
0.8 mm drill bit (DePuy Synthes, USA)	10 mL syringe
Air drill (DePuy Synthes, USA)	Scalpels blades size 10
Drill guides	Chlorhexidine
Scissors	Saline
Scalpel handle	Plastic sheet to cover rat
Forceps x 4	Drill cover
Saw blades and 1 mm spacer	Scalpel blade
Screw driver	Finger of glove
Wire cutter	Suture x 2 (Vicryl 5.0)

Surgical Procedure

1) The surgeon makes a 3-4cm incision along the femur, of the right leg, opening the skin and muscle to expose the lateral surface of the bone.

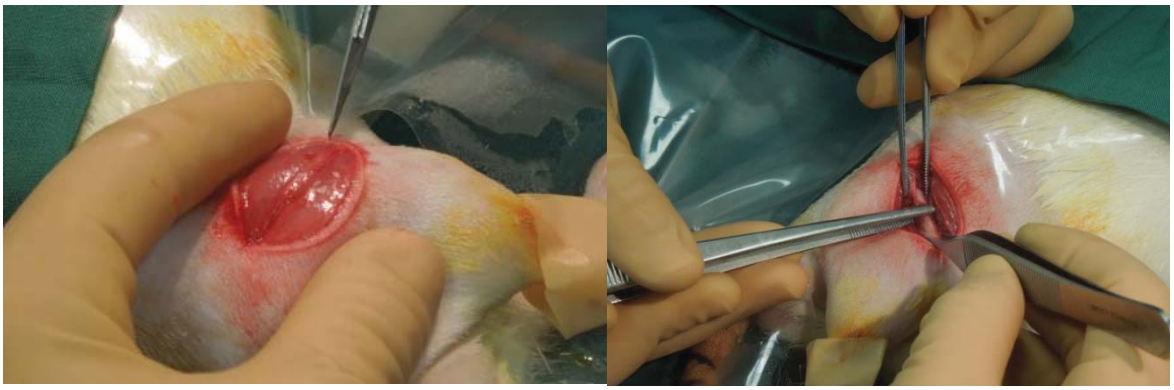

Figure A-1: Incision site and exposure of the lateral surface of the femur.

2) Surgical assistant holds the centre of the bone and retracts tissue from the proximal end of the bone. Surgeon places the first drill guide on the bone in position to drill the proximal hole. Placement of this hole is critical for the successful completion of the surgery. When in place, surgeon drills hole with irrigation (saline).

3) The first drill guide is then rotated and surgeon inserts the first pin.

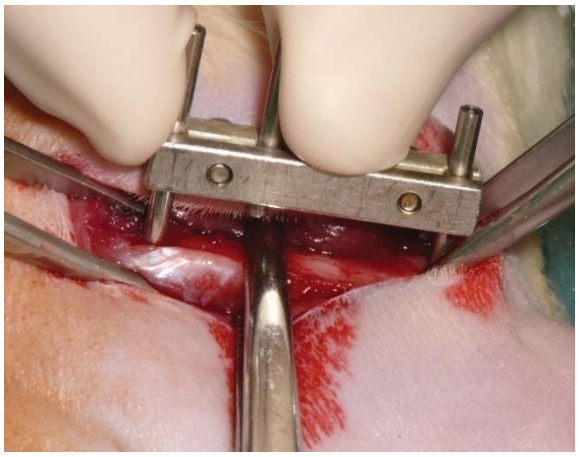

Figure A-2: Placement of first drill guide on surface of the femur.

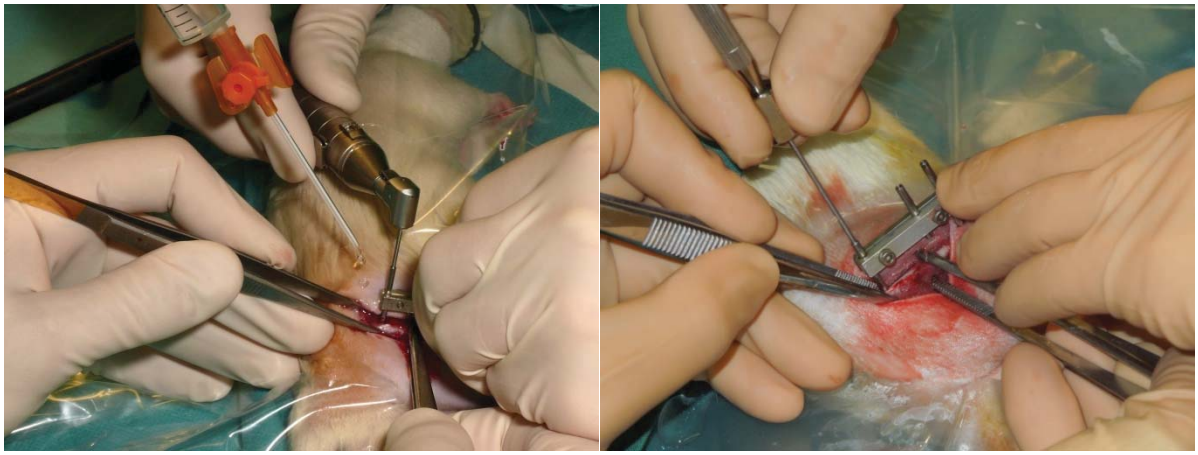

Figure A-3: Drilling of the first hole in the proximal end of the femur. The drill guide is then rotated to allow the insertion of the pin.

4) Before drilling the second hole at the distal end of the femur, it is important to check the placement of the drill guide with a pin inserted in the third hole. If this is in contact with the surface of the bone, the surgeon then proceeds to drill the distal hole.

5) To insert the distal pin, the first drill guide is replaced by the second drill guide. The pin is then inserted.

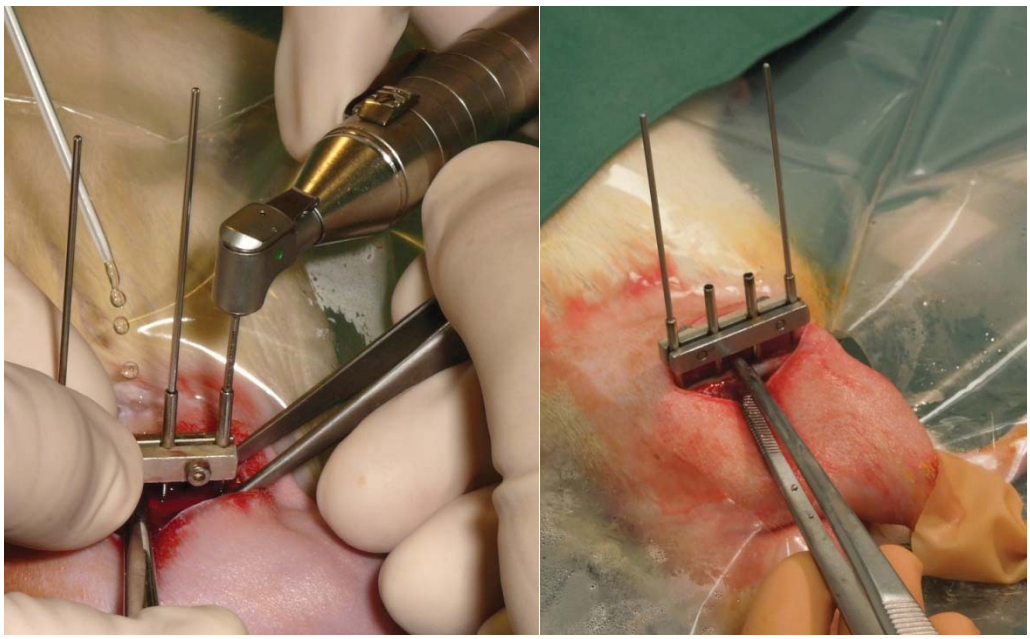

Figure A-4: Drilling the distal hole after checking the placement of the drill guide. The first drill guide is changed to the second one for insertion of the distal pin.

6) Using the second drill guide (already in place), the two inner holes are drilled.

7) The second drill guide is then replaced by the third guide for insertion of the inner pins. The third guide is then removed.

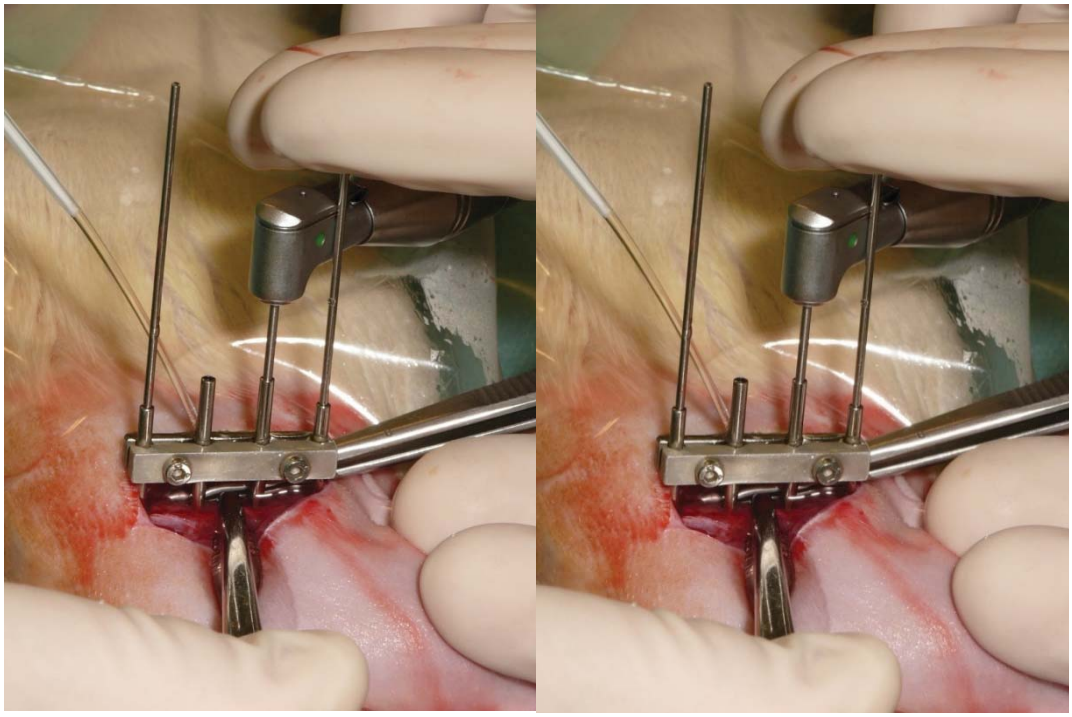

Figure A-5: Drilling of the inner two holes using the second drill guide.

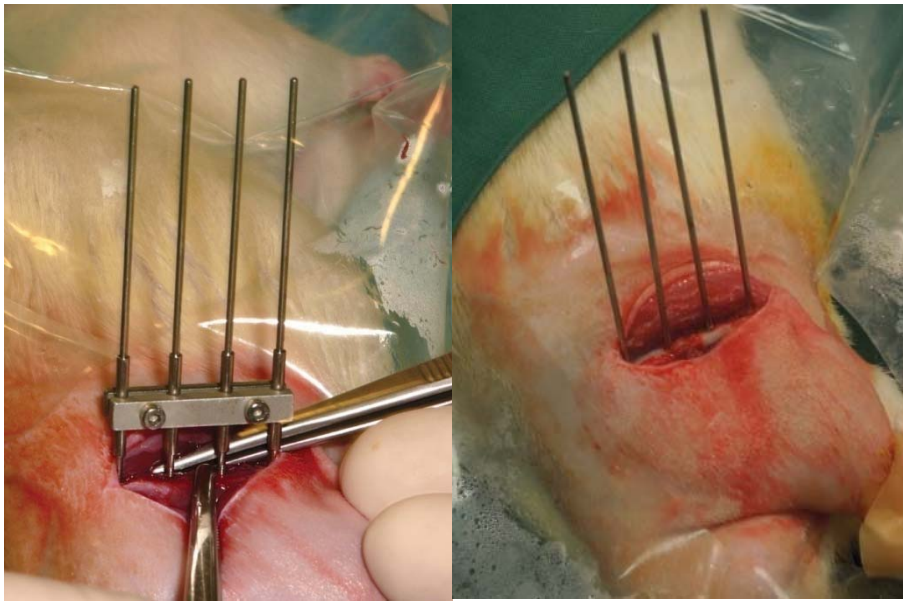

Figure A-6: Insertion of inner pins using the third guide. When this is completed the guide is removed.

8) The fixator bars are then places over the pins. A spacer of 6mm or 12mm is used to place the bars this distance from the bone for the stiff and flexible fixation conditions respectively. The distance between the bars is one bar width. Surgeon will hold the desired configuration firmly in place, while surgical assistant tightens the screws with an Allen key.

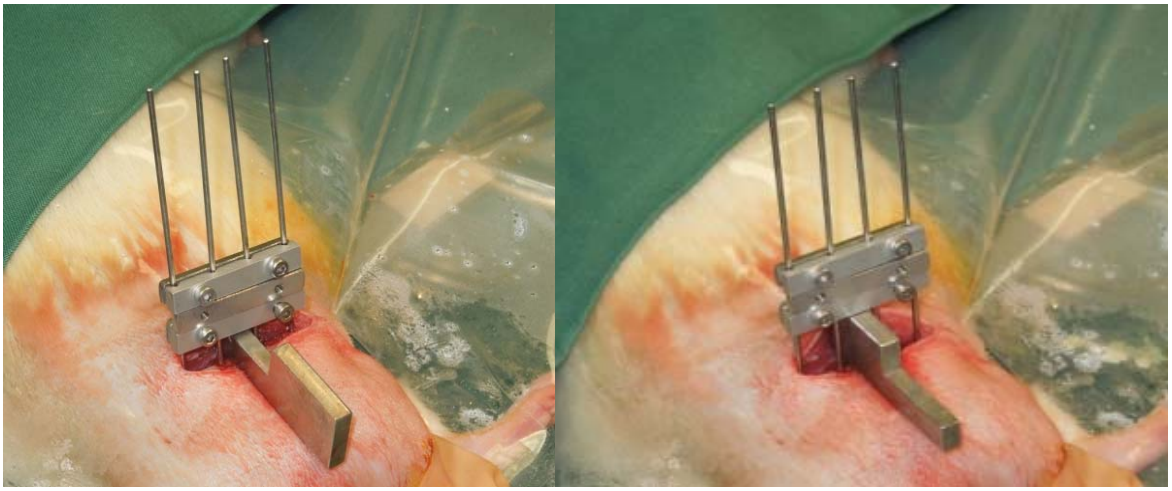

Figure A-7: Spacing for the stiff configuration (6mm) and flexible configuration (12mm) from the surface of the bone.

9) The inner bar is then removed and the extra length of the pins is cut with the wire cutters.

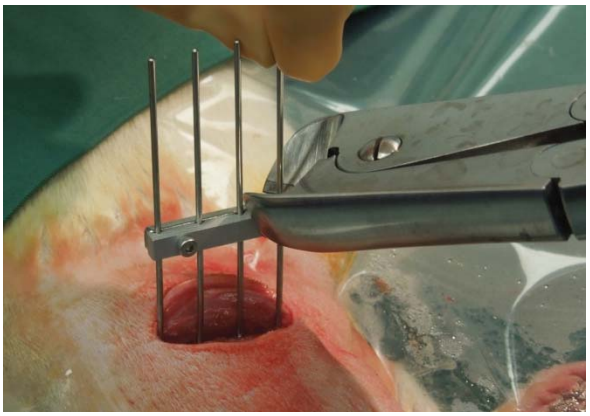

Figure A-8: Removal of inner fixator bar and cutting of excess length of the wire pins.

10) The osteotomy is then cut in the centre of the bone between the two inner pins. The saw used has two blades set 1mm apart in order to create the 1mm osteotomy.

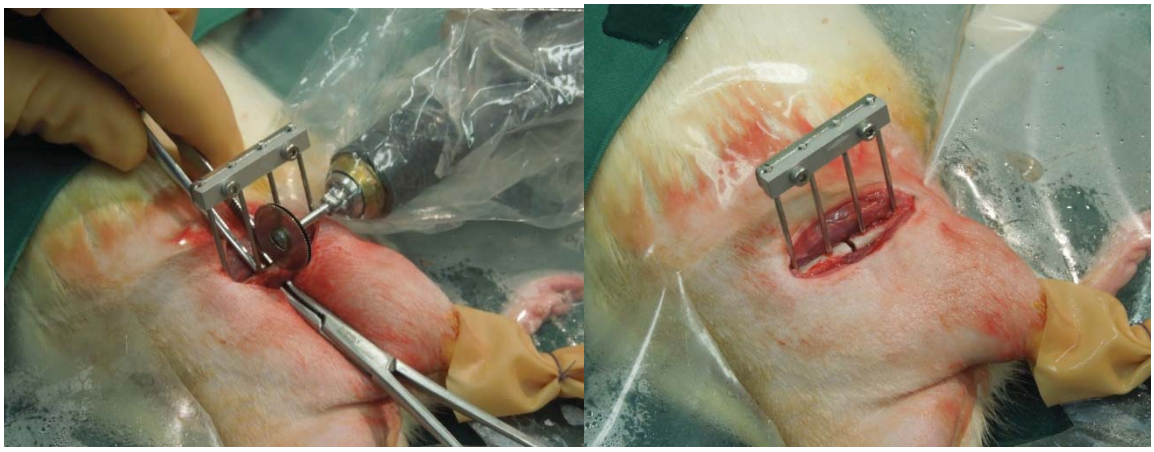

Figure A-9: 1mm osteotomy created between the two inner pins of the fixator.

11) Finally the muscle and skin are sutured closed. And the inner bar of the fixator is put back on, creating the final fixator configuration.

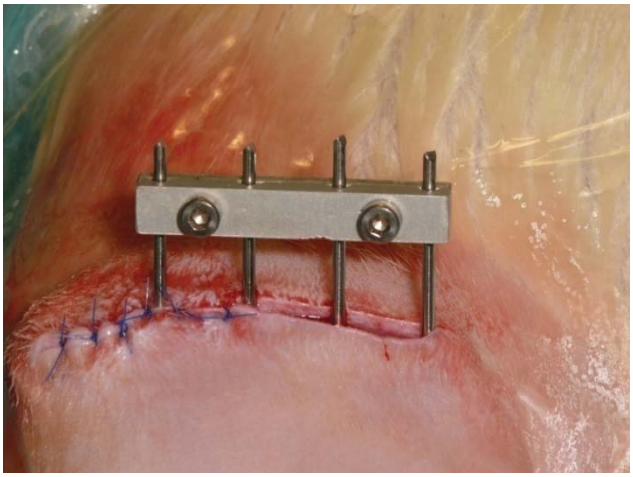

Figure A-10: Final step of suturing the muscle and skin to close the wound.